Curtin Medical School

An Absolutely Conserved Motif of the Essential Translocon Subunit, Sss1, Dictates Protein Function and Stability with Implications for Personalised Medicine

Christopher Michael Witham

This Thesis is Presented for the Degree of

Doctor of Philosophy

of

Curtin University

March 2023

Declaration

To the best of my knowledge and belief this thesis contains no material previously published by any other person except where due acknowledgment has been made. This thesis contains no material which has been accepted for the award of any other degree or diploma in any university.

Signature: … [redacted] ….

Date: 17/03/2023 ……..

Abstract

Secretory and integral membrane proteins contribute to approximately one third of the eukaryotic cellular proteome. Maturation of these proteins requires passage into the Endoplasmic reticulum (ER), a process facilitated by the heterotrimeric protein complex known as the Sec61 translocon. The three subunits that constitute the Sec61 translocon in yeast/mammals are Sec61/Sec61α, Sss1/Sec61γ and Sbh1/Sec61β. The functionality of the translocon is reliant on its ability to facilitate the induction of nascent proteins while maintaining the barrier between the two distinct environments of the ER and cytosol. However, the translocon is found to also participate in a controlled flux of essential metabolites, a role that is thought to be vital in maintaining these functional environments as well as for cellular processes such as Ca^{2+} signalling. The dynamic nature of the translocon is fundamental in the channels ability to participate in these collectively distinct functions; and while ER channels and components in translocation have been described with roles in disease progression, the involvement of dysregulated translocon dynamics is only recently being implicated.

The current literature that describes the mechanisms involved in regulating translocon conformational dynamics is very Sec61/Sec61α centric. Yet our own structural analysis revealed the extreme C-terminus of Sss1/Sec61γ to be juxtaposed to a key gating module of Sec61/Sec61α. We therefore hypothesised that the highly conserved C-terminus of Sss1/Sec61γ has a functional role in regulating translocon dynamics. This work is founded in the characterisation of a heptapeptide within the extreme C-terminus of the Sss1 subunit which we termed as the K_{69}LIHIPI_{75} motif. This region is absolutely conserved in all eukaryotes studied to date, which allowed us to take advantage of the well characterised and simplified biology of the model organism, *Saccharomyces cerevisiae*. Our characterisation of the K_{69}LIHIPI_{75} motif was instigated by the discovery of two temperature sensitive (TS) mutations of this region, termed *sss1-6* (P74A, I75A) and *sss1-7* (H72K), which yielded two main findings.

First, the TS phenotype of these mutants was found to be the result of dysregulated translocon dynamics, specifically that which stabilises the open conformation and perpetuates a leak across the translocon. We have leveraged the observable nature of this phenotype along with the high levels of conservation present in the translocon subunits in our design of a simplified system for assessing translocon gating dynamics. The utility for such a system lies in its ability to identify the manner in which disease associated mutations may be influencing translocon dynamics. This work has also served as a pilot study for such utility, where we show that cancer associated mutations of Sec61γ, that are conserved within Sss1, can influence the conformational stability of either the closed or open states of the translocon.

The second main outcome from our investigations involved an observed accumulation of Sss1 protein within the *sss1-6* mutant. This would be attributed to a disruption in the quality control of Sss1 that presented as increased protein stability and led us to conclude that the K_{69}LIHIPI_{75} peptide constitutes a degron for Sss1. Herein, we have proceeded to characterise the mechanisms of Sss1 degradation, finding an increased rate in degradation upon diminished presence of the major interacting partners, Sec61 and Ssh1. This outcome identified Sss1 as a quantity control substrate that is rapidly degraded when failing to interact with either protein. We also found that Sss1 protein demonstrated varying levels of stability across knockouts for three ER resident E3 ligase complexes, being HRD1, DOA10 and ASI. This tight control that cells appear to have over Sss1 was also demonstrated to be regulated via a family of peptidyl-prolyl cis-trans isomerases (PPI) known as cyclophilins.

In essence, we have identified a highly conserved region Sss1 which encodes the proteins degron and contributes to regulating translocon dynamics. Both findings are novel to this work and contribute to our greater understanding of eukaryotic cellular processes as well as the consequences to their dysregulation that can occur within disease.

Contents

Abstract ii

Contents iv

Table of Figures x

Table of Tables xii

Authorship Declarations xiii

Acknowledgements xvi

Abbreviations xix

Chapter 1:

Literature review 1

The Endoplasmic Reticulum 1

Sec61 Translocon Complex 2

The Signal Sequence and Protein Trafficking 6

Co-translational Translocation - Trafficking 8

Co-translational Translocation – Channel Interactions 11

Co-translational Translocation – Alternative Targeting 14

Post-translational Translocation 15

Post-translational Modifications 21

ER Homeostasis and The Translocon 26

Dysregulation and the Activation of UPR 29

Project Design & Hypothesis: Characterising the Outcomes of Dysfunctional Sss1 31

References 33

Chapter 2:

General Methodology 45

Growth Conditions 45

Yeast Transformation 45

Isolation of Yeast Genomic DNA 46

DNA Sequencing 46

Cell Lysates from Yeast Strains 47

Immunoblotting 47

β-Galactosidase Assays 48

Membrane Preparation 48

DSS Cross-linking 49

Solubilisation of Membranes with Digitonin 49

ConA Dependent Fractionation of SEC Proteins 49

Blue Native PAGE Analysis 50

Cycloheximide Chase Analysis 51

Mutagenesis and Selection for *SEC61* Suppressors of the *sss1-7* TS Phenotype 51

Fluorescence Microscopy 52

Glutathione Sensitive Growth Assay 52

Invertase Secretion 52

Reverse Transcription (RT)-PCR 53

Chapter 2 Tables 54

References 68

Chapter 3:

Investigating a Role for Sss1 in Translocon Gating Dynamics 69

Introduction 69

Sss1 Function 69

Temperature Sensitive Mutations 70

The Yeast of All Model Organisms 71

Experimental Design and Aims 72

Results 73
Structural Analysis Finds a Role for Sss1 in the Translocon Gating Module 73
Sec61 Mutants Suppress the Temperature Sensitivity of *sss1-7* 73
Characterisation of the Isolated *SEC61* Mutants 75
References 80
The Conserved C-terminus of Sss1p is Required to Maintain the ER Permeability Barrier 81
Abstract 82
Introduction 83
Results 85
The C-terminus of Sss1p is Highly Conserved 85
Mutations in the Sss1p C-terminus Disrupt ER Homeostasis 85
The ER is More Permeable in *sss1-6* and *sss1-7* 90
Mutations in Residues of Sec61p Located in Important Gating Modules Suppress *sss1-6* and *sss1-7* Temperature Sensitivity 93
Mutations in Residues Located in Important Sec61p Gating Modules Suppress the Elevated ER Permeability Observed in *sss1-6* and *sss1-7* 96
Discussion 99
The Extreme Sss1p/Sec61γ C-terminus Influences ER Permeability 99
Materials and Methods 102
Yeast Strains and Growth 102
Mutagenesis and Selection for *SEC61* Suppressors of *sss1-7* Temperature Sensitivity 102
Fluorescence Microscopy 102
DSS Cross-linking 103
Immunoblotting 103
ConA Dependent Fractionation of SEC Proteins 103
β-Galactosidase Assays 104

Glutathione Sensitive Growth Assay 104

References 106

Manuscript Supplementary Data 109

Chapter 4:

Characterising Cancer Associated Mutations of Sss1 that Impart Gating Dysregulation 120

Introduction 120

Calcium Regulation 120

Glutathione Regulation 122

Experimental Design and Aims 123

Results 126

The Translocon Establishes ER Redox Poise 126

Translocon Gating Defects Can Flood the Cytosol with Calcium 127

References 131

Cancer Associated Mutations in Sec61γ Alter the Permeability of the ER Translocase 134

Abstract 135

Author Summary 135

Introduction 136

Results 138

Sec61γ Cancer Associated Mutations do not Disrupt ER Translocation 138

The Sss1 H72R Mutation Affects Translocon Gating 142

Structural Rationale for Altered Translocon Gating in Sec61γ H58R Mutant 146

Other Sec61γ Cancer Associated Mutations Alter Translocon Gating 147

Discussion 154

A Possible Mechanism for *sss1*^{H72R} in Disrupting Gating Dynamics 154

Disrupting Translocon Dynamics: an Outcome in Cancer Related Mutations 155

Materials And Methods 158

Yeast Strains 158

Plasmid Construction – Site Directed Mutagenesis 158

Glutathione Sensitive Growth Assay 158

β-Galactosidase Assays 159

Cell Lysate Preparation and Immunoblotting 159

References 161

Manuscript Supplemental Data 165

Invertase Secretion 165

DSS Cross-linking 165

Blue Native PAGE Analysis 165

Reverse Transcription (RT)-PCR 166

Chapter 5:

Determining Protein Degradation Pathways Regulating Sss1 Abundance 180

Introduction 180

The HRD1 Pathway 182

The DOA10 Pathway 184

The ASI Pathway 185

Experimental Design and Aims 186

Results 186

The Conserved K_{69}LIHIPI$_{75}$ Heptapeptide Encodes the Sss1 Degron 186

P74A Individually Contributes to the Accumulation Observed in *sss1-6* 190

Sss1 is a Quantity Control Substrate Degraded by Three E3 Ligase Complexes 192

PPIs Appear to Coordinate ERAD for the Essential Translocon Component Sss1 196

Discussion 198

References 204

Chapter 6:

Concluding Remarks 209

The Complexity of Regulating Translocon Dynamics 209

Outcomes for Analysing Disease 212

How Can Yeast Help You 215

References 218

Table of Figures

Chapter 1:

Fig. 1.1. Ribbon diagram of the closed archaeal and open yeast translocon apparatus 4

Fig. 1.2. ER Trafficking 7

Fig. 1.3. Stepwise guide to co-translational translocation 13

Fig. 1.4. SRP-independent translocation 17

Fig. 1.5. Post translational modifications (PTM) 22

Chapter 3:

Fig. 2.1. *sss1-6* and *sss1-7* are mutants located at the extreme C-terminus of Sss1 and present with a temperature sensitive growth defect. 74

Fig. 2.2. Isolated suppressor colonies demonstrating restoration of the *sss1-7* growth defect. 76

Fig. 2.3. *SEC61*^{G262E} and *SEC61*^{L449M} demonstrate recessive suppression of *sss1-7*. .79

Chapter 3 Manuscript:

Fig. 3.1. The Sss1p C-terminus is highly conserved 86

Fig. 3.2. *sss1-6* and *sss1-7* are inserted into the ER membrane 87

Fig. 3.3. ER translocation is not affected in *sss1-6* and *sss1-7* 89

Fig. 3.4. ER homeostasis is perturbed in *sss1-6* and *sss1-7* 91

Fig. 3.5. Mutations in residues of Sec61p located in important gating modules suppress *sss1-6* and *sss1-7* temperature sensitivity 94

Fig. 3.6. SEC61 dependent suppressors of *sss1-6* and *sss1-7* are functional 95

Fig. 3.7. Mutations in the lumenal lateral gate genetically interact with *sss1-6* and *sss1-7* 97

Fig. 3.8. Mutations in residues of Sec61p located in important gating modules suppress ER permeability defects in *sss1-6* and *sss1-7* 98

Supp. Fig. S3.1 117

Supp. Fig. S3.2 118

Supp. Fig. S3.3 119

Chapter 4:

Fig. 4.1. uSil1 accumulates in *sss1^{ts}* gating mutants 128

Fig. 4.2. *sss1-7* is hypersensitive to FK506 129

Chapter 4 Manuscript:

Fig. 5.1. The Sss1p C-terminus is highly conserved 140

Fig. 5.2. The *sss1^{H72R}* mutation disrupts ER homeostasis 144

Fig. 5.3. The K27E and L56F mutations destabilise the closed conformation of the translocon 150

Fig. 5.4. The A39V and I64T mutations destabilise the open conformation of the translocon 153

Supp. Fig. S5.1. 174

Supp. Fig. S5.2. 175

Supp. Fig. S5.3. 177

Supp. Fig. S5.4. 178

Supp. Fig. S5.5. 179

Chapter 5:

Fig. 6.1. The major ERAD pathways of yeast 181

Fig. 6.2. Phenotypical characterisation of Sss1 abundance 188

Fig. 6.3. The C-terminus of Sss1 regulates protein turnover 189

Fig. 6.4. Characterisation of the P74A mutant finds it responsible for the accumulation of Sss1 protein observed within *sss1-6*. (A) 191

Fig. 6.5. Sss1 protein accumulates in knockouts for certain ERAD pathway components 193

Fig. 6.6. Characterisation of Sss1 degradation pathways by chx chase of ERAD defective strains 195

Fig. 6.7. Sss1 quality control is influenced via the action of cyclophilins 197

Table of Tables

Chapter 2:

Table 1.1. Yeast strains used in this study 54

Table 1.2. Plasmids used in this study 62

Table 1.3. Oligonucleotides used in this study 64

Table 1.4. Antibodies used in this study 67

Chapter 3:

Table 2.1. Each isolate signified by mutation, location, and number. 77

Chapter 3 Manuscript:

Supp. Table S3.1. Yeast strains used in this study 109

Supp. Table S3.2. Plasmids used in this study 113

Supp. Table S3.3. Oligonucleotides used in this study 114

Supp. Table S3.4. Antibodies used in this study 116

Chapter 4:

Table 4.1. Disease associated mutations of the translocon Sec61α subunit 125

Chapter 4 Manuscript:

Supp. Table S5.1. Yeast strains used in this study 167

Supp. Table S5.2. Plasmids used in this study 170

Supp. Table S5.3. Oligonucleotides used in this study 172

Supp. Table S5.4. Antibodies used in this study 173

Authorship Declarations

Two manuscripts contribute to the body of work presented within this thesis and I have obtained the appropriate permissions for their inclusion here.

Witham CM, Dassanayake HG, Paxman AL, Stevens KLP, Baklous L, White PF, et al. The conserved C-terminus of Sss1p is required to maintain the endoplasmic reticulum permeability barrier. J. Biol. Chem. 2020; 295(7):2125–34. pmid:31848225

Location in thesis: Chapter 3

This work was a collaborative effort from our group with the individual contributions of the co-authors indicated below and approved by Carl Mousley.

[redacted]

Christopher M. Witham – 50%

Involved in project design, data acquisition, critical analysis and co-wrote manuscript.

Hasindu G. Dassanayake – 4%

Provided technical assistance on experiments.

Aleshanee L. Paxman – 4%

Provided technical assistance on experiments and proofed final document.

Kofi L. P. Stevens – 5%

Supervisory role, providing critical analysis and proofed final document.

Lamprini Baklous – 4%

Provided technical assistance on experiments and generated vectors used in study.

Paris F. White – 2%

Provided technical assistance on experiments.

Amy L. Black – 1%

Generated a vector used in study.

Robert F. L. Steuart – 3%

Supervisory role, providing critical analysis and proofed final document.

Colin J. Stirling – 1%

Involved in early genesis of the work.

Benjamin L. Schulz – 2%

Provided expertise in field, providing critical analysis, and proofed final document.

Carl J. Mousley – 24%

Lead PI, involved in project conception, data acquisition, critical analysis and co-wrote manuscript.

Witham CM, Paxman AL, Baklous L, Steuart RFL, Schulz BL, Mousley CJ (2021) Cancer associated mutations in Sec61γ alter the permeability of the ER translocase. PLoS Genet 17(8): e1009780.

Location in thesis: Chapter 4

This work was a collaborative effort from our group with the individual contributions of the co-authors indicated below and approved by Carl Mousley.

Christopher M. Witham – 50%

Involved in project design, data acquisition, critical analysis and co-wrote manuscript.

Aleshanee L. Paxman – 10%

Provided technical assistance on experiments, critical analysis and co-wrote manuscript.

Lamprini Baklous – 10%

Provided technical assistance on experiments and generated vectors used in study.

Robert F. L. Steuart – 4%

Supervisory role, providing critical analysis and proofed final document.

Benjamin L. Schulz – 2%

Provided expertise in field, providing critical analysis, and proofed final document.

Carl J. Mousley – 24%

Lead PI, involved in project conception, data acquisition, critical analysis and co-wrote manuscript.

Acknowledgements

Firstly, I want to acknowledge the traditional owners of the land on which the Curtin Bentley campus is located, the Wadjuk people of the Nyungar Nation and pay my respects to the past, present and future traditional custodians, and elders of the nation's First Peoples as well as to the Aboriginal and Torres Strait Islander members of our community.

I would like to express my appreciation to my supervisors Dr Carl Mousley and Dr Rob Steuart. Carl, you have served as both a mentor and role model and for that I am grateful. You are as relentless in your pursuit for science as you are stuck in your ways, but it is that inherent passion you have for what we do that both inspired and drove me to be the scientist I am today. I will forever look back upon our impromptu meetings fondly where we would discuss new avenues to explore that, at times were doomed from the beginning, yet were always exhilarating in their prospects. To Rob, I appreciate both the support you have provided and the calm demeanour in which you approach situations. The time you have given to troubleshoot methods by going through each of the steps to identify issues or propose potential solutions has been invaluable and got me through several tough situations, placing me back into a positive mindset.

I am proud and grateful to count myself among those who have been a part of Carl's lab group. Through my time, I have had the pleasure to work with a great group of people and I appreciate all the patience, understanding and willingness to help I have received from those I have worked with. Specifically, I would like to thank:

Dr Kofi Stevens, I am indebted to you for all the time you so freely gave. Through your supervision I have gained innumerable skills and techniques which I will keep for a lifetime. I am also grateful for your approachability as it made asking the stupid questions easy and greatly helped my understanding, especially during the early days when I needed you to translate Carl. I am however most appreciative of your ability to identify shortcomings in either knowledge or skill and then be able to

adjust to accommodate for them, this has helped build confidence in myself as I am sure it has for others and did not go unnoticed.

Lesh, you have forced me out of my shell by yelling at me a lot and I appreciate that I guess. I also highly value your opinion as you, in almost stark contrast to your chaotic nature, have a great talent to ground the way we present our work to make it digestible to a wider audience.

Mark, the best of travelling companions. I value your friendship and intelligence, having learnt a lot from you. Your presence is also favourable on any occasion as you bring a sense of familiarity that has always made it easier to engage with new experiences.

Jared, I appreciate your friendship as I feel I can always speak my mind to you without judgment. You also always have something to say, for better or worse, do a great BBQ and you have helped keep me caffeinated, what more could I ask for.

Lee, you have been ever resourceful to me, and I appreciate the time you have given to teach me these skills as we all know the figures here wouldn't look nearly as good without you.

Most importantly Lamprini, you have always motivated me to strive for the best through your encouragement and belief in me. While you may not have known it at the time, I have always endeavoured to impress you, as the jubilant expressiveness in which you have responded to all my achievements has made all the hard work all the more worthwhile. You have supported me financially and emotionally, you have cared for me, and you have instilled a sense of belonging in me. For all these reasons you are my best friend and life partner and with you by my side I look forward to our future together so that I may give back all the love you have given me.

I would like to also extend my thanks to all those who have had a positive impact on my journey by providing both support and friendship, including Callum Verdonk, Amy Davis, Aleesha Davis, Tahlia Bastholm, Tom Mcleod, Merin Eapen, Ratish

Permala, Hasindu Dassanayake, Paris, Jaime, Zac, John and many more not listed here, as an exhaustive list would be impossible.

Finally, I would like to thank my family, my siblings Ben, Daniel, Josh, and Olivia as well as my parents Ian and Leanne. You have collectively given me so much support in pursuing my dreams, providing me with guidance when I have asked for it, understanding when I needed it and unfaltering compassion throughout.

I would like to give a special thanks to my mother, Leanne, as you were the first to believe in me. You pushed me to not only pursue my passion for science but did so against many roadblocks, most of which I must admit were placed there by my own actions. It is for this reason that I dedicate this thesis to you, thank you.

Abbreviations

4MαG	Methylumbelliferyl α-D-glucopyranoside
5-FOA	5-Fluoroorotic Acid
aa	Amino acids
ADTKD	Autosomal dominant tubulointerstitial kidney disease
ADP	Adenosine diphosphate
ATP	Adenosine triphosphate
BME	2-mercaptoethanol
BN-PAGE	Blue native polyacrylamide gel electrophoresis
Ca^{2+}	Calcium
CaM	Calmodulin
chx	Cycloheximide
CN	Calcineurin
ConA	Concanavalin A
CPR	Cyclosporin-sensitive proline rotamases
CsA	Cyclosporine A
DMSO	Dimethyl sulfoxide
DNA	Deoxyribonucleic acid
DSS	Disuccinimidyl suberate
DTT	Dithiothreitol
EP-PCR	Error-Prone PCR
ER	Endoplasmic reticulum
ERAD	ER-associated degradation
ERLAD	ER to lysosome associated degradation
Ero1	ER oxidoreductin 1
FAD	Flavin adenine dinucleotide
FFA	Free fatty acid
FPP	Farnesyl pyrophosphate
Fpp1	Farnesyl pyrophosphate synthetase

FPR	FK506-sensitive proline rotamases
GDP	Guanosine diphosphate
GET	Guided entry of tail anchored protein
GRX	Glutaredoxins
GSH	Reduced glutathione
GSSG	Oxidised glutathione
GTP	Guanosine triphosphate
HACS	High-affinity Ca^{2+} influx system
HCC	Hepatocellular carcinoma
Hgt1	High-affinity glutathione transporter
HNSCC	Head and neck squamous cell carcinoma
HSP	Heat shock protein
INM	Inner nuclear membrane
IP3R	Inositol trisphosphate receptor
K/O	Knock-out
LACS	Low-affinity Ca^{2+} influx system
LB	Luria Bertani
LUAD	Lung adenocarcinoma
MAMs	Mitochondria-associated ER membranes
Mg^{2+}	Magnesium
MHC	Major histocompatibility complex
Mn^{2+}	Manganese
NBD	Nucleotide binding domain
NE	Nuclear envelope
NEF	Nucleotide exchange factor
ONPG	Ortho-Nitrophenyl-β-galactoside
ORF	Open reading frame
OST	Oligosaccharide transferase
PCR	Polymerase chain reaction
PDI	Protein disulfide isomerase
PMSF	Phenylmethylsulfonyl fluoride

ppαf	Pre-pro-alpha factor
PPI	Peptidyl-prolyl cis-trans isomerases
PSIPRED	PSI-blast based secondary structure PREDiction
PTM	Post translational modifications
RAMPs	Ribosome attached membrane proteins
RET	Ribosomal exit tunnel
RING	Really interesting new gene
RNA	Ribonucleic acid
RNC	Ribosome nascent chain complex
RT	Reverse transcription
RYR	Ryanodine receptor
SBD	Substrate binding domain
SDM	Site directed mutagenesis
SERCA	Sarco/endoplasmic reticulum Ca^{2+}-ATPase
SND	SRP-independent
SOCE	Store operated calcium entry
SRP	Signal recognition particle
SR	SRP Receptor
SS	Signal sequence
TA	Tail anchored
tm	Tunicamycin
TM	Transmembrane
TMD	Transmembrane domain
TMH	Transmembrane helices
TPR	Tetratricopeptide repeat
TS	Temperature sensitive
UPR	Unfolded protein response
UPRE	Unfolded protein response element
uSil1	Unglycosylated Sil1
WT	Wildtype
YCp	Yeast centromere plasmid

YEp	Yeast episomal plasmid
YP	Yeast Peptone
YPD	Yeast Peptone supplemented with 2% w/v D-glucose
YNB	Yeast nitrogen base
Zn^{2+}	Zinc

Chapter 1

Literature review

The Endoplasmic Reticulum

The distribution of cellular processes to that of membrane bound organelles has proved to be one of the greatest evolutionary advantages afforded to eukaryotic cells. This compartmentalisation allows for specificity in an array of varying functions to meet the demands of a eukaryotic cell and achieves a level of efficiency required for such complexity observed in that of multicellular organisms. The endoplasmic reticulum (ER) is one of the largest organelles, forming a tubular network that can take up more than 10% of the cellular space at any given time (1). The size of the ER reflects its importance within a cell as the ER contributes to cellular function through lipid and steroid synthesis, protein maturation, transport and degradation, and the storage of Calcium ions (2-7). The ER itself has several morphologically distinct domains that specify in its many functions; the more peripheral regions are heavily involved in the movement of proteins and cellular organisation (8, 9), while the ER that envelopes the nucleus, known as the nuclear envelope (NE), is more focussed on processes relating to centrosome localisation and DNA repair (10-14).

On average, one third of the eukaryotic proteome is destined to the ER and includes integral membrane proteins and precursors to the secretory pathway (15). The secretory pathway exists for the processing and delivery of soluble proteins while also utilised by transmembrane (TM) proteins so too reach their destined location for functional expression. This pathway begins in the cytosol with the synthesis of an appropriate nascent polypeptide at the ribosome followed by trafficking to the ER membrane. The ER is the first point of contact for these proteins and performs the necessary post translational modifications (PTM) and folding to tertiary and quaternary structures. Proteins not resident to the ER are transported through vesicular movement from ER exit sites to those organelles in the endo/exo-cytosis

network (Golgi apparatus, endosome, vacuole/lysosome and trafficking vesicles), peroxisomes, lipid droplets, the mitochondria or the plasma membrane (15-17). At the Golgi apparatus soluble proteins are packaged for distribution to the extracellular space which is the process of secretion.

Sec61 Translocon Complex

Trafficking, and entry of nascent polypeptides to the ER is achieved via the process of translocation. A TM protein complex, aptly named the Sec61 Translocon, serves as the portal to the ER lumen and is cardinal in the translocation for the majority of proteins that must precede the ER. The Sec61 translocon is a heterotrimeric protein complex that is universally conserved, existing in prokaryota and archaea as SecYEG and SecYEβ respectively for the transport of protein across the plasma membrane (18-20). The conserved nature of the Sec61 translocon proved advantageous in providing the first structural insights. Initial studies dedicated to determining the crystal structure utilised the simple biology of archaeal systems in generating the homologous SecYEβ complex with X-ray crystallography (21). Advancements in structural analysis, particularly the advent of cryo-EM have allowed researchers to define translocon structure in eukaryotic systems with the initial discoveries still used as the template for comparative characterisation.

The three subunits that constitute the yeast translocon are Sec61, Sbh1 and Sss1, and represent the homologs to Sec61α, Sec61β and Sec61γ of the mammalian complex respectively (Fig. 1.1.). The Sec(retory)61 subunit is the largest component of the translocon. Ten TM domains form two half structures around an aqueous core that has been demonstrated to facilitate the translocating polypeptide (21-24). The two halves of Sec61 are organised into TM helices 1-5 and 6-10 which are connected by an external loop that extends between TM5 and 6 (L5/6) (Fig. 1.1., A & C). At the opposing face there exists a junction between TM helices 2/3 and 7/8 known as the lateral gate. Three polar residues of the lateral gate form a cluster that is sandwiched between an apolar patch of the plug domain and the hydrophobic core of the lipid bilayer (Fig. 1.1.). This structural component of the

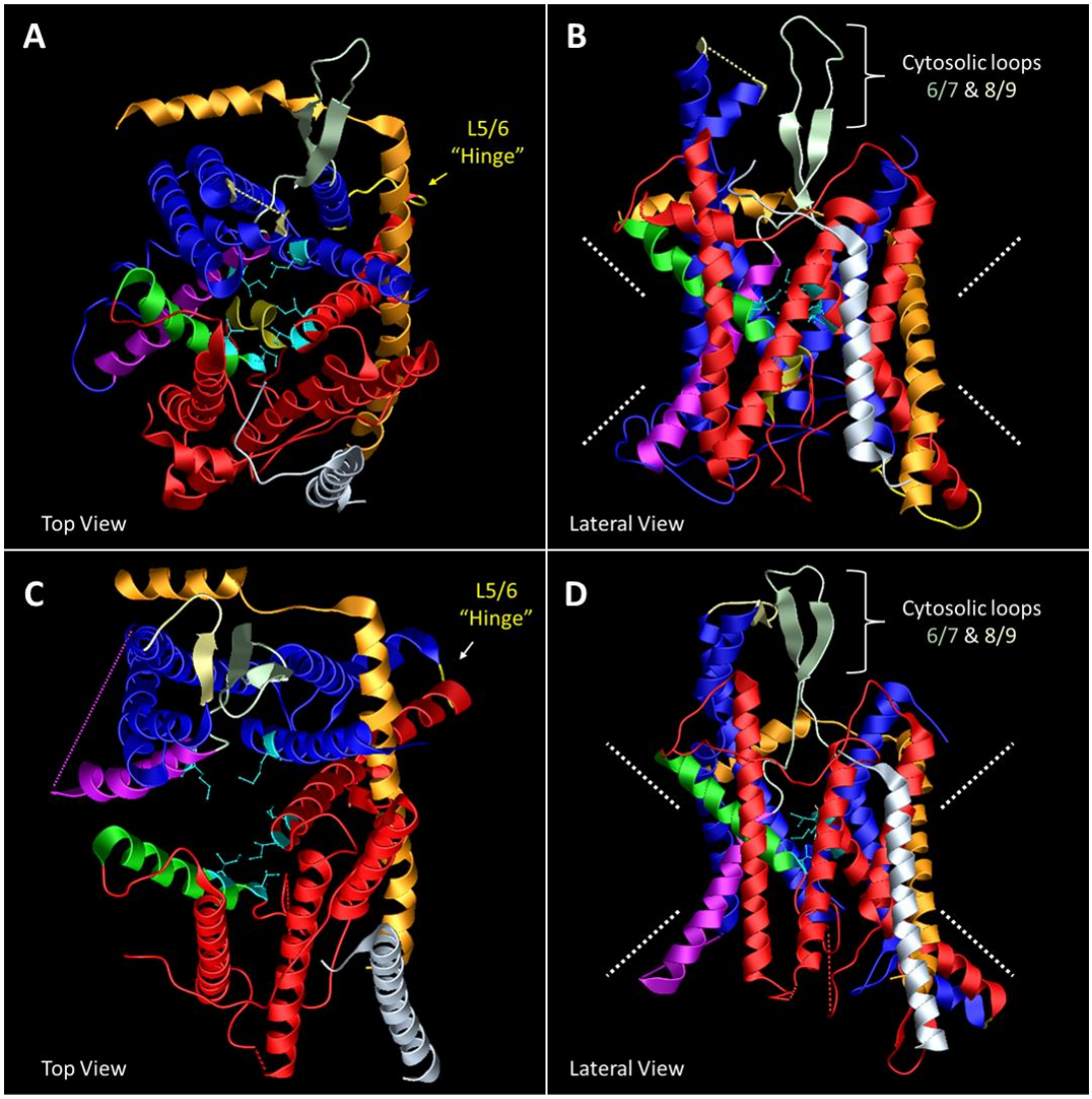
A
L5/6
"Hinge"
Top View
B
Cytosolic loops
6/7 & 8/9
Lateral View
C
L5/6
"Hinge"
Top View
D
Cytosolic loops
6/7 & 8/9
Lateral View

Fig. 1.1. Ribbon diagram of the closed archaeal and open yeast translocon apparatus. Illustration of the Sec61 crystal structure for the *Methanocaldococcus jannaschii* complex (1RH5.pdb) (21), representing a truly closed conformation, and the *Saccharomyces cerevisiae* SEC complex (6N3Q.pdb) (26) where Sec61 is engaged into the fully open conformation via interactions with Sec62/Sec63 complex (hidden in diagram). Diagrams composed using ICM-Browser software. Key structures are indicated: TM1-5 in red and green, and TM6-10 in blue and purple form the two halves of the translocon; The lateral gate is formed by the helices in purple and green; The pore ring and plug domain are highlighted in cyan and gold respectively; A "hinge" is formed by the external loop L5/6 in yellow which joins the two halves of the translocon; Cytosolic loops L6/7 and L8/9 are in pale green and pale yellow respectively. The Sbh1 subunit is shown in silver while Sss1 is depicted in orange. **(A)** Closed translocon, view looking from the cytosol inwards. The plug is central to the pore. **(B)** Lateral view of closed complex. **(C)** Open translocon, view looking from the cytosol inwards. The plug is displaced from the centre. **(D)** Lateral view of open complex. **(B,D)** Hourglass-like shape highlighted by white guidelines.

translocon is found to be critical for establishing a hydrogen bond network that stabilises the closed complex and coordinates interactions between the lateral and lumenal gates of the translocon (25). Six hydrophobic residues of Sec61 project their sidechains inwards at the approximate mid-section of the translocon. This creates a central constriction known as the pore ring and gives the complex a noticeably “hourglass-like” appearance (Fig. 1.1., B & D)(20, 21). The pore ring ultimately governs movement through the translocon and while inactive, a short helix of TM2 acts as a plug, interacting with the pore ring to seal the channel (27).

The Sbh1 and Sss1 subunits are less well characterised. Sss1 like Sec61 is an essential subunit of the translocon. Sec Sixty-one Suppressor (Sss1), as the name details, was discovered upon overexpression to supress a growth defect in a *sec61* mutant (28). An N-terminal amphipathic helix sits horizontally along the cytoplasmic face of the translocon while the C-terminus contains a transmembrane domain (TMD) that diagonally spans the Sec61 subunit and anchors Sss1 to the ER. The TM domain of Sss1 is positioned to stabilise the translocon at the opposing face to the lateral gate and has been implicated in regulating lateral access to the translocon (21, 29). The Sec61 Beta Homolog (Sbh1) is similarly anchored through a C-terminal TM domain and locates to the periphery of the translocon (21). Unlike the other two subunits, Sbh1 is only essential in higher eukaryotes, with the absence of the two yeast homologs instead resulting in only a mild TS growth phenotype (30, 31). The function of Sbh1 appears to be more regulatory with there being less reliance on this subunit for the purposes of translocation.

Eukaryotes encode for a paralog to the canonical Sec61 complex that is solely utilised for co-translational translocation, a protein trafficking pathway detailed below. In yeast this complex is referred to as the Ssh1 (Sec sixty-one homologue) while in mammals it is known as Sec61A2 (32). The Ssh1 complex comprises of three subunits. The Ssh1 subunit forms the pore and shares 34% identity with Sec61. Sbh2 is a second beta homolog with close relation to Sbh1. Interestingly, Sss1 remains present and might suggest the critical role that this subunit plays in the two complexes.

The Signal Sequence and Protein Trafficking

Currently protein sorting via the translocon is recognised to occur by one of two predominant branches, co- and post- translational translocation. These diverging pathways are described by the order of events in which trafficking of a substrate occurs in respect to translation at the ribosome. At times these terms have been synonymous with SRP-dependent and SRP-independent translocation respectively (20). These terms describe the involvement, or lack thereof in the latter case, of a highly conserved ribonucleoprotein known as the signal recognition particle (SRP) (33-35). The potential for a nascent polypeptide to interact with an SRP occurs during synthesis at the ribosome and is dependent on an amino-terminal signal sequence (36, 37). This signal sequence (SS) is common to all polypeptides destined to the ER as it is necessary for trafficking to the ER membrane and then for the priming of an active translocon (38). The signal sequence is observed to consist of a positively charged terminal region (N-region) followed by a hydrophobic core (H-region) of approximately 16-22 amino acids (aa) and finally a polar carboxy-terminus (C-region) that contains a cleavage site for recognition by a signal peptidase (Fig. 1.2., A)(38-40). The hydrophobicity of the H-region is a major determining factor in signal sequence recognition by the SRP, however, other primary peptide characteristics are also relevant and include the peptide's length and structure as well as the location of the signal sequence (38, 41-43). Initiation of translocation is dependent on successful intercalation of the signal sequence into the ER lipid bilayer, of which the N-region is critical for providing the charge that facilitates appropriate orientation at this locus (44). Furthermore, this has been in context for soluble proteins, yet these processes are reflected in TM proteins where amino-terminal transmembrane helices (TMH) share the characteristics of a signal sequence, retaining the essential function while having some structural differences (38, 45, 46). Positively charged aa residues remain important in orientating a TMH as it becomes imbedded into the lipid bilayer in accord with the established "positive inside" rule (45, 47). The location of the positively charged regions of a TMH can differ however, existing either N- or C-terminal to the H-region. TMHs are also of sufficient hydrophobicity to be recognised by an SRP and additionally lack

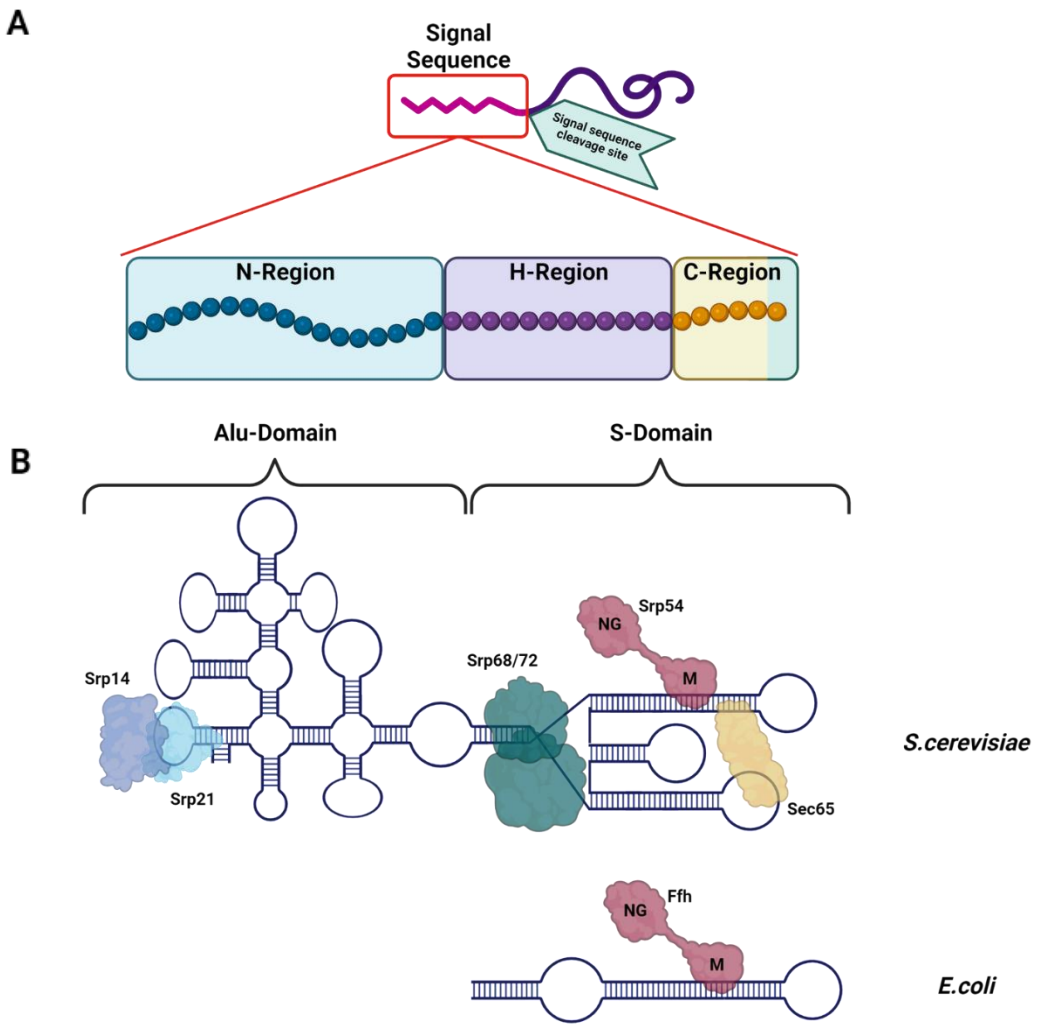

Fig. 1.2. ER Trafficking. (A) The signal sequence divided into three regions; a positively charged N-region, the H-region which consists of ~16-22 aa that form a hydrophobic core, and the polar C-region which contains the signal cleavage site that is highlighted in green. **(B)** Comparison of the yeast and bacterial SRP; Both contain the RNA S-Domain, significant in its association with the highly conserved Srp54/Ffh subunit in red. The M and NG domains are highlighted which are joined via a short linker. Yeast, as with other higher order organisms contain the Alu-domain for translation arrest. Yeast also contain additional subunits which are depicted here and critical in the stepwise assembly of SRP from the nucleus to the cytosol. Image created in BioRender.

the peptidase cleavage site of the SS as TMHs make up part of the functional protein.

Co-translational Translocation - Trafficking

While common to our understanding of protein trafficking in the current age, the existence of an aa sequence in coordinating the localisation of secretory proteins was first proposed by G. Blobel et al. In 1971 (48). This “signal hypothesis” as it is now known, would incite an insurgence in the field and later earn Blobel a Nobel prize for his work. Studies performing in vitro reconstitution assays would be the first to identify a key player, that of the mammalian SRP (49-53). A decade later, the discovery of the bacterial homologue would result in great strides in the functional characterisation of SRP due to the simplified biology and biochemical accessibility that these prokaryotic systems provide (33, 34, 54). Here, it is worth noting that significant homology is observed between these systems to such an extent that the prokaryotic machinery is capable of functionally replacing that of the eukaryotic/mammalian systems (54). An understanding of the mechanisms behind SRP functionality has not only provided comprehension for the protein targeting pathways but also for the processes that drive translocation. All of which will be described here and while a lot of the initial work in the characterisation was performed in prokaryotes I will henceforth focus on eukaryotic (yeast specific) terminology for both relevance and clarity.

Recognition of a signal sequence or TMH by SRP serves to traffic most ER proteins from the cytosol (55, 56). As previously mentioned, SRP is a ribonucleoprotein and consists of a 7S RNA molecule (4.5S RNA in prokaryotes) and six protein subunits that together make two observably distinct domains (Fig. 1.2., B) (55, 57). The Alu domain, absent in prokaryotes, is the shorter of the two and forms an elongated kinked structure that functions in translational arrest at the ribosome (58). The S-domain however is critical in the association it has with the universally conserved Srp54 subunit (Ffh in prokaryotes as the sole subunit) (55, 59). The C-terminal methionine rich domain (M-domain) of Srp54 anchors the subunit proximal to the

7S RNA and juxtaposed to a conserved tetraloop (60-62). A flexible linker extends from the M domain creating a junction to the remainder of Srp54 which consists of an N-terminal four helix bundle (N-domain) and a unique GTPase domain (G-domain) (63-65). The N- and G- domains are coupled in both Structure and function forming the NG-domain where nucleotide dependent dimerisation provides enzymatic activity (66, 67).

The SRP Receptor (SR) is a heterodimeric protein complex (SRα and SRβ) that localises to the ER. The Soluble SRα component possess an NG domain with high homology to that found in SRP (66, 67). Dimerisation between these shared domains supports the interaction between SRP and SR (SRP•SRα heterodimer) and further enables GTP hydrolysis. SRβ is a TM protein that associates with SRα through an X-domain present in the later hence causing SRα to be tethered to the ER membrane (68, 69). A GTPase domain in SRβ permits this association when bound with GTP (68).

With the key drivers now defined; SRP dependent translocation can be described as a series of stepwise conformational changes that accommodate a viable substrate on its passage to the ER membrane (Fig. 1.3.). Critical in the initiation of SRP-dependent translocation is the availability of an appropriate SS within a nascent polypeptide for the purposes of recognition by SRP. The key characteristics that facilitate this recognition have been already described yet the importance in the hydrophobicity of the H-region cannot be understated. The M-domain of Srp54 provides a hydrophobic groove to accommodate the H-region of the SS. The ability of the M-domain to recognise a diverse array of substrates is established through the enrichment of methionine residues. This phenomenon is explained by the recognised “methionine bristle” hypothesis whereby the side chains of methionine, while contributing to the hydrophobicity of the binding groove, also provide adequate plasticity (34, 70).

Recognition of a SS by a SRP occurs at the ribosome during translation of the nascent chain, forming the ribosome nascent chain complex (RNC). While SRP binding was first thought to occur as the nascent chain emerges from the ribosomal exit tunnel (RET), recent findings have demonstrated SRP to bind a ribosome with

80-100nM affinity as early as the nascent chain first enters the RET and in complete disregard of an appropriate SS (71-73). This event results in the first conformational change to occur in SRP, where the NG- and M-domain of Srp54 congregate to the RET (74-77). Specifically, the NG-domain in the “proximal” position makes contact with Rpl25 and Rpl35 while the M-domain is in contact with Rpl17 (58, 78-80). These specific Ribosomal Proteins of the Large subunit or RPL elements are part of the structure that forms a ring around the RET and also constitutes the sites at which the ribosome will contact the Sec61 translocon, suggesting competitive binding at this site.

The RET can house ~40-70 aa whereas substrate that extend greater than ~140 aa become inviable for recognition by SRP, this in conjunction with the relatively low stoichiometric abundance of SRP in the cytosol demonstrates the need for SRP to survey ribosomes (81-84) (Fig. 1.3., [2]). SRP bound RNC are placed into a standby phase as the SRP awaits the incoming nascent chain to ensure efficient targeting of substrate proteins (73, 74, 76). Incorrect cargo at the RNC drives disassembly of SRP so it may cycle between various ribosomes in search of a recognisable SS (73). In the event of a SS being recognised, further conformational changes take place in the SRP, increasing binding affinity 100-fold to an approximate 1nM affinity (71, 73, 77) (Fig. 1.3., [3]). Additionally, the highly structured Alu domain of SRP repositions into direct interference with the ribosomal binding site that catalyses tRNA translocation via elongation factor-2 and hence imparts translational arrest (58). The need for this inhibitory event in eukaryotic cells is in stark contrast to prokaryotes where it is absent and might reflect the grandeur scale at which these systems operate on.

The now quiescent RNC forms a high affinity targeting complex with SRP that finds itself locating to the SR at the ER membrane via the desired dimerisation of the collective NG-domains (84, 85) (Fig. 1.3., [4]). At this stage the ribosome has paused any further rearrangements from occurring at SRP as to remain competent for translocation (86). The presence of the anionic lipids, abundant at the ER membrane, has been observed to begin relieving this ribosomal pausing (87). Thought to aid in this event, the ribosome now at the SR will activate hydrolysis of

the GTP bound SRβ (88), resulting in dissociation of the SRα component. Occurring in tandem, the SRP•SRα heterodimer facilitates the detachment of the "proximal" NG-domain at the RET. Now mobile, the SRP•SRα heterodimer relocates "distally" to the SRP RNA (78, 89, 90). At this stage, crosslinking analysis has demonstrated the RNC remains associated with the now GDP bound SRβ (91) and with the NG-domain of SRP repositioned away from the RET this complex is primed for ribosomal handover to the translocon machinery (84, 90, 92) (Fig. 1.3., [5]). As the translocon associates with this oligomeric complex it is found to positively regulate the complete association of the SRP•SRα heterodimer into an active form for GTP hydrolysis that is also stimulated by the distal RNA (93) (Fig. 1.3., [6]). In the GDP bound state, SRP and SRα dissociate from each and are to be recycled for subsequent rounds of targeting (Fig. 1.3., [7]). Furthermore, Sbh1 has been demonstrated to serve as a nucleotide exchange factor (NEF) for SRβ resetting the subunit to be rebound with GTP and allowing it to reassociate with SRα (55).

Co-translational Translocation – Channel Interactions

Contact between the RNC and the translocon begins a cascading series of conformational changes that take the translocon from the inactive state to a status befitting the ability to accommodate protein translocation. The translocon lies within the ER membrane and therefore positioned to a junction that separates the distinct functional environments of the cytosol and ER lumen. As such a coordinated approach is necessary in facilitating protein translocation while maintaining the integrity of the ER membrane. The formation of the RNC-translocon oligomer is seen as the binding of an interacting partner which is this first step in the translocon entering a primed state capable of receiving a SS into the pore region. Cytosolic loops L6/7 and L8/9 extend from the translocon to associate with the ribosome at the common binding loci of RPL25 and RPL35 (Fig. 1.1., B & D) (94, 95). This interaction locks the translocon associated helices in place as a rotation is triggered in the rest of the complex. An asymmetrical repositioning in the structure of ~22° allows the cytosolic face to remain relatively unperturbed (19). At the

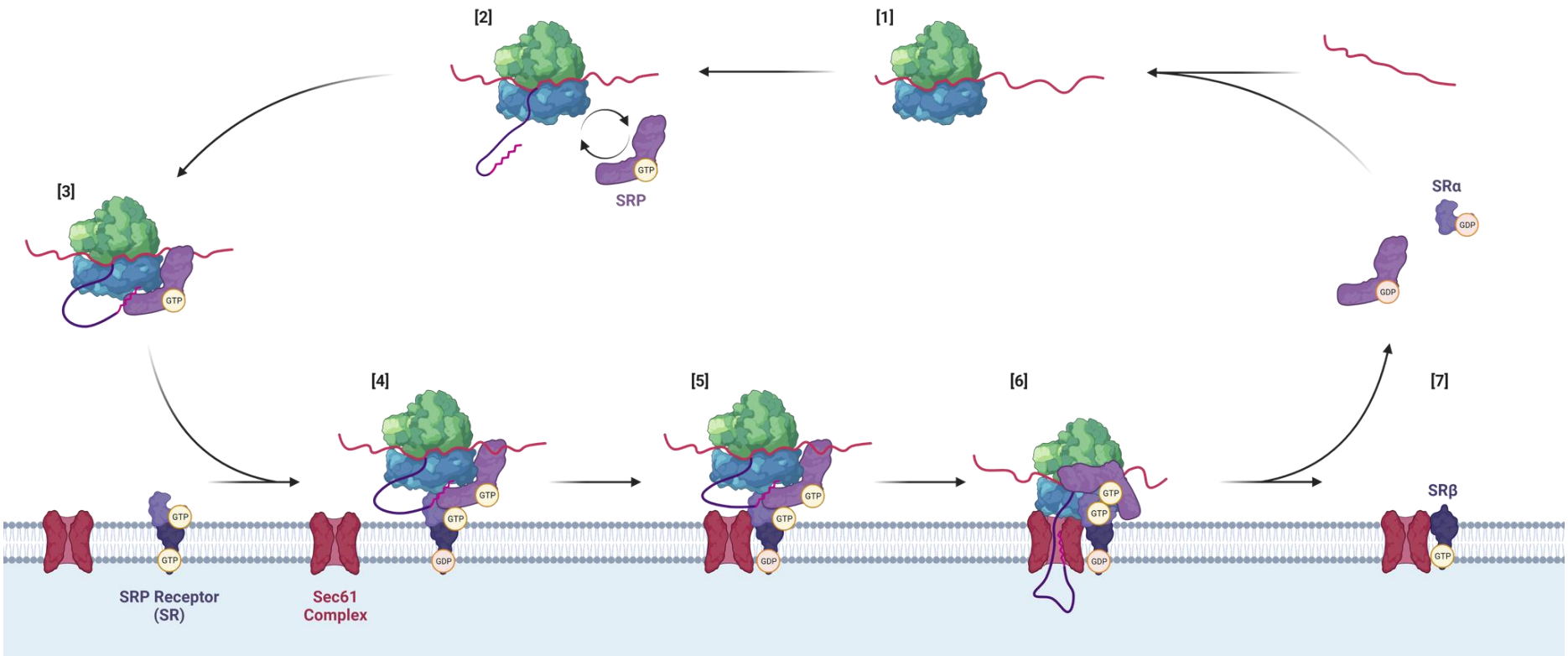
[1]
[2]
[3]
[4]
[5]
[6]
[7]
SRP
GTP
SRα
GDP
SRβ
SRP Receptor
(SR)
Sec61
Complex

Fig. 1.3. Stepwise guide to co-translational translocation. [1] Translation is initiated at the ribosome. **[2]** GTP bound SRP scans ribosomes with a bound SRP undergoing conformation changes that places the NG- and M-domains of Srp54 at the RET as it awaits the peptide. **[3]** A recognisable SS initiates the formation of a high affinity targeting complex which is directed to SR at the ER, translation is inhibited. **[4]** Now associated with SR, the ribosome facilitates hydrolysis of the GTP bound SRβ which allows the SRP•SRα heterodimer to move distally along the RNA. **[5]** The NG domain of SRP are now positioned away from the RET priming the complex for ribosomal handover to the translocon, reinitiating translation to drive translocation. **[6]** Association with the translocon regulates the complete association of the SRP•SRα heterodimer into an active form for GTP hydrolysis that is also stimulated by the distal RNA. **[7]** In the GDP bound State, SRP and SRα dissociate from each and are to be recycled for subsequent rounds of targeting, while SRβ is reset to a GTP bound state which is thought to occur via association with Sbh1 of the translocon. while several residues of the pore ring associate closely with TM2 to create a hydrophobic patch (19, 21). Image created in BioRender.

lumenal face however, the lateral gate is “cracked” to create a point of access to the lipid bilayer between helices TM2 and TM7 (19). The pore ring is also supplanted from the centre of the translocon at this time, initiating the displacement of the plug domain. The translocon is now primed to receive the SS/TMH of the nascent polypeptide. The determined hydrophobicity of the SS/TMH is relevant in drawing the peptide past the mostly hydrophilic external regions of the primed translocon and into the aqueous pore where the plug domain was previously situated (19). As the nascent polypeptide enters the channel the positively charged residues of the SS/TMH are attracted to the negatively charged head groups of the phospholipids that constitute the ER membrane (20, 96). The charged region is therefore retained in the cytosol resulting in ~45° kink to form in the polypeptide, bringing about looped insertion (20, 97). Attractive forces between the H-region of the SS/TMH and the hydrophobic patch, formed between non-polar residues of the lateral gate and pore ring, positions the SS/TMH adjacent TM2 at the “crack” in the lateral gate. This position allows the SS/TMH to intercalate into the accessible lipid bilayer and in doing so, further disrupts the lateral gate. The loop between TM5 and TM6 of the translocon act as a hinge at the opposing face which is further stabilised by interactions with Sss1 (19). As the lateral gate is fully extended, stability at the hinge results in unilateral opening at the translocon and secures the open conformation. Brownian motion allows for the random movement of the nascent polypeptide at the channel yet with SRP now dissociated from the ribosome, translation can provide direction (20, 21, 98). These forces provide the drive for unidirectional movement of the polypeptide into the ER lumen while the looped insertion of the peptide at ~45° prevents the possibility of self-interaction (20, 97).

Co-translational Translocation – Alternative Targeting

Despite the essential need for co-translational translocation, loss of SRP in *Saccharomyces cerevisiae* does not represent a lethal phenotype, instead presenting with cellular growth defects and an extended ER (35, 99). This poses the existence of alternative pathways to SRP that facilitate the transport of co-

translational substrates. Recently such a pathway has been described in yeast as a co-translational targeting mechanism occurring independent of SRP and hence known as the SRP-independent (SND) pathway (Fig. 1.4.) (100, 101). To this date only a single homologue, that of hSND2, has been identified in mammals. This pathway operates on a conceptual basis, quite similarly to that involving SRP where a cytosolic component (SND1) binds a translating ribosome to form a complex directed to a membrane bound heterodimer (SND2 & SND3) at the ER. The SND pathway operates in parallel to alternative targeting pathways, preferentially recognising substrate with TMHs relatively intermedial to those found at N- or C-termini.

Synthetic genetic interaction screens propose the SND pathway can also accommodate substrate that are trafficked by the SRP-dependent and GET pathways (100, 102). This interaction with the later pathway is particularly interesting as substrate to the GET pathway are usually translocated via an alternative GET complex, owing to the pathway's namesake. The guided entry of tail anchored protein (GET) pathway is involved in the translocation of proteins that contain a single C-terminally located TMH, otherwise known as tail anchored (TA) proteins and includes the Sbh1 and Sss1 subunits of the translocon (Fig. 1.4.) (103). Despite the specialised utility among each of these pathways an overlap is observed between the various schools of substrate that they traffic (104). This demonstrates a level of redundancy that may exist as a compensatory mechanism to relive substrate burden. The GET pathway also functions post translationally and may speak to conditional exchanges that could occur between the two broader branches of translocation.

Post-translational Translocation

A subset of polypeptides that are translated to completion in the cytoplasm are targeted to the ER as they still present with an appropriate SS/TMH. Due to the nature of these proteins, they have managed to evade SRP recognition at the ribosome and therefore must proceed by post-translational translocation (Fig. 1.4.).

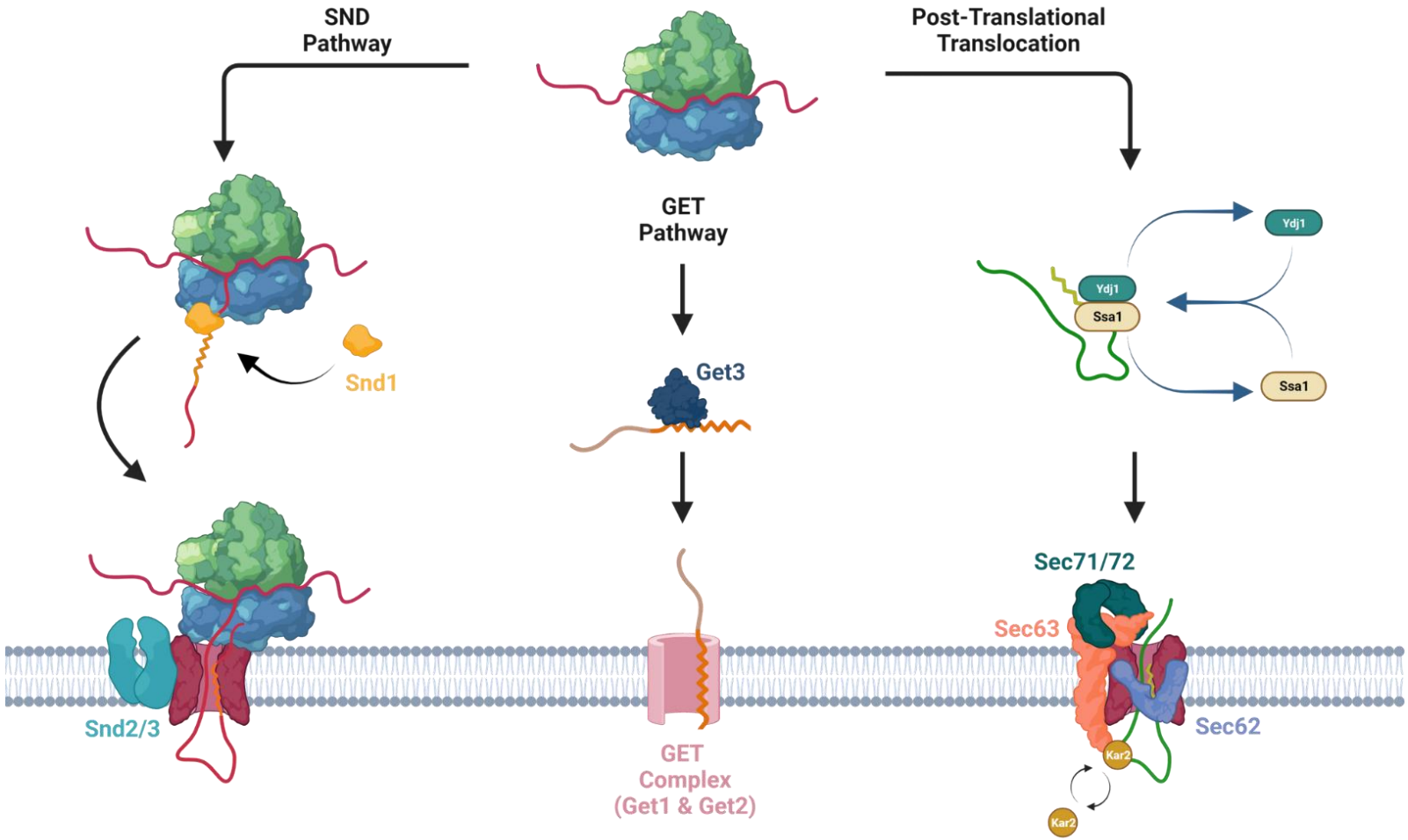
SND
Pathway
Post-Translational
Translocation
GET
Pathway
Snd1
Get3
Ydj1
Ydj1
Ssa1
Ssa1
Sec71/72
Sec63
Snd2/3
GET
Complex
(Get1 & Get2)
Sec62
Kar2
Kar2

Fig. 1.4. SRP-independent translocation. The SND pathway involves Snd1 binding to a translating ribosome and forming a complex directed to the membrane bound heterodimer of Snd2/3 at the ER. The SND pathway has a preference for centrally located TMHs bring substrate to the Sec61 translocon. The GET pathway is designed for the trafficking of TA proteins. Get1 and Get2 form the translocating complex with substrate targeted via Get3. Smaller peptides or those with only a moderately hydrophobic SS are directed via post-translational translocation. Substrate to this pathway are fully synthesised in the cytosol yet remain competent for translocation though the continual binding of HSP proteins, depicted here as the yeast proteins Ssa1 and Ydj1. The heptameric SEC complex consists of the Sec61 complex in addition to Sec62,63,71 and 72 which translocate substrate via a ratcheting mechanism with Kar2. Image created in BioRender.

Several occurrences can lead to this outcome, TA proteins for example contain a C-Terminal TMH and therefore are fully synthesised before their hydrophobic domain can engage an SRP (105). Smaller soluble proteins, namely pre-proteins (~<160 aa in length i.e. Pre-Pro-insulin) are shielded from SRP within the RET which can house an approximate ~40-70 aa (81, 106, 107). Even if large enough to emerge from the RET, post-translational substrates have only moderate hydrophobicity in their SS and are therefore incapable of efficiently engaging with an SRP (108).

Post translational translocation is an energy demanding process driven by nucleotide hydrolysis through the involvement of the 70kDa family of heat shock proteins (HSP70) at both substrate targeting and translocation (109, 110). This molecular chaperone is functionally characterised through two distinct domains that constitute of an N-terminal nucleotide binding domain (NBD) with weak ATPase activity which regulates the adjoined substrate binding domain (SBD). The bound nucleotide dictates the conformational related functions, with ATP bound HSP70 observed to have fast binding and release of substrate, while the ADP bound form slows these two processes (111-115). This approach to substrate binding is coordinated through interactions with a specialised family of co-chaperones that are characterised by the presence of a highly conserved J-domain (J-domain protein, JDP) (116). HSP70s bind at the J-domain which expedites activity at the NBD for efficient hydrolysis (117).

Post-translational polypeptides are fully synthesised in the cytosol where they are engaged by these two families of molecular chaperones to ensure translocation competency. The 40kDa family of Heat shock proteins (HSP40) are JDPs which recognise misfolded/unfolded polypeptides that are subsequently escorted to the HSP70. In the ATP bound state, HSP70 binds readily at exposed hydrophobic regions of the polypeptide where HSP40 induced hydrolysis facilitates the conversion into an ADP bound state with slowed substrate release (111, 118, 119). This is a cycled reaction with repeated substrate binding and release being critical in polypeptides gaining correct conformational status and preventing both the formation of protein aggregates and recognition by cytosolic proteasomes.

At the ER membrane the heterotrimeric translocon complex associates with a tetramer of accessory proteins that collectively form the heptameric SEC complex for post-translation translocation. The tetramer introduces the subunits Sec62, Sec63, Sec71 and Sec72 for the purposes of protein trafficking and priming the translocon for engagement with a polypeptide (120, 121). Sec63 makes extensive interactions with the translocon subunits and is the foundation by which the other accessory subunits associate, so that they too may facilitate interactions with the translocon machinery (26). Positioned at the back face of the translocon opposing the lateral gate, Sec63 has three TM domains that contact TM1 and TM5 of the Sec61 subunit as well as the TMs of both Sbh1 and Sss1 (26, 122). A prominent cytosolic tail at the C-terminal region of Sec63 contains the FN3 (Brl) domain which interacts with the L6/7 of Sec61 (26). This interaction interferes with the ability of the ribosome to bind to this loop; hence the ribosome cannot bind to the SEC complex.

Sec71 and Sec72 appear to be fungal specific with no human homologs as yet identified. Despite this, characterisation of Sec71/72 has elucidated the mechanisms for trafficking post-translational substrate to the ER. A tetratricopeptide repeat (TPR) in Sec72 creates a structural motif that provides the means by which an unfolded polypeptide bound by HSPs 40 & 70 will targeted to the ER (123). For context, the yeast proteins Ydj1 and Ssa1 are found in the roles of the cytosolic HSP40 and HSP70 respectively (124). As described previously these cytosolic chaperones will be involved in cycles of substrate binding and release, keeping the unfolded polypeptide competent for translocation, until binding of Ssa1 to the TPR domain of Sec72 through an acidic C-terminal tail (123). Sec72 is a peripheral membrane protein that is tethered to the ER by association with Sec71, a TM protein with a single membrane spanning domain at its N-terminus (125, 126). The Sec71/72 dimer clamps Sec63 at the FN3 domain positioned above the cytosolic face to the translocon channel (26, 127). This positioning is such that a tilt resulting from the spatial arrangement of Sec63/71/72 allows for the substrate peptide to be inserted straight into the translocon channel. Trafficking of polypeptides via Ssa1 is non-discriminatory however, as Ssa1 has also been

observed to traffic protein to the mitochondria via a similar mechanism with Tom70 (8, 128). Targeting specificity likely involves transient associations of Ssa1 with membrane bound channels that are stabilised when an appropriate signal is presented. These transient associations, however, could suffer from the relatively lower hydrophobicity that presents in the SS/TMH of post-translational substrates, as they would be met with a greater barrier of entry at the translocon. These shortcomings can be overcome with timely recruitment of the polypeptide into the translocon channel where interactions between Sec62/63 subunits and the translocon promote efficiency through a pre-opening of the channel (127, 129).

Much in the same as the interactions with the ribosome during co translational translocation, Sec62/63 cooperate as the interacting binding partner that initiates conformation changes in the translocon. The points of contact between Sec63 and the Sec61 subunit facilitate the initial “crack” in the lateral gate (130). Sec62 arrives at the translocon associated to Sec63 where a basic cluster at the N-terminus of Sec62 binds an acidic stretch of aa at the extreme C-terminus of Sec63 (131, 132). Sec62 contains two TM domains that arrange at the translocon in a V shape and positions the conjoining lumenal loop (L1/2) at the lateral gate (127). Localisation of Sec62 to the lateral gate has been associated with a rotation in TM7 and TM8 of the Sec61 subunit, causing further opening of the lateral gate and displacement of the plug domain (127). At this point the translocon is primed for substrate insertion. Sec62 is important at this stage for establishing protein topology as it has been found to establish the correct orientation of the incoming SS/TMH. Translocation proceeds in “ratcheting” process where Brownian motion again provides the passive movement of the polypeptide through the channel (133). However, lacking the translating ribosome, the process requires unidirectional moderation. The lumenal loop L2/3 of Sec63 contains a J domain that locates through an aperture between TM5 of Sec61 and the TM of Sss1 to the lumenal exit of the translocon (26). The J domain of Sec63 recruits an ER lumenal HSP70 chaperone protein known as Kar2p (BiP; the mammalian homolog). ATP bound Kar2 undergoes hydrolysis on association with Sec63, facilitating attachment of the ADP bound Kar2 to the translocating polypeptide. This is a continuous process whereby additional

molecules of Kar2 will subsequently bind, preventing the backflow of the polypeptide (133). Once translocated, NEFs in the lumen of the ER promote the dissociation of Kar2 from the polypeptide (133, 134).

Post-translational Modifications

Establishment of the 3D conformation of a protein is obligatory in maturation and ultimately, expression as a functional component of the proteome. Protein folding is a dynamic process that can be influenced by modification at specific aa residues following synthesis. These post-translational modifications (PTM) are diversified by the regions they function in as much as the nature of the modification itself, with certain PTMs demonstrating region specificity. The ER is no exception with several unique components initiating PTMs that include proteolytic cleavage, disulfide bond formation, glycosylation, and chaperone activity (Fig. 1.5.) (135, 136). Often considered to be the earliest modification to certain ER localised protein is the cleavage of the SS. The timing of SS cleavage is protein dependent yet regularly occurs during the translocation process (135, 137, 138). Lipid partitioning facilitates the SS to leave from its position at the lateral gate and diffuse away from the translocation machinery. At this time the once inaccessible SS is said to become extended at the polar C-region exposing the cleavage site for recognition by a signal peptidase (20, 135, 139). The SS is critical in protein localisation, establishing topology and can even influence folding and modification events; yet cleavage is necessary for the release of these proteins into ER lumen (135).

N-linked glycosylation is another PTM that can occur alongside protein translocation. The multimeric Oligosaccharide transferase (OST) complex associates with the translocon to permit the attachment of a core glycan to newly synthesised proteins (140, 141). Specifically, the presence of an acceptor sequence Asn-Xaa-Ser/Thr (where Xaa can be any aa expect for a proline and or aspartic acid) dictates the transfer of the membrane bound glycan from a lipid-linked dolichol pyrophosphate donor to the side chain amide group of the asparagine residue

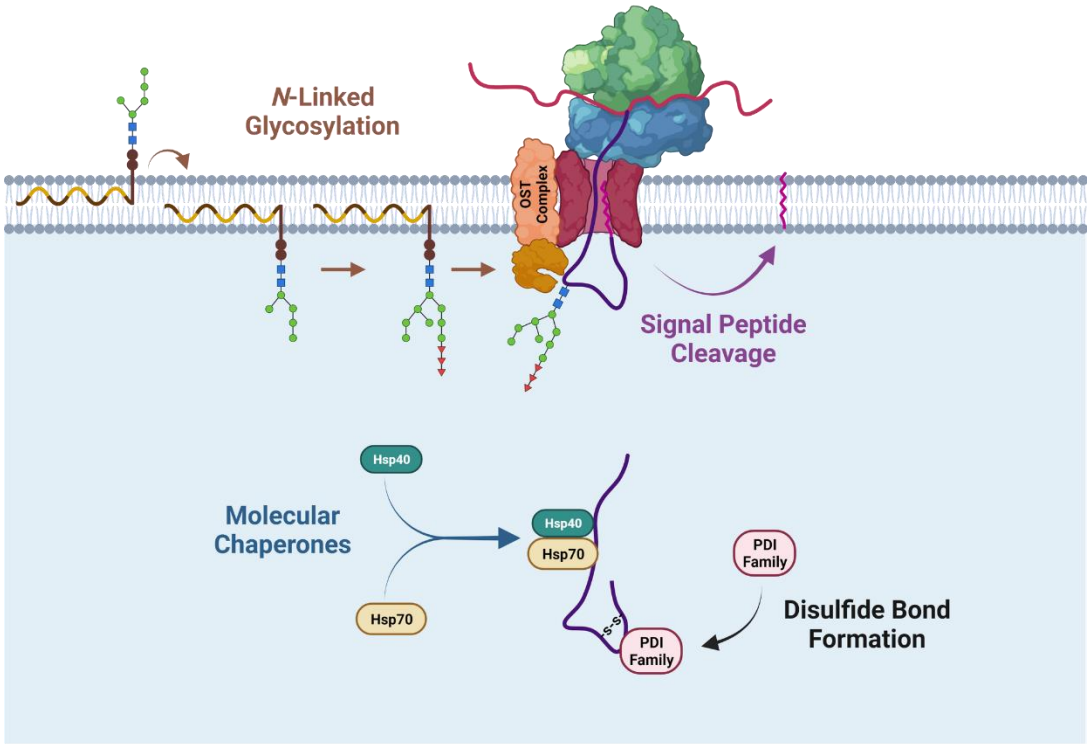

Fig. 1.5. Post translational modifications (PTM). The predominant PTM that take place at the ER include: The attachment of a glycan core through N-linked glycosylation via the OST complex; Cleavage of the SS from the translocated peptide by signal peptidase; Molecular chaperones for foldase and holdase activity which includes the action of HSPs 40 and 70 depicted here, binding to exposed hydrophobic regions to prevent aggregation; Formation of disulfide bonds facilitated via the activity of the PDI family of enzymes as well as the oxidising capacity of the ER lumen. Image created in BioRender.

(142, 143). The inclusion of glycoproteins is beneficial in enhancing the intrinsic physiochemical properties of the cellular proteome, permitting an enhanced rate of folding, greater thermodynamic stability, and a decreased propensity for forming aggregates (135, 136).

Molecular chaperones are a family of proteins that include the likes of HSPs 40 & 70. Chaperones are observed to complex with unfolded proteins as only intermediates to the native conformation, as they do not present in the final functional structure (144, 145). The various functions of chaperones include holdase and foldase activity which comes at a high energetic cost to cells as their functional cycle involves the hydrolysis of ATP. These functions are essential to keep proteins competent however, as they would otherwise become misfolded and targeted for degradation (135, 136).

Redox greatly contributes to the cellular homeostasis and is established by a ratio of reducing to oxidising agents. Glutathione presents as a major organic buffer for redox, existing in either reduced (GSH) or oxidised (GSSG) states. Initial studies investigating ER redox proposed a ratio of GSH to GSSG of 1:1 to 3:1 (146). These reports, in comparison to overall cellular ratios of 30:1 to 100:1, found that the ER harbours an environment which could be anywhere between 10-100 times more oxidative than that of the whole cell. These experiments into cellular redox were later proposed to be confounded by contamination from exogenous sources of oxygen and may explain the magnitude of difference in which these values exist between (147). More recent work has utilised fluorescent redox probes that can be targeted to cellular compartments to specifically gauge redox potential (Voltage; V) (148-151). Much in the same way that pH is a measure of free hydrogen ions, voltage is used as a readout for redox potential through the measure of free electrons. A more positive redox potential is representative of an analytes greater propensity to gain electrons, or more simply, as having a greater oxidising capability. Utilising the fluorescent redox reporters in yeast demonstrated the oxidising capacity of the ER with a redox potential of ~-208 mV, relative to ~-320 mV that was described in the cytosol (148-150).

A key rate limiting step in protein folding is the formation of a covalent bond between the thiol groups of two separate cysteine residues, otherwise known as a disulfide bond. Most secretory proteins will contain a disulfide bond to stabilise folds, restricting the conformational dynamics of the protein as it assumes a tertiary or even quaternary structure (152). A balanced redox poise is necessary for correct bond formation with oxidising conditions driving the enzymatic pathways in disulfide bond formation, while corrective mechanisms require significant reducing power in the advent of aberrant folding (152-154). The cytosol is a hive for GSH production and glutathione reductase activity and therefore maintains a high ratio of GSH to GSSG (152, 155). These conditions are inappropriate for establishing the oxidising requirement of disulfide bond production and as such this role is appropriated by the ER.

Disulfide bond formation is best described by the activity of two ER resident enzymes, Protein disulfide isomerase (PDI) and ER oxidoreductin 1 (Ero1). As an unfolded protein enters the ER, the close positioning of two cysteine side chains can permit coupling through the catalytic action of PDI (152, 156). However, to facilitate the formation of a disulfide bond, the internal pH must be sufficient to prompt deprotonation at the cysteine side chain, converting the thiol group to a reactive thiolate ion (151, 157). Catalysis by PDI then begins with a nucleophilic attack from the thiolate ion (152, 158). The PDI family of enzymes are characterised by the presence of a Cys-Xaa-Xaa-Cys thioredoxin-like motif within their catalytic domain. Oxidised PDI forms a disulfide bond between the cysteines that comprise thioredoxin-like motif (136, 159). The nucleophilic attack by thiolate resolves with an S_N2 reaction, reforming the disulfide bond to one existing between the cysteines of PDI and the substrate protein (152, 158). At this stage PDI has formed a mixed disulfide intermediate with the substrate protein whereby the activity of PDI donates the disulfide bond to the substrate, stabilising the protein fold and PDI becoming reduced in the process. PDI can be reutilised for further rounds of bond formation by reoxidation (160). Ero1 is a flavoprotein characterised by an association with the cofactor flavin adenine dinucleotide (FAD) and catalyses the restoration of PDI by the transfer of the electrons to itself (160, 161). FAD

subsequently promotes Ero1 catalysed oxidation which results in the electrons being dispensed to molecular oxygen, forming the reactive oxygen species H_2O_2 (136, 161).

Disulfide bond formation is ubiquitous to the ER and can occur even as the polypeptide is being translocated. Due to the low discriminatory nature of these modifications, cysteines are prone to mispairing and impact the early stages of folding (162, 163). Reduced PDI can resolve non-native structures, performing complementary to its oxidative state. This characterises the isomerase activity of PDI where the non-native bonds will be dissolved in favour of the correct disulfide bond that constitute part of the native structure (164).

Cells are unable to synthesise GSH in the ER lumen, instead GSH is imported into this organelle from the cytosol (165). Lumenal supply of GSH plays important regulatory roles in disulfide bond formation which extends to influences on overall ER homeostasis. GSH can attach at the thiol side chain of a cysteine residue in what is known as S-Glutathionylation. This PTM occurs ~0.1% of the time during normal growth conditions, increasing to ~15% in the result of oxidative stress and thought to protect protein thiols from irreversible over oxidation (151, 166). GSH is also utilised by a ubiquitous family of proteins known as Glutaredoxins (GRX). Enzymes of the GRX family demonstrate thioltransferase activity and perform a similar task to that of reduced PDI, as they reduce non-native disulfide bonds in substate proteins through the oxidation of GSH to GSSG (167, 168). Furthermore, GSH can act as a nucleophile and therefore competes with substrate for oxidation. In doing so GSH facilitates the reduction of PDI and therefore indirectly resolves protein misfolding (169, 170). Interestingly, these previous two outcomes also implicate GSH in promoting ER oxidation as it is converted to GSSG.

Accumulation of H_2O_2 from the intrinsic activity of Ero1 results in the detrimental hyperoxidation of the ER lumen. As such Ero1 must be regulated; a negative feedback loop under increasingly oxidising conditions leads to the formation of disulfide bonds at regulatory cysteines in Ero1, inhibiting activity and by association, the production of H_2O_2 (151, 171). The feedback loop is interrupted by the influx of GSH to the ER which reduces PDI and in turn Ero1, reinitiating the cycle and

establishing ER oxidation. Intuitively, GSH influx is also regulated under oxidising conditions to ensure it does not pre-emptively override the Ero1 feedback loop. Oxidation of the HSP70, Kar2, results in the chaperone interacting at the lumenal face of the translocon, inhibiting GSH import (165). This begins to speak to the translocons ability to influence ER homeostasis.

ER Homeostasis and The Translocon

Internal concentrations of metabolites control cellular function as they represent the underlying components to metabolism. This in turn determines enzyme binding site occupancy and the thermodynamics of metabolic reactions (172-174). Metabolite levels are usually tightly maintained at an optimal range yet display tolerance to accommodate the viability of organisms under changing conditions (175-177). Large scale adjustments are usually directed through the utilisation of active transporters, whereas the fundamental distribution of concentrates to an optimal range is established by a controlled flux (172).

The regulation of glutathione for maintaining the homeostatic redox status of the ER has already been discussed, yet the distribution of divalent cations between the ER lumen and cytosol is equally regulated. The broad functions to which these ions contribute include, cellular signalling, regulating molecular chaperones and establishing enzymatic activity. Magnesium (Mg^{2+}) for example is an important cofactor for several enzymes including ATPases and protein kinases (178). ER lumenal Mg^{2+} on the other hand is crucial for the functioning of mammalian MAGT1, the human ortholog to the Ost3 & Ost6 subunits of the yeast OST complex, and as such can indirectly regulate N-linked glycosylation (179-181). Manganese (Mn^{2+}) is an equally important cofactor to various enzymes. For instance, supply of Mn^{2+} impacts the sterol biosynthetic pathway, with cytosolic increases in Mn^{2+} upregulating the activity of farnesyl pyrophosphate (FPP) synthetase in the production of squalene, an intermediate to sterol (182). Finally, calcium (Ca^{2+}) and zinc (Zn^{2+}) ions are crucial cell signalling molecules that can be disseminated to numerous membrane receptors, transporters, and channels. Association of Ca^{2+} or

Zn^{2+} at these sites controls the regulation of upstream cellular processes which include gene transcription, exocytosis, proliferation, and the induction of apoptosis (183, 184).

It wasn't until recently that the true involvement of the translocon in regulating metabolite flux across the ER was revealed. Regarded as one of the largest membranous pores of the ER, the translocon can reach an observed diameter of approximately 40-60Å when open through ribosomal binding. Integrity at the ER membrane however, is maintained with the translocon in the inactive state presenting with a smaller diameter of 9–15Å (185, 186). Still, the nature in which the translocon can open to facilitate the translocation of polypeptide while maintaining ER homeostasis has been under much study. Taking advantage of the immediate effects of certain antibiotics and the conductance of analytes has allowed researchers to characterise not only the ability of molecules to cross through the translocon but the stages at which it is facilitated to do so.

Puromycin is an antibiotic that is highly selective at inhibiting translation through releasing the nascent polypeptide from the translocon and was used to first characterise the passage of small molecules via the translocon (187). Only following treatment with puromycin would a small, neutral dye; methylumbelliferyl α-D-glucopyranoside (4MαG) make its way into the ER lumen. There, association with α-glucosidase II would trigger activity in 4MαG which could be measured (188, 189). The requirement for puromycin in this process would leave the group surmising that a translationally inactive, ribosome-bound translocon could allow a flux yet the biological relevance was not alluded to. Furthermore, this work implicated the polypeptide in facilitating the integrity of the translocon during active translocation. True enough, a gasket like seal is observed to form between the pore ring side chains that contact the polypeptide as it transitions through the aqueous pore, preventing any flux from taking place (21, 190).

The use of puromycin was later applied to the assessment of Ca^{2+} across the ER in mouse pancreatic acinar cells. It was hypothesised that not unlike the dye, Ca^{2+} could cross the ER membrane by way of the translocon. In agreement with the initial predication, Ca^{2+} was found to be depleted from the ER after treatment with

puromycin (191). To collaborate that this was an outcome of flux through an inactive, ribosome-bound translocon another translational inhibitor, Anisomycin, was used. Anisomycin inhibits peptide elongation and therefore impacts upon the action from puromycin by preventing stabilisation of ribosomal bound translocons (192-194). The biological utility of the observed flux of Ca^{2+} across the translocon was later inferred to be necessary in cytosolic Ca^{2+} signalling and preventing Ca^{2+} overload (193, 194).

It is now evident that the translocon can facilitate the diffusion of molecules across the ER. But to what extent and at what stage in the translocons functional cycle does this occur? The puromycin experiments revealed that an actively translocating ribosome would interfere with the capacity to facilitate flux, ruling this state out. Even if you dismiss the established requirement of a bound ribosome; the closed lateral gate, localisation of the plug domain to the pore ring, as well as interactions from external factors such as Kar2, all collectively exclude any potential involvement of an inactive translocon in facilitating flux (186, 190). Some studies have found that a point of flux exists as the ribosome first docks to the translocon. This interaction initiates the conformational changes that “crack” the lateral gate, yet before the insertion of the polypeptide into the channel, the translocon is allowed to “breathe” which presents as a release of metabolites (97, 195). Even still, it wasn’t until work aiming to characterise the import of GSH, that the full extent by which facilitated diffusion occurs at the translocon could be demonstrated. Toledano and colleagues (165) would find that following translocation and departure of the polypeptide from the translocon, an idle ribosome will remain attached. A translocon bound by the idle ribosome remains open but is unburdened by substrate and so the facilitated diffusion of GSH into the ER lumen was observed. This introduced a third functional state to the translocon, one that operates outside of protein transport and instead contributes to cellular homeostasis through the facilitated diffusion of metabolites.

Dysregulation and the Activation of UPR

Eukaryotic organisms are dependent on the production and organisation of complex hetero-oligomeric proteins through ER function. The ER meets this demand with highly regulated systems for protein modification and delivery established by its unique lumenal environment. These systems are sensitive to dyshomeostasis and therefore justifying the stringent regulation placed on maintaining equilibrium. The merit of protein standard is determined during maturation with only properly folded protein allowed to exit from the ER to the Golgi. Yet even under tight control, disturbances to ER homeostasis can arise from Ca^{2+} depletion, hypoxia, altered glycosylation or viral infection (196). During these times efficiency is impacted which results in what is known as ER stress, typified by accumulation of misfolded/unfolded proteins. It is worth noting that ER stress can be experimentally induced using compounds such as tunicamycin, thapsigargin and dithiothreitol (DTT). These compounds impact N-glycosylation, Ca^{2+} homeostasis and disulfide bond formation respectively demonstrating again the importance in regulating these processes (197, 198). During times of ER stress, quality control systems are in place to slow production and clear misfolding. The unfolded protein response (UPR) is a signalling cascade triggered by the accumulation of unfolded/misfolded proteins in the ER. Coordinated activation of three lumenal sensors drives the response, being IRE1, PERK and ATF6. IRE1 and ATF6 expedite gene expression while PERK acts to reduce protein synthesis (199, 200). This represents the metazoan response to ER stress, as yeast only express Ire1. Human PERK expressed in yeast (201) however does demonstrate functionality suggesting that the final outcome is the same, just with less specificity under a single regulator.

The Ire1 pathway was first discovered in S*accharomyces cerevisiae* (202, 203) where it was used to define the UPR, and as such will be the focus here in. Ire1 has three functional domains, an N-terminal sensor domain that extend into the ER lumen and cytosolic domains at the C-terminus being a serine-threonine kinase and an endoribonuclease (199, 204, 205). The sensor domain contains a deep groove that has homology to a similar region found in the major histocompatibility complex (MHC). The groove is observed to bind protein with high specificity yet

located at a notable depth that is thought to be accessible to only unfolded proteins (196, 206). Under normal cellular conditions Kar2 is bound to the sensor domain to prevent unsolicited activation of Ire1. As unfolded protein accumulates, Kar2 is released from Ire1 to exert holdase activity at hydrophobic stretches of the unfolded protein, maintaining competency (199, 207, 208). In the absence of Kar2, Ire1 can bind along unfolded proteins and begin to form clusters. Oligomerisation at these clusters initiates autophosphorylation at the serine-threonine kinase and subsequently activation of the endoribonuclease domain (196, 199, 206, 209). The endoribonuclease domain performs spliceosome independent splicing of the Hac1 (XBP1; the mammalian ortholog) transcriptional factor (196, 199, 204, 210). Spliced Hac1 binds to an unfolded protein response element (UPRE) at the promoter of target genes with broad regulatory outcomes (211, 212). Protein synthesis is down regulated and membrane synthesis is enhanced, aiming to accommodate for the protein load. Expression of molecular chaperones is increased, Kar2 is one such target but also PDI which aids in protein re-folding through its inherent isomerase activity (196, 213). Protein degradation is also increased through upregulation of a pathway known as ER-associated degradation (ERAD).

ERAD aims to restore ER homeostasis through the removal of terminally misfolded proteins. Recognition of substrate for ERAD occurs through several means including, cis/trans configuration of peptidyl-prolyl bonds, disulfide bonds or the most well understood, glycan trimming (214-216). Attached N-glycans provides checkpoints during protein folding as progressively more extensive trimming events offers an opportunity for dynamic rearrangements to occur. However, at a terminal de-mannosylation event the protein is subsequently targeted for degradation. ERAD begins with the retro-translocation of a substate to the cytosol (215, 217). Retro-translocation is still not fully understood with some implicating Sec61 in this process yet the ubiquitin ligase complex Hrd1 serves as the better candidate (215, 218-220). At the cytosol the substrate associates with a ubiquitin ligase complex where exposed lysine residues are subject to covalent binding of ubiquitin chains in what is referred to as polyubiquitination. Polyubiquitin chains are recognised by the cytosolic 26s proteasome that finalises protein degradation (215, 221).

ER-phagy is an autophagic response that can also be enlisted by the cell for clearance of the ER to the vacuole/lysosome. The advantages of cellular compartmentalisation are apparent in these outcomes as problematic regions of the ER can be segregated to subdomains and relinquished for larger scale degradation. Regulation by autophagy is a newly emerging quality control pathway defined as ER to lysosome associated degradation (ERLAD) (216). ER-phagy is mediated by three differing classifications. Macro-phagy is the bulk delivery of ER constitutes to the vacuole via the formation of an autophagosome. Micro-phagy is characterised by portions of ER that contain misfolded proteins being directly engulfed by the vacuole. Finally, ER vesicles can be released for subsequent fusion and degradation by the vacuole/lysosome (216, 222). These events coordinate with UPR and ERAD to govern ER size, function, and homeostasis.

However, as stress on the ER persists, the chance for functionality to be restored and homeostasis re-established diminishes. In response the UPR may instead seek to prevent further reaching consequences, terminating the dysregulated cell via apoptosis (196, 200, 223). While this serves to eliminate the apparent dysregulation, significant apoptosis has been associated with several physiological imbalances and cellular diseases (224-227).

Project Design & Hypothesis: Characterising the Outcomes of Dysfunctional Sss1

Loss of ER homeostasis can impact intracellular function, leading to prolonged ER stress and presents as a risk factor to disease progression. Disturbances to ER channels and components in translocation have long been understood to have a role in disease progression and fall under the umbrella term of “Channelopathies” (228). While many of these channelopathies at the translocon have traditionally involved disruptions in protein translocation, the consequences of impaired gating are becoming more apparent. A study in mice observing the effects of defective Kar2 binding at the translocon was one of the first to demonstrate defective gating in propagating disease phenotypes. Here, a Y344H mutation in the ER lumenal L7 of Sec61α would result in significant apoptosis of pancreatic β-cells with the affected

mice presenting with phenotypes commonly associated with diabetes (229). Further work investing this mutation in a human cell line found the inability of Kar2 to bind the translocon was associated with Ca^{2+} depletion at the ER, providing novel insight to the pathological consequences of defective gating (230).

Our knowledge of cellular processes is determined through fundamental research which allows us to predict nature and elucidate not only function but subsequently the involvement of these processes in disease progression. At the start of this project, literature describing translocon function focused on the pore forming Sec61 subunit. Understanding of the equally essential subunit Sss1 was limited to simply stabilising the Sec61 subunit at this time. However, our structural analyses would find the extreme C-terminus of Sss1 was juxtaposed to a key gating module of Sec61. This led us to hypothesise that the highly conserved C-terminus of Sss1 may regulate gating of the translocon. In our possession are two mutants within this region of Sss1 that exhibit a temperature sensitivity (TS) growth defect, *sss1-6* (P74A, I75A) and *sss1-7* (H72K). The nature of the TS phenotype finds these strains inviable at an elevated temperature of 37°C through which phenotypical characterisation would serve as the basis of this project. Furthermore, this work has benefited from the genetic and biochemical tractability of the yeast, *Saccharomyces cerevisiae* when pursing our investigations. The degree of sequence and functional conservation observed between yeast and higher eukaryotes has resulted in yeast being extensively used for the understanding of fundamental eukaryotic processes, without the difficulties associated with the added complexity. Three aims were explored:

1. **Investigating a role for Sss1 in translocon gating dynamics**

2. **Characterising cancer associated mutations of Sss1 that impart gating dysregulation**

3. **Determining protein degradation pathways regulating Sss1 abundance**

References

1. Voeltz GK, Rolls MM, Rapoport TA. Structural organization of the endoplasmic reticulum. EMBO reports. 2002;3(10):944-50.
2. Hebert DN, Garman SC, Molinari M. The glycan code of the endoplasmic reticulum: asparagine-linked carbohydrates as protein maturation and quality-control tags. Trends in cell biology. 2005;15(7):364-70.
3. Clapham DE. Calcium signaling. Cell. 2007;131(6):1047-58.
4. Rapoport TA. Protein translocation across the eukaryotic endoplasmic reticulum and bacterial plasma membranes. Nature. 2007;450(7170):663-9.
5. Fagone P, Jackowski S. Membrane phospholipid synthesis and endoplasmic reticulum function. Journal of lipid research. 2009;50 Suppl(Suppl):S311-6.
6. Schwarz DS, Blower MD. The endoplasmic reticulum: structure, function and response to cellular signaling. Cellular and molecular life sciences : CMLS. 2016;73(1):79-94.
7. Daverkausen-Fischer L, Pröls F. Regulation of calcium homeostasis and flux between the endoplasmic reticulum and the cytosol. Journal of Biological Chemistry. 2022;298(7):102061.
8. English AR, Zurek N, Voeltz GK. Peripheral ER structure and function. Current opinion in cell biology. 2009;21(4):596-602.
9. Voeltz GK, Rolls MM, Rapoport TA. Structural organization of the endoplasmic reticulum. 2002;3(10):944-50.
10. Watson ML. The nuclear envelope; its structure and relation to cytoplasmic membranes. The Journal of biophysical and biochemical cytology. 1955;1(3):257-70.
11. Mattout A, Dechat T, Adam SA, Goldman RD, Gruenbaum Y. Nuclear lamins, diseases and aging. Current opinion in cell biology. 2006;18(3):335-41.
12. Salpingidou G, Smertenko A, Hausmanowa-Petrucewicz I, Hussey PJ, Hutchison CJ. A novel role for the nuclear membrane protein emerin in association of the centrosome to the outer nuclear membrane. Journal of Cell Biology. 2007;178(6):897-904.
13. Hetzer MW. The nuclear envelope. Cold Spring Harbor perspectives in biology. 2010;2(3):a000539.
14. Lei K, Zhu X, Xu R, Shao C, Xu T, Zhuang Y, et al. Inner Nuclear Envelope Proteins SUN1 and SUN2 Play a Prominent Role in the DNA Damage Response. Current Biology. 2012;22(17):1609-15.
15. Lang S, Zimmermann R. Mechanisms of ER Protein Import. International journal of molecular sciences. 2022;23(10).
16. Kurokawa K, Nakano A. The ER exit sites are specialized ER zones for the transport of cargo proteins from the ER to the Golgi apparatus. The Journal of Biochemistry. 2018;165(2):109-14.
17. Raote I, Ortega-Bellido M, Santos AJ, Foresti O, Zhang C, Garcia-Parajo MF, et al. TANGO1 builds a machine for collagen export by recruiting and spatially organizing COPII, tethers and membranes. eLife. 2018;7.
18. Jomaa A, Boehringer D, Leibundgut M, Ban N. Structures of the E. coli translating ribosome with SRP and its receptor and with the translocon. Nature Communications. 2016;7(1):10471.
19. Voorhees RM, Hegde RS. Structure of the Sec61 channel opened by a signal sequence. 2016;351(6268):88-91.
20. Rapoport TA, Li L, Park E. Structural and Mechanistic Insights into Protein Translocation. Annual Review of Cell and Developmental Biology. 2017;33(1):369-90.
21. Berg Bvd, Clemons WM, Collinson I, Modis Y, Hartmann E, Harrison SC, et al. X-ray structure of a protein-conducting channel. Nature. 2004;427(6969):36-44.

22. Simon SM, Blobel G. A protein-conducting channel in the endoplasmic reticulum. Cell. 1991;65(3):371-80.
23. Crowley KS, Reinhart GD, Johnson AE. The signal sequence moves through a ribosomal tunnel into a noncytoplasmic aqueous environment at the ER membrane early in translocation. Cell. 1993;73(6):1101-15.
24. Crowley KS, Liao S, Worrell VE, Reinhart GD, Johnson AE. Secretory proteins move through the endoplasmic reticulum membrane via an aqueous, gated pore. Cell. 1994;78(3):461-71.
25. Trueman SF, Mandon EC, Gilmore R. A gating motif in the translocation channel sets the hydrophobicity threshold for signal sequence function. The Journal of cell biology. 2012;199(6):907-18.
26. Itskanov S, Park E. Structure of the posttranslational Sec protein-translocation channel complex from yeast. Science (New York, NY). 2019;363(6422):84-7.
27. Li W, Schulman S, Boyd D, Erlandson K, Beckwith J, Rapoport TA. The Plug Domain of the SecY Protein Stabilizes the Closed State of the Translocation Channel and Maintains a Membrane Seal. Molecular Cell. 2007;26(4):511-21.
28. Esnault Y, Blondel MO, Deshaies RJ, Scheckman R, Képès F. The yeast SSS1 gene is essential for secretory protein translocation and encodes a conserved protein of the endoplasmic reticulum. The EMBO journal. 1993;12(11):4083-93.
29. Wilkinson BM, Brownsword JK, Mousley CJ, Stirling CJ. Sss1p Is Required to Complete Protein Translocon Activation*. Journal of Biological Chemistry. 2010;285(42):32671-7.
30. Toikkanen J, Gatti E, Takei K, Saloheimo M, Olkkonen VM, Söderlund H, et al. Yeast protein translocation complex: isolation of two genes SEB1 and SEB2 encoding proteins homologous to the Sec61 beta subunit. Yeast (Chichester, England). 1996;12(5):425-38.
31. Zhu Y, Zhang G, Lin S, Shi J, Zhang H, Hu J. Sec61β facilitates the maintenance of endoplasmic reticulum homeostasis by associating microtubules. Protein & Cell. 2018;9(7):616-28.
32. Finke K, Plath K, Panzner S, Prehn S, Rapoport TA, Hartmann E, et al. A second trimeric complex containing homologs of the Sec61p complex functions in protein transport across the ER membrane of S. cerevisiae. The EMBO journal. 1996;15(7):1482-94.
33. Römisch K, Webb J, Herz J, Prehn S, Frank R, Vingron M, et al. Homology of 54K protein of signal-recognition particle, docking protein and two E. coli proteins with putative GTP–binding domains. Nature. 1989;340(6233):478-82.
34. Bernstein HD, Poritz MA, Strub K, Hoben PJ, Brenner S, Walter P. Model for signal sequence recognition from amino-acid sequence of 54K subunit of signal recognition particle. Nature. 1989;340(6233):482-6.
35. Hann BC, Walter P. The signal recognition particle in S. cerevisiae. Cell. 1991;67(1):131-44.
36. Blobel G, Dobberstein B. Transfer of proteins across membranes. I. Presence of proteolytically processed and unprocessed nascent immunoglobulin light chains on membrane-bound ribosomes of murine myeloma. The Journal of cell biology. 1975;67(3):835-51.
37. Martoglio B, Dobberstein B. Signal sequences: more than just greasy peptides. Trends in cell biology. 1998;8(10):410-5.
38. Lang S, Nguyen D, Bhadra P, Jung M, Helms V, Zimmermann R. Signal Peptide Features Determining the Substrate Specificities of Targeting and Translocation Components in Human ER Protein Import. Frontiers in physiology. 2022;13:833540.
39. von Heijne G. Signal sequences. The limits of variation. Journal of molecular biology. 1985;184(1):99-105.

40. Hegde RS, Bernstein HD. The surprising complexity of signal sequences. Trends in biochemical sciences. 2006;31(10):563-71.
41. Peterson JH, Woolhead CA, Bernstein HD. Basic amino acids in a distinct subset of signal peptides promote interaction with the signal recognition particle. The Journal of biological chemistry. 2003;278(46):46155-62.
42. Walter P, Ibrahimi I, Blobel G. Translocation of proteins across the endoplasmic reticulum. I. Signal recognition protein (SRP) binds to in-vitro-assembled polysomes synthesizing secretory protein. The Journal of cell biology. 1981;91(2 Pt 1):545-50.
43. Jones JD, McKnight CJ, Gierasch LM. Biophysical studies of signal peptides: implications for signal sequence functions and the involvement of lipid in protein export. Journal of bioenergetics and biomembranes. 1990;22(3):213-32.
44. Goder V, Spiess M. Molecular mechanism of signal sequence orientation in the endoplasmic reticulum. The EMBO journal. 2003;22(14):3645-53.
45. von Heijne G, Gavel Y. Topogenic signals in integral membrane proteins. European journal of biochemistry. 1988;174(4):671-8.
46. Rapoport TA, Goder V, Heinrich SU, Matlack KE. Membrane-protein integration and the role of the translocation channel. Trends in cell biology. 2004;14(10):568-75.
47. Baker JA, Wong WC, Eisenhaber B, Warwicker J, Eisenhaber F. Charged residues next to transmembrane regions revisited: "Positive-inside rule" is complemented by the "negative inside depletion/outside enrichment rule". BMC biology. 2017;15(1):66.
48. Blobel G, Sabatini DD. Ribosome-Membrane Interaction in Eukaryotic Cells. In: Manson LA, editor. Biomembranes: Volume 2. Boston, MA: Springer US; 1971. p. 193-5.
49. Gilmore R, Blobel G, Walter P. Protein translocation across the endoplasmic reticulum. I. Detection in the microsomal membrane of a receptor for the signal recognition particle. The Journal of cell biology. 1982;95(2 Pt 1):463-9.
50. Gilmore R, Walter P, Blobel G. Protein translocation across the endoplasmic reticulum. II. Isolation and characterization of the signal recognition particle receptor. The Journal of cell biology. 1982;95(2 Pt 1):470-7.
51. Walter P, Blobel G. Purification of a membrane-associated protein complex required for protein translocation across the endoplasmic reticulum. Proceedings of the National Academy of Sciences of the United States of America. 1980;77(12):7112-6.
52. Walter P, Blobel G. Disassembly and reconstitution of signal recognition particle. Cell. 1983;34(2):525-33.
53. Walter P, Gilmore R, Blobel G. Protein translocation across the endoplasmic reticulum. Cell. 1984;38(1):5-8.
54. Bernstein HD, Zopf D, Freymann DM, Walter P. Functional substitution of the signal recognition particle 54-kDa subunit by its Escherichia coli homolog. Proceedings of the National Academy of Sciences of the United States of America. 1993;90(11):5229-33.
55. Akopian D, Shen K, Zhang X, Shan SO. Signal recognition particle: an essential protein-targeting machine. Annual review of biochemistry. 2013;82:693-721.
56. Shao S, Hegde RS. Membrane protein insertion at the endoplasmic reticulum. Annu Rev Cell Dev Biol. 2011;27:25-56.
57. Walter P, Blobel G. Signal recognition particle contains a 7S RNA essential for protein translocation across the endoplasmic reticulum. Nature. 1982;299(5885):691-8.
58. Halic M, Becker T, Pool MR, Spahn CM, Grassucci RA, Frank J, et al. Structure of the signal recognition particle interacting with the elongation-arrested ribosome. Nature. 2004;427(6977):808-14.
59. Ciufo LF, Brown JD. Nuclear export of yeast signal recognition particle lacking Srp54p by the Xpo1p/Crm1p NES-dependent pathway. Current biology : CB. 2000;10(20):1256-64.

60. Lütcke H, High S, Römisch K, Ashford AJ, Dobberstein B. The methionine-rich domain of the 54 kDa subunit of signal recognition particle is sufficient for the interaction with signal sequences. The EMBO journal. 1992;11(4):1543-51.
61. Janda CY, Li J, Oubridge C, Hernández H, Robinson CV, Nagai K. Recognition of a signal peptide by the signal recognition particle. Nature. 2010;465(7297):507-10.
62. Batey RT, Rambo RP, Lucast L, Rha B, Doudna JA. Crystal structure of the ribonucleoprotein core of the signal recognition particle. Science. 2000;287(5456):1232-9.
63. Montoya G, Svensson C, Luirink J, Sinning I. Crystal structure of the NG domain from the signal-recognition particle receptor FtsY. Nature. 1997;385(6614):365-8.
64. Freymann DM, Keenan RJ, Stroud RM, Walter P. Structure of the conserved GTPase domain of the signal recognition particle. Nature. 1997;385(6614):361-4.
65. Keenan RJ, Freymann DM, Walter P, Stroud RM. Crystal Structure of the Signal Sequence Binding Subunit of the Signal Recognition Particle. Cell. 1998;94(2):181-91.
66. Focia PJ, Shepotinovskaya IV, Seidler JA, Freymann DM. Heterodimeric GTPase core of the SRP targeting complex. Science. 2004;303(5656):373-7.
67. Egea PF, Shan SO, Napetschnig J, Savage DF, Walter P, Stroud RM. Substrate twinning activates the signal recognition particle and its receptor. Nature. 2004;427(6971):215-21.
68. Schwartz T, Blobel G. Structural basis for the function of the beta subunit of the eukaryotic signal recognition particle receptor. Cell. 2003;112(6):793-803.
69. Tajima S, Lauffer L, Rath VL, Walter P. The signal recognition particle receptor is a complex that contains two distinct polypeptide chains. Journal of Cell Biology. 1986;103(4):1167-78.
70. Saraogi I, Shan SO. Molecular mechanism of co-translational protein targeting by the signal recognition particle. Traffic (Copenhagen, Denmark). 2011;12(5):535-42.
71. Bornemann T, Jöckel J, Rodnina MV, Wintermeyer W. Signal sequence-independent membrane targeting of ribosomes containing short nascent peptides within the exit tunnel. Nature structural & molecular biology. 2008;15(5):494-9.
72. Flanagan JJ, Chen JC, Miao Y, Shao Y, Lin J, Bock PE, et al. Signal recognition particle binds to ribosome-bound signal sequences with fluorescence-detected subnanomolar affinity that does not diminish as the nascent chain lengthens. The Journal of biological chemistry. 2003;278(20):18628-37.
73. Zhang X, Rashid R, Wang K, Shan SO. Sequential checkpoints govern substrate selection during cotranslational protein targeting. Science. 2010;328(5979):757-60.
74. Holtkamp W, Lee S, Bornemann T, Senyushkina T, Rodnina MV, Wintermeyer W. Dynamic switch of the signal recognition particle from scanning to targeting. Nature structural & molecular biology. 2012;19(12):1332-7.
75. Lee JH, Chandrasekar S, Chung S, Hwang Fu Y-H, Liu D, Weiss S, et al. Sequential activation of human signal recognition particle by the ribosome and signal sequence drives efficient protein targeting. Proceedings of the National Academy of Sciences. 2018;115(24):E5487-E96.
76. Mercier E, Holtkamp W, Rodnina MV, Wintermeyer W. Signal recognition particle binds to translating ribosomes before emergence of a signal anchor sequence. Nucleic acids research. 2017;45(20):11858-66.
77. Voorhees RM, Hegde RS. Structures of the scanning and engaged states of the mammalian SRP-ribosome complex. eLife. 2015;4.
78. Pool MR, Stumm J, Fulga TA, Sinning I, Dobberstein B. Distinct modes of signal recognition particle interaction with the ribosome. Science. 2002;297(5585):1345-8.
79. Halic M, Blau M, Becker T, Mielke T, Pool MR, Wild K, et al. Following the signal sequence from ribosomal tunnel exit to signal recognition particle. Nature. 2006;444(7118):507-11.

80. Schaffitzel C, Oswald M, Berger I, Ishikawa T, Abrahams JP, Koerten HK, et al. Structure of the E. coli signal recognition particle bound to a translating ribosome. Nature. 2006;444(7118):503-6.
81. Joiret M, Rapino F, Close P, Geris L. Ribosome exit tunnel electrostatics. bioRxiv. 2020:2020.10.20.346684.
82. Siegel V, Walter P. The affinity of signal recognition particle for presecretory proteins is dependent on nascent chain length. The EMBO journal. 1988;7(6):1769-75.
83. Chartron JW, Hunt KC, Frydman J. Cotranslational signal-independent SRP preloading during membrane targeting. Nature. 2016;536(7615):224-8.
84. O'Keefe S, Pool MR, High S. Membrane protein biogenesis at the ER: the highways and byways. The FEBS Journal. 2022;289(22):6835-62.
85. Connolly T, Gilmore R. GTP hydrolysis by complexes of the signal recognition particle and the signal recognition particle receptor. The Journal of cell biology. 1993;123(4):799-807.
86. Zhang X, Schaffitzel C, Ban N, Shan SO. Multiple conformational switches in a GTPase complex control co-translational protein targeting. Proceedings of the National Academy of Sciences of the United States of America. 2009;106(6):1754-9.
87. Lam VQ, Akopian D, Rome M, Henningsen D, Shan SO. Lipid activation of the signal recognition particle receptor provides spatial coordination of protein targeting. The Journal of cell biology. 2010;190(4):623-35.
88. Bacher G, Pool M, Dobberstein B. The ribosome regulates the GTPase of the beta-subunit of the signal recognition particle receptor. The Journal of cell biology. 1999;146(4):723-30.
89. Halic M, Gartmann M, Schlenker O, Mielke T, Pool MR, Sinning I, et al. Signal recognition particle receptor exposes the ribosomal translocon binding site. Science. 2006;312(5774):745-7.
90. Jomaa A, Eitzinger S, Zhu Z, Chandrasekar S, Kobayashi K, Shan S-O, et al. Molecular mechanism of cargo recognition and handover by the mammalian signal recognition particle. Cell Reports. 2021;36(2):109350.
91. Fulga TA, Sinning I, Dobberstein B, Pool MR. SRβ coordinates signal sequence release from SRP with ribosome binding to the translocon. 2001;20(9):2338-47.
92. Wild K, Juaire KD, Soni K, Shanmuganathan V, Hendricks A, Segnitz B, et al. Reconstitution of the human SRP system and quantitative and systematic analysis of its ribosome interactions. Nucleic acids research. 2019;47(6):3184-96.
93. Shen K, Arslan S, Akopian D, Ha T, Shan S-o. Activated GTPase movement on an RNA scaffold drives co-translational protein targeting. Nature. 2012;492(7428):271-5.
94. Voorhees Rebecca M, Fernández Israel S, Scheres Sjors HW, Hegde Ramanujan S. Structure of the Mammalian Ribosome-Sec61 Complex to 3.4 Å Resolution. Cell. 2014;157(7):1632-43.
95. Gogala M, Becker T, Beatrix B, Armache J-P, Barrio-Garcia C, Berninghausen O, et al. Structures of the Sec61 complex engaged in nascent peptide translocation or membrane insertion. Nature. 2014;506(7486):107-10.
96. Devaraneni PK, Conti B, Matsumura Y, Yang Z, Johnson AE, Skach WR. Stepwise insertion and inversion of a type II signal anchor sequence in the ribosome-Sec61 translocon complex. Cell. 2011;146(1):134-47.
97. Li L, Park E, Ling J, Ingram J, Ploegh H, Rapoport TA. Crystal structure of a substrate-engaged SecY protein-translocation channel. Nature. 2016;531(7594):395-9.
98. Matlack KES, Mothes W, Rapoport TA. Protein Translocation: Tunnel Vision. Cell. 1998;92(3):381-90.

99. Mutka SC, Walter P. Multifaceted physiological response allows yeast to adapt to the loss of the signal recognition particle-dependent protein-targeting pathway. Molecular biology of the cell. 2001;12(3):577-88.
100. Aviram N, Ast T, Costa EA, Arakel EC, Chuartzman SG, Jan CH, et al. The SND proteins constitute an alternative targeting route to the endoplasmic reticulum. Nature. 2016;540(7631):134-8.
101. Haßdenteufel S, Sicking M, Schorr S, Aviram N, Fecher-Trost C, Schuldiner M, et al. hSnd2 protein represents an alternative targeting factor to the endoplasmic reticulum in human cells. 2017;591(20):3211-24.
102. Hegde RS, Keenan RJ. The mechanisms of integral membrane protein biogenesis. Nature Reviews Molecular Cell Biology. 2022;23(2):107-24.
103. Schuldiner M, Metz J, Schmid V, Denic V, Rakwalska M, Schmitt HD, et al. The GET Complex Mediates Insertion of Tail-Anchored Proteins into the ER Membrane. Cell. 2008;134(4):634-45.
104. Lang S, Pfeffer S, Lee P-H, Cavalié A, Helms V, Förster F, et al. An Update on Sec61 Channel Functions, Mechanisms, and Related Diseases. 2017;8.
105. Kutay U, Hartmann E, Rapoport TA. A class of membrane proteins with a C-terminal anchor. Trends in cell biology. 1993;3(3):72-5.
106. Zimmermann R, Eyrisch S, Ahmad M, Helms V. Protein translocation across the ER membrane. Biochimica et Biophysica Acta (BBA) - Biomembranes. 2011;1808(3):912-24.
107. Lakkaraju AK, Thankappan R, Mary C, Garrison JL, Taunton J, Strub K. Efficient secretion of small proteins in mammalian cells relies on Sec62-dependent posttranslational translocation. Molecular biology of the cell. 2012;23(14):2712-22.
108. Ng DT, Brown JD, Walter P. Signal sequences specify the targeting route to the endoplasmic reticulum membrane. Journal of Cell Biology. 1996;134(2):269-78.
109. Müller G, Zimmermann R. Import of honeybee prepromelittin into the endoplasmic reticulum: energy requirements for membrane insertion. The EMBO journal. 1988;7(3):639-48.
110. Ngosuwan J, Wang NM, Fung KL, Chirico WJ. Roles of Cytosolic Hsp70 and Hsp40 Molecular Chaperones in Post-translational Translocation of Presecretory Proteins into the Endoplasmic Reticulum*. Journal of Biological Chemistry. 2003;278(9):7034-42.
111. Alderson TR, Kim JH, Markley JL. Dynamical Structures of Hsp70 and Hsp70-Hsp40 Complexes. Structure (London, England : 1993). 2016;24(7):1014-30.
112. Bertelsen EB, Chang L, Gestwicki JE, Zuiderweg ER. Solution conformation of wild-type E. coli Hsp70 (DnaK) chaperone complexed with ADP and substrate. Proceedings of the National Academy of Sciences of the United States of America. 2009;106(21):8471-6.
113. Qi R, Sarbeng EB, Liu Q, Le KQ, Xu X, Xu H, et al. Allosteric opening of the polypeptide-binding site when an Hsp70 binds ATP. Nature structural & molecular biology. 2013;20(7):900-7.
114. Sekhar A, Rosenzweig R, Bouvignies G, Kay LE. Hsp70 biases the folding pathways of client proteins. 2016;113(20):E2794-E801.
115. Rüdiger S, Germeroth L, Schneider-Mergener J, Bukau B. Substrate specificity of the DnaK chaperone determined by screening cellulose-bound peptide libraries. The EMBO journal. 1997;16(7):1501-7.
116. Cho H, Shim WJ, Liu Y, Shan S-O. J-domain proteins promote client relay from Hsp70 during tail-anchored membrane protein targeting. Journal of Biological Chemistry. 2021;296:100546.
117. Mayer MP. Hsp70 chaperone dynamics and molecular mechanism. Trends in biochemical sciences. 2013;38(10):507-14.
118. Rüdiger S, Schneider-Mergener J, Bukau B. Its substrate specificity characterizes the DnaJ co-chaperone as a scanning factor for the DnaK chaperone. 2001;20(5):1042-50.

119. Rodriguez F, Arsène-Ploetze F, Rist W, Rüdiger S, Schneider-Mergener J, Mayer MP, et al. Molecular Basis for Regulation of the Heat Shock Transcription Factor σ32 by the DnaK and DnaJ Chaperones. Molecular Cell. 2008;32(3):347-58.
120. Panzner S, Dreier L, Hartmann E, Kostka S, Rapoport TA. Posttranslational protein transport in yeast reconstituted with a purified complex of Sec proteins and Kar2p. Cell. 1995;81(4):561-70.
121. Harada Y, Li H, Wall JS, Li H, Lennarz WJ. Structural Studies and the Assembly of the Heptameric Post-translational Translocon Complex *. Journal of Biological Chemistry. 2011;286(4):2956-65.
122. Bhadra P, Yadhanapudi L, Römisch K, Helms V. How does Sec63 affect the conformation of Sec61 in yeast? PLoS computational biology. 2021;17(3):e1008855.
123. Tripathi A, Mandon EC, Gilmore R, Rapoport TA. Two alternative binding mechanisms connect the protein translocation Sec71-Sec72 complex with heat shock proteins. Journal of Biological Chemistry. 2017;292(19):8007-18.
124. Becker J, Walter W, Yan W, Craig EA. Functional interaction of cytosolic hsp70 and a DnaJ-related protein, Ydj1p, in protein translocation in vivo. Molecular and Cellular Biology. 1996;16(8):4378-86.
125. Feldheim D, Schekman R. Sec72p contributes to the selective recognition of signal peptides by the secretory polypeptide translocation complex. The Journal of cell biology. 1994;126(4):935-43.
126. Feldheim D, Yoshimura K, Admon A, Schekman R. Structural and functional characterization of Sec66p, a new subunit of the polypeptide translocation apparatus in the yeast endoplasmic reticulum. Molecular biology of the cell. 1993;4(9):931-9.
127. Itskanov S, Kuo KM, Gumbart JC, Park E. Stepwise gating of the Sec61 protein-conducting channel by Sec63 and Sec62. Nature structural & molecular biology. 2021;28(2):162-72.
128. Young JC, Hoogenraad NJ, Hartl FU. Molecular chaperones Hsp90 and Hsp70 deliver preproteins to the mitochondrial import receptor Tom70. Cell. 2003;112(1):41-50.
129. Jung S-j, Kim H. Emerging View on the Molecular Functions of Sec62 and Sec63 in Protein Translocation. 2021;22(23):12757.
130. Wu X, Cabanos C, Rapoport TA. Structure of the post-translational protein translocation machinery of the ER membrane. Nature. 2019;566(7742):136-9.
131. Willer M, Jermy AJ, Young BP, Stirling CJ. Identification of novel protein–protein interactions at the cytosolic surface of the Sec63 complex in the yeast ER membrane. 2003;20(2):133-48.
132. Wittke S, Dünnwald M, Johnsson N. Sec62p, A Component of the Endoplasmic Reticulum Protein Translocation Machinery, Contains Multiple Binding Sites for the Sec-Complex. Molecular biology of the cell. 2000;11(11):3859-71.
133. Matlack KES, Misselwitz B, Plath K, Rapoport TA. BiP Acts as a Molecular Ratchet during Posttranslational Transport of Prepro-α Factor across the ER Membrane. Cell. 1999;97(5):553-64.
134. Liebermeister W, Rapoport TA, Heinrich R. Ratcheting in post-translational protein translocation: a mathematical model11Edited by G. von Heijne. Journal of molecular biology. 2001;305(3):643-56.
135. Braakman I, Hebert DN. Protein Folding in the Endoplasmic Reticulum. Cold Spring Harbor perspectives in biology. 2013;5(5):a013201-a.
136. Ellgaard L, McCaul N, Chatsisvili A, Braakman I. Co- and Post-Translational Protein Folding in the ER. Traffic (Copenhagen, Denmark). 2016;17(6):615-38.
137. Li Y, Bergeron JJ, Luo L, Ou WJ, Thomas DY, Kang CY. Effects of inefficient cleavage of the signal sequence of HIV-1 gp 120 on its association with calnexin, folding, and

intracellular transport. Proceedings of the National Academy of Sciences of the United States of America. 1996;93(18):9606-11.
138. Nicchitta CV, Murphy EC, 3rd, Haynes R, Shelness GS. Stage- and ribosome-specific alterations in nascent chain-Sec61p interactions accompany translocation across the ER membrane. The Journal of cell biology. 1995;129(4):957-70.
139. Weihofen A, Binns K, Lemberg MK, Ashman K, Martoglio B. Identification of signal peptide peptidase, a presenilin-type aspartic protease. Science. 2002;296(5576):2215-8.
140. Braunger K, Pfeffer S, Shrimal S, Gilmore R, Berninghausen O, Mandon EC, et al. Structural basis for coupling protein transport and N-glycosylation at the mammalian endoplasmic reticulum. Science. 2018;360(6385):215-9.
141. Ramírez AS, Kowal J, Locher KP. Cryo-electron microscopy structures of human oligosaccharyltransferase complexes OST-A and OST-B. Science. 2019;366(6471):1372-5.
142. Nilsson IM, von Heijne G. Determination of the distance between the oligosaccharyltransferase active site and the endoplasmic reticulum membrane. The Journal of biological chemistry. 1993;268(8):5798-801.
143. Czuba LC, Hillgren KM, Swaan PW. Post-translational modifications of transporters. Pharmacology & Therapeutics. 2018;192:88-99.
144. Ellis RJ. Assembly chaperones: a perspective. Philosophical transactions of the Royal Society of London Series B, Biological sciences. 2013;368(1617):20110398.
145. Hartl FU, Hayer-Hartl M. Converging concepts of protein folding in vitro and in vivo. Nature structural & molecular biology. 2009;16(6):574-81.
146. Hwang C, Sinskey AJ, Lodish HF. Oxidized Redox State of Glutathione in the Endoplasmic Reticulum. 1992;257(5076):1496-502.
147. Dixon BM, Heath SH, Kim R, Suh JH, Hagen TM. Assessment of endoplasmic reticulum glutathione redox status is confounded by extensive ex vivo oxidation. Antioxidants & redox signaling. 2008;10(5):963-72.
148. Birk J, Meyer M, Aller I, Hansen HG, Odermatt A, Dick TP, et al. Endoplasmic reticulum: reduced and oxidized glutathione revisited. Journal of cell science. 2013;126(Pt 7):1604-17.
149. Morgan B, Ezeriņa D, Amoako TN, Riemer J, Seedorf M, Dick TP. Multiple glutathione disulfide removal pathways mediate cytosolic redox homeostasis. Nature chemical biology. 2013;9(2):119-25.
150. Schafer FQ, Buettner GR. Redox environment of the cell as viewed through the redox state of the glutathione disulfide/glutathione couple. Free radical biology & medicine. 2001;30(11):1191-212.
151. Ulrich K, Jakob U. The role of thiols in antioxidant systems. Free radical biology & medicine. 2019;140:14-27.
152. Robinson PJ, Bulleid NJ. Mechanisms of Disulfide Bond Formation in Nascent Polypeptides Entering the Secretory Pathway. 2020;9(9):1994.
153. Hudson DA, Gannon SA, Thorpe C. Oxidative protein folding: from thiol-disulfide exchange reactions to the redox poise of the endoplasmic reticulum. Free radical biology & medicine. 2015;80:171-82.
154. Ellgaard L, Sevier CS, Bulleid NJ. How Are Proteins Reduced in the Endoplasmic Reticulum? Trends in biochemical sciences. 2018;43(1):32-43.
155. Couto N, Wood J, Barber J. The role of glutathione reductase and related enzymes on cellular redox homoeostasis network. Free radical biology & medicine. 2016;95:27-42.
156. Welker E, Wedemeyer WJ, Narayan M, Scheraga HA. Coupling of conformational folding and disulfide-bond reactions in oxidative folding of proteins. Biochemistry. 2001;40(31):9059-64.
157. Poole LB. The basics of thiols and cysteines in redox biology and chemistry. Free radical biology & medicine. 2015;80:148-57.

158. Bach RD, Dmitrenko O, Thorpe C. Mechanism of thiolate-disulfide interchange reactions in biochemistry. The Journal of organic chemistry. 2008;73(1):12-21.
159. Okumura M, Kadokura H, Inaba K. Structures and functions of protein disulfide isomerase family members involved in proteostasis in the endoplasmic reticulum. Free radical biology & medicine. 2015;83:314-22.
160. Frand AR, Kaiser CA. Ero1p Oxidizes Protein Disulfide Isomerase in a Pathway for Disulfide Bond Formation in the Endoplasmic Reticulum. Molecular Cell. 1999;4(4):469-77.
161. Tu BP, Weissman JS. The FAD- and O(2)-dependent reaction cycle of Ero1-mediated oxidative protein folding in the endoplasmic reticulum. Mol Cell. 2002;10(5):983-94.
162. Wedemeyer WJ, Welker E, Narayan M, Scheraga HA. Disulfide bonds and protein folding. Biochemistry. 2000;39(15):4207-16.
163. Fu J, Gao J, Liang Z, Yang D. PDI-Regulated Disulfide Bond Formation in Protein Folding and Biomolecular Assembly. Molecules (Basel, Switzerland). 2020;26(1).
164. Kojer K, Riemer J. Balancing oxidative protein folding: the influences of reducing pathways on disulfide bond formation. Biochimica et biophysica acta. 2014;1844(8):1383-90.
165. Ponsero AJ, Igbaria A, Darch MA, Miled S, Outten CE, Winther JR, et al. Endoplasmic Reticulum Transport of Glutathione by Sec61 Is Regulated by Ero1 and Bip. Mol Cell. 2017;67(6):962-73.e5.
166. Hansen RE, Roth D, Winther JR. Quantifying the global cellular thiol-disulfide status. Proceedings of the National Academy of Sciences of the United States of America. 2009;106(2):422-7.
167. Luo M, Jiang Y-L, Ma X-X, Tang Y-J, He Y-X, Yu J, et al. Structural and Biochemical Characterization of Yeast Monothiol Glutaredoxin Grx6. Journal of molecular biology. 2010;398(4):614-22.
168. Berndt C, Lillig CH, Holmgren A. Thioredoxins and glutaredoxins as facilitators of protein folding. Biochimica et biophysica acta. 2008;1783(4):641-50.
169. Deponte M. Glutathione catalysis and the reaction mechanisms of glutathione-dependent enzymes. Biochimica et Biophysica Acta (BBA) - General Subjects. 2013;1830(5):3217-66.
170. Cuozzo JW, Kaiser CA. Competition between glutathione and protein thiols for disulphide-bond formation. Nature Cell Biology. 1999;1(3):130-5.
171. Zhang L, Niu Y, Zhu L, Fang J, Wang X, Wang L, et al. Different interaction modes for protein-disulfide isomerase (PDI) as an efficient regulator and a specific substrate of endoplasmic reticulum oxidoreductin-1α (Ero1α). The Journal of biological chemistry. 2014;289(45):31188-99.
172. Bennett BD, Kimball EH, Gao M, Osterhout R, Van Dien SJ, Rabinowitz JD. Absolute metabolite concentrations and implied enzyme active site occupancy in Escherichia coli. Nature chemical biology. 2009;5(8):593-9.
173. Park JO, Rubin SA, Xu YF, Amador-Noguez D, Fan J, Shlomi T, et al. Metabolite concentrations, fluxes and free energies imply efficient enzyme usage. Nature chemical biology. 2016;12(7):482-9.
174. Henry CS, Broadbelt LJ, Hatzimanikatis V. Thermodynamics-based metabolic flux analysis. Biophysical journal. 2007;92(5):1792-805.
175. Kitano H. Towards a theory of biological robustness. 2007;3(1):137.
176. Hackett SR, Zanotelli VRT, Xu W, Goya J, Park JO, Perlman DH, et al. Systems-level analysis of mechanisms regulating yeast metabolic flux. 2016;354(6311):aaf2786.
177. Küken A, Eloundou-Mbebi JMO, Basler G, Nikoloski Z. Cellular determinants of metabolite concentration ranges. PLoS computational biology. 2019;15(1):e1006687.

178. Pilchova I, Klacanova K, Tatarkova Z, Kaplan P, Racay P. The Involvement of Mg(2+) in Regulation of Cellular and Mitochondrial Functions. Oxidative medicine and cellular longevity. 2017;2017:6797460.
179. Karaoglu D, Kelleher DJ, Gilmore R. Functional characterization of Ost3p. Loss of the 34-kD subunit of the Saccharomyces cerevisiae oligosaccharyltransferase results in biased underglycosylation of acceptor substrates. The Journal of cell biology. 1995;130(3):567-77.
180. Kelleher DJ, Gilmore R. The Saccharomyces cerevisiae oligosaccharyltransferase is a protein complex composed of Wbp1p, Swp1p, and four additional polypeptides. The Journal of biological chemistry. 1994;269(17):12908-17.
181. Matsuda-Lennikov M, Biancalana M, Zou J, Ravell JC, Zheng L, Kanellopoulou C, et al. Magnesium transporter 1 (MAGT1) deficiency causes selective defects in N-linked glycosylation and expression of immune-response genes. The Journal of biological chemistry. 2019;294(37):13638-56.
182. Cohen Y, Megyeri M, Chen OCW, Condomitti G, Riezman I, Loizides-Mangold U, et al. The Yeast P5 Type ATPase, Spf1, Regulates Manganese Transport into the Endoplasmic Reticulum. PLOS ONE. 2014;8(12):e85519.
183. Huang EP. Metal ions and synaptic transmission: think zinc. Proceedings of the National Academy of Sciences of the United States of America. 1997;94(25):13386-7.
184. Hershfinkel M, Moran A, Grossman N, Sekler I. A zinc-sensing receptor triggers the release of intracellular Ca2+ and regulates ion transport. Proceedings of the National Academy of Sciences of the United States of America. 2001;98(20):11749-54.
185. Hamman BD, Chen J-C, Johnson EE, Johnson AE. The Aqueous Pore through the Translocon Has a Diameter of 40–60 Å during Cotranslational Protein Translocation at the ER Membrane. Cell. 1997;89(4):535-44.
186. Hamman BD, Hendershot LM, Johnson AE. BiP Maintains the Permeability Barrier of the ER Membrane by Sealing the Lumenal End of the Translocon Pore before and Early in Translocation. Cell. 1998;92(6):747-58.
187. Traut RR, Monro RE. THE PUROMYCIN REACTION AND ITS RELATION TO PROTEIN SYNTHESIS. Journal of molecular biology. 1964;10:63-72.
188. Heritage D, Wonderlin WF. Translocon pores in the endoplasmic reticulum are permeable to a neutral, polar molecule. The Journal of biological chemistry. 2001;276(25):22655-62.
189. Roy A, Wonderlin WF. The permeability of the endoplasmic reticulum is dynamically coupled to protein synthesis. The Journal of biological chemistry. 2003;278(7):4397-403.
190. Park E, Rapoport TA. Preserving the membrane barrier for small molecules during bacterial protein translocation. Nature. 2011;473(7346):239-42.
191. Lomax RB, Camello C, Van Coppenolle F, Petersen OH, Tepikin AV. Basal and physiological Ca(2+) leak from the endoplasmic reticulum of pancreatic acinar cells. Second messenger-activated channels and translocons. The Journal of biological chemistry. 2002;277(29):26479-85.
192. Rodriguez-Fonseca C, Amils R, Garrett RA. Fine structure of the peptidyl transferase centre on 23 S-like rRNAs deduced from chemical probing of antibiotic-ribosome complexes. Journal of molecular biology. 1995;247(2):224-35.
193. Van Coppenolle F, Vanden Abeele F, Slomianny C, Flourakis M, Hesketh J, Dewailly E, et al. Ribosome-translocon complex mediates calcium leakage from endoplasmic reticulum stores. Journal of cell science. 2004;117(Pt 18):4135-42.
194. Parys JB, Van Coppenolle F. Sec61 complex/translocon: The role of an atypical ER Ca(2+)-leak channel in health and disease. Frontiers in physiology. 2022;13:991149.

195. Bhadra P, Dos Santos S, Gamayun I, Pick T, Neumann C, Ogbechi J, et al. Mycolactone enhances the Ca2+ leak from endoplasmic reticulum by trapping Sec61 translocons in a Ca2+ permeable state. The Biochemical journal. 2021;478(22):4005-24.
196. Read A, Schröder M. The Unfolded Protein Response: An Overview. 2021;10(5):384.
197. DuRose JB, Tam AB, Niwa M. Intrinsic Capacities of Molecular Sensors of the Unfolded Protein Response to Sense Alternate Forms of Endoplasmic Reticulum Stress. Molecular biology of the cell. 2006;17(7):3095-107.
198. Messias Sandes J, Nascimento Moura DM, Divina da Silva Santiago M, Barbosa de Lima G, Cabral Filho PE, da Cunha Gonçalves de Albuquerque S, et al. The effects of endoplasmic reticulum stressors, tunicamycin and dithiothreitol on Trypanosoma cruzi. Experimental Cell Research. 2019;383(2):111560.
199. Hernández-Elvira M, Torres-Quiroz F, Escamilla-Ayala A, Domínguez-Martin E, Escalante R, Kawasaki L, et al. The Unfolded Protein Response Pathway in the Yeast Kluyveromyces lactis. A Comparative View among Yeast Species. Cells. 2018;7(8).
200. Walter P, Ron D. The unfolded protein response: from stress pathway to homeostatic regulation. Science. 2011;334(6059):1081-6.
201. Yap WS, Thibault G. Human PERK rescues unfolded protein response-deficient yeast cells. microPublication biology. 2022;2022.
202. Mori K. The unfolded protein response: the dawn of a new field. Proceedings of the Japan Academy Series B, Physical and biological sciences. 2015;91(9):469-80.
203. Nikawa J, Yamashita S. IRE1 encodes a putative protein kinase containing a membrane-spanning domain and is required for inositol phototrophy in Saccharomyces cerevisiae. Molecular microbiology. 1992;6(11):1441-6.
204. Sidrauski C, Walter P. The transmembrane kinase Ire1p is a site-specific endonuclease that initiates mRNA splicing in the unfolded protein response. Cell. 1997;90(6):1031-9.
205. Mori K, Ma W, Gething MJ, Sambrook J. A transmembrane protein with a cdc2+/CDC28-related kinase activity is required for signaling from the ER to the nucleus. Cell. 1993;74(4):743-56.
206. Credle JJ, Finer-Moore JS, Papa FR, Stroud RM, Walter P. On the mechanism of sensing unfolded protein in the endoplasmic reticulum. Proceedings of the National Academy of Sciences of the United States of America. 2005;102(52):18773-84.
207. Okamura K, Kimata Y, Higashio H, Tsuru A, Kohno K. Dissociation of Kar2p/BiP from an ER sensory molecule, Ire1p, triggers the unfolded protein response in yeast. Biochemical and biophysical research communications. 2000;279(2):445-50.
208. Bertolotti A, Zhang Y, Hendershot LM, Harding HP, Ron D. Dynamic interaction of BiP and ER stress transducers in the unfolded-protein response. Nat Cell Biol. 2000;2(6):326-32.
209. Kimata Y, Ishiwata-Kimata Y, Ito T, Hirata A, Suzuki T, Oikawa D, et al. Two regulatory steps of ER-stress sensor Ire1 involving its cluster formation and interaction with unfolded proteins. The Journal of cell biology. 2007;179(1):75-86.
210. Hooks KB, Griffiths-Jones S. Conserved RNA structures in the non-canonical Hac1/Xbp1 intron. RNA biology. 2011;8(4):552-6.
211. Mori K, Kawahara T, Yoshida H, Yanagi H, Yura T. Signalling from endoplasmic reticulum to nucleus: transcription factor with a basic-leucine zipper motif is required for the unfolded protein-response pathway. Genes to cells : devoted to molecular & cellular mechanisms. 1996;1(9):803-17.
212. Fordyce PM, Pincus D, Kimmig P, Nelson CS, El-Samad H, Walter P, et al. Basic leucine zipper transcription factor Hac1 binds DNA in two distinct modes as revealed by

microfluidic analyses. Proceedings of the National Academy of Sciences of the United States of America. 2012;109(45):E3084-93.
213. Mori K, Sant A, Kohno K, Normington K, Gething MJ, Sambrook JF. A 22 bp cis-acting element is necessary and sufficient for the induction of the yeast KAR2 (BiP) gene by unfolded proteins. 1992;11(7):2583-93.
214. Vembar SS, Brodsky JL. One step at a time: endoplasmic reticulum-associated degradation. Nature Reviews Molecular Cell Biology. 2008;9(12):944-57.
215. Thibault G, Ng DT. The endoplasmic reticulum-associated degradation pathways of budding yeast. Cold Spring Harbor perspectives in biology. 2012;4(12).
216. Molinari M. ER-phagy responses in yeast, plants, and mammalian cells and their crosstalk with UPR and ERAD. Developmental Cell. 2021;56(7):949-66.
217. Zhang J, Wu J, Liu L, Li J. The Crucial Role of Demannosylating Asparagine-Linked Glycans in ERADicating Misfolded Glycoproteins in the Endoplasmic Reticulum. 2021;11.
218. Plemper RK, Egner R, Kuchler K, Wolf DH. Endoplasmic reticulum degradation of a mutated ATP-binding cassette transporter Pdr5 proceeds in a concerted action of Sec61 and the proteasome. The Journal of biological chemistry. 1998;273(49):32848-56.
219. Pilon M, Schekman R, Römisch K. Sec61p mediates export of a misfolded secretory protein from the endoplasmic reticulum to the cytosol for degradation. The EMBO journal. 1997;16(15):4540-8.
220. Carvalho P, Stanley AM, Rapoport TA. Retrotranslocation of a misfolded luminal ER protein by the ubiquitin-ligase Hrd1p. Cell. 2010;143(4):579-91.
221. Jarosch E, Taxis C, Volkwein C, Bordallo J, Finley D, Wolf DH, et al. Protein dislocation from the ER requires polyubiquitination and the AAA-ATPase Cdc48. Nat Cell Biol. 2002;4(2):134-9.
222. Duve Cd, Wattiaux R. Functions of Lysosomes. 1966;28(1):435-92.
223. Urano F, Wang X, Bertolotti A, Zhang Y, Chung P, Harding HP, et al. Coupling of Stress in the ER to Activation of JNK Protein Kinases by Transmembrane Protein Kinase IRE1. 2000;287(5453):664-6.
224. Demirtas L, Guclu A, Erdur FM, Akbas EM, Ozcicek A, Onk D, et al. Apoptosis, autophagy & endoplasmic reticulum stress in diabetes mellitus. The Indian journal of medical research. 2016;144(4):515-24.
225. Hotamisligil GS. Endoplasmic reticulum stress and the inflammatory basis of metabolic disease. Cell. 2010;140(6):900-17.
226. Tadic V, Prell T, Lautenschlaeger J, Grosskreutz J. The ER mitochondria calcium cycle and ER stress response as therapeutic targets in amyotrophic lateral sclerosis. Frontiers in cellular neuroscience. 2014;8:147.
227. Tsai YC, Weissman AM. The Unfolded Protein Response, Degradation from Endoplasmic Reticulum and Cancer. Genes & cancer. 2010;1(7):764-78.
228. Sicking M, Lang S, Bochen F, Roos A, Drenth JPH, Zakaria M, et al. Complexity and Specificity of Sec61-Channelopathies: Human Diseases Affecting Gating of the Sec61 Complex. Cells. 2021;10(5):1036.
229. Lloyd DJ, Wheeler MC, Gekakis N. A point mutation in Sec61alpha1 leads to diabetes and hepatosteatosis in mice. Diabetes. 2010;59(2):460-70.
230. Schäuble N, Lang S, Jung M, Cappel S, Schorr S, Ulucan Ö, et al. BiP-mediated closing of the Sec61 channel limits Ca2+ leakage from the ER. The EMBO journal. 2012;31(15):3282-96.

Chapter 2

General Methodology

Growth Conditions

S. cerevisiae were grown in Yeast Peptone (YP) media (1% w/v yeast extract, 2% w/v peptone) supplemented with 2% w/v D-glucose (YPD) or minimal media (0.67% w/v yeast nitrogen base, 0.5% w/v Ammonium Sulphate (Difco©, BD)) supplemented with 2% w/v D-glucose (YNB), 0.002% w/v amino acids (100x stock; Leu, His, Lys, Ura, Trp, Ade) and lacking in one or more of the essential amino acids used as a selectable marker on a plasmid at either 30°C or 37°C. Counter selection of *URA3* selective plasmids was achieved by the addition of 5-Fluoroorotic Acid (5-FOA) at 1 mg/mL. *E. coli* was cultured in Luria Bertani (LB) media (0.5% w/v yeast extract, 1% w/v tryptone, 1% w/v NaCl) at 37°C with the addition of 110 µg/mL ampicillin when selecting for transformants. Solid media was made by supplementing with 2% w/v bacteriological agar. The Biophotometer Plus (Eppendorf) was utilised to assess growth via Optical density (OD) at 600 nm. All media were from FORMEDIUM (Hunstanton, U.K.). For growth assays yeast were spotted in a 10-fold dilution series on YPD agar and grown at either 30°C, 34°C or 37°C for 2-3 days.

Yeast Transformation

Cells grown overnight were isolated via centrifugation at 3000g for 10 minutes at 4°C, resuspended in 5 mL of LTE buffer (100 mM lithium acetate (LiOAc), 10 mM Tris.acetate, pH 7.4, 1 mM EDTA) and incubated at 30°C for 1 hour with shaking. Cells were isolated as before and resuspended in 0.2 mL of LTE buffer. Transformation reactions consisted of 34 µL of yeast cells, 6 µL of single-stranded DNA (8 mg/mL salmon sperm DNA dissolved in LTE), up to 2 µL of plasmid/PCR and 200 µL of LTE PEG (LTE containing 40% w/v PEG4000), vortexed and then incubated

at room temperature for ~30 minutes. Finally, cells were heat shocked for 15-30 minutes at 42°C and then immediately plated on the appropriate selective media.

Isolation of Yeast Genomic DNA

Yeast was grown to saturation, OD_{600nm}>4 and isolated by centrifugation at 3000g for 3 minutes. Cells were resuspended in 0.5 mL of water, transferred to a 1.5 mL microfuge tube and then centrifuged at 11,000g for 5 minutes at room temperature. Cells were retained and resuspended in 0.2 mL of buffer A (2% v/v Triton X-100, 100 mM NaCl, 10 mM Tris.HCl, 1 mM EDTA pH 8.0), and 200 µL of acid washed beads and 0.2 mL of phenol:chloroform:isoamyl alcohol (25:24:1) (PCI) was added. Samples were homogenised with the FastPrep-24™ 5G (6.0m/sec for 40sec). After microcentrifugation (described above) the aqueous layer was transferred to a new tube containing 0.2 mL of PCI and vortexed. This was repeated twice with chloroform instead of PCI and 0.2 mL of TE (10 mM Tris.HCl, pH 8, 1 mM EDTA) was added to the final extraction. 40 µL of 3M NaOAc pH 5.2 and 1 mL 100% EtOH was added to each aqueous sample and incubated at -20°C for 20 minutes. Samples were centrifuged at 11,000 g for 5 minutes at room temperature and the pellet was washed with 500 µL of 70% EtOH. Following a final spin at 11,000 g for 5 minutes the pellet was left to dry and resuspended in 100 µL of sterile H_2O.

DNA Sequencing

Big Dye PCR reactions were setup as 10 µL reactions containing 1 µL BigDye, 1.5 µL 5xBigDye buffer, 1.5 µL water, 0.32 µL of an appropriate primer, and either ~40ng PCR product or ~300ng plasmid DNA as template. After amplification, 1 µL of 125mM EDTA, 1 µL of 3M sodium acetate and 25 µL of 100% ethanol was added to the reaction mixture which was then incubated at room temperature for 25 minutes. Samples were then centrifuged at 18,000g for 28 minutes at room temperature, the pellet washed in 125 µL of 70% ethanol and then centrifuged at 18,000g at room temperature for a further 5 minutes. The supernatant was

discarded with the pellets left to dry in the dark. Samples were taken to Murdoch University SABC sequencing facility where the sequencing was performed.

Cell Lysates from Yeast Strains

Yeast cells were grown to mid-log phase ($OD_{600nm} \leq 1$) and 10 OD_{600nm} of cells were isolated by centrifugation at 3000 g for 3 minutes at 4°C, washed twice in 1 mL of sterile H_20 and transferred to a 1.5 mL screw top tube and centrifuged, isolating cells. Laemmli Buffer (63 mM Tris pH6.8, 10% glycerol, 5% β-mercaptoethanol, 2% SDS, 0.005% bromophenol blue) was added to cells at 200 µL per 10 OD_{600} in combination with acid washed beads to the meniscus. Samples were heated to 95°C for 5 minutes and cell lysis achieved utilising the FastPrep-24™ 5G (6.0m/sec for 40sec). The samples were then heated for a second time at 95°C for 5 minutes before loading onto a polyacrylamide gel or storage at -20°C.

Immunoblotting

Gels were run with SDS running buffer at 25 mA with 5-10 µL of sample used alongside 2 µL of protein ladder. Samples underwent semi-dry transfer at 150 mA, 25 V for 1.5 hrs to PVDF membranes. After transfer, membranes were blocked for ≥30 minutes in TBST (130 mM NaCl, 2.6mM KCl, 2 mM Tris pH 7.6, 0.1% v/v tween 20) containing 5% w/v skim milk powder (TBSTM) with shaking. Primary antibody was applied with TBSTM at designated concentrations and left for ≥2 hours with shaking. Membranes were washed three times in TBST for 5-10mins with shaking. Blots were incubated with secondary antibody for an hour with shaking. Following another wash done as previously, SuperSignal® West Pico chemiluminescent substrate (Thermo Scientific) was applied to develop the blot which was then visualised using the ChemiDoc™ MP System (BioRad).

β-Galactosidase Assays

β-Galactosidase assays were performed according to Tyson and Stirling 2000 (1). Briefly, yeast cells were grown at 30 °C in minimal medium containing 2% glucose and appropriate supplements. Cultures were diluted to an $A_{600\ nm}$ of 0.2 and grown for a further 4 h. Cells were isolated and resuspended in 2 mL of Z buffer (60 mM Na_2HPO_4, 40 mM NaH_2PO_4, 10 mM KCl, 10 mM $MgSO_4$, 50 mM 2-mercaptoethanol, pH 7.0). Aliquots (0.8 mL) were collected, cells were permeabilised in 50 µL of 0.1% (w/v) SDS and 100 µL of $CHCl_3$, and samples were equilibrated to 30°C. Assays were initiated by addition of 160 µL of o-nitrophenyl-galactopyranoside (4 mg/mL stock solution in Z buffer) and incubated at 30°C for 20 min. Reactions were terminated by addition of 400 µL of 1 M Na_2CO_3, pH 9.0, the $OD_{420\ nm}$ was measured, and LacZ activity (U) was calculated by multiplying $OD_{420\ nm}/OD_{600\ nm}$ by 1000. Three independent biological replicates and at least two technical replicates were performed.

Membrane Preparation

Yeast were grown in YPD to OD_{600nm} = 0.5 - 2, harvested by centrifugation at 3000g for 3 minutes at 4°C. The harvested cells were then washed with 10 mL of resuspension buffer (100 mM Tris.SO_4 pH 9.4, 10 mM DTT) before being resuspended in this buffer at 1 mL per 50 OD_{600nm} and incubated at room temperature for 10 minutes. Cells were isolated by centrifugation at 3000g for 5 minutes at 4°C and resuspended in spheroplast buffer (0.7 M sorbitol, 0.5% w/v glucose, 50 mM Tris.HCl pH 7.4) at 1 mL per 100 OD_{600nm} plus 1.5 U of lyticase per OD_{600nm} and Phenylmethylsulfonyl fluoride (PMSF) at 10 µL per mL of buffer (PMSF was added to all subsequent buffers) and incubated at 30°C for 30 minutes. Following centrifugation at 2500g for 5mins at 4°C the spheroplasts were resuspended in ice cold lysis buffer (0.1 M sorbitol, 50 mM KOAc, 20 mM HEPES pH 7.4, 2 mM EDTA, 1 mM DTT) at 1 mL per 200 OD_{600nm}. Acid washed beads were then added to approximately 75% of the sample volume and samples were vortexed at 30 second intervals for 5 cycles. This was followed by centrifugation at 1000g for 10

minutes at 4°C to remove debris. The soluble fraction was retained and then centrifuged at 10000g for 20 minutes at 4°C to isolate membranes. The pellet was washed twice in 1 mL of ice-cold membrane storage buffer (250 mM sorbitol, 20 mM HEPES pH 7.4, 50 mM KOAc, 1 mM DTT, 2 mM MgOAc) and then resuspended in a final volume of 1 mL per 50 OD_{280nm} and snap frozen until use.

DSS Cross-linking

Yeast microsomes were prepared according to Rothblatt and Meyer, 1986 (2). Microsomes were incubated at 30°C for 30 min in the presence of either 1 mM DSS or equivalent volume of DMSO. The addition of 10 mM lysine and 10 mM Tris (final concentration) supplied excess amine groups to quench the reaction. Crosslinking was assessed through subsequent SDS PAGE, transfer and immunoblot.

Solubilisation of Membranes with Digitonin

Two O_{D280nm} units of microsomes were harvested by centrifugation at 10,000 g for 5 minutes at 4°C. The membrane pellet was resuspended in 100 µL of solubilisation buffer (S-buffer; 2% digitonin, 250 mM NaCl, 2 mM DTT, 30 mM Tris.HCl pH 7.6, 5 mM MgOAc, 12% glycerol, 1% v/v PIC) and incubated for 30 minutes on ice. Samples were centrifuged at 10,000g for 15 minutes after which the soluble fraction was retained and subject to ultracentrifugation at 400,000g for 1 hour to separate the ribosome associated material. Finally, the soluble fraction was retained and diluted to a total volume of 180 µL with S-buffer without NaCl and digitonin.

ConA Dependent Fractionation of SEC Proteins

The fractionation of SEC proteins by ConA was performed according to Pilon et al., 1998 (3). Briefly, microsomes were isolated and resuspended in 100 µL of solubilisation buffer (50 mM HEPES/KOH, pH 7.4, 400 mM KAc, 5 mM MgAc, 10% [wt/vol] glycerol, 0.05% [vol/vol] β-mercaptoethanol) on ice containing protease

inhibitors (5 µg/mL leupeptin, 0.5 µg/mL pepstatin, 1 mM amino-benzamidine, 2.5 µg/mL chymostatin, and 0.1 mM PMSF). Membranes were solubilised by the addition of 400 µL solubilisation buffer containing 3.75% (wt/vol) digitonin. Next, samples were centrifuged at 100,000 x g in a Beckman TLA100.3 rotor for 60 min at 4°C to isolate the ribosome attached membrane proteins (RAMPs). The supernatant fraction was added to 100 µL of a suspension of concanavalin A (Con-A)-Sepharose equilibrated in 50 mM HEPES/KOH (pH 7.4), 10% (wt/vol) glycerol, 0.05% (vol/vol) β-mercaptoethanol, 1% (wt/vol) digitonin, and protease inhibitors, and incubated for 60 mins at 4°C. The beads were recovered by centrifugation at 2500 × g and the supernatant fraction was cleared from any remaining beads at 12,000 × g (free fraction). The Con-A beads were washed three times with 1 mL of equilibration buffer. Equal aliquots of both fractions were analysed by SDS-PAGE and immunoblotting with the indicated antibodies.

Blue Native PAGE Analysis

BN-PAGE was performed according to Jermy et al., 2006 (4). Two A280nm units of microsomes were harvested by centrifugation at 10,000 × g, resuspended in 100 µL of S-buffer (20 mM Tris-HCl, pH 7.6, 250 mM NaCl, 2 mM dithiothreitol, 5 mM MgOAc, 2% digitonin, 12% glycerol, 1% (v/v) protease inhibitor mixture (Sigma)) and then incubated on ice for 30 min. The insoluble material was removed by centrifugation at 10,000 × g, and then ribosomes were removed by centrifugation for 60 min at 400,000 × g. The supernatant was then diluted to 180 µL with S-buffer without NaCl and digitonin, followed by the addition of 20 µL of 10× sample buffer (5% Coomassie Brilliant Blue G250, 500 mM 6-aminocaproic acid, 100 mM Bistris-HCl, pH 7.0). 0.8 A280nm unit aliquots were loaded onto a 6–16% polyacrylamide gradient gel (buffered with 500 mM 6-aminocaproic acid, 50 mM Tris-HCl, pH 7.0). The samples were run at 200 V for 18 h with Coomassie-containing cathode buffer (50 mM Tricine, pH 7.0, 15 mM Bistris-HCl, pH 7.0, 0.02% Coomassie Brilliant Blue G250) and then for a further 3 h at 500 V in buffer lacking Coomassie (50 mM Tricine, pH 7.0, 15 mM Bistris-HCl, pH 7.0). Anode buffer (50 mM Bistris-HCl, pH 7.0) was constant throughout. The samples were then transferred to polyvinylidene

difluoride membrane and analysed by Western blotting. Complex sizes were determined using the high molecular weight calibration kit for native electrophoresis (Amersham Biosciences).

Cycloheximide Chase Analysis

Yeast cells were grown in YPD overnight at 30°C. Overnight cultures were then diluted back to 0.2 OD_{600nm} in 15 mL of fresh medium and left to recover until they reach log growth phase (0.8-1.2 OD_{600nm}). When cells have reached log growth, 2 OD_{600nm} of cells were collected for each time point that was to be taken. Cells were centrifuged at 3000g for 3 mins and the supernatant was subsequently discarded. Cell pellets were then resuspended in fresh YPD to reach the desired 2 OD_{600nm} culture which was placed back at 30°C for 5 mins to re-equilibrate. To initiate the chase, cultures were treated with cycloheximide (chx) to final concentration of 250 ug/mL and timer swiftly started following treatment to the first sample, with chx added to subsequent samples in 30 sec intervals. Following a 10-minute pre-treatment, 950 ul of cells were collected every 30 minutes, over a 90-minute time course and placed in a screw cap tube on ice with 50 µL of 20x stop mix (200 mM sodium azide, 5 mg/mL bovine serum albumin). Samples were processed as soon as possible following collection, in-between collection time point as per the cell lysate protocol and then placed at -80°C until all samples were processed and ready to be run on polyacrylamide gels. Samples were resolved on 15% polyacrylamide gels and then immunoblotted as described above.

Mutagenesis and Selection for *SEC61* Suppressors of the *sss1-7* TS Phenotype

EP-PCR was carried out with Taq DNA polymerase in the presence of 500 µM $MnCl_2$ and run for 10 cycles. Reactions were also performed with inverse dNTP concentrations. Samples were pooled after EP-PCR and digested with *Hind III* for 1 hour at 37°C. *sss1-7* yeast were transformed with restricted PCR product and transformants were plated on YPD agar and incubated at 37°C for up to 5 days. The *SEC61* locus of suppressor colonies was sequenced, and individual mutations were

introduced in pBW11 by site-directed mutagenesis using the Q5® Site Directed Mutagenesis Protocol (NEB).

Fluorescence Microscopy

The GFP ORF was amplified with oligonucleotides flanked with 5' *PacI* and 3' *SphI* and ligated into pJKB2 in which nucleotides -8 to -1 and 1 to 6 were mutated to encode *PacI* and *SphI* restriction sites respectively giving pLB4 (YCp GFP-*SSS1*). The *sss1-6* and *sss1-7* mutations were incorporated into pLB4 using the Q5® Site Directed Mutagenesis Protocol (NEB) givig pLB5 and pLB6 respectively. Oligonucleotides used are listed in Table 1.3. Static images were collected of live cells attached to a concanavalin A-coated slide using an Ultraview Spinning Disk Confocal Microscope (Perkin Elmer Life Sciences).

Glutathione Sensitive Growth Assay

Yeast strains containing the Yep *HGT1* were cultured at 30°C to mid-logarithmic phase. Sub-cultures at 0.01 OD_{600nm} in SC medium were produced omitting uracil and with the addition of 0-10 µM of L-reduced glutathione. Growth was followed and recorded at several key time points. Three independent biological replicates and at least two technical replicates were performed. These results were averaged with each concentration compared as a factor of the 0 µM result.

Invertase Secretion

Cells were grown in YPD (2% glucose) at 30°C, cultures were split, and cells incubated at 30°C or 37°C for 1h in YPD (2% glucose). Cells were then pelleted (2000g), washed twice with pre-warmed low glucose (0.1% glucose) YPD, resuspended in the low glucose YPD medium, and incubated as before for 1.5 hrs. To halt trafficking, samples were adjusted to 10mM NaN3, and incubated on ice. The samples were washed 3X with 500 µL ice-cold 10mM NaN3 and re-suspended in 500 µL of the same. The samples were split into 10mM NaN3 buffers ± 0.2 %

Triton X-100 (final) with the Triton-solubilised fractions also being subjected to one cycle of freeze-thaw to generate the permeabilised cell fraction. The partner non-permeabilised and permeabilised samples were used to determine extracellular and total invertase activities, respectively. The pool of secreted invertase is expressed as a fraction.

Reverse Transcription (RT)-PCR

Total RNA was isolated from cells using the FavorPrepTM blood cultured cell total RNA mini-Kit and 1 µg was used to template reverse transcription using WarmStart® RTx Reverse Transcriptase to generate cDNA (20 µL final volume). H_2O was used in no RT controls. To analyse *HGT1*, *PMR1* or *ACT1* expression, PCR was performed using 1 µL of cDNA fraction as template and specific oligonucleotides as primers. Products were quantified with Image J software.

Chapter 2 Tables

Table 1.1. Yeast strains used in this study.

Yeast	Genotype	Reference
BWY12	*MATα ade2- 1 ura3-1 his3-11,15 trp1-1 leu2-3,112 can1-100 sec61Δ::HIS3* pBW7	Wilkinson et al. 1997 (5)
BWY530	*MATα ade2- 1 ura3-1 his3-11,15 trp1-1 leu2-3,112 can1-100 sss1Δ::KanMX4* FKp53	Wilkinson et al. 2010 (6)
BWY531	*MATa ade2- 1 ura3-1 his3-11,15 trp1-1 leu2-3,112 can1-100 sss1Δ::KanMX4* FKp53	Wilkinson et al. 2010 (6)
SSS1	*MATα ade2- 1 ura3-1 his3-11,15 trp1-1 leu2-3,112 can1-100 sss1Δ::KanMX4* pJKB2	Wilkinson et al. 2010 (6)
SSS1-3	*MATα ade2- 1 ura3-1 his3-11,15 trp1-1 leu2-3,112 can1-100 sss1Δ::KanMX4* pHD1	This study
SSS1-4	*MATα ade2- 1 ura3-1 his3-11,15 trp1-1 leu2-3,112 can1-100 sss1Δ::KanMX4* pHD2	This study
SSS1-5	*MATα ade2- 1 ura3-1 his3-11,15 trp1-1 leu2-3,112 can1-100 sss1Δ::KanMX4* pHD3	This study
sss1-6	*MATα ade2- 1 ura3-1 his3-11,15 trp1-1 leu2-3,112 can1-100 sss1Δ::KanMX4* pJKB16	This study
sss1-7	*MATα ade2- 1 ura3-1 his3-11,15 trp1-1 leu2-3,112 can1-100 sss1Δ::KanMX4* pCM205	This study
CMY5	*MATα ade2- 1 ura3-1 his3-11,15 trp1-1 leu2-3,112 can1-100 sec61Δ::HIS3 sss1Δ::KanMX4* YCp *SEC61 SSS1 URA3*	This study
CWY1	*sss1-7* + YCp *SEC61*^{V82F} (pCW2)	This study
CWY2	*sss1-7* + YCp *SEC61*^{S289F} (pCW3)	This study
CWY3	*sss1-7* + YCp *SEC61*^{N302K} (pCW4)	This study
CWY4	*sss1-7* + YCp *SEC61*^{N302Y} (pCW5)	This study
CWY5	*sss1-7* + YCp *SEC61*^{T379A} (pCW6)	This study

CWY6	*sss1-7* + YCp *SEC61*^{N302L} (pCW7)	This study
CWY8	*sss1-7* + YCp *SEC61*^{V82F} (pCW2) + pJT30	This study
CWY9	*sss1-7* + YCp *SEC61*^{S289F} (pCW3) + pJT30	This study
CWY10	*sss1-7* + YCp *SEC61*^{N302K} (pCW4) + pJT30	This study
CWY11	*sss1-7* + YCp *SEC61*^{N302Y} (pCW5) + pJT30	This study
CWY12	*sss1-7* + YCp *SEC61*^{T379A} (pCW6) + pJT30	This study
CWY13	*sss1-7* + YCp *SEC61*^{N302L} (pCW7) + pJT30	This study
CWY15	*sss1-6* + YCp *SEC61*^{V82F} (pCW2) + pCW10	This study
CWY16	*sss1-6* + YCp *SEC61*^{S289F} (pCW3) + pCW10	This study
CWY17	*sss1-6* + YCp *SEC61*^{N302K} (pCW4) + pCW10	This study
CWY18	*sss1-6* + YCp *SEC61*^{N302Y} (pCW5) + pCW10	This study
CWY19	*sss1-6* + YCp *SEC61*^{T379A} (pCW6) + pCW10	This study
CWY20	*sss1-6* + YCp *SEC61*^{N302L} (pCW7) + pCW10	This study
CWY22	*sss1-6* + YCp *SEC61*^{V82F} (pCW2) + pJT30	This study
CWY23	*sss1-6* + YCp *SEC61*^{S289F} (pCW3) + pJT30	This study
CWY24	*sss1-6* + YCp *SEC61*^{N302K} (pCW4) + pJT30	This study
CWY25	*sss1-6* + YCp *SEC61*^{N302Y} (pCW5) + pJT30	This study
CWY26	*sss1-6* + YCp *SEC61*^{T379A} (pCW6) + pJT30	This study
CWY27	*sss1-6* + YCp *SEC61*^{N302L} (pCW7) + pJT30	This study
CWY29	*MATα ade2- 1 ura3-1 his3-11,15 trp1-1 leu2-3,112 can1-100 sec61Δ::HIS3* pCW8	This study
CWY30	*MATα ade2- 1 ura3-1 his3-11,15 trp1-1 leu2-3,112 can1-100 sec61Δ::HIS3 sss1Δ::KanMX4* pBW11 pLB1	This study
CWY31	*MATα ade2- 1 ura3-1 his3-11,15 trp1-1 leu2-3,112 can1-100 sec61Δ::HIS3 sss1Δ::KanMX4* pCW8 pLB1	This study
CWY32	*MATα ade2- 1 ura3-1 his3-11,15 trp1-1 leu2-3,112 can1-100 sec61Δ::HIS3 sss1Δ::KanMX4* pBW11 pLB2	This study

CWY33	*MATα ade2- 1 ura3-1 his3-11,15 trp1-1 leu2-3,112 can1-100 sec61Δ::HIS3 sss1Δ::KanMX4* pCW8 pLB2	This study
CWY34	*MATα ade2- 1 ura3-1 his3-11,15 trp1-1 leu2-3,112 can1-100 sec61Δ::HIS3 sss1Δ::KanMX4* pBW11 pLB3	This study
CWY35	*MATα ade2- 1 ura3-1 his3-11,15 trp1-1 leu2-3,112 can1-100 sec61Δ::HIS3 sss1Δ::KanMX4* pCW8 pLB3	This study
CWY36	*MATα ade2- 1 ura3-1 his3-11,15 trp1-1 leu2-3,112 can1-100 sec61Δ::HIS3* YCp *SEC61* (pBW11)	This study
CWY37	*MATα ade2- 1 ura3-1 his3-11,15 trp1-1 leu2-3,112 can1-100 sec61Δ::HIS3* YCp *SEC61*^{V82F} (pCW2)	This study
CWY38	*MATα ade2- 1 ura3-1 his3-11,15 trp1-1 leu2-3,112 can1-100 sec61Δ::HIS3* YCp *SEC61*^{S289F} (pCW3)	This study
CWY39	*MATα ade2- 1 ura3-1 his3-11,15 trp1-1 leu2-3,112 can1-100 sec61Δ::HIS3* YCp *SEC61*^{N302K} (pCW4)	This study
CWY40	*MATα ade2- 1 ura3-1 his3-11,15 trp1-1 leu2-3,112 can1-100 sec61Δ::HIS3* YCp *SEC61*^{N302Y} (pCW5)	This study
CWY41	*MATα ade2- 1 ura3-1 his3-11,15 trp1-1 leu2-3,112 can1-100 sec61Δ::HIS3* YCp *SEC61*^{T379A} (pCW6)	This study
CWY42	*MATα ade2- 1 ura3-1 his3-11,15 trp1-1 leu2-3,112 can1-100 sec61Δ::HIS3* YCp *SEC61*^{N302L} (pCW7)	This study

CWY43	*MATα ade2- 1 ura3-1 his3-11,15 trp1-1 leu2-3,112 can1-100 sss1Δ::KanMX4* pLB4 pSM1960	This study
CWY44	*MATα ade2- 1 ura3-1 his3-11,15 trp1-1 leu2-3,112 can1-100 sss1Δ::KanMX4* pLB5 pSM1960	This study
CWY45	*MATα ade2- 1 ura3-1 his3-11,15 trp1-1 leu2-3,112 can1-100 sss1Δ::KanMX4* pLB6 pSM1960	This study
sss1-8	*MATα ade2- 1 ura3-1 his3-11,15 trp1-1 leu2-3,112 can1-100 sss1Δ::KanMX4* pCW11	This study
sss1-KI	*MATα ade2- 1 ura3-1 his3-11,15 trp1-1 leu2-3,112 can1-100 sss1Δ::KanMX4* pCW12	This study
sss1-KE	*MATα ade2- 1 ura3-1 his3-11,15 trp1-1 leu2-3,112 can1-100 sss1Δ::KanMX4* pCW13	This study
sss1-AV	*MATα ade2- 1 ura3-1 his3-11,15 trp1-1 leu2-3,112 can1-100 sss1Δ::KanMX4* pCW14	This study
sss1-LF	*MATα ade2- 1 ura3-1 his3-11,15 trp1-1 leu2-3,112 can1-100 sss1Δ::KanMX4* pCW15	This study
sss1-VT	*MATα ade2- 1 ura3-1 his3-11,15 trp1-1 leu2-3,112 can1-100 sss1Δ::KanMX4* pCW16	This study
sss1-6 KI	*MATα ade2- 1 ura3-1 his3-11,15 trp1-1 leu2-3,112 can1-100 sss1Δ::KanMX4* pCW17	This study
sss1-6 KE	*MATα ade2- 1 ura3-1 his3-11,15 trp1-1 leu2-3,112 can1-100 sss1Δ::KanMX4* pCW18	This study
sss1-6 AV	*MATα ade2- 1 ura3-1 his3-11,15 trp1-1 leu2-3,112 can1-100 sss1Δ::KanMX4* pCW19	This study
sss1-6 LF	*MATα ade2- 1 ura3-1 his3-11,15 trp1-1 leu2-3,112 can1-100 sss1Δ::KanMX4* pCW20	This study
sss1-6 VT	*MATα ade2- 1 ura3-1 his3-11,15 trp1-1 leu2-3,112 can1-100 sss1Δ::KanMX4* pCW21	This study
sss1-7 KI	*MATα ade2- 1 ura3-1 his3-11,15 trp1-1 leu2-3,112 can1-100 sss1Δ::KanMX4* pCW22	This study

sss1-7 KE	*MATα ade2- 1 ura3-1 his3-11,15 trp1-1 leu2-3,112 can1-100 sss1Δ::KanMX4 pCW23*	This study
sss1-7 AV	*MATα ade2- 1 ura3-1 his3-11,15 trp1-1 leu2-3,112 can1-100 sss1Δ::KanMX4 pCW24*	This study
sss1-7 LF	*MATα ade2- 1 ura3-1 his3-11,15 trp1-1 leu2-3,112 can1-100 sss1Δ::KanMX4 pCW25*	This study
sss1-7 VT	*MATα ade2- 1 ura3-1 his3-11,15 trp1-1 leu2-3,112 can1-100 sss1Δ::KanMX4 pCW26*	This study
CWY46	*sss1-8* + YCp *SEC61* (pBW11)	This study
CWY47	*sss1-8* + YCp *SEC61*^{N302K} (pCW4)	This study
CWY48	*sss1-8 +* YCp *SEC61*^{N302L} (pCW7)	This study
CWY49	*sss1-8 +* YCp *SEC61*^{Q48A} (pCW27)	This study
CWY50	*sss1-6 KE* + pRS315	This study
CWY51	*sss1-6 KE* + YCp *SEC61* (pBW11)	This study
CWY52	*sss1-6 KE + YCp SEC61*^{N302L} (pCW7)	This study
CWY53	*sss1-6 KE* + YCp *SEC61*^{N302K} (pCW4)	This study
CWY54	*sss1-7 KE* + pRS315	This study
CWY55	*sss1-7 KE* + YCp *SEC61* (pBW11)	This study
CWY56	*sss1-7 KE* + YCp *SEC61*^{N302L} (pCW7)	This study
CWY57	*sss1-7 KE* + YCp *SEC61*^{N302K} (pCW4)	This study
CWY58	*SSS1*+ YCp *SEC61* (pBW11) + pJT30	Witham et al., 2020 (7)
CWY59	*sss1-6* + YCp *SEC61* (pBW11) + pJT30	Witham et al., 2020 (7)

CWY60	*sss1-7* + YCp *SEC61* (pBW11) + pJT30	Witham et al., 2020 (7)
CWY61	*sss1-6 LF* + YCp *SEC61* (pBW11) + pJT30	This study
CWY62	*sss1-7 LF* + YCp *SEC61* (pBW11) + pJT30	This study
CWY63	*sss1-6 AV* + YCp *SEC61* (pBW11) + pJT30	This study
CWY64	*sss1-7 AV* + YCp *SEC61* (pBW11) + pJT30	This study
CWY65	*sss1-7 VT* + YCp *SEC61* (pBW11) + pJT30	This study
CWY66	*sss1-8* + YCp *SEC61* (pBW11) + pJT30	This study
CWY67	*sss1-8* + YCp *SEC61*^{N302K} (pCW4) + pJT30	This study
CWY68	*sss1-8* + YCp *SEC61*^{N302L} (pCW7) + pJT30	This study
CWY69	*sss1-8* + YCp *SEC61*^{Q48A} (pCW27) + pJT30	This study
CWY70	*SSS1* + YCp *SEC61* (pBW11) + pCW10	Witham et al., 2020 (7)
CWY71	*sss1-6* + YCp *SEC61* (pBW11) + pCW10	Witham et al., 2020 (7)
CWY72	*sss1-7* + YCp *SEC61* (pBW11) + pCW10	Witham et al., 2020 (7)
CWY73	*sss1-6 LF* + YCp *SEC61* (pBW11) + pCW10	This study
CWY74	*sss1-7 LF* + YCp *SEC61* (pBW11) + pCW10	This study
CWY75	*sss1-6 AV* + YCp *SEC61* (pBW11) + pCW10	This study
CWY76	*sss1-7 AV* + YCp *SEC61* (pBW11) + pCW10	This study
CWY77	*sss1-7 VT* + YCp *SEC61* (pBW11) + pCW10	This study
CWY78	*sss1-8* + YCp *SEC61* (pBW11) + pCW10	This study

CWY79	*sss1-8* + YCp *SEC61*^{N302K} (pCW4) + pCW10	This study
CWY80	*sss1-8* + YCp *SEC61*^{N302L} (pCW7) + pCW10	This study
CWY81	*sss1-8* + YCp *SEC61*^{Q48A} (pCW27) + pCW10	This study
CWY82	*sss1-7 +* YCp *SEC61*^{G262E} (pCW31)	This study
CWY83	*sss1-7 +* YCp *SEC61*^{L449M} (pCW32)	This study
CWY84	*MATα ade2- 1 ura3-1 his3-11,15 trp1-1 leu2-3,112 can1-100 sec61Δ::HIS3* YCp *SEC61*^{G262E} (pCW31)	This study
CWY85	*MATα ade2- 1 ura3-1 his3-11,15 trp1-1 leu2-3,112 can1-100 sec61Δ::HIS3* YCp *SEC61*^{L449M} (pCW32)	This study
BY4742	*MATα his3Δ1 leu2Δ0 lys2Δ0 ura3Δ0*	Winston et al. 1995 (8)
BWY530t	*MATa ade2- 1 ura3-1 his3-11,15 trp1-1 leu2-3,112 can1-100 sss1Δ::TRP1* FKp53	This study
PRY14	*MATα ade2- 1 ura3-1 his3-11,15 trp1-1 leu2-3,112 can1-100 ssh1Δ::kanMX4, HIS3-pMET3-SEC61*	This study
sss1^{P74A}	*MATα ade2- 1 ura3-1 his3-11,15 trp1-1 leu2-3,112 can1-100 sss1Δ::KanMX4* pCW28	This study
sss1^{I75A}	*MATα ade2- 1 ura3-1 his3-11,15 trp1-1 leu2-3,112 can1-100 sss1Δ::KanMX4* pCW29	This study
sss1$^{K20R, K38R}$	*MATα ade2- 1 ura3-1 his3-11,15 trp1-1 leu2-3,112 can1-100 sss1Δ::KanMX4* pCW30	This study
lhs1Δ	*MATα his3Δ1 leu2Δ0 lys2Δ0 ura3Δ0 lhs1Δ::KanMX4*	Winzeler et al. 1999 (9)
pmr1Δ	*MATα his3Δ1 leu2Δ0 lys2Δ0 ura3Δ0 pmr1Δ::KanMX4*	Winzeler et al. 1999 (9)

hrd1Δ	*MATα his3Δ1 leu2Δ0 lys2Δ0 ura3Δ0 hrd1Δ::KanMX4*	Winzeler et al. 1999 (9)
der1Δ	*MATα his3Δ1 leu2Δ0 lys2Δ0 ura3Δ0 der1Δ::KanMX4*	Winzeler et al. 1999 (9)
usa1Δ	*MATα his3Δ1 leu2Δ0 lys2Δ0 ura3Δ0 usa1Δ::KanMX4*	Winzeler et al. 1999 (9)
ubc7Δ	*MATα his3Δ1 leu2Δ0 lys2Δ0 ura3Δ0 ubc71Δ::KanMX4*	Winzeler et al. 1999 (9)
doa10Δ	*MATα his3Δ1 leu2Δ0 lys2Δ0 ura3Δ0 doa10Δ::KanMX4*	Winzeler et al. 1999 (9)
530t *hrd1Δ*	*MATa ade2- 1 ura3-1 his3-11,15 trp1-1 leu2-3,112 can1-100 sss1Δ::TRP1 hrd1Δ::KanMX6*	This study
530t *doa10Δ*	*MATa ade2- 1 ura3-1 his3-11,15 trp1-1 leu2-3,112 can1-100 sss1Δ::TRP1 doa10Δ::KanMX6*	This study
530t *asi1Δ*	*MATa ade2- 1 ura3-1 his3-11,15 trp1-1 leu2-3,112 can1-100 sss1Δ::TRP1 asi1Δ::KanMX6*	This study
530t *cpr5Δ*	*MATa ade2- 1 ura3-1 his3-11,15 trp1-1 leu2-3,112 can1-100 sss1Δ::TRP1 cpr5Δ::KanMX6*	This study

Table 1.2. Plasmids used in this study.

Plasmid	Description	Reference
pJT30	UPRE-LacZ reporter	Tyson and Stirling, 2000 (1)
pBW11	YCp *SEC61 LEU2*	Wilkinson et al., 1997 (5)
pDR195	YEp *URA3* containing the *PMA1* promoter and *CYC1* terminator to enable high level gene expression.	Rentsch et al. 1995 (10)
pSM1960	YEp *SEC63*-mRFP *URA3*	Metzger et al., 2008 (11)
pJKB2	YCp *SSS1 HIS3*	Wilkinson et al., 2010. (6)
pJKB16	YCp *sss1*$^{P74A\ I75A}$ *HIS3*	This study
pCM203	YCp *SEC61 SSS1 URA3*	This study
pCM205	YCp *sss1*^{H72K} *HIS3*	This study
FKp52	YCp *SSS1 URA3*	Esnault et al., 1993 (12)
FKp53	YEp *SSS1 URA3*	Esnault et al., 1993 (12)
pFA6a-kanMX6	Kanamycin resistance cassette	Bähler et al., 1998 (13)
pRS316	Yeast centromeric *URA3* vector	Sikorski and Hieter., 1989 (14)
pCW2	YCp *SEC61*^{V82F} *LEU2*	This study
pCW3	YCp *SEC61*^{S289F} *LEU2*	This study
pCW4	YCp *SEC61*^{N302K} *LEU2*	This study
pCW5	YCp *SEC61*^{N302Y} *LEU2*	This study
pCW6	YCp *SEC61*^{T379A} *LEU2*	This study
pCW7	YCp *SEC61*^{N302L} *LEU2*	This study
pCW8	YCp *SEC61*^{N302D} *LEU2*	This study
pCW10	YEp *HGT1 URA3*	This study
pCW11	YCp *sss1*^{H72R} *HIS3*	This study
pCW12	YCp *sss1*^{K38I} *HIS3*	This study
pCW13	YCp *sss1*^{K41E} *HIS3*	This study
pCW14	YCp *sss1*^{A53V} *HIS3*	This study

pCW15	YCp *sss1*^{L70F} *HIS3*	This study
pCW16	YCp *sss1*^{V78T} *HIS3*	This study
pCW17	YCp *sss1*$^{K38I\ P74A\ I75A}$ *HIS3*	This study
pCW18	YCp *sss1*$^{K41E\ P74A\ I75A}$ *HIS3*	This study
pCW19	YCp *sss1*$^{A53V\ P74A\ I75A}$ *HIS3*	This study
pCW20	YCp *sss1*$^{L70F\ P74A\ I75A}$ *HIS3*	This study
pCW21	YCp *sss1*$^{V78T\ P74A\ I75A}$ *HIS3*	This study
pCW22	YCp *sss1*$^{K38I\ H72K}$ *HIS3*	This study
pCW23	YCp *sss1*$^{K41E\ H72K}$ *HIS3*	This study
pCW24	YCp *sss1*$^{A53V\ H72K}$ *HIS3*	This study
pCW25	YCp *sss1*$^{L70F\ H72K}$ *HIS3*	This study
pCW26	YCp *sss1*$^{V78T\ H72K}$ *HIS3*	This study
pCW27	YCp *SEC61*^{Q48A} *LEU2*	This study
pCW28	YCp *sss1*^{P74A} *HIS3*	This study
pCW29	YCp *sss1* ^{I75A} *HIS3*	This study
pCW30	YCp *sss1*$^{K20R\ K38R}$ *HIS3*	This study
pCW31	YCp *SEC61*^{G262E} *LEU2*	This study
pCW32	YCp *SEC61*^{L449M} *LEU2*	This study
pHD1	YCp *sss1*$^{I68A\ K69A}$ *HIS3*	This study
pHD2	YCp *sss1*$^{L70A\ I71A}$ *HIS3*	This study
pHD3	YCp *sss1*$^{H72A\ I73A}$ *HIS3*	This study
pLB1	YCp *SSS1 TRP1*	This study
pLB2	YCp *sss1*$^{P74A,\ I75A}$ *TRP1*	This study
pLB3	YCp *sss1*^{H72K} *TRP1*	This study
pLB4	Ycp GFP-*SSS1 HIS3*	This study
pLB5	Ycp GFP-*sss1*$^{P74A,\ I75A}$ *HIS3*	This study
pLB6	YCp GFP-*sss1*^{H72K} *HIS3*	This study

Table 1.3. Oligonucleotides used in this study.

Name	Sequence
M13_F	GTAAAACGACGGCCAGT
M13_R	CAGGAAACAGCTATGAC
SEC61 5'_F	CCGTGTTCTAGACTTGTTTAAGC
SEC61 V82F_F	AATTGGGTTTTTCGCCCATCATCAC
SEC61 G262E_F	ATATTTACAAGaaTTCCGTTACGAATTGCCCATC
SEC61 G262E_R	GTAACGGAAttCTTGTAAATATAAAACAAAGAGG
SEC61 V82F_R	CCAGTAAAGTACCACGGTTGG
SEC61 S289F_F	CTTTTATACTTtCAACACCCCAATCATGTT
SEC61 S289F_R	TGGGGTGTTGaAAGTATAAAAGAGTTTGAT
SEC61 N302K_F	CATTGACTTCTAAaATTTTCTTGATCTCTC
SEC61 N302K_R	CAAGAAAATtTTAGAAGTCAATGCACTCTG
SEC61 N302Y_F	CATTGACTTCTttCATTTTCTTGATCTCTC
SEC61 N302Y_R	CAAGAAAATGgaAGAAGTCAATGCACTCTG
SEC61 T379A_F	ATTTTCCAAGgCATGGATCGAAATCTCCGG
SEC61 T379A_R	TTCGATCCATGcCTTGGAAAATACTGCGCA
SEC61 L449M_F	CATCCATTaTGATGGCTACTACCACCATCTAC
SEC61 L448M_R	GTAGCCATCAtAATGGATGCCCCAGAACCTAA
SEC61 N302L_F	CATTGACTTCTctCATTTTCTTGATCTCTC
SEC61 N302L_R	CAAGAAAATGagAGAAGTCAATGCACTCTG
SEC61 N302D_F	CATTGACTTCTgaCATTTTCTTGATCTCTC
SEC61 N302D_R	CAAGAAAATGtcAGAAGTCAATGCACTCTG
SSS1 I68A K69A_F	TTACGCCgcCgcGTTGATTCATATTCCAAT
SSS1 I68A K69A_R	GAATCAACgcGgcGGCGTAACCAATGATAC
SSS1 L70A I71A_F	CATCAAGgcGgcTCATATTCCAATCAGATA
SSS1 L70A I71A_R	GAATATGAgcCgcCTTGATGGCGTAACCAA
SSS1 H72A I73A_F	GTTGATTgcTgcTCCAATCAGATACGTTAT
SSS1 H72A I73A_R	TGATTGGAgcAgcAATCAACTTGATGGCGT
SSS1 P74A I75A_F	GATTCATATTgCAgcCAGATACGTTATTGT
SSS1 P74A I75A _R	GTATCTGgcTGcAATATGAATCAACTTGAT

SSS1 H72K_F	AAGTTGATTaAaATTCCAATCAGATACGTTATTG
SSS1 H72K _R	TGATTGGAATtTtAATCAACTTGATGGCGTAAC
SphI pJKB2_F	gcatgcAGAGCTAGTGAAAAAGGTGAAGAG
pJKB2 PacI_R	ttaattaaTCAATGTTATACGTGATTTTATCTTTGG
PacI GFP_F	tttttttttaattaaatgAGTAAAGGAGAAGAACTTTTCAC
SphI GFP_R	tttttgcatgcTTTGTATAGTTCATCCATGCC
*HGT*1_F	ATATAGCGGCCGCATGAGTACCATTTATAGGGAGAGCG
*HGT*1_R	ATATAGGATCCTTACCACCATTTATCATAACC
SSS1 P74A I75A_F	GATTCATATTgCAgcCAGATACGTTATTGT
SSS1 P74A I75A_R	GTATCTGgcTGcAATATGAATCAACTTGAT
SSS1 H72K_F	AAGTTGATTaAaATTCCAATCAGATACGTTATTG
SSS1 H72K_R	TGATTGGAATtTtAATCAACTTGATGGCGTAAC
SSS1 K38I_F	AATTCTTGGCCAttTGTAAGAAACCTGATT
SSS1 K38I _R	TTCTTACAaaTGGCCAAGAATTGAGTACCT
SSS1 K41E_F	CAAGTGTAAGgAACCTGATTTGAAGGAATA
SSS1 K41E_R	CAAATCAGGTTCCTTACACTTGGCCAAGAA
SSS1 A53V_F	GATTGTCAAGGtTGTTGGTATTGGTTTTAT
SSS1 A53V_R	AATACCAACAaCCTTGACAATCTTGGTGTA
SSS1 L70F_F	CATCAAGTTtATTCATATTCCAATCAGATACG
SSS1 L70F_R	GCTGCAATATGAATaAACTTGATGGCGTAACC
SSS1 H72R_F	CATCAAGTTGATTagaATTCCAATCAGATACG
SSS1 H72R_R	ATTGGAATtctAATCAACTTGATGGCGTAACC
SSS1 V78T_F	CAGATACacTATTGTTTAAAAGAGATAAAAG
SSS1 V78T_R	TCTTTTAAACAATAgtGTATCTGATTGGAAT
SSS1 L70F P74A I75A_F	CATCAAGTTtATTCATATTGCAGCCAGATACG
SSS1 L70F P74A I75A_R	ATTGGAATATGAATaAACTTGATGGCGTAACC
SSS1 L70F H72K_F	CATCAAGTTtATTaAaATTCCAATCAGATACG
SSS1 L70F H72K_R	ATTGGAATtTtAATaAACTTGATGGCGTAACC
SSS1 V78T P74A I75A_R	TCTTTTAAACAATAgtGTATCTGGCTGGAAT
*HGT1*_qpcr_F	CCCAATTGGTAGGATACTGG
*HGT1*_qpcr_R	GTAAGACCTGCAGCACCATAAC

*PMR*1_qpcr_F	GGCAACCAAGATTCTCAACC
*PMR1*_qpcr_R	GCCATAGAATTTGCGCACTC
*ACT1*_qpcr_F	GCCTTCTACGTTTCCATCCA
*ACT1*_qpcr_R	GGCCAAATCGATTCTCAAAA
SSS1 P74A_FWD	GATTCATATTGCAATCAGATACGTTATTGTTTAAAAG
SSS1 P74A_RVS	AACGTATCTGATTGCAATATGAATCAACTTGATGGCG
SSS1 I75A_FWD	GATTCATATTCCAGCCAGATACGTTATTGTTTAAAAG
SSS1 I75A_RVS	AACGTATCTGGCTGGAATATGAATCAACTTGATGGCG
SSS1 K20R_FWD	CAACCAGGTTGAAAGGCTGGTTGAAGCACCTG
SSS1 K20R_RVS	CAACCAGCCTTTCAACCTGGTTGTTGCTCTGC
SSS1 K38R_FWD	CTTGGCCAGGTGTAAGAAACCTGATTTGAAGG
SSS1 K38R_RVS	GGTTTCTTACACCTGGCCAAGAATTGAGTACC
*HRD1*_FWD	GCTTCACCACTAGTTATACTGTCG
*HRD1*_RVS	GGTCAGACGTAGCTGATCGATGTAG
*DOA10*_FWD	GACCGATCTATGAAGCCATAAG
*DOA10*_RVS	CTTGAAAGCACTCGCACGCATAG
*ASI1*_KO_FWD	TTTTTTTCTTCTTTTTACAAAGAAACTATGCTAAGAATATGC GTACGCTGCAGGTCGAC
*ASI1*_KO_RVS	AAACCTCTTTTAGATACCATGCAAAAGTTCTTAAACTATTA ATCGATGAATTCGAGCTC
*CPR5*_KO_FWD	CAATAAACAAAAGGCACAGCGATATCCGCAATTATGCGTA CGCTGCAGGTCGAC
*CPR5*_KO_RVS	GCTGGCCTATACATCTCCTGAATAGTGATGCAGTTTACGAT GAATTCGAGCTCG
*HRD1*_Check_FWD	CGATAAATTTCCATACGTGCCG
*DOA10*_Check_FWD	CGCATCGATTGAGGACATTG
*CPR5*_Check_FWD	CCATCCTTACTACTTTCCTCGAGGAG
*ASI1*_Check_FWD	GGGAATACTCAGGTATCGTAAGATGC
*KAN*_Check_RVS	GATGTGAGAACTGTATCCTAGC

Table 1.4. Antibodies used in this study.

Antibody	Dilution	Reference
Anti-Sec61p, rabbit polyclonal	1:10,000	Stirling et al., 1992 (15)
Anti-Sss1p, sheep polyclonal	1:5000	Wilkinson et al., 2010 (6)
Anti-Sec63p, sheep polyclonal	1:10,000	Young et al., 2001 (16)
Anti-DPAP B, sheep polyclonal	1:5000	Tyson and Stirling 2000 (1)
Anti-Kar2p, sheep polyclonal	1:10,000	Tyson and Stirling 2000 (1)
Anti-Prepro alpha factor, sheep polyclonal	1:10,000	Young et al., 2001 (16)
Anti-Sil1, sheep polyclonal	1:10,000	Tyson and Stirling 2000 (1)
Anti-GAPDH, mouse polyclonal	1:20,000	N/A
HRP conjugated anti-sheep	1:20,000	N/A
HRP conjugated anti-rabbit	1:20,000	N/A
HRP conjugated anti-mouse	1:10,000	N/A

References

1. Tyson JR, Stirling CJ. LHS1 and SIL1 provide a lumenal function that is essential for protein translocation into the endoplasmic reticulum. The EMBO journal. 2000;19(23):6440-52.
2. Rothblatt JA, Meyer DI. Secretion in yeast: translocation and glycosylation of prepro-alpha-factor in vitro can occur via an ATP-dependent post-translational mechanism. The EMBO journal. 1986;5(5):1031-6.
3. Pilon M, Romisch K, Quach D, Schekman R. Sec61p serves multiple roles in secretory precursor binding and translocation into the endoplasmic reticulum membrane. Molecular biology of the cell. 1998;9(12):3455-73.
4. Jermy AJ, Willer M, Davis E, Wilkinson BM, Stirling CJ. The Brl domain in Sec63p is required for assembly of functional endoplasmic reticulum translocons. The Journal of biological chemistry. 2006;281(12):7899-906.
5. Wilkinson BM, Esnault Y, Craven RA, Skiba F, Fieschi J, K'Epes F, et al. Molecular architecture of the ER translocase probed by chemical crosslinking of Sss1p to complementary fragments of Sec61p. The EMBO journal. 1997;16(15):4549-59.
6. Wilkinson BM, Brownsword JK, Mousley CJ, Stirling CJ. Sss1p is required to complete protein translocon activation. The Journal of biological chemistry. 2010;285(42):32671-7.
7. Witham CM, Dassanayake HG, Paxman AL, Stevens KLP, Baklous L, White PF, et al. The conserved C-terminus of Sss1p is required to maintain the endoplasmic reticulum permeability barrier. The Journal of biological chemistry. 2020;295(7):2125-34.
8. Winston F, Dollard C, Ricupero-Hovasse SL. Construction of a set of convenient saccharomyces cerevisiae strains that are isogenic to S288C. 1995;11(1):53-5.
9. Winzeler EA, Shoemaker DD, Astromoff A, Liang H, Anderson K, Andre B, et al. Functional characterization of the S. cerevisiae genome by gene deletion and parallel analysis. Science. 1999;285(5429):901-6.
10. Rentsch D, Laloi M, Rouhara I, Schmelzer E, Delrot S, Frommer WB. NTR1 encodes a high affinity oligopeptide transporter in Arabidopsis. FEBS Lett. 1995;370(3):264-8.
11. Metzger MB, Maurer MJ, Dancy BM, Michaelis S. Degradation of a cytosolic protein requires endoplasmic reticulum-associated degradation machinery. The Journal of biological chemistry. 2008;283(47):32302-16.
12. Esnault Y, Blondel MO, Deshaies RJ, Scheckman R, Képès F. The yeast SSS1 gene is essential for secretory protein translocation and encodes a conserved protein of the endoplasmic reticulum. The EMBO journal. 1993;12(11):4083-93.
13. Bähler J, Wu JQ, Longtine MS, Shah NG, McKenzie A, 3rd, Steever AB, et al. Heterologous modules for efficient and versatile PCR-based gene targeting in Schizosaccharomyces pombe. Yeast (Chichester, England). 1998;14(10):943-51.
14. Sikorski RS, Hieter P. A system of shuttle vectors and yeast host strains designed for efficient manipulation of DNA in Saccharomyces cerevisiae. Genetics. 1989;122(1):19-27.
15. Stirling CJ, Rothblatt J, Hosobuchi M, Deshaies R, Schekman R. Protein translocation mutants defective in the insertion of integral membrane proteins into the endoplasmic reticulum. Molecular biology of the cell. 1992;3(2):129-42.
16. Young BP, Craven RA, Reid PJ, Willer M, Stirling CJ. Sec63p and Kar2p are required for the translocation of SRP-dependent precursors into the yeast endoplasmic reticulum in vivo. The EMBO journal. 2001;20(1-2):262-71.

Chapter 3

Investigating a Role for Sss1 in Translocon Gating Dynamics

Introduction

The Endoplasmic Reticulum (ER) is a multifunctional organelle that acts as the entry point to the secretory pathway and is a major site for protein biogenesis. The heterotrimeric Sec61 translocon forms the channel through which secretory and integral membrane proteins are translocated. This function demands that the channel sits a junction between the ER and cytosol, and as such must be structured to prevent the free flow of various solutes. During the inception of this project, we found that the current mechanisms describing how the translocon is gated to be very Sec61 centric.

Sss1 Function

Sss1 is an essential subunit of the heterotrimeric Sec61 complex. Structural analysis shows Sss1 to be a small C-terminal anchor protein consisting of an N-terminal cytosolic domain and a C-terminal TM domain. Sss1 was previously indicated to act as a clamp to hold both halves of the Sec61 subunit together and hence regulate lateral access to the translocon (1, 2). Some of the first characterisation of Sss1 involved a series of novel mutations within the cytosolic and TMDs of the protein (2). This work found that the cytosolic domain was responsible in establishing interactions with the Sec61 subunit. Analysis at the TMD of Sss1 however, revealed that deletion of this domain led to a loss of cell viability due to defective protein translocation. To further characterise this outcome fusion mutants were created using the two domains of Sss1 with those corresponding to another single membrane spanning protein, that of the ubiquitin conjugating enzyme Ubc6. The generated fusion mutants were able to associate with Sec61 but could not supress the lethality of a *sss1Δ* mutation which was

attributed to an obstruction in translocation. This was the first study to indicate a requirement for the Sss1 TMD in the activation of protein translocation. These findings would be complemented with a later study that found point mutations within the tail anchored TMD of Sss1 led to diminished growth, defects in co- and post- translational translocation, inefficient ribosome binding to Sec61 complex, reduction in the stability of both heterotrimeric Sec61 and heptameric SEC complexes and a complete breakdown of ER structure (3).

Our own structural analysis revealed that the highly conserved extreme C-terminus of Sss1 is juxtaposed to a key gating module of Sec61. Therefore, we hypothesised that the C-terminus of Sss1 is important for gating the Sec61 translocon. This work would become the first to detail a role for the Sss1 subunit in regulating translocon gating. With its completion, we have furthered the fundamental understanding of how the translocon is regulated which is a critical step in understanding the pathways to dysfunction that arise in disease. This was achieved through the characterisation of two mutants within the extreme C-terminus of Sss1 which exhibited temperature sensitivity at 37°C, being *sss1-6* (P74A, I75A) and *sss1-7* (H72K) (4).

Temperature Sensitive Mutations

The study of temperature sensitive (TS) mutations has served fundamental biology from as early as 1963 (5, 6). This class of mutants has been utilised in both the identification of genes as well as analysing their essential functions within a cell. TS alleles are generally missense variants that provide a straightforward mechanism to control gene function. Standard growing conditions are permissive to cellular growth of these mutants. However, the essential function of the mutated genes becomes ablated under elevated temperatures which can be observed at both, high non-permissive temperatures, and intermediate, semi permissive temperatures. This provides an inducible environment where the impact of these mutations on cellular physiology can

be assessed, and by characterising the loss of an essential function, we can implicate the assessed gene in regulating these processes.

The Yeast of All Model Organisms

Despite the compelling utility of TS mutants, the task of generating them can be quite arduous. These mutations must be incorporated into the genome of the organism of interest and as such the screening process requires a large number of isolates. This number is only exacerbated as the size of the organism's genome increases. Using the fruit-fly, *Drosophila melanogaster* as an example, the screening process to isolate TS mutations can be in the order of several hundred thousand separate isolates (7, 8). Such a task is considered infeasible, especially if you take the fact that more complex organisms require longer culturing times. Therefore, it has become necessary to use simple model organisms in such screens.

Escherichia coli is commonly used due to its unburdened and well described biology in addition to the fact it can be cultured quite rapidly. However bacterial systems can be inappropriate in the study of eukaryotic genes due to the lack of PTMs such as proteolytic cleavage of signal sequences and glycosylation. It is for this reason that the budding yeast, *Saccharomyces cerevisiae* has been extensively used in the understanding of fundamental eukaryotic processes. In addition to fast culturing and an ability to perform PTMs, Yeast possess a genetic system that allows for complementation and dominant versus recessive studies, a transformation efficiency of up to 1×10^8 transformants/µg of DNA and a highly developed and conserved secretory pathway (9). *S. cerevisiae* also demonstrates a high frequency of homologous DNA recombination which can be performed with DNA elements with as few as 40 base pairs that are homologous to the gene of interest (9, 10). Collectively these characteristics make yeast ideal for creating genetic libraries as part of a study, particularly those conducting directed evolution screens.

Experimental Design and Aims

Directed evolution in a laboratory setting takes a Darwinian approach which involves generating genetic diversity followed by selection through function. Random mutagenesis is generally used to achieve diversity in the genes of interest and can be performed using Error-Prone PCR (EP-PCR), chemical mutagenesis and DNA shuffling (11). We endeavoured to generate a library of *sec61* mutants through EP-PCR to determine whether mutations in this major interacting partner to Sss1 could supress the temperature sensitivity of our *sss1* mutants. Any difficulty associated to directed evolution usually comes at selection stage and as is the benefit to our approach, whereby using our TS mutants we can select for suppression. We also take advantage of the fact that the Sec61 subunit was well-described in the literature and has a strong association with our gene of interest, *SSS1*. Therefore, by exploiting the genetics of Sec61 we subsequently infer similar functionality to Sss1. We found several mutations within key gating modules of Sec61 that were capable of supressing the TS phenotypes of both *sss1-6* and *sss1-7*. We also further characterised the TS phenotype to be a consequence of disturbed gating at the translocon which perpetuates an uncontrolled flux of metabolites across the channel. These collective outcomes granted a greater understanding of the consequences that the TS mutations had on cellular anatomy and offers direction in exploring the physiology and associated pathologies at the mammalian ER.

*** The greater part of this work has undergone peer review and was subsequently accepted for publication. The submitted manuscript has been included to form part of this chapter together with supplementary results that we found relevant in our path to discovery yet didn't make it to submission. This is followed by a brief discussion on the topic matter that includes some deeper insights upon reflection.**

Results

Structural Analysis Finds a Role for Sss1 in the Translocon Gating Module

Sss1 is a small C-terminal anchor protein and an essential component of the heterotrimeric Sec61 complex. Clustal omega sequence analysis of Sss1/Sec61γ protein sequences identifies the TM domain of these orthologues to be 57% identical and 83% similar (Fig. 2.1., A) thus indicating substantial conservation. Further structural analysis revealed that the extreme C-terminus of Sss1/Sec61γ lies at the opening of the translocation channel within the ER lumen, juxtaposed to the key gating module of Sec61/Sec61α which comprises the lumenal loop connecting TM1 and the TM2a plug domain (Fig. 2.1., B).

Two mutants of *sss1* were generated to query the functional importance of the Sss1 C-terminus. The first of these mutants contains a substitution of a highly conserved histidine residue to a lysine (H72K) and was termed *sss1-7*. The other mutant, which is the outcome of a substitution to two highly conserved residues being that of a proline and isoleucine for alanine residues (P74A, I75A), was termed *sss1-6*. These two mutants confer TS growth at 37°C (Fig. 2.1., C).

Sec61 Mutants Suppress the Temperature Sensitivity of *sss1-7*

A genetic approach was used to discern the nature of the TS *sss1* mutations and the physiological impact they impose onto the ER. This involved a directed evolution screen where EP-PCR served as the conduit for mutagenesis to introduce point mutations into the gene encoding for the major interacting partner of Sss1, Sec61. This allowed us to identify intergenic suppressors of *sss1-7* TS growth (Ts+). Error prone PCR (EP-PCR) utilises the low fidelity of Taq polymerase which is exacerbated when Mn^{2+} is introduced into the reaction. Increased Mg^{2+} and unequal dNTP concentrations were also applied. After 5 PCR cycles the mutagenised PCR product was transformed into *sss1-7* cells and transformants grown at 37°C. 203 Ts+ colonies were isolated and the

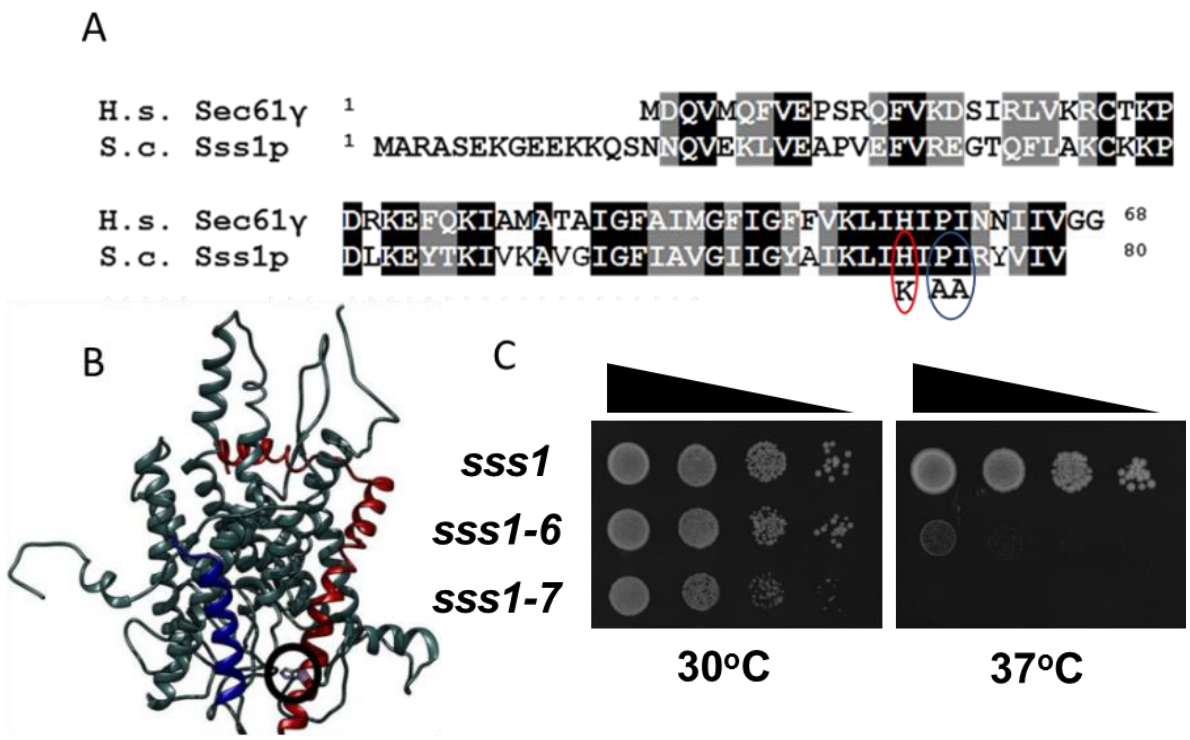

Fig. 2.1. *sss1-6* and *sss1-7* are mutants located at the extreme C-terminus of Sss1 and present with a temperature sensitive growth defect. (A) Sequence alignment of *Homo sapiens* (H.s.) Sec61γ and budding yeast (S.c.) Sss1p using Clustal omega sequence alignment software. Sequence identity and similarity are noted in black, and grey respectively. **(B)** Crystal structure of the Ssh1 translocon. Ssh1p is indicated in slate, Sss1p in red and Sbh2p in blue. The Sec61 complex remains to be crystallised. Sss1p H72 is circled. **(C)** WT, *sss1-6* and *sss1-7* cells were spotted on YPD in a 10-fold dilution series and incubated at 30 and 37°C for 3 days.

complete nucleotide sequences of 50 determined. On average EP-PCR yielded 3.5 mutations per 1 kb yet only 25 of the 50 sequenced mutants contained a single nucleotide substitution in the *SEC61* open reading frame (ORF). In total seven different *SEC61* mutant alleles, V82F, G262E, S289F, N302K, N302Y, T379A, and L449M, were obtained from this screen and their ability to suppress the TS growth defect of *sss1-7* cells was reconfirmed (Fig. 2.2.). The *SEC61*^{T379A} and *SEC61*^{L449M} mutants were each identified in ten different suppressor colonies, giving confidence that these represent *bona fide* suppressors of *sss1-7*. Mapping each mutation on the crystal structure of the Sec61 homologue Ssh1 revealed these mutations to localise at critical sites for translocation that include the site adjacent to the ribosomal binding site and the pore ring (Table 2.1).

Characterisation of the Isolated *SEC61* Mutants

To confirm the validity of each of these Sec61 mutants, site directed mutagenesis was performed to recreate the exact mutation within a plasmid system using the YCp Sec61, pBW11. All mutant plasmid variants were successfully generated and confirmed with sangar sequencing. The generated plasmids were then transformed into the *sss1-7* mutant yeast strain to confirm the previously noted suppressive effect. The *sss1-7* strain holds an endogenous chromosomal copy of Sec61 so any potential suppressive effects observed post transformation with the mutant plasmids would indicate that they are of a dominant nature. We were pleased to find *SEC61*^{V82F}, *SEC61*^{S289F}, *SEC61*^{N302K}, *SEC61*^{N302Y} and *SEC61*^{T379A} all demonstrated suppressive capabilities in our *sss1-7* strain as a second copy of Sec61. The full characterisation of the dominant mutants served as the basis for the attached manuscript.

The *SEC61*^{G262E} and *SEC61*^{L449M} mutants however, did not show any dominance within *sss1-7* which could be explained through one of two possible scenarios, first is that these are silent mutants that arose secondary to the main effector or second, that they are recessive in nature. To test the later outcome we transformed pBW11, *SEC61*^{G262E}

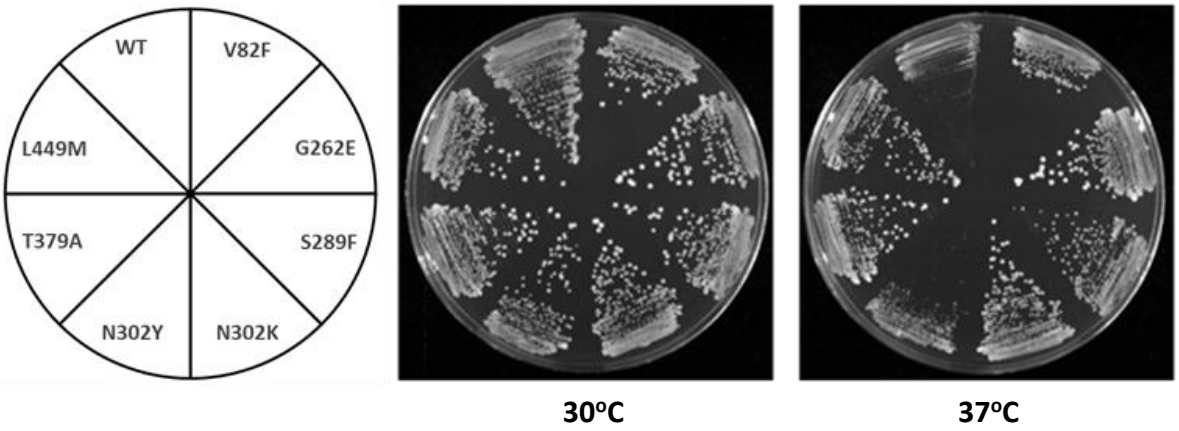

Fig. 2.2. Isolated suppressor colonies demonstrating restoration of the *sss1-7* growth defect. Single representation of a WT yeast strain (BWY530 + pJKB2) and each of the isolated suppressors with mutations that were successfully sequenced within the *SEC61* ORF as they were streaked onto YPD medium and incubated at 30°C and 37°C for 2 days.

Table 2.1. Each isolate signified by mutation, location, and number.

Mutation	Location	Number of isolates
V82F	**Pore ring**	**1**
G262D	**TM6**	**1**
S289F	**TM7 (*Prl*$_{adjacent}$)**	**1**
N302K/Y	**Lateral and lumenal gate**	**2**
T379A	**TM8**	**10**
L449M	**TM10 (*Prl*)**	**10**

Prl$_{adjacent}$= Mutations found lying adjacent to identified *Prl* residues

and *SEC61*^{L449M}, along with pJKB2 and pCM205 into the yeast strain CMY5 (*sss1Δ::KanMX4* and *sec61Δ::HIS3* pCM203). Both *SEC61* and *SSS1* are essential and as such viability of the CMY5 strain is maintained though pCM203 which contain both genes on a *URA3* plasmid backbone. Following transformation with of our Sec61 and Sss1 plasmids of interest, cells were plated onto 5-FOA medium to counter select for the *URA3* containing plasmid as it converts the FOA into a toxic by-product. Strains harbouring pBW11 and pJKB2 yielded viable colonies, as did the mutant plasmids, whereas strains transformed with vector alone could not. The CWY32 (*SEC61*^{L449M} + pCM205) strain, but not CWY31 (*SEC61*^{G262E} + pCM205), demonstrated suppression of the TS phenotype at both 34°C and 37°C, indicating that the L449M was a true recessive suppressor (Fig. 2.3.).

The inability for the G262E to demonstrate any suppression in both the dominant and recessive screens may be indicative of false positive by one of two outcomes. G262E may have been an artefact of the sequencing reaction or arose as a secondary silent mutation to a spontaneous mutation located elsewhere in the isolated suppressors genome.

The L449M mutant impacts upon a site of TM10 at the Sec61 complex that can harbour a *prl* phenotype. The *prl* phenotype belongs to a class of well characterised mutations found to reduce the hydrophobicity threshold at the translocon that is necessary for integration of the signal sequence (12, 13). Such mutations are described to destabilise the closed state of the translocon at critical gating sites such as the plug, lateral gate and site of ribosomal binding and hence allow for a less specific signal sequence to be integrated for translocation (12-15). We therefore predict that the L449M is a *prl* located suppressor that is having the inverse effect, creating a more stringent threshold to compensate a channel suspected to be in a more open state.

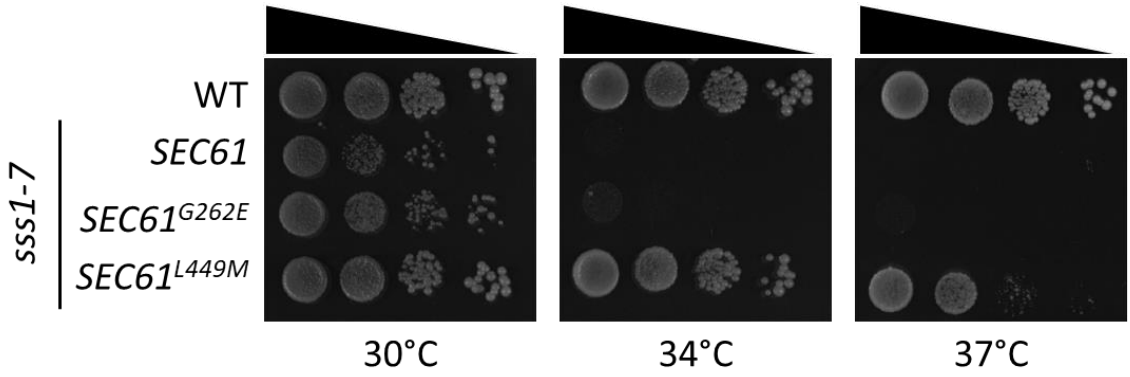

Fig. 2.3. *SEC61^{G262E}* and *SEC61^{L449M}* demonstrate recessive suppression of *sss1-7*. CMY5 yeast were transformed with either YCp *SEC61*, YCp *SEC61^{G262E}* or YCp *SEC61^{L449M}* alongside either YCp *SSS1* or YCp *sss1-7* and were subsequently spotted on YPD agar in a 10-fold dilution series and incubated at 30°C, 34°C or 37°C for 2 days. The L449M is shown here to demonstrate suppression at both 34 ^{o}C and 37 ^{o}C.

References

1. Van den Berg B, Clemons WM, Jr., Collinson I, Modis Y, Hartmann E, Harrison SC, et al. X-ray structure of a protein-conducting channel. Nature. 2004;427(6969):36-44.
2. Wilkinson BM, Brownsword JK, Mousley CJ, Stirling CJ. Sss1p is required to complete protein translocon activation. The Journal of biological chemistry. 2010;285(42):32671-7.
3. Falcone D, Henderson MP, Nieuwland H, Coughlan CM, Brodsky JL, Andrews DW. Stability and function of the Sec61 translocation complex depends on the Sss1p tail-anchor sequence. The Biochemical journal. 2011;436(2):291-303.
4. Mousley CJ. Functional analysis of the ER translocon component Sss1p [Ph. D. Thesis]: University of Manchester; 2005.
5. Ben-Aroya S, Pan X, Boeke JD, Hieter P. Making temperature-sensitive mutants. Methods in enzymology. 2010;470:181-204.
6. Edgar RS, Lielausis I. TEMPERATURE-SENSITIVE MUTANTS OF BACTERIOPHAGE T4D: THEIR ISOLATION AND GENETIC CHARACTERIZATION. Genetics. 1964;49(4):649-62.
7. Suzuki DT, Grigliatti T, Williamson R. Temperature-sensitive mutations in Drosophila melanogaster. VII. A mutation (para-ts) causing reversible adult paralysis. Proceedings of the National Academy of Sciences of the United States of America. 1971;68(5):890-3.
8. Varadarajan R, Nagarajaram HA, Ramakrishnan C. A procedure for the prediction of temperature-sensitive mutants of a globular protein based solely on the amino acid sequence. Proceedings of the National Academy of Sciences of the United States of America. 1996;93(24):13908-13.
9. Gonzalez-Perez D, Garcia-Ruiz E, Alcalde M. Saccharomyces cerevisiae in directed evolution: An efficient tool to improve enzymes. Bioengineered bugs. 2012;3(3):172-7.
10. Gibson DG. Synthesis of DNA fragments in yeast by one-step assembly of overlapping oligonucleotides. Nucleic acids research. 2009;37(20):6984-90.
11. Cobb RE, Chao R, Zhao H. Directed Evolution: Past, Present and Future. AIChE journal American Institute of Chemical Engineers. 2013;59(5):1432-40.
12. Junne T, Kocik L, Spiess M. The Hydrophobic Core of the Sec61 Translocon Defines the Hydrophobicity Threshold for Membrane Integration. Molecular biology of the cell. 2010;21(10):1662-70.
13. Trueman SF, Mandon EC, Gilmore R. A gating motif in the translocation channel sets the hydrophobicity threshold for signal sequence function. The Journal of Cell Biology. 2012;199(6):907.
14. Junne T, Schwede T, Goder V, Spiess M. Mutations in the Sec61p channel affecting signal sequence recognition and membrane protein topology. The Journal of biological chemistry. 2007;282(45):33201-9.
15. Smith MA, Clemons WM, Jr., DeMars CJ, Flower AM. Modeling the effects of prl mutations on the Escherichia coli SecY complex. Journal of bacteriology. 2005;187(18):6454-65.

The Conserved C-terminus of Sss1p is Required to Maintain the ER Permeability Barrier

Christopher M. Witham [1,2], Hasindu G. Dassanayake [1], Aleshanee L. Paxman [1], Kofi L. P. Stevens [1,2], Lamprini Baklous [1,2], Paris F. White [1], Amy L. Black [1,2], Robert F. L. Steuart [2], Colin J. Stirling [3,4], Benjamin L. Schulz [5] and Carl J. Mousley [1,2*].

[1] School of Pharmacy and Biomedical Sciences, Curtin University, Bentley, WA 6102, Australia. [2] Curtin Health Innovation Research Institute, Curtin University, Bentley, WA 6102, Australia. [3] University of Manchester, School of Biological Sciences, Oxford Road, Manchester, M13 9PT, United Kingdom. [4] Current address: Office of the Vice Chancellor, Flinders University, Sturt Rd, Bedford Park, SA 5042, Australia [5] School of Chemistry and Molecular Biosciences, University of Queensland, Brisbane St Lucia, QLD 4072, Australia.

Running title: The Sss1p C-terminus is important for ER homeostasis

*To whom correspondence should be addressed: Carl J. Mousley, School of Pharmacy and Biomedical Sciences, Curtin University, Bentley, WA 6102, Australia; Carl.Mousley@curtin.edu.au;

Telephone. +61 8 9266 5617, Facsimile : +61 8 9266 2342

Keywords: Endoplasmic reticulum (ER), Sec61 complex, Sec61p/Sec61α, Sss1p/Sec61 γ, translocon gating.

Abstract

The endoplasmic reticulum (ER) is the entry point to the secretory pathway and major site of protein biogenesis. Translocation of secretory and integral membrane proteins across or into the ER membrane occurs via the evolutionarily conserved Sec61 complex, a heterotrimeric channel that comprises the Sec61p/Sec61α, Sss1p/Sec61γ and Sbh1p/Sec61β subunits. In addition to forming a protein conducting channel, the Sec61 complex also functions to maintain the ER permeability barrier, preventing the mass free flow of essential ER enriched molecules and ions. Loss in Sec61 integrity is detrimental and implicated in the progression of disease. The Sss1p/Sec61γ C-terminus is juxtaposed to the key gating module of Sec61p/Sec61α and we hypothesise it is important for gating the ER translocon. The ER stress response was found to be constitutively induced in two temperature sensitive *sss1* mutants (*sss1*^{ts}) that are still proficient to conduct ER translocation. A screen to identify intergenic mutations that allow for *sss1*^{ts} cells to grow at 37°C suggests the ER permeability barrier to be compromised in these mutants. We propose the extreme C-terminus of Sss1p/Sec61γ is an essential component of the gating module of the ER translocase and is required to maintain the ER permeability barrier.

Introduction

The endoplasmic reticulum (ER) plays a major role in the biosynthesis of about a third of a cell's proteome (1). Proteins are targeted to and translocated across the ER membrane either co- or post-translationally. Co-translational translocation is initiated upon recognition of the hydrophobic signal sequence by the signal recognition particle (SRP) as it emerges from the ribosome (2-6). The resulting complex is targeted to the ER by association of the SRP with the SRP receptor (3, 5, 6). Interaction with the translocon results in SRP dissociation followed by looped insertion of the nascent chain into the translocation channel (3, 7, 8). Upon resumption of translation the nascent chain moves through the pore and into the lumen of the ER where cleavable signal sequences are processed by the signal peptidase complex (9-12).

Smaller proteins or those containing a moderately hydrophobic signal sequence are completely synthesised in the cytoplasm and translocated post-translationally (3, 13). Cytosolic chaperones associate with these substrates in order to maintain them in a translocation competent state (12, 14, 15). Post-translational translocation proceeds via the SEC complex, an assembly of the translocon and the Sec62p/Sec63p/Sec71p/Sec72p sub-complex (3, 16-20). Upon association with the SEC complex, chaperones are released and the signal peptide of the secretory precursor is inserted into the translocation channel after which translocation is facilitated by Kar2p (BiP in mammals) (16, 21).

The translocon is formed by the conserved heterotrimeric Sec61 complex. It comprises two essential subunits, Sec61p and Sss1p, and the non-essential Sbh1p subunit (Sec61α , Sec61γ and Sec61β in mammals respectively) (3, 16, 22). This complex forms an hourglass shaped structure with an aqueous pore. At the centre lies the pore ring, formed by hydrophobic amino acids, the side chains of which form a gasket through which a polypeptide is threaded during translocation (12, 23, 24). In the closed conformation the pore is sealed by a short helix of TM2 in Sec61p, TM2a, which acts as a plug (23, 25). A Sec61 paralog exists that exclusively functions in the co-translational pathway (26-28). This paralog is known as Ssh1 and Sec61A2

in yeast and mammals respectively (29). In yeast the Ssh1 complex comprises Ssh1p and Sbh2p, related to Sec61p and Sbh1p respectively, as well as Sss1p (26, 27).

The conformational changes that take place within the translocon upon the initiation of translocation are best understood for co-translational translocation. Interaction of the ribosome-nascent chain complex (RNC) with cytosolic loops 6 and 8 of Sec61p is critical for initiating the preliminary conformational changes that facilitate translocation (3, 30-33). This includes partial displacement of the plug and opening of the lateral gate, formed by TM2b and TM7 of Sec61p, to allow the intercalation of the signal sequence (23, 34). The latter promotes further conformational changes that includes full displacement of the plug and further lateral gate separation to establish an open channel to allow protein translocation to proceed.

Previous studies have shown Sss1p/Sec61γ to stabilise the translocon; defects in the Sss1p/Sec61γ TMD lead to various outcomes such as inefficient ribosomal binding, breakdown of ER structure, defective co and post translational translocation and loss of cell viability (22, 35). Additionally, structural analyses show the extreme C-terminus of Sss1p is juxtaposed to the key gating module of Sec61p (32, 36). Therefore, we hypothesised that the highly-conserved C-terminus of Sss1p is critical in gating the ER translocon. Through phenotypical characterisation of two mutants, *sss1-6* and *sss1-7*, we show that the C-terminus of Sss1p is important for ER homeostasis but does not influence the stability of the ER translocation machinery. Furthermore, we found that mutations in key gating modules of Sec61p, suppress the temperature sensitivity of *sss1-6* and *sss1-7*. Together, this provides insight into the role of Sss1p/Sec61γ plays in translocon function and in mammalian ER physiology and pathology associated with dysregulated diffusion of small molecules through the ER translocon.

Results

The C-terminus of Sss1p is Highly Conserved

The Sec61 complex comprises Sec61/Sec61α, Sbh1p/Sec61β and Sss1p/Sec61γ. Eukaryotes also encode for a second ER translocase which contains Ssh1p/Sec61α2, Sss1p/Sec61γ and Sbh2p/Sec61β, (Fig. 3.1., A). Given that Sss1p/Sec61γ is the only essential protein to be a component of both ER translocases we considered the possibility that its activity may be tightly regulated. The Sss1p transmembrane domain is highly conserved, in particular the C-terminal portion where the K_{69}LIHIPI_{75} heptapeptide is absolutely conserved. We hypothesised this region to be functionally important, and performed double-alanine scanning mutagenesis throughout it, creating variants Sss1p^{I68A,K69A}, Sss1p^{L70A,I71A}, Sss1p^{H72A,I73A}, and Sss1p^{P74A,I75A} (Fig. 3.1., B), to investigate the role of these residues in Sss1p function. As *SSS1* is essential we tested if expression of these variants could sustain cell viability. YCp *SSS1* and each mutant was transformed into BWY530 (*sss1Δ::KanMX4* FKp53) and tested for the ability of these strains to grow after loss of FKp53 on 5-FOA medium. Strains harbouring YCp *SSS1* or any of the mutants, unlike cells transformed with vector alone, produced viable colonies that expressed stable Sss1 protein (Fig. 3.1., C & D).

Mutations in the Sss1p C-terminus Disrupt ER Homeostasis

The growth of cells expressing the *sss1*$^{P74A,\ I75A}$ double mutant, referred to as *sss1-6* herein, is temperature sensitive as they grow poorly at 37°C (Fig. 3.2., A). We have isolated a second mutation within the C-terminus that is temperature sensitive (Fig. 3.2., A). The Sss1p^{H72K} variant (referred to as *sss1-7*) was originally generated to enable us to identify potential lumenal interacting proteins by cross-linking. The resulting strain was even more temperature sensitive than *sss1-6* cells (Fig. 3.2., A & B).

The hydrophobicity of the extreme C-terminus of tail anchored proteins is a critical property that allows their stable integration into membranes by the GET complex (37). Hydropathy analysis shows that the mutations in the C-terminus of Sss1-6p and

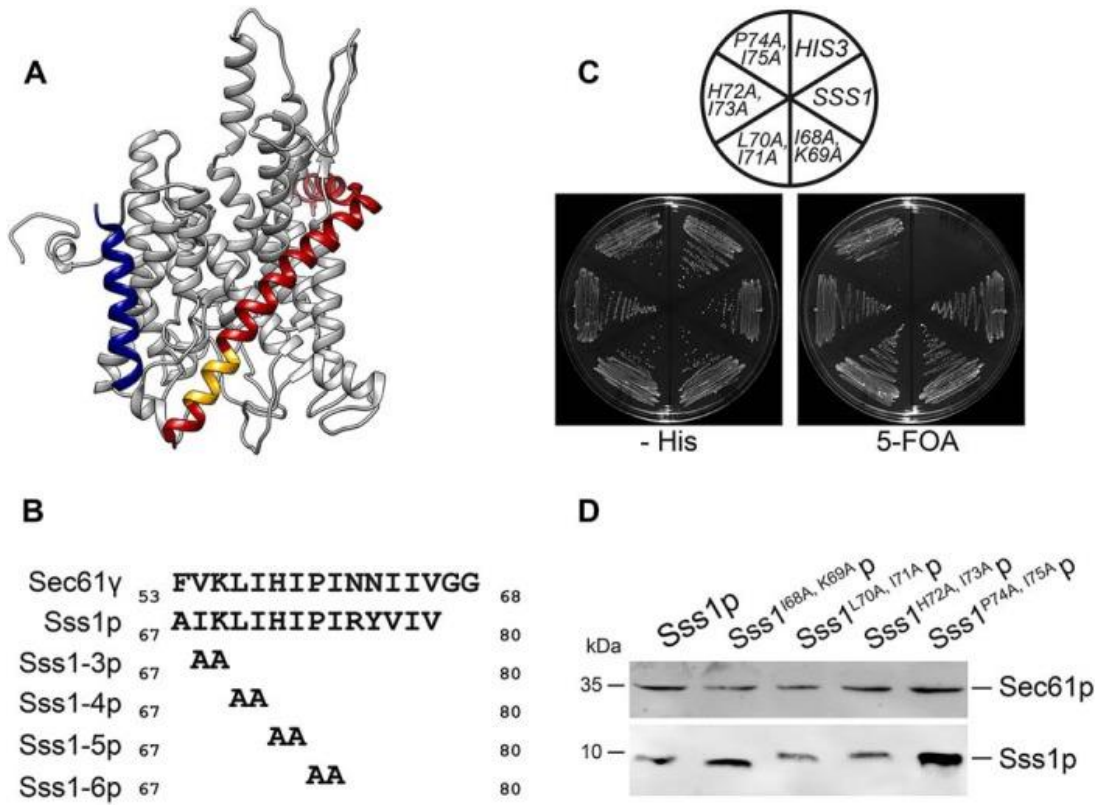

Fig. 3.1. The Sss1p C-terminus is highly conserved. (A) Ribbon diagram of the Sec61 homologue complex crystal structure (2WWA.pdb) (32) was composed using Chimera software. Ssh1p, Sbh2p and Sss1p are coloured grey, blue and red respectively. The highly conserved KLIHIPI heptapeptide is highlighted in gold. **(B)** The sequence of the extreme C-terminus of Sec61γ and Sss1p are aligned using clustal omega sequence alignment software and the position of each double alanine scanning mutation indicated. **(C)** BWY530 yeast transformed with either YCp *HIS3*, YCp *SSS1*, YCp *SSS11*$^{I68A,\ K69A}$, YCp *SSS1*$^{L70A,\ I71A}$, YCp *SSS1*$^{H72A,\ I73A}$ or YCp *SSS1*$^{P74A,\ I75A}$ were streaked onto –His selective medium and medium containing FOA and incubated at 30°C for 2 days. **(D)** Cell extracts derived from wildtype cells or cells expressing either *SSS1*$^{I68A,\ K69A}$, *SSS1*$^{L70A,\ I71A}$, *SSS1*$^{H72A,\ I73A}$ or *SSS1*$^{P74A,\ I75A}$ were immunoblotted with anti-Sss1p or anti-Sec61p antibodies.

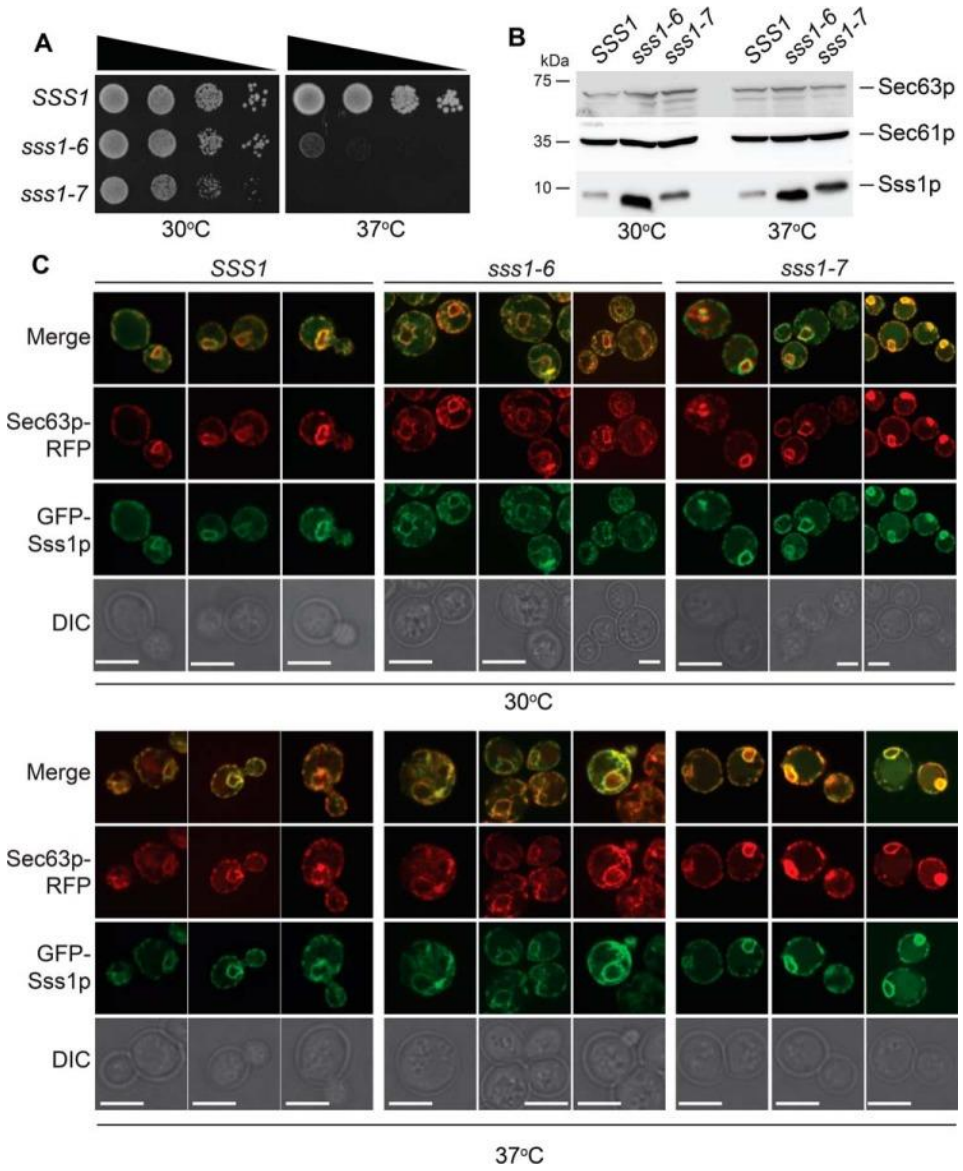

Fig. 3.2. *sss1-6* and *sss1-7* are inserted into the ER membrane. (A) Wildtype, *sss1-6* or *sss1-7* yeast were spotted on YPD agar in a 10-fold dilution series and incubated at 30°C or 37°C for 2 days. **(B)** Cell extracts derived from wildtype *sss1-6* or *sss1-7* yeast were immunoblotted with anti- Sss1p, anti-Sec61p and anti-Sec63p antibodies. **(C)** GFP-Sss1p, GFP-Sss1-6p and GFP-Sss1-7p was visualised in cells grown at 30°C and 37°C and co-localised with Sec63p-RFP (5 µM bar).

Sss1-7p have little effect on the hydrophobicity of this region relative to Sss1p (Supp. Fig. S3.1.). We used fluorescence microscopy to investigate if these mutations affect the integration of Sss1p into the ER membrane. GFP-Sss1p shows a perinuclear and peripheral locality and co-localises with the ER resident protein Sec63p (Fig. 3.2., C). As with GFP-Sss1p, we observe GFP-Sss1-6p and GFP-Sss1-7p to localise to the perinuclear and peripheral ER and both entirely co-localise with Sec63p (Fig. 3.2., C).

Given that Sss1p is an essential translocon component, we investigated if the integrity of the translocation apparatus was affected in Sss1p variants by measuring the stability of other essential translocon associated proteins. We find the stability of both Sec61p and Sec63p to be unaffected in *sss1-6* and *sss1-7* at 30°C or 37°C (Fig. 3.2., B). Next, we investigated the integrity of the translocon. The interaction between Sss1p and Sec61p required to form the translocon can be stabilised by the crosslinking reagent disuccinimidyl suberate (DSS) (38, 39). We detected a DSS-dependent immunoreactive band of ≈ 46 kDa with both anti-Sss1p and anti-Sec61p specific antibodies in membranes isolated from wildtype cells (Fig. 3.3., A). This adduct was also detected in membranes isolated from either *sss1-6* or *sss1-7* cells treated with DSS, regardless of whether cells were grown at 30°C or 37°C (Fig. 3.3., A).

Binding of the Sec71p glycoprotein with the lectin concanavalin A (ConA) enables the affinity purification of the heptameric SEC complex (20, 40). Digitonin solubilised membranes isolated from WT, *sss1-6* and *sss1-7* cells were incubated with ConA coupled sepharose beads, the bound fraction retained and Sec61p, Sss1p and Sec63p, were visualised by immunoblot analysis (Fig. 3.3., B). As expected, Sec61p, Sss1p and Sec63p were associated with the ConA bound fraction of digitonin solubilised membranes isolated from WT cells. Likewise, these proteins were associated with the ConA bound fraction of digitonin solubilised membranes isolated from *sss1-6* and *sss1-7* cells, grown at 30°C or 37°C. Therefore, neither the $sss1^{H72K}$ nor the $sss1^{P74A,\ I75A}$ mutations disrupted the ability to form protein complexes required for ER translocation.

The biogenesis of DPAP B, which is translocated co-translationally, as well as Lhs1p and α-factor, which are translocated by post-translational translocation (41), were

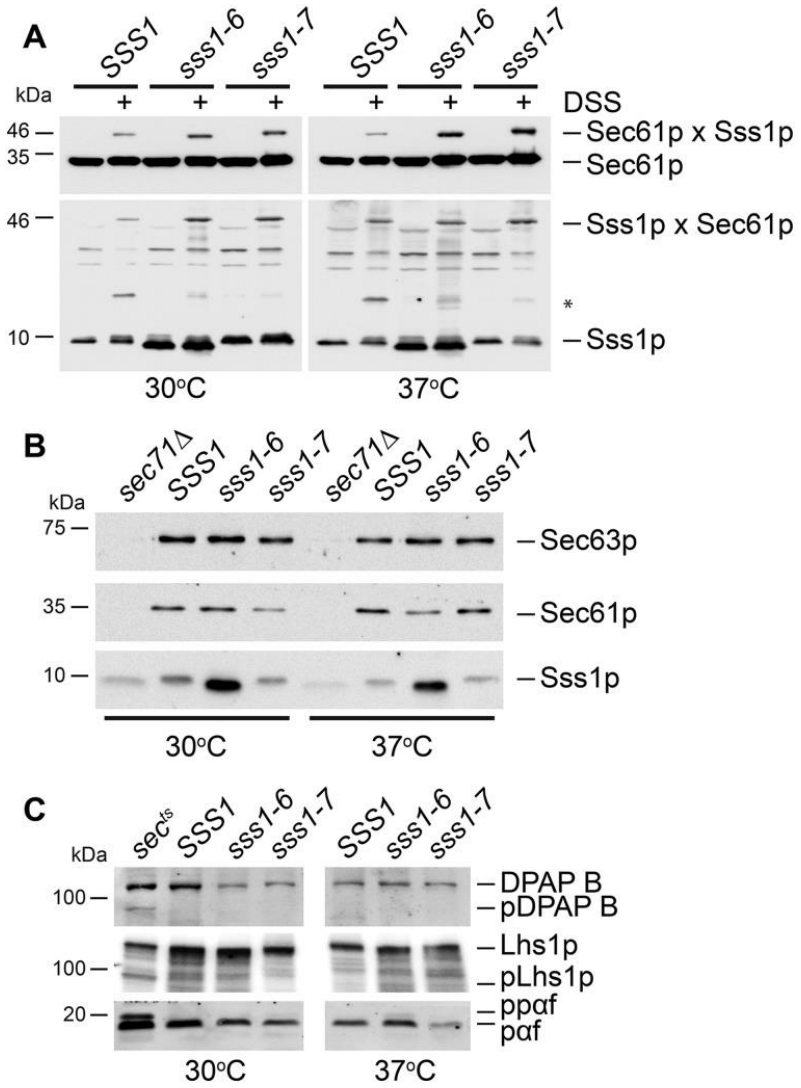

Fig. 3.3. ER translocation is not affected in *sss1-6* and *sss1-7*. (A) Membranes derived from wildtype *sss1-6* or *sss1-7* yeast incubated with and without 1 mM DSS were immunoblotted with anti-Sss1p and anti-Sec61p antibodies. **(B)** Membranes prepared from wildtype *sss1-6* or *sss1-7* yeast were subject to ConA chromatography. An equal portion of each fraction was analysed by immunoblotting with either anti-Sss1p, anti-Sec61p or anti-Sec63p specific antibodies. The bound fraction is shown. **(C)** Cell extracts derived from wildtype *sss1-6* or *sss1-7* yeast were immunoblotted with anti-Sss1p, anti-Sec61p, anti-α factor and anti-DPAP B antibodies. Secretory mutants, *sec63-1* and *sec65-1* (*sects*) were included as a negative control for α-factor and DPAP B respectively.

monitored to determine whether ER translocation is compromised in *sss1-6* and *sss1-7*. There was no obvious translocation defect in *sss1-6* and *sss1-7* mutants, irrespective of growth conditions, as the levels of both pDPAP B and Lhs1p did not exceed that that accumulates in wildtype cells (Fig. 3.3., C). This was also the case for a second post-translational translocation substrate pre-pro-alpha factor (ppαf) (Fig. 3.3., C). To further validate this, we reasoned that the mating efficiency of *MATα* variants of both *sss1-6* and *sss1-7* would be comparable to wildtype cells at both permissive and semi-permissive temperatures. Indeed, we observed no difference in the ability of these *sss1* mutants to mate as compared to wildtype cells (Supp. Fig. S3.2., A).

We observed significant ER distension and expansion in *sss1-6,* in particular, and *sss1-7* indicating the ER to be stressed in these mutants (Fig. 3.2., C). Given this, we tested if the unfolded protein response (UPR) was induced in *sss1-6* and *sss1-7* mutants. For this we used a lacZ reporter placed under transcriptional control of a yeast UPR enhancer (UPRE) (Wilkinson et al., 2000). WT cells were treated with the reducing agent dithiothreitol (DTT) to gauge a typical UPR response. UPR dependent Lac Z activity was significantly elevated in DTT treated cells compared to WT (Fig. 3.4., A), ensuring the range of response expected from these controls. LacZ activity in both *sss1* mutants at 30°C and 37°C was up to 11-fold greater than that of WT. This confirms that the UPR is constitutively induced in *sss1-6* and *sss1-7* cells.

Together, these experiments confirmed that despite their large effects on cell viability at 37˚C and causing constitutive induction of the UPR, these Sss1p point mutations did not affect the abundance, overall integrity, or general translocational activity of the translocon. This suggested that the role of this conserved section of Sss1p is independent of protein translocation.

The ER is More Permeable in *sss1-6* and *sss1-7*

The Sec61 complex has been shown by Toledano and colleagues to facilitate the diffusion of reduced glutathione into the ER (42). Furthermore, it has also been suggested that the Sec61 complex may facilitate the diffusion of other small

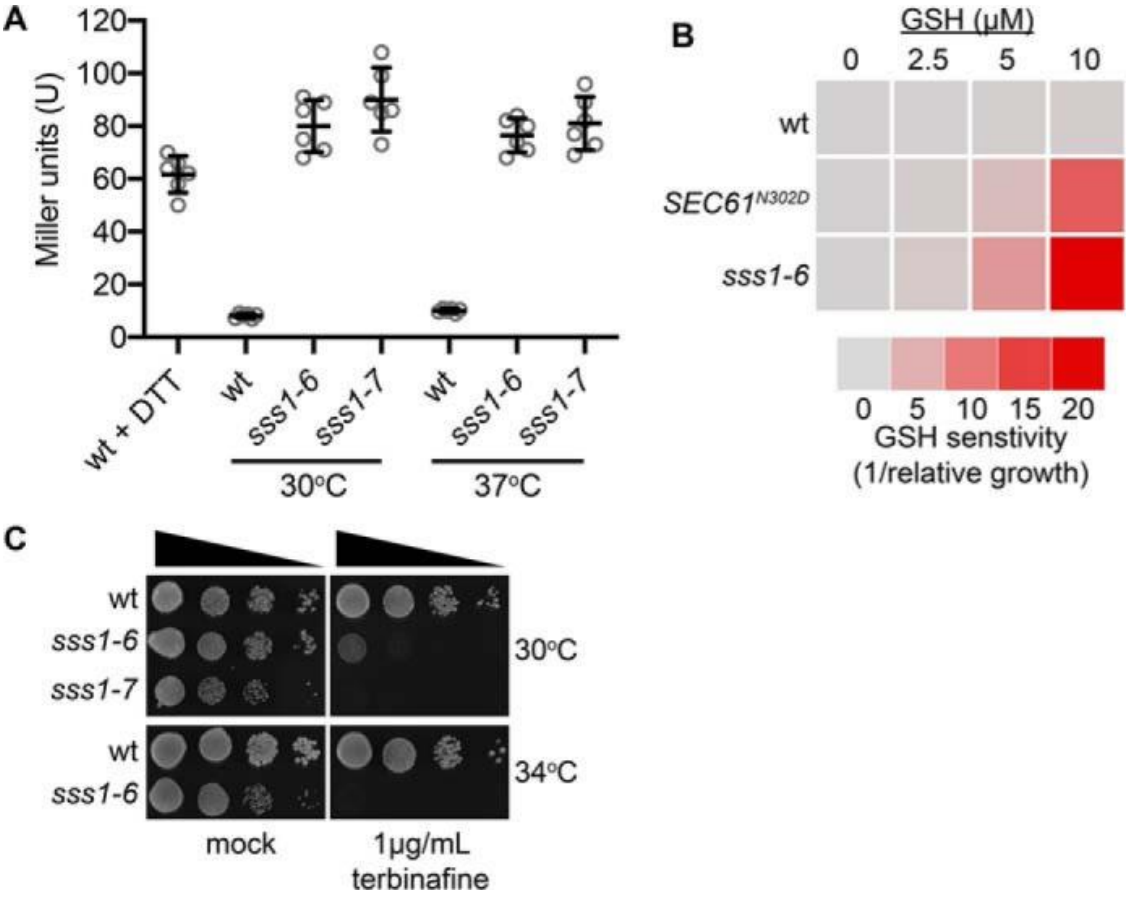

Fig. 3.4. ER homeostasis is perturbed in *sss1-6* and *sss1-7*. (A) Wildtype, *sss1-6* and *sss1-7* yeast transformed with pJT30 (UPRE-LacZ) were grown in –Ura medium and β-Galactosidase activity determined. Wildtype cells treated with 5 mM DTT for 2 hours were used as a positive control. **(B)** Wildtype, *SEC61^{N302D}* and *sss1-6* yeast transformed with YEp *HGT1* were grown in –Ura selective medium with increasing concentrations of GSH. The relative growth of each strain determined and the GSH sensitivity (1/relative growth) presented. **(C)** Wildtype, *sss1-6* and *sss1-7* yeast were spotted on YPD agar or YPD agar containing 1 µg/mL terbinafine in a 10-fold dilution series and incubated at 30°C or 34°C for 2 days.

molecules across the ER membrane. We wanted to determine whether *sss1-6* and *sss1-7* cells possessed phenotypes consistent with altered ER permeability. WT cells that overexpress Hgt1p, the plasma membrane high-affinity GSH transporter (↑*HGT1* cells hereafter), accumulate high levels of glutathione when supplied with exogenous GSH, which becomes cytotoxic due to hyper-oxidation of the ER (42, 43). *HGT1* is overexpressed in ↑*HGT1* cells by placing the *HGT1* open reading frame under transcriptional control of the constitutive and robust *PMA1* promoter on a multicopy plasmid (YEp). In our hands WT ↑Hgt1p cells easily tolerate up to 10 µM GSH (Fig. 3.4., B) whereas the growth of *SEC61*^{N302D} ↑Hgt1p cells is hypersensitive (Fig. 3.4., B). *sss1-6* ↑Hgt1p growth is also hypersensitive to GSH as it was severely perturbed by 2.5 µM GSH and 5 µM GSH, and completely arrested by 10 µM GSH (Fig. 3.4., B).

Mn^{2+} is an essential cofactor for cytoplasmic farnesyl pyrophosphate (FPP) synthetase (Fpp1p) (44-46). Schuldiner and colleagues have shown that Fpp1p activity is elevated upon deletion of the ER resident Mn^{2+} transporter Spf1p due to a failure to store Mn^{2+} in the ER which gives rise to elevated Mn^{2+} levels in the cytosol (44). Elevated Fpp1p activity leads to increased squalene synthesis, which inhibits cell proliferation if cells cannot remove it through metabolism; such as when cells are challenged with the squalene epoxidase inhibitor terbinafine (44). We used this system to test if Sss1p mutants were also defective in maintaining normal Mn^{2+} homeostasis, and possessed increased Fpp1p activity. *sss1-6* and *sss1-7*, in particular, cell growth is extremely sensitive to terbinafine as, unlike wildtype, 1 µg/mL terbinafine completely inhibited the growth of *sss1-7* and *sss1-6* at 30ºC and 34ºC respectively (Fig. 3.4., C). Importantly, neither *sss1-6* nor *sss1-7* cells are hypersensitive to the 14α-sterol demethylase inhibitor miconazole (Supp. Fig. S3.2., B). Therefore, the hypersensitivity of both *sss1-6* and *sss1-7* cells to terbinafine is not simply due to these mutants being hypersensitive to small molecules that inhibit ergosterol biosynthesis.

Mutations in Residues of Sec61p Located in Important Gating Modules Suppress *sss1-6* and *sss1-7* Temperature Sensitivity

To understand how mutations in the C-terminus of Sss1p disrupt ER homeostasis we sought to identify mutations in the major interacting partner of Sss1p, Sec61p, which could suppress *sss1-7* temperature sensitive growth. Missense mutations were incorporated into the *SEC61* gene by error-prone PCR and mutagenised *SEC61* genes were then transfected into *sss1-7* yeast and integrated into the *SEC61* genetic locus by homologous recombination. In total 203 Ts^+ colonies were isolated and the complete nucleotide sequence of 50 was determined. On average EP-PCR yielded 3.5 mutations per 1 kb and 23 of the 50 mutants sequenced contained a single nucleotide substitution in the *SEC61* open reading frame (ORF). In total five different *SEC61* mutant alleles, V82F, S289F, N302K, N302Y and T379A were obtained from this screen. We were surprised to discover that each mutation was able to suppress the temperature sensitive growth of *sss1-6* and *sss1-7* (Fig. 3.5., A) and reduced UPR induction (Fig. 3.5., B) in these *sss1* mutants when expressed from a low-copy, centromeric plasmid, avoiding the need to integrate these mutations into the *SEC61* locus.

The functionality of these suppressive *SEC61* mutants is not compromised as each mutant supports the robust growth of cells when expressed as the only copy of *SEC61* (Fig. 3.6., A & B). Furthermore, neither mutant possessed temperature growth phenotype (Fig. 3.6., A). We did not detect any major SRP dependent or SRP independent translocation defects in these mutants. The SRP dependent precursor pDPAP B readily accumulates in the *sec65-1^{ts}* control at both permissive and non-permissive temperatures but not in our panel of *SEC61* mutants (Fig. 3.6., C). Also, neither SRP independent translocation precursor pLhs1p nor ppαf accumulated in these *SEC61* mutants at 30°C and 37°C unlike the *sec62-1^{ts}* control (Fig. 3.6., C).

Mapping each mutation on the crystal structure of the Sec61 homologue Ssh1 revealed them to be positioned at critical sites for translocon gating including the pore ring (V82) and the lateral and lumenal gate (S289F, N302K/Y and T379A) (Supp. Fig. S3.3.). Residue N302 is part of a network that is responsible for the opening and closing of the lateral and lumenal gates of the translocon. That the *SEC61^{N302K}* and

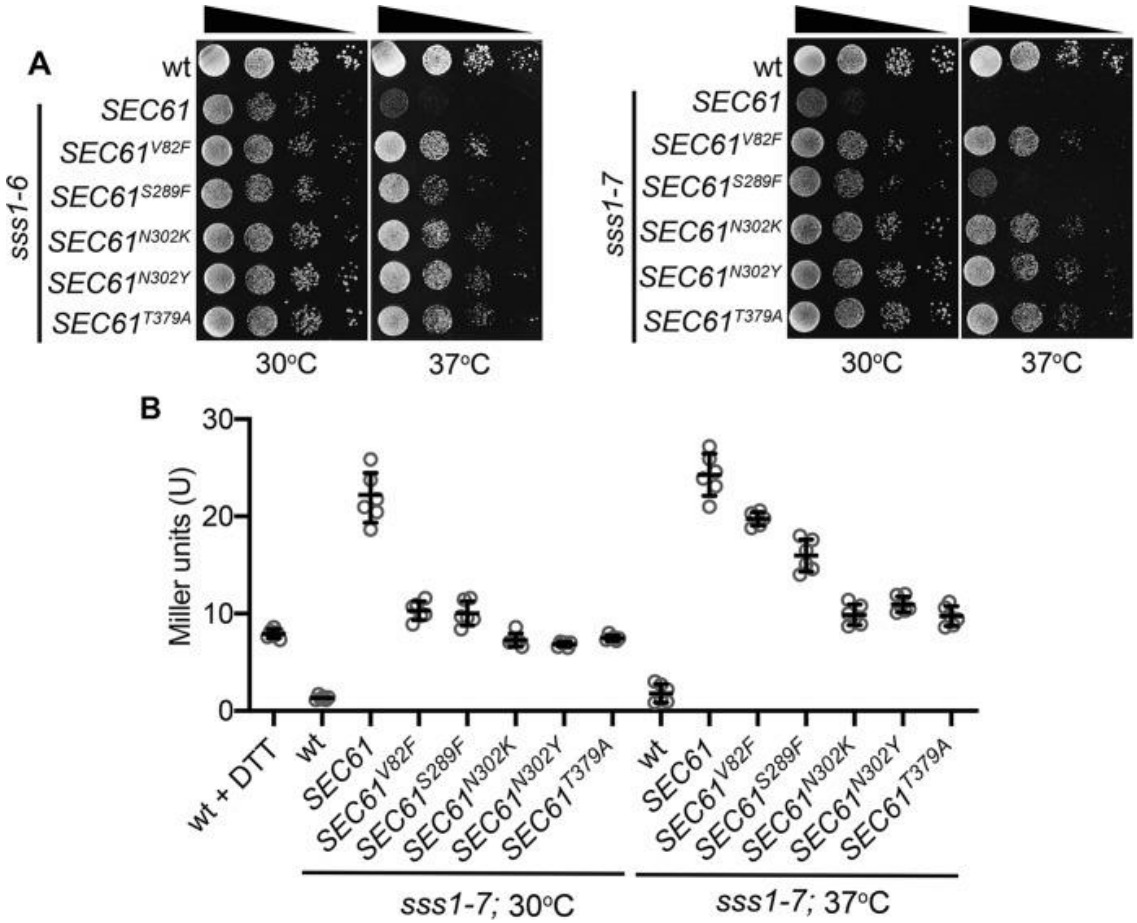

Fig. 3.5. Mutations in residues of Sec61p located in important gating modules suppress *sss1-6* and *sss1-7* temperature sensitivity. (A) Wildtype, *sss1-6* or *sss1-7* yeast transformed with either YCp *SEC61*, YCp *SEC61^{V82F}*, YCp *SEC61^{S289F}*, YCp *SEC61^{N302K}*, YCp *SEC61^{N302Y}* or YCp *SEC61^{T379A}* were spotted on YPD agar in a 10-fold dilution series and incubated at 30°C or 37°C for 2 days. (B) Wildtype, *sss1-6* or *sss1-7* yeast transformed with either YCp *SEC61*, YCp *SEC61^{V82F}*, YCp *SEC61^{S289F}*, YCp *SEC61^{N302K}*, YCp *SEC61^{N302Y}* or YCp *SEC61^{T379A}* and with pJT30 (UPRE-LacZ) were grown in –Ura selective medium and β-Galactosidase activity determined. As a positive control wildtype cells were treated with 5mM DTT for 2 hours.

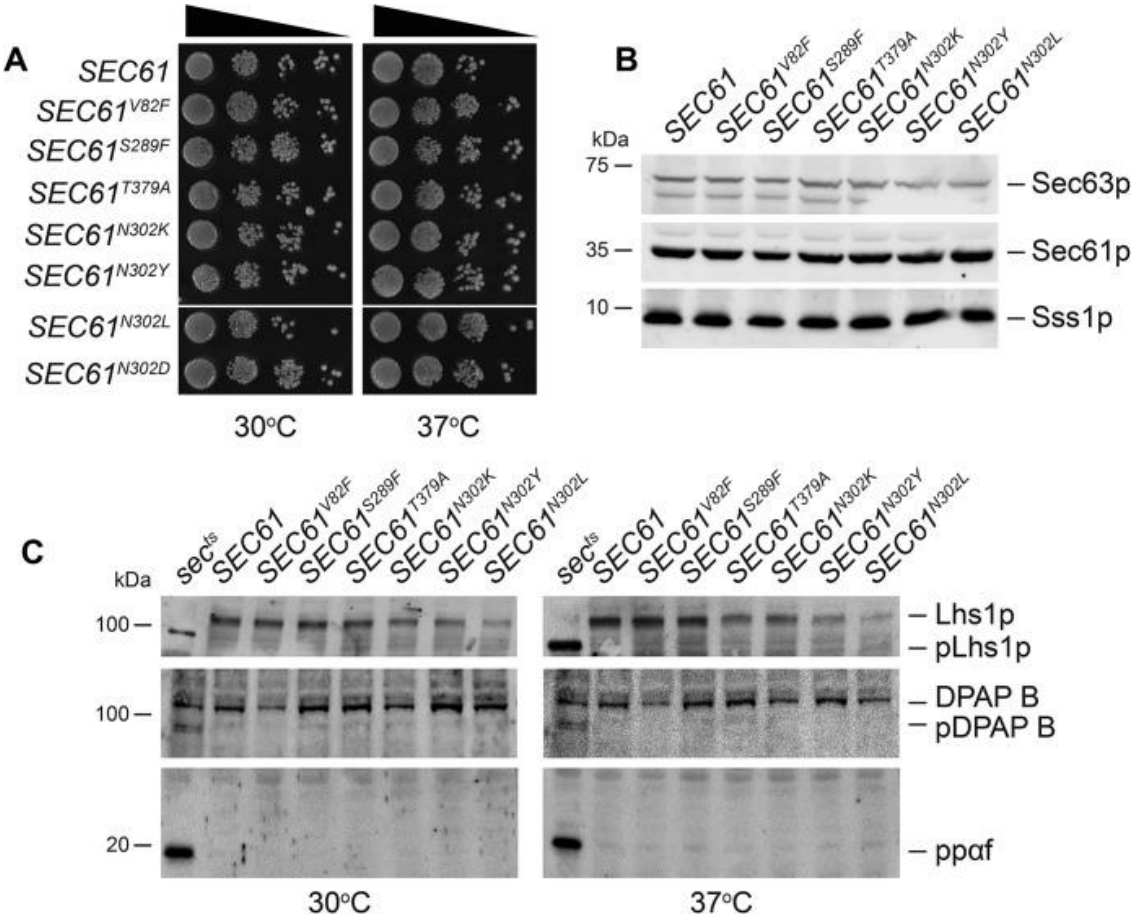

Fig. 3.6. SEC61 dependent suppressors of *sss1-6* and *sss1-7* are functional. (A) Wildtype, *SEC61^{V82F}*, *SEC61^{S289F}*, *SEC61^{N302K}*, *SEC61^{N302Y}*, *SEC61^{T379A}*, *SEC61^{N302L}* or *SEC61^{N302D}* yeast were spotted on YPD agar in a 10-fold dilution series and incubated at 30°C or 37°C for 2 days. **(B)** Cell extracts derived from wildtype *SEC61^{V82F}*, *SEC61^{S289F}*, *SEC61^{N302K}*, *SEC61^{N302Y}*, *SEC61^{T379A}* or *SEC61^{N302L}* yeast were immunoblotted with anti- Sss1p, anti-Sec61p and anti-Sec63p antibodies. **(C)** Cell extracts derived from wildtype *SEC61^{V82F}*, *SEC61^{S289F}*, *SEC61^{N302K}*, *SEC61^{N302Y}*, *SEC61^{T379A}* or *SEC61^{N302L}* yeast grown at 30°C or 37°C were immunoblotted with anti-Lhs1p, anti-DPAP B and anti- alpha factor antibodies.

SEC61^{N302Y} mutations suppresses both *sss1-6* and *sss1-7* suggests that dynamics of the lateral and lumenal gate of the translocon is altered somehow in these *sss1* mutants. Substitution of N302 to a polar (N302D) or hydrophobic residue (N302L) destabilises the closed or open conformation of the Sec61 complex, respectively (47). To investigate if *sss1*^{H72K} and *sss1*$^{P74A,\ I75A}$ mutations destabilise either the open or closed conformation of the translocon we tested if the *SEC61*^{N302L} or the *SEC61*^{N302D} mutation suppressed *sss1-6* and *sss1-7* temperature sensitivity. The *SEC61*^{N302L} mutant suppressed *sss1-6* and *sss1-7* temperature sensitive growth (Fig. 3.7., A) and reduced UPR induction (Fig. 3.7., B) like *SEC61*^{N302K} and *SEC61*^{N302Y}. In contrast, co-expression of *SEC61*^{N302D} with either *sss1-6* or *sss1-7* exacerbated the growth defects of these mutants (Fig. 3.7., C & D). Furthermore, we were unable to isolate *sss1-7 sec61*^{N302D} double mutants (Fig. 3.7., C), suggesting the possibility that these mutations, when co-expressed, are synthetically lethal. Together, this suggests that the *sss1-6* and *sss1-7* mutations may destabilise the closed conformation of the translocon.

Mutations in Residues Located in Important Sec61p Gating Modules Suppress the Elevated ER Permeability Observed in *sss1-6* and *sss1-7*

Given the impressive manner in which our *SEC61* mutants were able to diminish the level of ER stress in both *sss1-6* and *sss1-7* we were keen to determine whether these mutants were also able to suppress phenotypes associated with altered ER permeability. Co-expression of each of the *SEC61* suppressors of *sss1-7* temperature sensitive growth were able to suppress the hypersensitivity of the *sss1-6* mutant to GSH (Fig. 3.8., A & B). Furthermore, co-expression of the *SEC61* mutants that suppressed *sss1-6* and *sss1-7* temperature sensitive growth also suppressed their hypersensitivity to terbinafine, albeit with varying strength (Fig. 3.8., C & D).

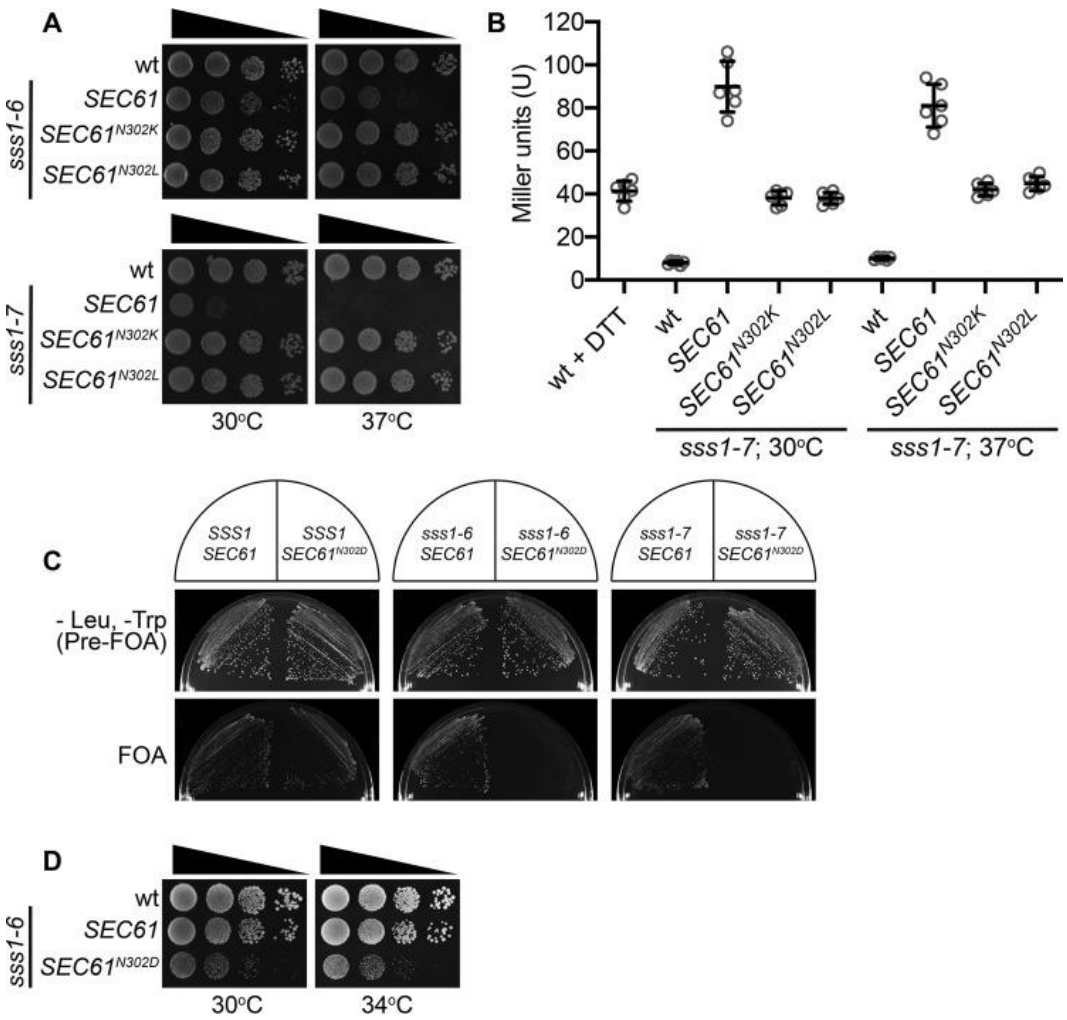

Fig. 3.7. Mutations in the lumenal lateral gate genetically interact with *sss1-6* and *sss1-7*. (A) Wildtype, and *sss1-6* or *sss1-7* yeast transformed with either YCp *SEC61*, YCp *SEC61*^{N302K} or YCp *SEC61*^{N302L} were spotted on YPD agar in a 10-fold dilution series and incubated at 30°C or 37°C for 2 days. **(B)** Wildtype or *sss1-7* yeast transformed with either YCp *SEC61*, YCp *SEC61*^{N302K} or YCp *SEC61*^{N302L} and with pJT30 (UPRE-LacZ) were grown in –Ura selective medium and β-Galactosidase activity was determined. As a positive control wildtype cells were treated with 5mM DTT for 2 hours. **(C)** CMY5 yeast were co-transformed with either YCp *SSS1*, YCp *sss1-6* or YCp *sss1-7* and either YCp *SEC61* or YCp *SEC61*^{N302D}. Transformants were streaked out onto either –Leu, -Trp selective medium or medium containing FOA and incubated at 30°C for 3 days. **(D)** CMY5 yeast co-transformed with YCp *sss1-6* and either YCp *SEC61* or YCp *SEC61*^{N302D} recovered from FOA containing medium were spotted on YPD agar in a 10-fold dilution series and incubated at 30°C or 37°C for 2 days.

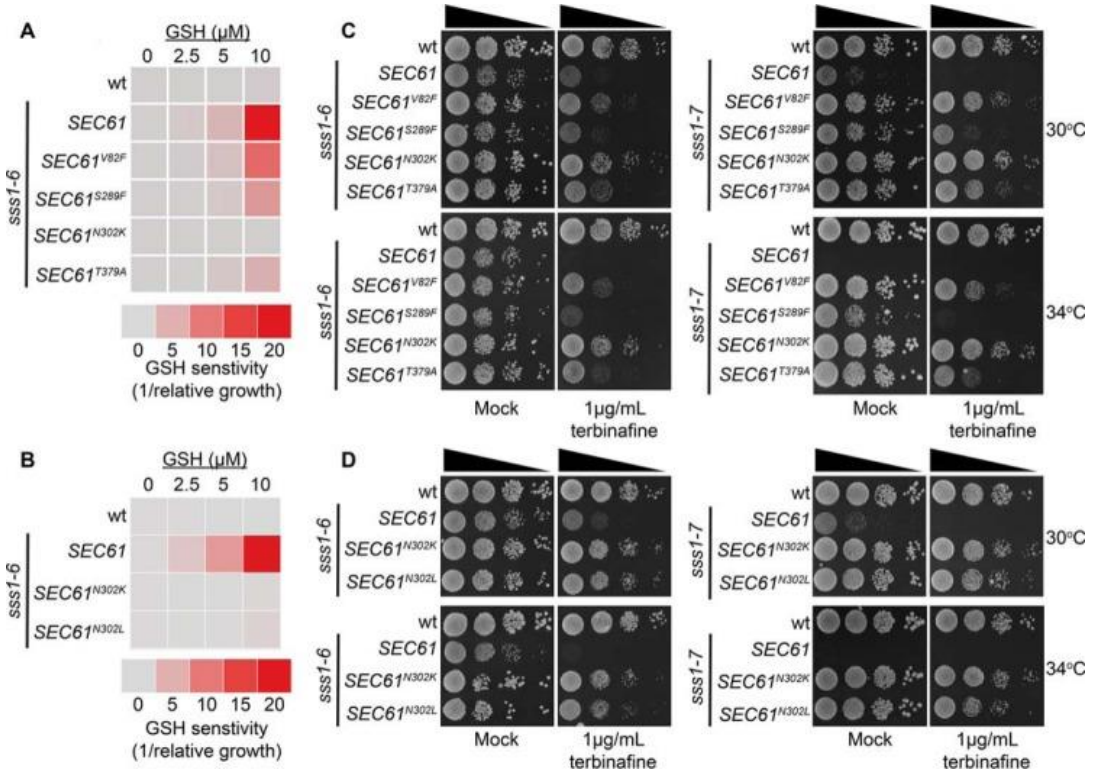

Fig. 3.8. Mutations in residues of Sec61p located in important gating modules suppress ER permeability defects in *sss1-6* and *sss1-7*. (A) Wildtype, or *sss1-6* yeast transformed with either YCp *SEC61*, YCp *SEC61*^{V82F}, YCp *SEC61*^{S289F}, YCp *SEC61*^{N302K}, or YCp *SEC61*^{T379A} were transformed with YEp *HGT1* were grown in –Ura selective medium with increasing concentrations of GSH. The relative growth of each strain determined and the GSH sensitivity (1/relative growth) presented. **(B)** Wildtype, *sss1-6* or *sss1-6* yeast transformed with either YCp *SEC61*^{N302K} or YCp *SEC61*^{N302L} and YEp *HGT1* were grown in –Ura medium with increasing concentrations of GSH, the relative growth of each strain determined and the GSH sensitivity (1/relative growth) presented. **(C)** Wildtype, and *sss1-6* or *sss1-7* yeast transformed with either YCp *SEC61*, YCp *SEC61*^{V82F}, YCp *SEC61*^{S289F}, YCp *SEC61*^{N302K}, or YCp *SEC61*^{T379A} were spotted on YPD agar or YPD agar containing 1 µg/mL terbinafine in a 10-fold dilution series and incubated at 30°C or 34°C for 2 days. **(D)** Wildtype, *sss1-6*, *sss1-7* or *sss1-6* and *sss1-7* yeast transformed with either YCp *SEC61*^{N302K} or YCp *SEC61*^{N302L} were spotted on YPD agar or YPD agar supplemented with 1 µg/mL terbinafine in a 10-fold dilution series and incubated at 30°C or 34°C for 2 days.

Discussion

Sss1p/Sec61γ is an essential and highly conserved subunit of the ER translocase yet its function is poorly understood. A heptapeptide, KLIHIPI, located towards the C-terminus of the protein is absolutely conserved in all eukaryotes studied to date. Herein, we discover the KLIHIPI peptide to be an important factor that influences ER permeability.

The Extreme Sss1p/Sec61γ C-terminus Influences ER Permeability

Cells expressing *sss1* mutants with defective TM domains have been shown to be defective in ER translocation (22, 35). We were surprised to find no ER translocation defect in both *sss1-6* and *sss1-7* cells even though the UPR was highly induced in both mutants. Sss1p, like Sec61p, is essential for both SRP dependent and SRP independent ER translocation. That we find no evidence of the accumulation of secretory precursor proteins at steady state suggests that mutation of the highly conserved C-terminus of Sss1p does not result in the gross perturbation in the formation of protein complexes that are required to conduct ER translocation. Given that Sss1p/Sec61γ is a C-terminally anchored protein it is possible that both Sss1-6p and Sss1-7p may not be efficiently targeted to and incorporated into the ER membrane. Our data does not support this notion. We do not observe a decrease in either the membrane associated pool of Sss1-6p and Sss1-7p nor do we observe a decreased ability to crosslink both Sec61p and Sss1p with DSS. The latter point is crucial to this conclusion as the insertion of C-terminal anchored proteins proceeds via the GET complex and not the ER translocase. Therefore, the cross-linking of Sec61p with both Sss1-6p and Sss1-7p reflects a functional interaction rather than a trivial interaction of Sec61p with a translocation intermediate. In further support, we observe no reduction in the ability to isolate components of the ER SEC complex by Con A pull down.

Those secretory proteins that are N-glycosylated are modified by the Oligosaccharyl transferase (OST) as they are translocated through the translocation channel. Sss1p is physically located at the interface between the translocon and OST. It is possible that mutation of the highly conserved Sss1p C-terminus perturbs the association of

OST with the translocon. However, we find no evidence of N-glycosylation being perturbed in *sss1-6* and *sss1-7*, the N-glycosylation status of Lhs1p and DPAP B is indistinguishable from wildtype. Furthermore, *MAT α* derivatives of both *sss1-6* and *sss1-7* secrete sufficient quantity of α factor to enable their mating with *MAT a* strains. We therefore have to consider other possibilities to explain the severe ER stress in *sss1-6* and *sss1-7* mutants.

A directed evolution approach was therefore used to obtain *SEC61* mutants that suppressed the temperature sensitive growth defect of *sss1-7* cells in order to understand what aspect of translocon function was disrupted in these *sss1* mutants. We isolated two different classes of suppressor mutation: class one mutations (V82F) mutations are located in the pore ring and class two mutations (S289F, N302K/Y and T379A) are located in the lateral and lumenal gate that coordinates the opening and closing of the protein conducting channel. A common feature of both classes of suppressor mutation is that they are situated in regions of the Sec61 protein that are required to gate the channel. The lateral gate, formed by TMs 2 and 7 of Sec61p, enables the incorporation of signal peptides or transmembrane helices into the lipid bilayer once they have emerged from the ribosome. Thus, the opening of the "lateral gate" is a critical process that allows protein translocation to proceed whilst maintaining the ER permeability barrier to ensure that ER lumenal equivalents do not leak into the cytosol and vice versa. Apolar residues in the lumenal gate and a cluster of polar residues within the lateral gate forms a highly conserved gating motif that regulates the opening and closing of the Sec61 complex (47). One critical residue is Sec61p N302. Importantly, mutations that reconfigure the hydrogen bonding network have been shown to elicit a Prl phenotype (47). In contrast, mutations that increase the hydrophobicity enhance the nonpolar interactions between the lateral and lumenal gates, stabilises the closed conformation. Enhancing the non-polar interaction network suppressed both *sss1-6* and *sss1-7* temperature sensitivity.

Taken together this suggests the possibility that the ER is more permeable in *sss1-6* and *sss1-7*. We consider that our panel of *SEC61* mutations in the lumenal and lateral gate negate the ability of *sss1-6* and *sss1-7* to destabilise the closed conformation of the Sec61 complex. It is possible that these mutations suppress *sss1-6* and *sss1-7* by

reducing the rate of ER translocation to such an extent that a translocating intermediate can seal the channel by clogging the translocon. However, we consider this to be highly unlikely as each mutant is fully functional with no detectable defect in either SRP dependent or SRP independent translocation.

The Sec61 complex has been shown by Toledano and colleagues to facilitate the diffusion of reduced glutathione into the ER (42). It is important to note that the *SEC61*^{N302L} mutation in the lumenal-lateral gate was also utilised in this study to verify that the translocon forms the channel that facilitates the diffusion of GSH into the ER. Our panel of *SEC61* suppressors as well as *SEC61*^{N302L} suppresses *sss1-6* hypersensitivity to GSH. These *SEC61* mutations also rescues the hypersensitivity of both *sss1-6* and *sss1-7* to terbinafine, a phenotype that has been previously shown to arise in mutants defective in ER Mn^{2+} storage (44). We appreciate that the hypersensitivity of both *sss1-6* and *sss1-7* growth to terbinafine is itself an indirect measure of increased ER permeability in these mutants. However, both *sss1-6* and *sss1-7* are not hypersensitive to the 14α-sterol demethylase inhibitor, miconazole ruling out that this phenotype is due to these *sss1* mutants being hypersensitive to reagents that inhibit ergosterol biosynthesis. Together we hypothesise that the C-terminus of Sss1p/Sec61γ constitutes an important component of the gating module that coordinates the opening and closing of the translocon with both *sss1-6* and *sss1-7* destabilising the closed state. Future work will provide a mechanistic insight in to the role of this domain. The importance of the C-terminus of Sss1p as a key component of the translocon gating module is reflected in the absolute conservation of the KLIHIPI heptapeptide throughout the *eukaryota*.

Materials and Methods

Yeast Strains and Growth

Saccharomyces cerevisiae strains are listed in Supp. Table S3.1. and plasmids are listed in Supp. Table S3.2. Yeast strains were grown routinely at 30°C in YP medium (2% peptone, 1% yeast extract) containing 2% glucose (YPD) or in minimal medium (0.67% yeast nitrogen base; YNB) with 2% glucose plus appropriate supplements for selective growth. All media were from FORMEDIUM (Hunstanton, U.K.). For growth assays yeast were spotted in a 10-fold dilution series on YPD agar and grown at either 30°C, 34°C or 37°C for 2-3 days. 1 µg/mL terbinafine or DMSO was added to YPD agar where indicated.

Mutagenesis and Selection for *SEC61* Suppressors of *sss1-7* Temperature Sensitivity

EP-PCR was carried out with Taq DNA polymerase in the presence of 500 µM $MnCl_2$ and run for 10 cycles. Reactions were also performed with inverse dNTP concentrations. Samples were pooled after EP-PCR and digested with *Hind III* for 1 hour at 37°C. *sss1-7* yeast were transformed with restricted PCR product and transformants were plated on YPD agar and incubated at 37°C for upto 5 days. The *SEC61* locus of suppressor colonies was sequenced and individual mutations were introduced in pBW11 by site-directed mutagenesis using the Q5® Site Directed Mutagenesis Protocol (NEB), oligonucleotides used are listed in Supp. Table S3.3.

Fluorescence Microscopy

The GFP ORF was amplified with oligonucleotides flanked with 5' *PacI* and 3' *SphI* and ligated into pJKB2 in which nucleotides -8 to -1 and 1 to 6 were mutated to encode *PacI* and *SphI* restriction sites respectively giving pLB4 (YCp GFP-*SSS1*). The *sss1-6* and *sss1-7* mutations were incorporated into pLB4 using the Q5® Site Directed

Mutagenesis Protocol (NEB) givig pLB5 and pLB6 respectively. Oligonucleotides used are listed in Supp. Table S3.3. Static images were collected of live cells attached to a concanavalin A-coated slide using an Ultraview Spinning Disk Confocal Microscope (Perkin Elmer Life Sciences).

DSS Cross-linking

Yeast microsomes were prepared according to Rothblatt and Meyer, 1986 (48). Membranes were treated with DMSO or 1 mM DSS at 30 °C or 37 °C for 30 min and then quenched by the addition of 10 mM lysine and 100 mM Tris for 10 mins.

Immunoblotting

Antibodies used are listed in Supp. Table S3.4.

ConA Dependent Fractionation of SEC Proteins

The fractionation of SEC proteins by ConA was performed according to Pilon et al., 1998 (40). Briefly, microsomes were isolated and resuspended in 100 µL of solubilisation buffer (50 mM HEPES/KOH, pH 7.4, 400 mM KAc, 5 mM MgAc, 10% [wt/vol] glycerol, 0.05% [vol/vol] β-mercaptoethanol) on ice containing protease inhibitors (5 µg/mL leupeptin, 0.5 µg/mL pepstatin, 1 mM amino-benzamidine, 2.5 µg/mL chymostatin, and 0.1 mM PMSF). Membranes were solubulised by the addition of 400 µL solubilisation buffer containing 3.75% (wt/vol) digitonin. Next, samples were centrifuged at 100,000 x g in a Beckman TLA100.3 rotor for 60 min at 4°C to isolate the ribosome attached membrane proteins (RAMPs). The supernatant fraction was added to 100 µL of a suspension of concanavalin A (Con-A)-Sepharose equilibrated in 50 mM HEPES/KOH (pH 7.4), 10% (wt/vol) glycerol, 0.05% (vol/vol) β-mercaptoethanol, 1% (wt/vol) digitonin, and protease inhibitors, and incubated for 60 mins at 4°C. The beads were recovered by centrifugation at 2500 × g and the supernatant fraction was cleared from any remaining beads at 12,000 × g (free

fraction). The Con-A beads were washed three times with 1 mL of equilibration buffer. Equal aliquots of both fractions were analysed by SDS-PAGE and immunoblotting with the indicated antibodies.

β-Galactosidase Assays

β-Galactosidase assays were performed according to Tyson and Stirling 2000 (49). Briefly, yeast cells were grown at 30 °C in minimal medium containing 2% glucose and appropriate supplements. Cultures were diluted to $A_{600\,nm}$ of 0.2 and grown for a further 4 h. Cells were isolated, and resuspended in 2 mL of Z buffer (60 mM Na_2HPO_4, 40 mM NaH_2PO_4, 10 mM KCl, 10 mM $MgSO_4$, 50 mM 2-mercaptoethanol, pH 7.0). Aliquots (0.8 mL) were collected, cells were permeabilised in 50 µL of 0.1% (w/v) SDS and 100 µL of $CHCl_3$, and samples were equilibrated to 30°C. Assays were initiated by addition of 160 µL of o-nitrophenyl-galactopyranoside (4 mg/mL stock solution in Z buffer) and incubated at 30°C for 20 min. Reactions were terminated by addition of 400 µL of 1 M Na_2CO_3, pH 9.0, the $OD_{420\ nm}$ was measured, and LacZ activity (U) was calculated by multiplying $OD_{420\ nm}/OD_{600\ nm}$ by 1000. Three independent biological replicates and at least two technical replicates were performed.

Glutathione Sensitive Growth Assay

Cells harbouring YEp *HGT1* were grown to mid logarithmic-phase and then sub-cultured to 0.01 OD_{600nm} in SC media without uracil containing 0-10 µM GSH and the growth rate recorded. The growth rate of cells cultured in the absence of GSH was set to 100% and relative growth rates plotted. Three independent biological replicates and at least two technical replicates were performed.

Footnotes

Acknowledgments: We would like to thank Curtin University School of Pharmacy and Biomedical Sciences for funding.

Conflict of interest: The authors declare that they have no conflicts of interest with the contents of this article.

Author contributions: C.J.M, C.J.S. and B.J.S conceived, designed, and analysed the research; C.M.W., H.G.D., A.L.P., K.L.P.S and P.W. performed the research; L.B. and A.L.B constructed and prepared plasmids, C.J.M. and R.F.L.S supervised C.M.W., H.G.D., A.L.P., K.L.P.S., P.W., L.B. and A.L.B.; C.J.M., R.F.L.S., B.L.S and C.M.W. wrote the paper.

References

1. Behnke J, Feige MJ, Hendershot LM. BiP and its nucleotide exchange factors Grp170 and Sil1: mechanisms of action and biological functions. Journal of molecular biology. 2015;427(7):1589-608.
2. Janda CY, Li J, Oubridge C, Hernandez H, Robinson CV, Nagai K. Recognition of a signal peptide by the signal recognition particle. Nature. 2010;465(7297):507-10.
3. Rapoport TA, Li L, Park E. Structural and Mechanistic Insights into Protein Translocation. Annual review of cell and developmental biology. 2017;33:369-90.
4. Voorhees RM, Hegde RS. Structures of the scanning and engaged states of the mammalian SRP-ribosome complex. eLife. 2015;4:e07975.
5. Walter P II, Blobel G. Translocation of proteins across the endoplasmic reticulum. I. Signal recognition protein (SRP) binds to in-vitro-assembled polysomes synthesizing secretory protein. The Journal of cell biology. 1981;91(2):545-50.
6. Keenan RJ, Freymann DM, Stroud RM, Walter P. The signal recognition particle. Annual review of biochemistry. 2001;70:755-75.
7. Luirink J, Sinning I. SRP-mediated protein targeting: structure and function revisited. Biochimica et biophysica acta. 2004;1694(1-3):17-35.
8. Ulbrandt ND, Newitt JA, Bernstein HD. The E. coli Signal Recognition Particle Is Required for the Insertion of a Subset of Inner Membrane Proteins. Cell. 1997;88(2):187-96.
9. Bohni PC, Deshaies RJ, Schekman RW. SEC11 is required for signal peptide processing and yeast cell growth. The Journal of cell biology. 1988;106(4):1035-42.
10. Evans EA, Gilmore R, Blobel G. Purification of microsomal signal peptidase as a complex. Proceedings of the National Academy of Sciences of the United States of America. 1986;83(3):581-5.
11. Braakman I, Hebert DN. Protein folding in the endoplasmic reticulum. Cold Spring Harbor perspectives in biology. 2013;5(5):a013201.
12. Zimmermann R, Eyrisch S, Ahmad M, Helms V. Protein translocation across the ER membrane. Biochimica et Biophysica Acta (BBA) - Biomembranes. 2011;1808(3):912-24.
13. Lakkaraju AK, Thankappan R, Mary C, Garrison JL, Taunton J, Strub K. Efficient secretion of small proteins in mammalian cells relies on Sec62-dependent posttranslational translocation. Molecular biology of the cell. 2012;23(14):2712-22.
14. Jensen RE, Johnson AE. Protein translocation: Is Hsp70 pulling my chain? Current Biology. 1999;9(20):R779-R82.
15. Ngosuwan J, Wang NM, Fung KL, Chirico WJ. Roles of Cytosolic Hsp70 and Hsp40 Molecular Chaperones in Post-translational Translocation of Presecretory Proteins into the Endoplasmic Reticulum. Journal of Biological Chemistry. 2003;278(9):7034-42.
16. Park E, Rapoport TA. Mechanisms of Sec61/SecY-mediated protein translocation across membranes. Annu Rev Biophys. 2012;41:21-40.
17. Plath K, Rapoport TA. Spontaneous Release of Cytosolic Proteins from Posttranslational Substrates before Their Transport into the Endoplasmic Reticulum. The Journal of cell biology. 2000;151(1):167-78.
18. Young BP, Craven RA, Reid PJ, Willer M, Stirling CJ. Sec63p and Kar2p are required for the translocation of SRP-dependent precursors into the yeast endoplasmic reticulum in vivo. The EMBO journal. 2001;20(1-2):262-71.
19. Deshaies RJ, Sanders SL, Feldheim DA, Schekman R. Assembly of yeast Sec proteins involved in translocation into the endoplasmic reticulum into a membrane-bound multisubunit complex. Nature. 1991;349(6312):806-8.

20. Panzner S, Dreier L, Hartmann E, Kostka S, Rapoport TA. Posttranslational protein transport in yeast reconstituted with a purified complex of Sec proteins and Kar2p. Cell. 1995;81(4):561-70.
21. Matlack KE, Misselwitz B, Plath K, Rapoport TA. BiP acts as a molecular ratchet during posttranslational transport of prepro-alpha factor across the ER membrane. Cell. 1999;97(5):553-64.
22. Falcone D, Henderson MP, Nieuwland H, Coughlan CM, Brodsky JL, Andrews DW. Stability and Function of the Sec61 Translocation Complex Depends on the Sss1p Tail-Anchor Sequence. The Biochemical journal. 2011;436(2):291-303.
23. Berg Bvd, Clemons WM, Collinson I, Modis Y, Hartmann E, Harrison SC, et al. X-ray structure of a protein-conducting channel. Nature. 2004;427(6969):36-44.
24. Mandon EC, Trueman SF, Gilmore R. Protein Translocation across the Rough Endoplasmic Reticulum. Cold Spring Harbor perspectives in biology. 2013;5(2):a013342.
25. Li W, Schulman S, Boyd D, Erlandson K, Beckwith J, Rapoport TA. The plug domain of the SecY protein stabilizes the closed state of the translocation channel and maintains a membrane seal. Molecular cell. 2007;26(4):511-21.
26. Finke K, Plath K, Panzner S, Prehn S, Rapoport TA, Hartmann E, et al. A second trimeric complex containing homologs of the Sec61p complex functions in protein transport across the ER membrane of S. cerevisiae. The EMBO journal. 1996;15(7):1482-94.
27. Jiang Y, Cheng Z, Mandon EC, Gilmore R. An interaction between the SRP receptor and the translocon is critical during cotranslational protein translocation. The Journal of cell biology. 2008;180(6):1149-61.
28. Prinz A, Hartmann E, Kalies KU. Sec61p is the main ribosome receptor in the endoplasmic reticulum of Saccharomyces cerevisiae. Biological chemistry. 2000;381(9-10):1025-9.
29. Grupe A, Li Y, Rowland C, Nowotny P, Hinrichs AL, Smemo S, et al. A Scan of Chromosome 10 Identifies a Novel Locus Showing Strong Association with Late-Onset Alzheimer Disease. American Journal of Human Genetics. 2006;78(1):78-88.
30. Gogala M, Becker T, Beatrix B, Armache J-P, Barrio-Garcia C, Berninghausen O, et al. Structures of the Sec61 complex engaged in nascent peptide translocation or membrane insertion2014. 107-10 p.
31. Voorhees RM, Fernandez IS, Scheres SH, Hegde RS. Structure of the mammalian ribosome-Sec61 complex to 3.4 A resolution. Cell. 2014;157(7):1632-43.
32. Becker T, Bhushan S, Jarasch A, Armache JP, Funes S, Jossinet F, et al. Structure of monomeric yeast and mammalian Sec61 complexes interacting with the translating ribosome. Science. 2009;326(5958):1369-73.
33. Cheng Z, Jiang Y, Mandon EC, Gilmore R. Identification of cytoplasmic residues of Sec61p involved in ribosome binding and cotranslational translocation. The Journal of cell biology. 2005;168(1):67-77.
34. Plath K, Mothes W, Wilkinson BM, Stirling CJ, Rapoport TA. Signal sequence recognition in posttranslational protein transport across the yeast ER membrane. Cell. 1998;94(6):795-807.
35. Wilkinson BM, Brownsword JK, Mousley CJ, Stirling CJ. Sss1p is required to complete protein translocon activation. The Journal of biological chemistry. 2010;285(42):32671-7.
36. Van den Berg B, Clemons WM, Jr., Collinson I, Modis Y, Hartmann E, Harrison SC, et al. X-ray structure of a protein-conducting channel. Nature. 2004;427(6969):36-44.
37. Schuldiner M, Metz J, Schmid V, Denic V, Rakwalska M, Schmitt HD, et al. The GET complex mediates insertion of tail-anchored proteins into the ER membrane. Cell. 2008;134(4):634-45.

38. Esnault Y, Feldheim D, Blondel MO, Schekman R, Kepes F. SSS1 encodes a stabilizing component of the Sec61 subcomplex of the yeast protein translocation apparatus. The Journal of biological chemistry. 1994;269(44):27478-85.
39. Wilkinson BM, Esnault Y, Craven RA, Skiba F, Fieschi J, K'Epes F, et al. Molecular architecture of the ER translocase probed by chemical crosslinking of Sss1p to complementary fragments of Sec61p. The EMBO journal. 1997;16(15):4549-59.
40. Pilon M, Romisch K, Quach D, Schekman R. Sec61p serves multiple roles in secretory precursor binding and translocation into the endoplasmic reticulum membrane. Molecular biology of the cell. 1998;9(12):3455-73.
41. Ng DT, Brown JD, Walter P. Signal sequences specify the targeting route to the endoplasmic reticulum membrane. J Cell Biol. 1996;134(2):269-78.
42. Ponsero AJ, Igbaria A, Darch MA, Miled S, Outten CE, Winther JR, et al. Endoplasmic Reticulum Transport of Glutathione by Sec61 Is Regulated by Ero1 and Bip. Molecular cell. 2017;67(6):962-73 e5.
43. Kumar C, Igbaria A, D'Autreaux B, Planson AG, Junot C, Godat E, et al. Glutathione revisited: a vital function in iron metabolism and ancillary role in thiol-redox control. The EMBO journal. 2011;30(10):2044-56.
44. Cohen Y, Megyeri M, Chen OC, Condomitti G, Riezman I, Loizides-Mangold U, et al. The yeast p5 type ATPase, spf1, regulates manganese transport into the endoplasmic reticulum. PLoS One. 2013;8(12):e85519.
45. Davis CD, Ney DM, Greger JL. Manganese, iron and lipid interactions in rats. J Nutr. 1990;120(5):507-13.
46. Hansen SL, Spears JW, Lloyd KE, Whisnant CS. Growth, reproductive performance, and manganese status of heifers fed varying concentrations of manganese. J Anim Sci. 2006;84(12):3375-80.
47. Trueman SF, Mandon EC, Gilmore R. A gating motif in the translocation channel sets the hydrophobicity threshold for signal sequence function. The Journal of cell biology. 2012;199(6):907-18.
48. Rothblatt JA, Meyer DI. Secretion in yeast: translocation and glycosylation of prepro-alpha-factor in vitro can occur via an ATP-dependent post-translational mechanism. The EMBO journal. 1986;5(5):1031-6.
49. Tyson JR, Stirling CJ. LHS1 and SIL1 provide a lumenal function that is essential for protein translocation into the endoplasmic reticulum. The EMBO journal. 2000;19(23):6440-52.
50. Rentsch D, Laloi M, Rouhara I, Schmelzer E, Delrot S, Frommer WB. NTR1 encodes a high affinity oligopeptide transporter in Arabidopsis. FEBS Lett. 1995;370(3):264-8.
51. Metzger MB, Maurer MJ, Dancy BM, Michaelis S. Degradation of a cytosolic protein requires endoplasmic reticulum-associated degradation machinery. The Journal of biological chemistry. 2008;283(47):32302-16.
52. Stirling CJ, Rothblatt J, Hosobuchi M, Deshaies R, Schekman R. Protein translocation mutants defective in the insertion of integral membrane proteins into the endoplasmic reticulum. Molecular biology of the cell. 1992;3(2):129-42.
53. Wilkinson BM, Tyson JR, Reid PJ, Stirling CJ. Distinct domains within yeast Sec61p involved in post-translational translocation and protein dislocation. The Journal of biological chemistry. 2000;275(1):521-9.

Manuscript Supplementary Data

Supp. Table S3.1. Yeast strains used in this study.

Yeast	Genotype	Reference
BWY12	*MATα ade2- 1 ura3-1 his3-11,15 trp1-1 leu2-3,112 can1-100 sec61Δ::HIS3* pBW7	Wilkinson et al. 1997 (39)
BWY530	*MATα ade2- 1 ura3-1 his3-11,15 trp1-1 leu2-3,112 can1-100 sss1Δ::KanMX4* FKp53	Wilkinson et al. 2010 (35)
BWY531	*MATa ade2- 1 ura3-1 his3-11,15 trp1-1 leu2-3,112 can1-100 sss1Δ::KanMX4* FKp53	Wilkinson et al. 2010 (35)
SSS1	*MATα ade2- 1 ura3-1 his3-11,15 trp1-1 leu2-3,112 can1-100 sss1Δ::KanMX4* pJKB2	Wilkinson et al. 2010 (35)
SSS1-3	*MATα ade2- 1 ura3-1 his3-11,15 trp1-1 leu2-3,112 can1-100 sss1Δ::KanMX4* pHD1	This study
SSS1-4	*MATα ade2- 1 ura3-1 his3-11,15 trp1-1 leu2-3,112 can1-100 sss1Δ::KanMX4* pHD2	This study
SSS1-5	*MATα ade2- 1 ura3-1 his3-11,15 trp1-1 leu2-3,112 can1-100 sss1Δ::KanMX4* pHD3	This study
sss1-6	*MATα ade2- 1 ura3-1 his3-11,15 trp1-1 leu2-3,112 can1-100 sss1Δ::KanMX4* pJKB16	This study
sss1-7	*MATα ade2- 1 ura3-1 his3-11,15 trp1-1 leu2-3,112 can1-100 sss1Δ::KanMX4* pCM205	This study
CMY5	*MATα ade2- 1 ura3-1 his3-11,15 trp1-1 leu2-3,112 can1-100 sec61Δ::HIS3 sss1Δ::KanMX4* YCp *SEC61 SSS1 URA3*	This study
CWY1	*sss1-7* + YCp *SEC61*^{V82F} (pCW2)	This study
CWY2	*sss1-7* + YCp *SEC61*^{S289F} (pCW3)	This study
CWY3	*sss1-7* + YCp *SEC61*^{N302K} (pCW4)	This study
CWY4	*sss1-7* + YCp *SEC61*^{N302Y} (pCW5)	This study
CWY5	*sss1-7* + YCp *SEC61*^{T379A} (pCW6)	This study

CWY6	*sss1-7* + YCp *SEC61*^{N302L} (pCW7)	This study
CWY8	*sss1-7* + YCp *SEC61*^{V82F} (pCW2) + pJT30	This study
CWY9	*sss1-7* + YCp *SEC61*^{S289F} (pCW3) + pJT30	This study
CWY10	*sss1-7* + YCp *SEC61*^{N302K} (pCW4) + pJT30	This study
CWY11	*sss1-7* + YCp *SEC61*^{N302Y} (pCW5) + pJT30	This study
CWY12	*sss1-7* + YCp *SEC61*^{T379A} (pCW6) + pJT30	This study
CWY13	*sss1-7* + YCp *SEC61*^{N302L} (pCW7) + pJT30	This study
CWY15	*sss1-6* + YCp *SEC61*^{V82F} (pCW2) + pCW10	This study
CWY16	*sss1-6* + YCp *SEC61*^{S289F} (pCW3) + pCW10	This study
CWY17	*sss1-6* + YCp *SEC61*^{N302K} (pCW4) + pCW10	This study
CWY18	*sss1-6* + YCp *SEC61*^{N302Y} (pCW5) + pCW10	This study
CWY19	*sss1-6* + YCp *SEC61*^{T379A} (pCW6) + pCW10	This study
CWY20	*sss1-6* + YCp *SEC61*^{N302L} (pCW7) + pCW10	This study
CWY22	*sss1-6* + YCp *SEC61*^{V82F} (pCW2) + pJT30	This study
CWY23	*sss1-6* + YCp *SEC61*^{S289F} (pCW3) + pJT30	This study
CWY24	*sss1-6* + YCp *SEC61*^{N302K} (pCW4) + pJT30	This study
CWY25	*sss1-6* + YCp *SEC61*^{N302Y} (pCW5) + pJT30	This study
CWY26	*sss1-6* + YCp *SEC61*^{T379A} (pCW6) + pJT30	This study
CWY27	*sss1-6* + YCp *SEC61*^{N302L} (pCW7) + pJT30	This study
CWY29	*MATα ade2- 1 ura3-1 his3-11,15 trp1-1 leu2-3,112 can1-100 sec61Δ::HIS3* pCW8	This study
CWY30	*MATα ade2- 1 ura3-1 his3-11,15 trp1-1 leu2-3,112 can1-100 sec61Δ::HIS3 sss1Δ::KanMX4* pBW11 pLB1	This study
CWY31	*MATα ade2- 1 ura3-1 his3-11,15 trp1-1 leu2-3,112 can1-100 sec61Δ::HIS3 sss1Δ::KanMX4* pCW8 pLB1	This study
CWY32	*MATα ade2- 1 ura3-1 his3-11,15 trp1-1 leu2-3,112 can1-100 sec61Δ::HIS3 sss1Δ::KanMX4* pBW11 pLB2	This study

CWY33	*MATα ade2- 1 ura3-1 his3-11,15 trp1-1 leu2-3,112 can1-100 sec61Δ::HIS3 sss1Δ::KanMX4* pCW8 pLB2	This study
CWY34	*MATα ade2- 1 ura3-1 his3-11,15 trp1-1 leu2-3,112 can1-100 sec61Δ::HIS3 sss1Δ::KanMX4* pBW11 pLB3	This study
CWY35	*MATα ade2- 1 ura3-1 his3-11,15 trp1-1 leu2-3,112 can1-100 sec61Δ::HIS3 sss1Δ::KanMX4* pCW8 pLB3	This study
CWY36	*MATα ade2- 1 ura3-1 his3-11,15 trp1-1 leu2-3,112 can1-100 sec61Δ::HIS3* YCp *SEC61* (pBW11)	This study
CWY37	*MATα ade2- 1 ura3-1 his3-11,15 trp1-1 leu2-3,112 can1-100 sec61Δ::HIS3* YCp *SEC61*^{V82F} (pCW2)	This study
CWY38	*MATα ade2- 1 ura3-1 his3-11,15 trp1-1 leu2-3,112 can1-100 sec61Δ::HIS3* YCp *SEC61*^{S289F} (pCW3)	This study
CWY39	*MATα ade2- 1 ura3-1 his3-11,15 trp1-1 leu2-3,112 can1-100 sec61Δ::HIS3* YCp *SEC61*^{N302K} (pCW4)	This study
CWY40	*MATα ade2- 1 ura3-1 his3-11,15 trp1-1 leu2-3,112 can1-100 sec61Δ::HIS3* YCp *SEC61*^{N302Y} (pCW5)	This study
CWY41	*MATα ade2- 1 ura3-1 his3-11,15 trp1-1 leu2-3,112 can1-100 sec61Δ::HIS3* YCp *SEC61*^{T379A} (pCW6)	This study
CWY42	*MATα ade2- 1 ura3-1 his3-11,15 trp1-1 leu2-3,112 can1-100 sec61Δ::HIS3* YCp *SEC61*^{N302L} (pCW7)	This study
CWY43	*MATα ade2- 1 ura3-1 his3-11,15 trp1-1 leu2-3,112 can1-100 sss1Δ::KanMX4* pLB4 pSM1960	This study

CWY44	*MATα ade2- 1 ura3-1 his3-11,15 trp1-1 leu2-3,112 can1-100 sss1Δ::KanMX4* pLB5 pSM1960	This study
CWY45	*MATα ade2- 1 ura3-1 his3-11,15 trp1-1 leu2-3,112 can1-100 sss1Δ::KanMX4* pLB6 pSM1960	This study

Supp. Table S3.2. Plasmids used in this study.

Plasmid	Description	Reference
pJT30	UPRE-LacZ reporter	Tyson and Stirling, 2000 (49)
pBW11	YCp *SEC61 LEU2*	Wilkinson et al., 1997 (39)
pDR195	YEp *URA3* containing the *PMA1* promoter and *CYC1* terminator to enable high level gene expression.	Rentsch et al. 1995 (50)
pSM1960	YEp *SEC63*-mRFP *URA3*	Metzger et al., 2008 (51)
pJKB2	YCp *SSS1 HIS3*	Wilkinson et al., 2010. (35)
pJKB16	YCp *sss1*$^{P74A,\ I75A}$ *HIS3*	This study
pCM203	YCp *SEC61 SSS1 URA3*	This study
pCM205	YCp *sss1*^{H72K} *HIS3*	This study
pCW2	YCp *SEC61*^{V82F} *LEU2*	This study
pCW3	YCp *SEC61*^{S289F} *LEU2*	This study
pCW4	YCp *SEC61*^{N302K} *LEU2*	This study
pCW5	YCp *SEC61*^{N302Y} *LEU2*	This study
pCW6	YCp *SEC61*^{T379A} *LEU2*	This study
pCW7	YCp *SEC61*^{N302L} *LEU2*	This study
pCW8	YCp *SEC61*^{N302D} *LEU2*	This study
pCW10	YEp *HGT1 URA3*	This study
pHD1	YCp *sss1*$^{I68A\ K69A}$ *HIS3*	This study
pHD2	YCp *sss1*$^{L70A\ I71A}$ *HIS3*	This study
pHD3	YCp *sss1*$^{H72A\ I73A}$ *HIS3*	This study
pLB1	YCp *SSS1 TRP1*	This study
pLB2	YCp *sss1*$^{P74A,\ I75A}$ *TRP1*	This study
pLB3	YCp *sss1*^{H72K} *TRP1*	This study
pLB4	Ycp GFP-*SSS1 HIS3*	This study
pLB5	Ycp GFP-*sss1*$^{P74A,\ I75A}$ *HIS3*	This study
pLB6	YCp GFP-*sss1*^{H72K} *HIS3*	This study

Supp. Table S3.3. Oligonucleotides used in this study.

Name	Sequence
M13_F	GTAAAACGACGGCCAGT
M13_R	CAGGAAACAGCTATGAC
SEC61 5'_F	CCGTGTTCTAGACTTGTTTAAGC
SEC61 V82F_F	AATTGGGTTTTTCGCCCATCATCAC
SEC61 V82F_R	CCAGTAAAGTACCACGGTTGG
SEC61 S289F_F	CTTTTATACTTtCAACACCCCAATCATGTT
SEC61 S289F_R	TGGGGTGTTGaAAGTATAAAAGAGTTTGAT
SEC61 N302K_F	CATTGACTTCTAAaATTTTCTTGATCTCTC
SEC61 N302K_R	CAAGAAAATtTTAGAAGTCAATGCACTCTG
SEC61 N302Y_F	CATTGACTTCTttCATTTTCTTGATCTCTC
SEC61 N302Y_R	CAAGAAAATGgaAGAAGTCAATGCACTCTG
SEC61 T379A_F	ATTTTCCAAGgCATGGATCGAAATCTCCGG
SEC61 T379A_R	TTCGATCCATGcCTTGGAAAATACTGCGCA
SEC61 N302L_F	CATTGACTTCTctCATTTTCTTGATCTCTC
SEC61 N302L_R	CAAGAAAATGagAGAAGTCAATGCACTCTG
SEC61 N302D_F	CATTGACTTCTgaCATTTTCTTGATCTCTC
SEC61 N302D_R	CAAGAAAATGtcAGAAGTCAATGCACTCTG
SSS1 I68A K69A_F	TTACGCCgcCgcGTTGATTCATATTCCAAT
SSS1 I68A K69A_R	GAATCAACgcGgcGGCGTAACCAATGATAC
SSS1 L70A I71A_F	CATCAAGgcGgcTCATATTCCAATCAGATA
SSS1 L70A I71A_R	GAATATGAgcCgcCTTGATGGCGTAACCAA
SSS1 H72A I73A_F	GTTGATTgcTgcTCCAATCAGATACGTTAT
SSS1 H72A I73A_R	TGATTGGAgcAgcAATCAACTTGATGGCGT
SSS1 P74A I75A_F	GATTCATATTgCAgcCAGATACGTTATTGT
SSS1 P74A I75A _R	GTATCTGgcTGcAATATGAATCAACTTGAT
SSS1 H72K_F	AAGTTGATTaAaATTCCAATCAGATACGTTATTG
SSS1 H72K _R	TGATTGGAATtTtAATCAACTTGATGGCGTAAC
SphI pJKB2_F	gcatgcAGAGCTAGTGAAAAAGGTGAAGAG
pJKB2 PacI_R	ttaattaaTCAATGTTATACGTGATTTTATCTTTGG

PacI GFP_F	tttttttttaattaaatgAGTAAAGGAGAAGAACTTTTCAC
SphI GFP_R	tttttttgcatgcTTTGTATAGTTCATCCATGCC
*HGT*1_F	ATATAGCGGCCGCATGAGTACCATTTATAGGGAGAGCG
*HGT*1_R	ATATAGGATCCTTACCACCATTTATCATAACC

Supp. Table S3.4. Antibodies used in this study.

Antibody	Dilution	Reference
Anti-Sec61p, rabbit polyclonal	1:10,000	Stirling et al., 1992 (52)
Anti-Sss1p, sheep polyclonal	1:5000	Wilkinson et al., 2010 (35)
Anti-Sec63p, sheep polyclonal	1:10,000	Young et al., 2001 (18)
Anti-DPAP B, sheep polyclonal	1:5000	Wilkinson et al., 2000 (53)
Anti-α factor, sheep polyclonal	1:10,000	Tyson and Stirling 2000 (49)
HRP conjugated anti-sheep	1:20,000	N/A
HRP conjugated anti-rabbit	1:20,000	N/A

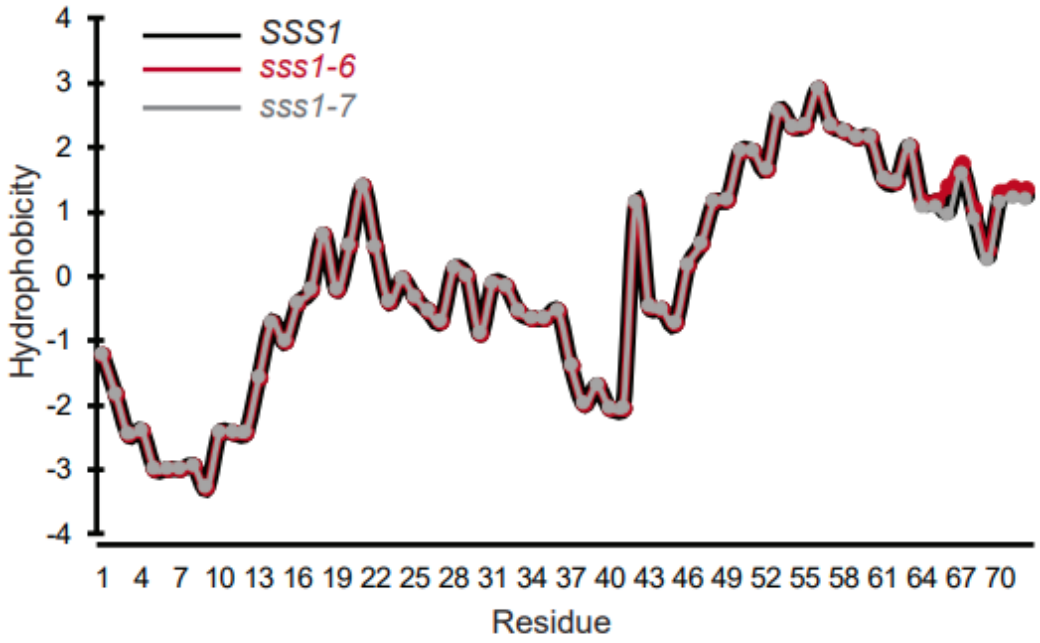

Supp. Fig. S3.1. The hydrophobicity of the Sss1-6p and Sss1-7p C-terminus is not compromised. Kyte-Doolittle analysis of Sss1p, Sss1-6p and Sss1-7p.

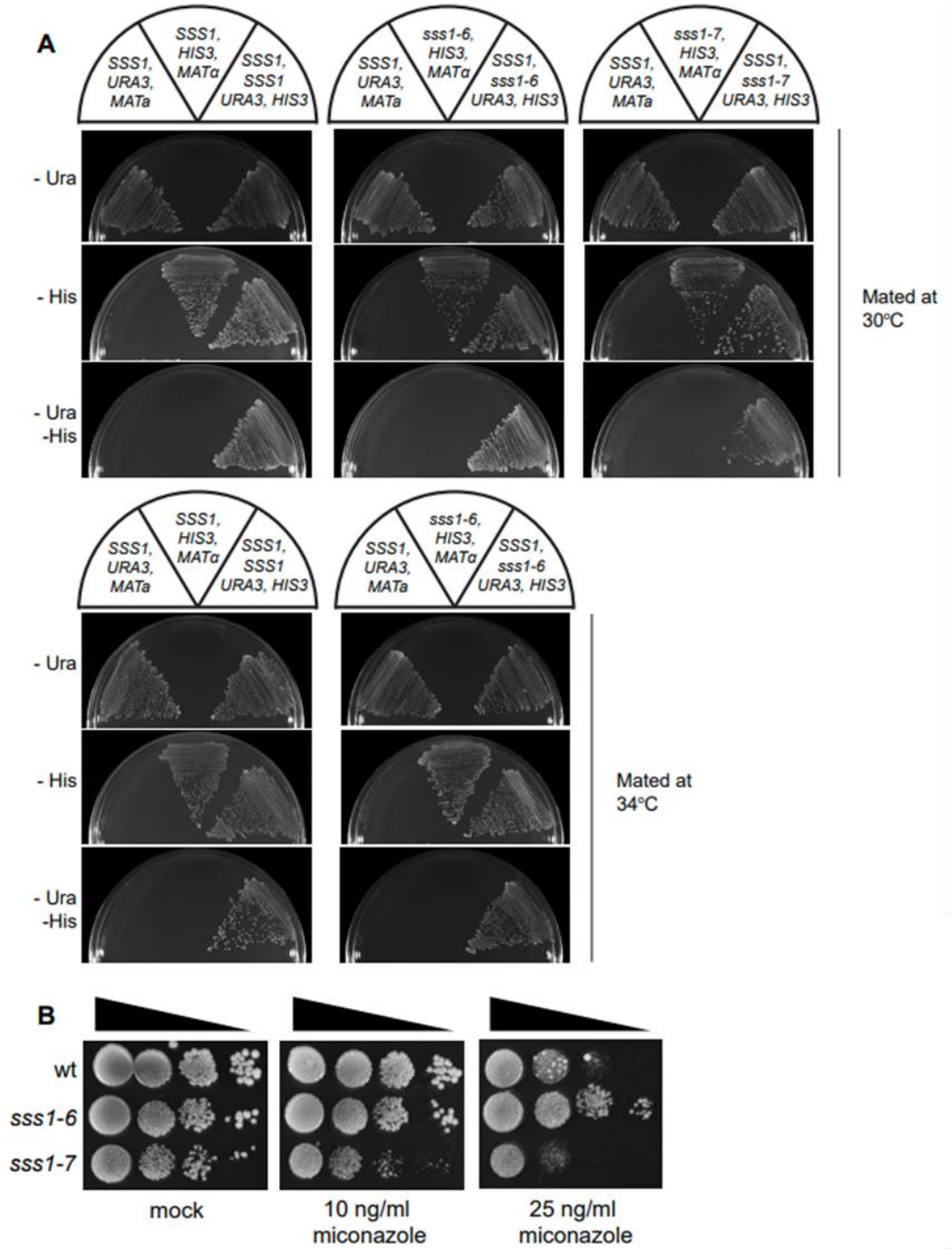

Supp. Fig. S3.2. (A) Wildtype, *sss1-6* and *sss1-7* cells were mated, overnight, with BWY531 (wildtype, Mat a) at 30°C and 34°C. After mating cells were grown on either -Ura, -His or synthetic complete media containing 1g/L 5'Fluororotic acid and grown at 30°C for 2 days. **(B)** Wildtype, *sss1-6* and *sss1-7* yeast were grown on either YPD or YPD containing 10 ng/mL or 25 ng/mL miconazole at 30°C.

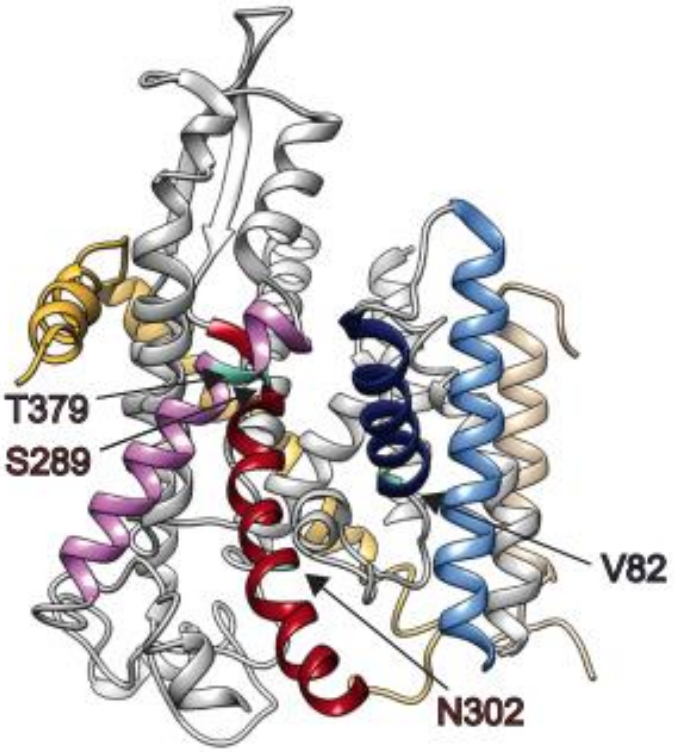

Supp. Fig. S3.3. Mutations in residues of Sec61p located in important gating modules suppress sss1-6 and sss1-7 temperature sensitivity. The equivalent residues of V82, S289, N302 and T379 are highlighted on the crystal structure of the Ssh1 complex (2WWA.pdb) (32).

Chapter 4

Characterising Cancer Associated Mutations of Sss1 that Impart Gating Dysregulation

Introduction

Translocon gating is an important regulatory process that enables the Sec61 complex to perform its essential function in protein translocation while simultaneously maintaining the integrity of the ER. However, the translocon has also been implicated to function as a leak channel that facilitates the flux of essential metabolites. This function is attributed to a third state of the translocon that follows the complete delivery of the polypeptide into the ER lumen. At this stage the translocon is found to remain bound to an idle ribosome, keeping the complex in the open conformation, and with the polypeptide no longer blocking the channel a facilitated flux of metabolites can occur (1). The facilitated flux of both Ca^{2+} and GSH have been demonstrated to occur through this process (1-3). These important biological metabolites are involved in establishing cellular signalling and redox status respectively, which demands that they are kept within an optimal range through the cooperation of active transporters and passive leak channels.

Calcium Regulation

In mammalian cells, the ER facilitates the storage of Ca^{2+} (4). A local supply of Ca^{2+} at the ER is necessary for optimal function with depletion having a negative impact on protein folding as many ER resident chaperones demonstrate an affinity for the ion (5). However, the role of Ca^{2+} far exceeds its action at the ER with involvement in critical cellular signalling, metabolism, autophagy, and apoptosis (6). The involvement of Ca^{2+} in these pivotal cellular events, places it under significant scrutiny. Mammalian cells evolved to have a highly responsive network of Ca^{2+} transporters that respond to Ca^{2+} oscillations. Depletion of Ca^{2+} at the ER results in

activation of store operated calcium entry (SOCE). This process begins as the ER transmembrane protein STIM1 senses the diminished lumenal Ca^{2+} and responds by aggregating at the ORI1 channel on the plasma membrane. This engages the influx of Ca^{2+} into the cytosol from the extracellular environment (7, 8). At the ER the local Ca^{2+} environment is controlled via influx and efflux channels. Sarco/endoplasmic reticulum Ca^{2+}-ATPase (SERCA) predominately enables influx while inositol trisphosphate receptors (IP3Rs) and ryanodine receptors (RYRs) in co-operation with calcium leak channels (i.e. Sec61 translocon) permit Ca^{2+} efflux (6-9). More specifically Ca^{2+} leak channels and the more ubiquitously present isoform, IP3R1, impact steady state Ca^{2+} levels, working to preventing Ca^{2+} overload (10, 11). RYRs and the IP3R3 isoform are more generally localised to contact sites between the ER and mitochondria known as mitochondria-associated ER membranes (MAMs) (12). Ca^{2+} flux from these receptors fuels the mitochondria in a manner that drives bioenergetics (i.e TCA cycle for ATP synthesis) (12, 13).

The management of Ca^{2+} is similar in yeast which possess functional homologs to the mammalian Ca^{2+} transporters. The most prominent difference is in the storage of Ca^{2+} at the vacuole instead of the ER (14, 15). Even so, Ca^{2+} remains important in optimal ER function and as signalling molecule, vital for cellular physiology. Yeast permit the influx of Ca^{2+} through the high-affinity Ca^{2+} influx system (HACS) and the low-affinity Ca^{2+} influx system (LACS) which collectively respond to depleted Ca^{2+} in the secretory pathway (14-16). HACS is the better described of the two systems and utilises a pair of TM proteins, Mid1 and Cch1. These two proteins localise to the plasma membrane where they interact to form a high affinity channel for the import of Ca^{2+} from the exogenous environment (15, 17). Intracellular Ca^{2+} is then sequestered to the vacuole through the action of two resident transporters the Ca^{2+} ATPase Pmc1 and the Ca^{2+}/H^{+} exchanger Vcx1. The yeast vacuole can contain up to 95% of the cells total Ca^{2+} which is found in complex with inorganic polyphosphate (14). Pmr1 and Spf1/Cod1 represent to two leading Ca^{2+} ATPase pumps that supply the secretory pathway with Ca^{2+} (15, 18, 19). Pmr1 and Spf1/Cod1 are also crucial in the maintenance of Ca^{2+} homeostasis and cellular physiology as deletion of both

these transporters leads to fragmentation of the vacuole and disturbances to protein folding (14, 15).

The intracellular levels of Ca^{2+} are maintained at relatively low concentrations (50-200 nM) (14, 15). In response to certain stimuli however, Ca^{2+} channels open to flood the intracellular space with Ca^{2+} from both the exogenous environment and internal stores. This sudden spike of Ca^{2+} triggers a cascading series of events that drive Ca^{2+} requiring biosynthetic pathways such as those involved in ATP synthesis and autophagy (6, 12, 13). To avoid persistent signalling that is incongruous to the needs of the cell, basal levels become restored through the coordinated activity of two molecular chaperones calmodulin (CaM) and calcineurin (CN). CaM is a Ca^{2+} binding protein that can respond to increases in intracellular [Ca^{2+}] (20, 21). In such an event the Ca^{2+} bound CaM interacts with CN stimulating its activity as a phosphatase. Upon activation, CN responds via dephosphorylating a series of C_2H_2-type zinc finger transcriptional factors such as Crz1 (21-23). Activation of Crz1 and its orthologues initiates their translocation from the cytosol to the nucleus where they tune the expression of certain Ca^{2+} regulatory genes. Import channels such as Pmc1 and Pmr1 become upregulated, yet Ca^{2+} uptake via the vacuole is limited through repression of Vcx1 (21-24). The combined activity of this transcriptional regulation serves to sequester Ca^{2+} to organelles and in turn reduces intracellular Ca^{2+} to basal levels.

Glutathione Regulation

The acquisition of glutathione within the cytosol is achieved via both local production as well as through transporters such as the yeast high affinity glutathione transporter, Hgt1 (25). The ER is not privy to such mechanisms however and is demonstrated to obtain GSH through facilitated diffusion at the translocon (1). The ER establishes an internal redox with higher oxidising capabilities than that of the cytosol, which is key in driving several PTMs such as disulfide bond formation and the glycosylation of certain proteins. A component of the oligosaccharyltransferase complex (OST) complex, Ost3, contains a conserved CxxC

thioredoxin motif that allows this subunit to sense the redox status of the ER (26). The function of Ost3 is regulated via this mechanism with reductive stress resulting in a downregulation in the activity of Ost3. N-glycosylation is an essential PTM to certain proteins, assisting in folding and stability so that they may achieve their native conformation (27-29). The ER NEF, Sil1, presents as a substrate to Ost3 for glycosylation, yet this interaction has an interesting connotation to establishing ER homeostasis. In times of reductive stress, the activity of Ost3 is absent which results in an accumulation of unglycosylated Sil1 (uSil1). This outcome has been associated with a gain of function to Sil1 where its NEF activity is enhanced, demonstrated through the ability of uSil1 to compensate for the loss of Lhs1, another ER resident NEF (30). This implicates an accumulation of uSil1 in having a regulatory function during reductive stress and demonstrates the level of dynamic control the redox status has on the functionality of the ER proteome.

I have previously indicated that the import of GSH operates on a feedback loop. The activity of Ero1 in the formation of disulfide bonds leads to the production of H_2O_2 which oxidises the ER lumen (31, 32). As a reactive oxygen species, hyperoxidation through the accumulation of H_2O_2 is detrimental to cellular physiology. In these conditions however Ero1 activity is supressed through disulfide bond formation at a pair of regulatory cystines (33, 34). Likewise, oxidation of the HSP70, Kar2 halts any further import of GSH which could be utilised to reinitiate the activity of Ero1. This prevents any further exacerbation to the ER environment as quality control measures begin to restore homeostasis (1). The actions of Sil1 and Kar2 collectively provide examples of regulatory mechanisms within the ER that are designed to restore an optimal redox environment. Additionally, by permitting the import of GSH into the ER, the translocon acts as regulatory hub that contributes to establishing optimal redox conditions.

Experimental Design and Aims

In Chapter 1 I discussed the literature surrounding dysregulated gating at the translocon and how this can impact upon the homeostatic levels of certain

metabolites of which can consequently lead to pathologies associated with disease. These outcomes are described as channelopathies, and I provided an example where perturbed Ca^{2+} flux at the translocon presents with phenotypes often associated to diabetes. The literature describes similar outcomes with a mutation at the pore ring region of the translocon that is also involved in forming the hydrophobic patch during translocation, being found to result in autosomal dominant tubulointerstitial kidney disease (ADTKD) (35, 36). A non-exhaustive list of similar mutations and their clinical outcomes can be found in Table 4.1 and demonstrates the diversity in which these Sec61 associated channelopathies present. Furthermore, with the reliance on metabolites in regulating certain biosynthetic pathways it is not surprising to find that several components of the translocon machinery are manipulated to the benefit of cancer. This link became extremely relevant to us when we discovered a cancer associated mutation within a Sec61 gating motif we had previously characterised as part of Aim1. The mutation, N302S, is at a critical residue found in regulating the dynamics of the translocon's lateral gate (1, 3). When we expressed this mutation within our gating defective *sss1-7* strain, we found that it had a suppressive effect and hence implies that this mutation was regulating translocon gating dynamics to some extent. This observation demonstrated the utility of *sss1-7* as part of a novel system that can be used to routinely screen for disease associated mutations that may be affecting gating dynamics at the translocon. Not only that, but we could assess the manner in which they do so. I.e., those supressing the phenotype of *sss1-7*, as is observed with N302S, are due more stringent gating. While those found to exacerbate the TS phenotype demonstrate an ability to perpetuate a leak through the channel. This is an important distinction to make as the way a mutation alters gating at the translocon can reveal the metabolic demands of the associated disease and should be a consideration in clinical settings for both developing treatment plans and when designing personalised approaches to medicine. In this aim we characterise the mechanism by which *sss1-7* (H72K), and its cancer associated variant *sss1-8* (H72R), perpetuate a leak through stabilising the open conformation of the translocon. This work has also served as a pilot study for utilising *sss1-7* in a system to characterise gating defects in disease. We found that cancer associated mutations of

Table 4.1. Disease associated mutations of the translocon Sec61α subunit.

Gene	Mutation	Location	Disease Association
Sec61α (Mammalian)	Y334H	BiP (Kar2) binding site	Type 2 diabetes
	Q92R	TMH 2 Lateral gate	Autosomal dominant severe congenital neutropenia
	V85D	Pore ring	Plasma cell deficiency
	V67G	Plug helix	Autosomal dominant tubulointerstitial kidney disease
	T185A	TMH 5, Pore ring adjacent	Congenital anaemia neutropenia

Sec61γ/Sss1 present with an ability to influence the conformation of the translocon through stabilising either the closed or open state.

*** The greater part of this work has undergone peer review and was subsequently accepted for publication. The submitted manuscript has been included to form part of this chapter together with supplementary results that we found relevant in our path to discovery yet didn't make it to submission. This is followed by a brief discussion on the topic matter that includes some deeper insights upon reflection.**

Results

The Translocon Establishes ER Redox Poise

In the attached manuscript of Chapter 3 we developed an assay that assessed translocon gating via a cells tolerance to increased supply of exogenous reduced glutathione (GSH). This assay is established on the basis that cells overexpressing the high-affinity glutathione transporter (Hgt1) at the plasma membrane, accumulate increase levels of GSH within the cytosol. WT cells overexpressing *HGT1* are found to become sensitive to increasing concentrations of GSH supplemented to the media as the ER becomes hyper-oxidised (37, 38). Overexpression of *HGT1* is achieved by placing the open reading frame under transcriptional control of the constitutive and robust *PMA1* promoter on a multicopy episomal plasmid (YEp). Our analysis of *sss1-6* and *sss1-7* within this system found the cell lines to be hypersensitive to GSH, which we attributed to the increase permeability afforded to these mutants. Furthermore, this outcome could be averted via introducing any of suppressive Sec61 mutations which highlights the translocons direct role. We have also utilised this approach to characterise a series of cancer associated mutations of Sss1 within this chapter. While this assay is useful in characterising the nature by which certain mutations influence translocon gating, it also implicates a potential for these mutations to cause dysregulation in ER redox poise. The ER of WT cells is

found to become hyper-oxidised upon increased supply of GSH, yet we hypothesised that the perpetual flux of *sss1-6* and *sss1-7* would result in hyper-reduction of the ER. In our characterisation of the TS *sss1* mutants, we assessed levels of UPR induced proteins Lhs1 and Kar2 (See chapter 3) in addition to Sil1. As mentioned in the introduction, Sil1 glycosylation status is dependent upon the redox sensing thioredoxin motif of Ost3, with a reduced ER environment leaving Sil unglycosylated. We were elated to find then that immunoblotting for Sil1 within our TS *sss1* mutants revealed an accumulation of uSil1 (Fig. 4.1.). This result, in collaboration with the GSH analysis implicates mutations that lead to a more open translocon in not only an uncontrolled flux of GSH but in manner that reduces the redox potential of the ER.

Translocon Gating Defects Can Flood the Cytosol with Calcium

The ability of yeast cells to react to increasing concentrations of Ca^{2+} in the cytosol is dependent on the Czr1 response. This response is reliant on the phosphatase activity of calcineurin within the cytosol which can become silenced upon treatment with calcineurin inhibitors such as the macrolide, FK506 (39). Yeast cells that a defective in their capacity to regulate the transport and storage of Ca^{2+} from the cytosol are found to be hyper-sensitive to treatment with FK506 (40-43). Should *sss1-7* truly represent an uncontrolled flux of metabolites we would expect an accumulation of Ca^{2+} at the cytosol and a reliance on Crz1 to maintain cell viability. Therefore, we hypothesised that *sss1-7* would be hypersensitive to treatment with FK506. To test this, we spotted WT and *sss1-7* yeast at permissive temperature on media containing varying concentration of FK506. We found that *sss1-7* growth was inviable on media containing 1 ug/mL of FK506 where WT growth seemed largely unperturbed (Fig. 4.2.). In support of this being a local effect from dysregulated translocon gating dynamics, a characterised suppressor, *Sec61*^{Q48A}, demonstrated restored growth of *sss1-7* on FK506 containing media (Fig. 4.2.). The UPR is constitutively induced in *sss1-7* cells which we attribute to ER stress. It is worth noting that the activity of calcineurin is required to maintain cell viability during times of ER stress and as such the effects of FK506 on *sss1-7* might

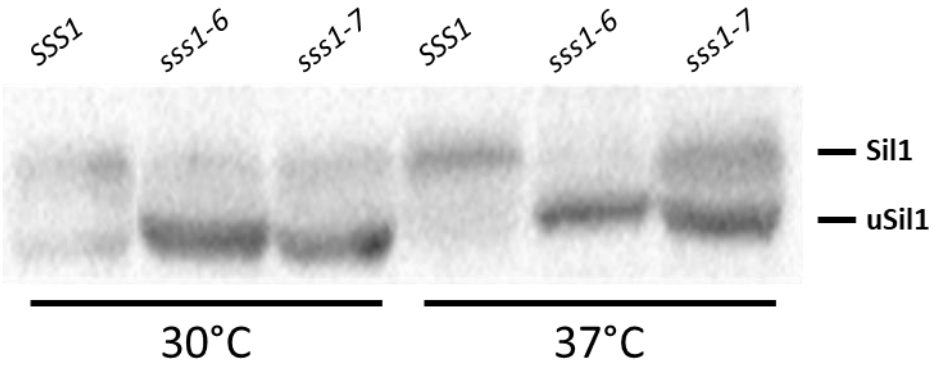

Fig. 4.1. uSil1 accumulates in *sss1^{ts}* gating mutants. Cell extracts derived from cells expressing either *SSS1, sss1-6 or sss1-7* were immunoblotted with anti-Sil1 antibody at both 30°C and 37°C. Accumulation of uSil1 identified in both ts Sss1 mutant strains.

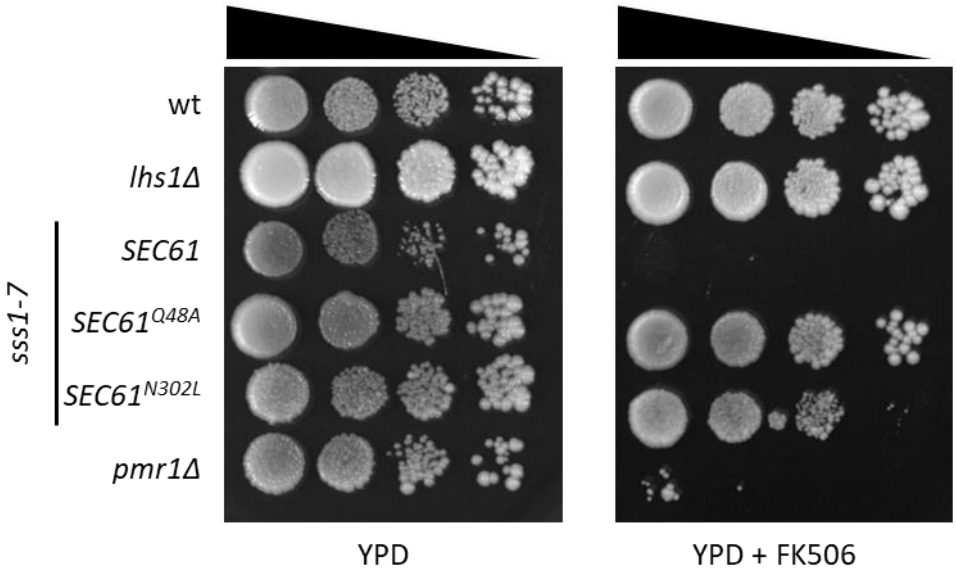

Fig. 4.2. *sss1-7* is hypersensitive to FK506. Wildtype, *lhs1Δ*, *pmr1Δ* or *sss1-7 (sss1^{H72k})* yeast transformed with either YCp *SEC61,* YCp *SEC61^{N302L}* or YCp *SEC61^{Q48A}* were spotted on YPD agar or YPD agar containing 1 ug/mL FK506 in a 10-fold dilution series and incubated at 30°C for 3 days.

be attributed to this outcome and hence irrelevant to cytosolic Ca^{2+} (44). To address this, we plated *lhs1Δ* mutant yeast cells on media containing FK506. Like *sss1-7*, the UPR within *lhs1Δ* cells is constitutively induced, yet we saw no effects on growth at the concentration demonstrated to ablate the viability of *sss1-7* (45). Therefore, we confidently suggest that the sensitivity of *sss1-7* to FK506 is attributed to perturbed Ca^{2+} homeostasis.

References

1. Ponsero AJ, Igbaria A, Darch MA, Miled S, Outten CE, Winther JR, et al. Endoplasmic Reticulum Transport of Glutathione by Sec61 Is Regulated by Ero1 and Bip. Molecular cell. 2017;67(6):962-73.e5.
2. Lang S, Erdmann F, Jung M, Wagner R, Cavalie A, Zimmermann R. Sec61 complexes form ubiquitous ER Ca2+ leak channels. Channels (Austin, Tex). 2011;5(3):228-35.
3. Trueman SF, Mandon EC, Gilmore R. A gating motif in the translocation channel sets the hydrophobicity threshold for signal sequence function. The Journal of cell biology. 2012;199(6):907-18.
4. Lam AKM, Galione A. The endoplasmic reticulum and junctional membrane communication during calcium signaling. Biochimica et Biophysica Acta (BBA) - Molecular Cell Research. 2013;1833(11):2542-59.
5. Mekahli D, Bultynck G, Parys JB, De Smedt H, Missiaen L. Endoplasmic-Reticulum Calcium Depletion and Disease. 2011;3(6).
6. Ivanova H, Kerkhofs M, La Rovere RM, Bultynck G. Endoplasmic Reticulum–Mitochondrial Ca2+ Fluxes Underlying Cancer Cell Survival. 2017;7(70).
7. Parekh AB, Putney JW. Store-Operated Calcium Channels. Physiological Reviews. 2005;85(2):757-810.
8. Roberts-Thomson SJ, Chalmers SB, Monteith GR. The Calcium-Signaling Toolkit in Cancer: Remodeling and Targeting. 2019;11(8).
9. Berridge MJ. Inositol trisphosphate and calcium signalling mechanisms. Biochimica et Biophysica Acta (BBA) - Molecular Cell Research. 2009;1793(6):933-40.
10. Hattori M, Suzuki AZ, Higo T, Miyauchi H, Michikawa T, Nakamura T, et al. Distinct roles of inositol 1,4,5-trisphosphate receptor types 1 and 3 in Ca2+ signaling. The Journal of biological chemistry. 2004;279(12):11967-75.
11. Kania E, Roest G, Vervliet T, Parys JB, Bultynck G. IP3 Receptor-Mediated Calcium Signaling and Its Role in Autophagy in Cancer. 2017;7(140).
12. Morciano G, Marchi S, Morganti C, Sbano L, Bittremieux M, Kerkhofs M, et al. Role of Mitochondria-Associated ER Membranes in Calcium Regulation in Cancer-Specific Settings. Neoplasia. 2018;20(5):510-23.
13. Rowland AA, Voeltz GK. Endoplasmic reticulum-mitochondria contacts: function of the junction. Nat Rev Mol Cell Biol. 2012;13(10):607-25.
14. D'hooge P, Coun C, Van Eyck V, Faes L, Ghillebert R, Mariën L, et al. Ca2+ homeostasis in the budding yeast Saccharomyces cerevisiae: Impact of ER/Golgi Ca2+ storage. Cell Calcium. 2015;58(2):226-35.
15. Lange M, Peiter E. Calcium Transport Proteins in Fungi: The Phylogenetic Diversity of Their Relevance for Growth, Virulence, and Stress Resistance. 2020;10.
16. Cunningham KW. Acidic calcium stores of Saccharomyces cerevisiae. Cell Calcium. 2011;50(2):129-38.
17. Locke EG, Bonilla M, Liang L, Takita Y, Cunningham KW. A Homolog of Voltage-Gated Ca²⁺Channels Stimulated by Depletion of Secretory Ca²⁺ in Yeast. 2000;20(18):6686-94.
18. Rudolph HK, Antebi A, Fink GR, Buckley CM, Dorman TE, LeVitre J, et al. The yeast secretory pathway is perturbed by mutations in PMR1, a member of a Ca2+ ATPase family. Cell. 1989;58(1):133-45.
19. Cronin SR, Khoury A, Ferry DK, Hampton RY. Regulation of Hmg-Coa Reductase Degradation Requires the P-Type Atpase Cod1p/Spf1p. Journal of Cell Biology. 2000;148(5):915-24.
20. Cyert MS. Genetic analysis of calmodulin and its targets in Saccharomyces cerevisiae. Annual review of genetics. 2001;35:647-72.

21. Liu S, Hou Y, Liu W, Lu C, Wang W, Sun S. Components of the calcium-calcineurin signaling pathway in fungal cells and their potential as antifungal targets. Eukaryotic cell. 2015;14(4):324-34.
22. Bodvard K, Jörhov A, Blomberg A, Molin M, Käll M. The yeast transcription factor Crz1 is activated by light in a Ca2+/calcineurin-dependent and PKA-independent manner. PLoS One. 2013;8(1):e53404.
23. Karababa M, Valentino E, Pardini G, Coste AT, Bille J, Sanglard D. CRZ1, a target of the calcineurin pathway in Candida albicans. Molecular microbiology. 2006;59(5):1429-51.
24. Cunningham KW, Fink GR. Calcineurin inhibits VCX1-dependent H+/Ca2+ exchange and induces Ca2+ ATPases in Saccharomyces cerevisiae. Mol Cell Biol. 1996;16(5):2226-37.
25. Bourbouloux A, Shahi P, Chakladar A, Delrot S, Bachhawat AK. Hgt1p, a High Affinity Glutathione Transporter from the Yeast Saccharomyces cerevisiae*. Journal of Biological Chemistry. 2000;275(18):13259-65.
26. Schulz BL, Stirnimann CU, Grimshaw JP, Brozzo MS, Fritsch F, Mohorko E, et al. Oxidoreductase activity of oligosaccharyltransferase subunits Ost3p and Ost6p defines site-specific glycosylation efficiency. Proceedings of the National Academy of Sciences of the United States of America. 2009;106(27):11061-6.
27. Johnson AE, van Waes MA. The translocon: a dynamic gateway at the ER membrane. Annu Rev Cell Dev Biol. 1999;15:799-842.
28. Shental-Bechor D, Levy Y. Folding of glycoproteins: toward understanding the biophysics of the glycosylation code. Current opinion in structural biology. 2009;19(5):524-33.
29. SolÁ RJ, Griebenow KAI. Effects of Glycosylation on the Stability of Protein Pharmaceuticals. Journal of pharmaceutical sciences. 2009;98(4):1223-45.
30. Stevens KLP, Black AL, Wells KM, Yeo KYB, Steuart RFL, Stirling CJ, et al. Diminished Ost3-dependent N-glycosylation of the BiP nucleotide exchange factor Sil1 is an adaptive response to reductive ER stress. 2017;114(47):12489-94.
31. Tu BP, Weissman JS. The FAD- and O(2)-dependent reaction cycle of Ero1-mediated oxidative protein folding in the endoplasmic reticulum. Mol Cell. 2002;10(5):983-94.
32. Ellgaard L, McCaul N, Chatsisvili A, Braakman I. Co- and Post-Translational Protein Folding in the ER. Traffic (Copenhagen, Denmark). 2016;17(6):615-38.
33. Ulrich K, Jakob U. The role of thiols in antioxidant systems. Free radical biology & medicine. 2019;140:14-27.
34. Zhang L, Niu Y, Zhu L, Fang J, Wang X, Wang L, et al. Different interaction modes for protein-disulfide isomerase (PDI) as an efficient regulator and a specific substrate of endoplasmic reticulum oxidoreductin-1α (Ero1α). The Journal of biological chemistry. 2014;289(45):31188-99.
35. Schubert D, Klein M-C, Hassdenteufel S, Caballero-Oteyza A, Yang L, Proietti M, et al. Plasma cell deficiency in human subjects with heterozygous mutations in Sec61 translocon alpha 1 subunit (SEC61A1). Journal of Allergy and Clinical Immunology. 2018;141(4):1427-38.
36. Sicking M, Lang S, Bochen F, Roos A, Drenth JPH, Zakaria M, et al. Complexity and Specificity of Sec61-Channelopathies: Human Diseases Affecting Gating of the Sec61 Complex. Cells. 2021;10(5):1036.
37. Kumar C, Igbaria A, D'Autreaux B, Planson AG, Junot C, Godat E, et al. Glutathione revisited: a vital function in iron metabolism and ancillary role in thiol-redox control. The EMBO journal. 2011;30(10):2044-56.
38. Ponsero AJ, Igbaria A, Darch MA, Miled S, Outten CE, Winther JR, et al. Endoplasmic Reticulum Transport of Glutathione by Sec61 Is Regulated by Ero1 and Bip. Molecular cell. 2017;67(6):962-73 e5.

39. Thomson AW, Bonham CA, Zeevi A. Mode of action of tacrolimus (FK506): molecular and cellular mechanisms. Therapeutic drug monitoring. 1995;17(6):584-91.
40. Ghanegolmohammadi F, Yoshida M, Ohnuki S, Sukegawa Y, Okada H, Obara K, et al. Systematic analysis of Ca(2+) homeostasis in Saccharomyces cerevisiae based on chemical-genetic interaction profiles. Molecular biology of the cell. 2017;28(23):3415-27.
41. Maeda T, Sugiura R, Kita A, Saito M, Deng L, He Y, et al. Pmr1, a P-type ATPase, and Pdt1, an Nramp homologue, cooperatively regulate cell morphogenesis in fission yeast: The importance of Mn2+ homeostasis. 2004;9(1):71-82.
42. Puigpinós J, Casas C, Herrero E. Altered intracellular calcium homeostasis and endoplasmic reticulum redox state in Saccharomyces cerevisiae cells lacking Grx6 glutaredoxin. 2015;26(1):104-16.
43. Tanida I, Hasegawa A, Iida H, Ohya Y, Anraku Y. Cooperation of Calcineurin and Vacuolar H⁺-ATPase in Intracellular Ca²⁺Homeostasis of Yeast Cells &#x2217. Journal of Biological Chemistry. 1995;270(17):10113-9.
44. Dudgeon DD, Zhang N, Ositelu OO, Kim H, Cunningham KW. Nonapoptotic death of Saccharomyces cerevisiae cells that is stimulated by Hsp90 and inhibited by calcineurin and Cmk2 in response to endoplasmic reticulum stresses. Eukaryotic cell. 2008;7(12):2037-51.
45. Tyson JR, Stirling CJ. LHS1 and SIL1 provide a lumenal function that is essential for protein translocation into the endoplasmic reticulum. The EMBO journal. 2000;19(23):6440-52.

Cancer Associated Mutations in Sec61γ Alter the Permeability of the ER Translocase

Christopher M. Witham [1,2], Aleshanee L. Paxman [1,2], Lamprini Baklous [1,2], Robert F. L. Steuart [2], Benjamin L. Schulz [3] and Carl J. Mousley [1,2*].

[1] Curtin Medical School, Curtin University, Bentley, WA 6102, Australia

[2] Curtin Health Innovation Research Institute, Curtin University, Bentley, WA 6102, Australia

[3] School of Chemistry and Molecular Biosciences, University of Queensland, Brisbane St Lucia, QLD 4072, Australia

Keywords: Endoplasmic reticulum (ER), Sec61 complex, Sss1p/Sec61 γ, translocon gating.

*Corresponding Author:

Email: Carl.Mousley@curtin.edu.au

Telephone: +61 8 9266 5617

Facsimile : +61 8 9266 2342

Abstract

Translocation of secretory and integral membrane proteins across or into the ER membrane occurs via the Sec61 complex, a heterotrimeric protein complex possessing two essential sub-units, Sec61p/Sec61α and Sss1p/Sec61γ and the non-essential Sbh1p/Sec61β subunit. In addition to forming a protein conducting channel, the Sec61 complex maintains the ER permeability barrier, preventing flow of molecules and ions. Loss of Sec61 integrity is detrimental and implicated in the progression of disease. The Sss1p/Sec61γ C-terminus is juxtaposed to the key gating module of Sec61p/Sec61α and is important for gating the translocon. Inspection of the cancer genome database identifies six mutations in highly conserved amino acids of Sec61γ/Sss1p. We identify that five out of the six mutations identified affect gating of the ER translocon, albeit with varying strength. Together, we find that mutations in Sec61γ that arise in malignant cells result in altered translocon gating dynamics, this offers the potential for the translocon to represent a target in co-therapy for cancer treatment.

Author Summary

The first step in the biogenesis of secretory proteins is the targeting and translocation into the endoplasmic reticulum (ER). Secretory proteins enter the ER via a gated channel in the ER membrane called the translocon, a protein complex composed of Sec61p/Sec61α, Sbh1p/Sec61β and Sss1p/Sec61γ. As a protein conducting channel the translocon must be sealed in a regulated manner to prevent the free flow of ions and small molecules between the ER and cytosol. We have discovered that mutations in Sec61γ that arise in cancer affect this seal but not the ability of this protein complex to translocate secretory proteins into the ER. We hypothesise that altered translocon gating contributes to malignancy by influencing factors such as migration, autophagy and chemotherapy resistance.

Introduction

The endoplasmic reticulum (ER) is the entry point into the secretory pathway (1, 2). To enter this organelle proteins are conducted through a channel known as the translocon (3). Secretory proteins are marked by the presence of a signal sequence that comprises an N-terminal positively charged N-domain, a largely hydrophobic central H-domain, and a polar C-terminal cleavage site or C-domain (4, 5). The signal peptide instructs the targeting and subsequent translocation of a precursor through the ER translocase by one of two distinct mechanisms (6, 7). Proteins that possess a signal sequence of sufficient hydrophobicity are translocated co-translationally by a mechanism dependent on the signal recognition particle (SRP) (8-10). Translocation may also occur independent of the SRP (6) whereby a secretory protein is fully synthesised and then maintained in an unfolded, translocation competent state by cytosolic chaperones prior to post-translational translocation via the SEC complex in yeast (11, 12).

The ER translocase is formed by the conserved Sec61 heterotrimeric complex (3). In yeast the Sec61 complex is comprised of Sec61p, Sss1p and Sbh1p with the equivalent in mammalian organisms being Sec61α, Sec61γ and Sec61β respectively (7, 13). Within the complex, Sec61p forms the subunit through which proteins pass (14, 15). This essential subunit contains ten transmembrane domains (TMDs) (13) which create the two halves of Sec61p, TMDs 1-5 and TMDs 6-10 (13, 16). These halves are joined by an external loop between TMD 5 and TMD 6 (loop 5/6) (13). A distinct hourglass shape results from the central constriction of the channel created by the pore ring, a series of hydrophobic residues that help to form a seal during translocation. While inactive, a plug formed by the first portion of TMD 2 (2a) resides within the pore ring (13). This plug is partially displaced to allow for translocation to occur (13). The two halves of Sec61p also form the lateral gate (13). A hinge is formed between loop 5/6 which acts as an important regulator of translocon opening via facilitating exposure to the lipid bilayer of the ER membrane (13, 17). Ribosomal binding initiates partial opening of the lateral gate which is completed through the integration of the signal sequence between TMD 2 and TMD 7 (13, 17).

Sss1p is an essential component of the translocon, acting to stabilise the conformation of the channel (18). The amphipathic N-terminal helix and the TMD of Sss1p wraps around Sec61p on the surface and diagonally around TMDs 1, 5, 6 and 10 of Sec61p respectively, clamping the two halves of the structure. Sbh1p is only essential in higher eukaryotes. It contains one TM domain, the N-terminus of which makes contact with Sec61p (12, 19, 20). The cytosolic domain of Sbh1p is largely unstructured and not visible in any of the available structures. As such, it is unknown to what extent this domain makes direct contact with Sec61, however, it is highly likely that it does so as this domain can be crosslinked to polypeptides as they translocate through the Sec61 complex (21).

The translocon must allow for passage of a protein while maintaining the permeability barrier between the cytosol and ER lumen. The ER environment facilitates lumenal processes such as protein folding and appropriate cellular signalling. Disturbances to this system can result in ER stress which can lead to induction of recovery mechanisms including the unfolded protein response (UPR) (22, 23). During translocation there is opportunity for the movement of small molecules into and out of the ER (24, 25). Docking of the ribosome to the translocon during co-translational translocation initiates displacement of the plug usually residing within the inactive Sec61 complex (26). As plug displacement occurs the translating protein is thread through the translocon, keeping the pore blocked and preventing the flow of molecules (24). Upon the immediate completion of translation, the ribosome remains docked to the translocon in an idle state. (27, 28). Here, the Sec61 complex remains open and empty prior to the detachment of ribosomes (24, 25). At this stage small molecules can pass between the different cellular environments through the translocon (24, 29). The dissociation of the idle ribosome from the translocon causes a conformational shift within the Sec61 complex, closing the channel once again (30). Work by Trueman *et al.* and Ponsero *et al.* demonstrated that mutations in Sec61p can destabilise the closed or open conformation of the translocon (24, 29). Destabilisation of the closed translocon increases the opportunity for molecules to pass into and out of the ER (24).

Conversely, destabilisation of the open Sec61 complex decreases movement of small molecules through the translocon (24).

The extreme C-terminus of Sss1p has been shown to be located adjacent to key amino acids in Sec61p that gate this channel and genetic analyses suggest a role for this region in gating the translocon (13). Inspection of the cancer genome database identifies several mutations in highly conserved amino acids of Sss1p. We identify that five out of the six mutations identified could affect gating of the ER translocon, albeit with varying strength. Together, we find that mutations in Sec61γ that arise in malignant cells result in altered translocon gating dynamics, this offers the potential for the translocon to represent a target in co-therapy for cancer treatment.

Results

Sec61γ Cancer Associated Mutations do not Disrupt ER Translocation

Cancer genome databases provide a repository of naturally occurring mutations in genes that potentially impact the function of a protein they encode given their association with disease. We were interested to determine whether mutations in Sec61γ that arise in cancer alter gating dynamics of the Sec61 complex. Mining the COSMIC database identified 6 mutations in Sec61γ in residues that are highly conserved in eukaryotes (Fig. 5.1., A). The R24I mutation was identified in a patient with colorectal cancer, the K27E and I64T mutations were identified in patients with endometrial cancer, the A39V mutation in a patient with pancreatic cancer and the L56F and H58R mutations identified in patients with lung cancer. The equivalent mutations in Sss1p are K38I, K41E, A53V, L70F, H72R and V78T respectively and these are found throughout the protein (Fig. 5.1., B). Importantly, these mutations do not represent natural SEC61γ polymorphisms as none of these mutations are annotated in the genome aggregation database (gnomAD) that spans 125748 exome sequences and 15708 whole genome sequences from unrelated individuals (31). We exploited our yeast model to test whether these mutations grossly alter Sss1p function. *SSS1* is an essential gene as *sss1Δ* cells are not viable. Therefore, we firstly tested if expression of these cancer associated variants could sustain cell viability via a

Fig. 1

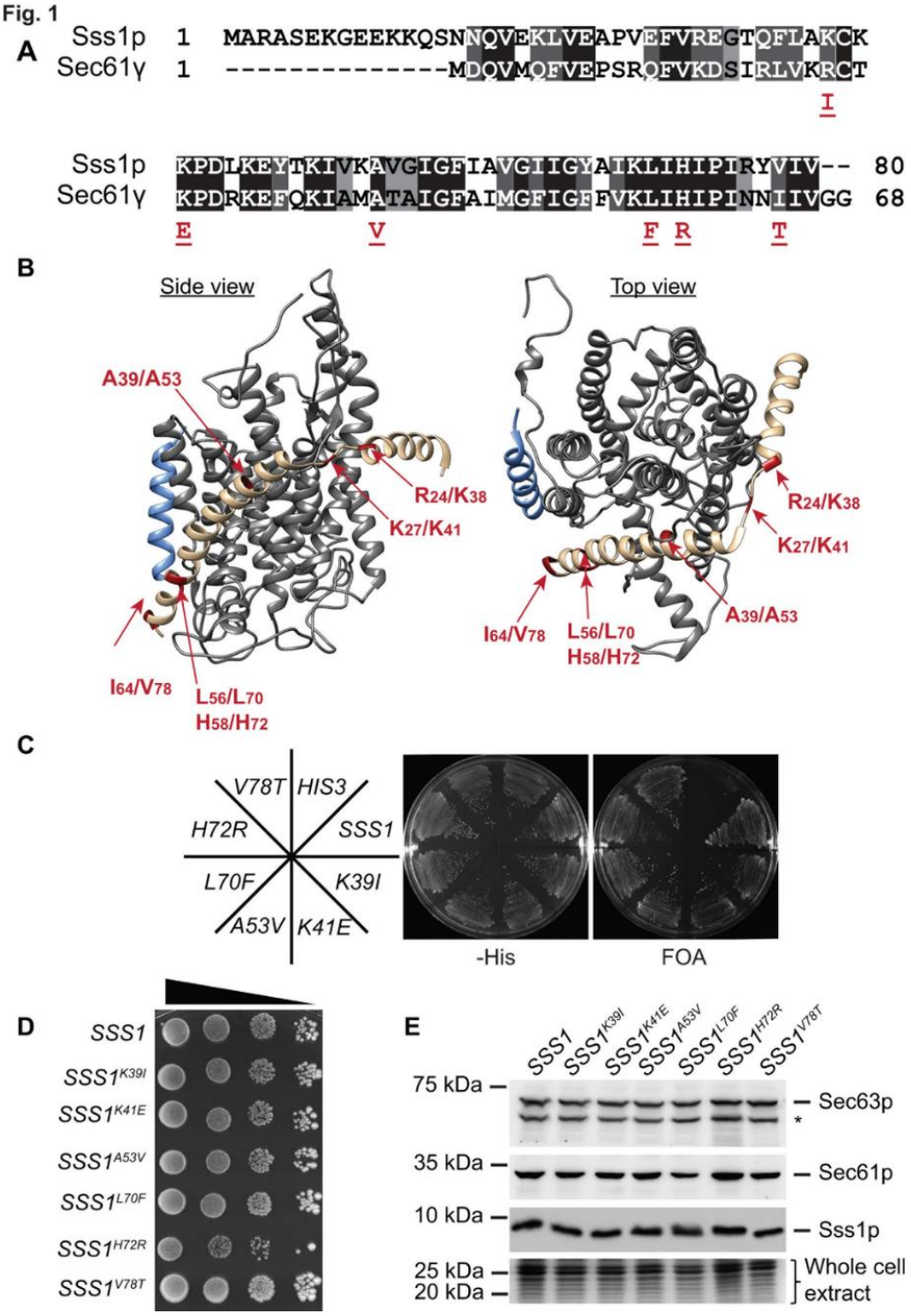
A
Sss1p 1 MARASEKGEEKKQSNNQVEKLVEAPVEFVREGTQFLAKCK
Sec61γ 1 ----------MDQVMQFVEPSRQFVKDSIRLVKRCT
I
Sss1p KPDLKEYTKIVKAVGIGFIAVGIIGYAIKLIHIPIRYVIV-- 80
Sec61γ KPDRKEFQKIAMATAIGFAIMGFIGFFVKLIHIPINNIIVGG 68
E V F R T
B
Side view
Top view
A39/A53
R24/K38
K27/K41
I64/V78
L56/L70
H58/H72
C
V78T
HIS3
H72R
SSS1
L70F
K39I
A53V
K41E
-His
FOA
D
SSS1
SSS1K39I
SSS1K41E
SSS1A53V
SSS1L70F
SSS1H72R
SSS1V78T
E
SSS1
SSS1K39I
SSS1K41E
SSS1A53V
SSS1L70F
SSS1H72R
SSS1V78T
75 kDa
35 kDa
10 kDa
25 kDa
20 kDa
Sec63p
Sec61p
Sss1p
Whole cell extract

Fig. 5.1. The Sss1p C-terminus is highly conserved. (A) The sequence of *Sec61γ* and Sss1p are aligned using clustal omega sequence alignment software and the position of cancer associated mutations indicated. **(B)** Ribbon diagram of the Sec61 complex crystal structure (4CG7.pdb) (32) was composed using Chimera software. *Sec61α*, *Sec61β* and *Sec61γ*, are coloured grey, blue and sand respectively. Cancer associated mutations are indicated in red. **(C)** BWY530 yeast transformed with either YCp *HIS3*, YCp *SSS1*, YCp $SSS1^{K39I}$, YCp $SSS1^{K41E}$, YCp $SSS1^{A53V}$, YCp $SSS1^{L70F}$, YCp $SSS1^{H72R}$ or YCp $SSS1^{V78T}$ were streaked onto –His selective medium and medium containing FOA and incubated at 30°C for 2 days. **(D)** Wildtype or cells expressing either $SSS1^{K39I}$, $SSS1^{K41E}$, $SSS1^{A53V}$, $SSS1^{L70F}$, $SSS1^{H72R}$ or $SSS1^{V78T}$ as the sole source of *SSS1* were spotted in a 10 fold dilution series and grown on YPD at 30°C for 3 days. **(E)** Cell extracts derived from wildtype cells or cells expressing either $SSS1^{K39I}$, $SSS1^{K41E}$, $SSS1^{A53V}$, $SSS1^{L70F}$, $SSS1^{H72R}$ or $SSS1^{V78T}$ were immunoblotted with anti-Sss1p, anti-Sec61p or anti-Sec63p antibodies. * identifies a proteolysed product of Sec63p.

plasmid shuffle assay. This method involves introduction of a plasmid containing a mutated copy of an essential gene into a strain carrying the wild-type gene on a *URA3* plasmid to complement the disruption of the chromosomal copy of the gene. This is followed by growth in the presence of 5-fluoroorotic acid (5-FOA) to prevent propagation of the *URA3* plasmid. 5-FOA resistant cells can only be isolated if the mutated copy of the gene retains sufficient essential activity. We transformed YCp *SSS1* and each mutant into BWY530 (*sss1Δ::KanMX4* FKp53) and tested for the ability of these strains to grow after counter-selecting for FKp53 on 5-FOA medium. Cells expressing plasmid derived copies of *SSS1* or any of the mutants produced viable colonies, whereas those transformed with vector alone could not, indicating that these mutations do not ablate function (Fig. 5.1., C & D).

Structurally Sss1p is composed almost exclusively of alpha helices. Importantly, the PSI-blast based secondary structure PREDiction (PSIPRED) program that uses artificial neural network machine learning algorithms to predict secondary structure (32) indicated that the cancer associated mutations did not alter Sss1p secondary structure (Supp. Fig. S5.1.). Neither are key translocon subunits Sss1p and Sec61p and accessory proteins (e.g. Sec63p) affected in these mutants (Fig. 5.1., E). The biogenesis of DPAP B, which is translocated in an SRP dependent manner, prepro alpha factor, which is translocated post-translationally and Kar2p which can be translocated by both pathways were monitored to determine whether ER translocation is affected in these mutants. There was no obvious translocation defects in these mutants (Supp. Fig. S5.2., A). Finally, we investigated invertase secretion to determine if the secretory capacity of the cell is altered by our panel of cancer associated mutations. We observed no significant difference in the fraction of invertase that is secreted by the cell in each mutant when compared to wild type (Supp. Fig. S5.2., B). Therefore, the mutations in conserved residues in Sec61γ that arise in cancer do not perturb the essential translocation activity of the Sec61 complex nor do they alter the secretory capacity of the cell.

The Sss1 H72R Mutation Affects Translocon Gating

The H58 residue in Sec61γ is absolutely conserved in all homologues identified to date and corresponds to H72 in Sss1p (33, 34). Interestingly, the growth of cells expressing *sss1*^{H72R} is temperature sensitive as they are inviable at temperatures greater than 37°C (Fig. 5.2., A). However, the temperature sensitivity of *sss1*^{H72R} is not due to the stability of the key translocon subunits Sss1p and Sec61p and key accessory proteins Sec62p and Sec63p being affected in this mutant (see above; Fig. 5.1., D). Furthermore, the integrity of the translocon itself was not compromised in the *sss1*^{H72R} mutant. The Sss1p and Sec61p interaction can be stabilised by the crosslinking reagent disuccinimidyl suberate (DSS) (18, 35). We detected a DSS-dependent immunoreactive band of ≈ 46 kDa with both anti-Sss1p and anti-Sec61p specific antibodies in membranes isolated from wildtype or *sss1*^{H72R} cells treated with DSS, regardless of whether they were grown at 30°C or 37°C (Supp. Fig. S5.2., B).

Blue native polyacrylamide gel electrophoresis (BN-PAGE) has been used to resolve important translocation structures; specifically the Sec61 complex, the Sec63/71/72 subcomplex and the SEC' and SEC complex (36). We therefore used BN-PAGE to complement our cross-linking analysis. Microsomes isolated from wildtype cells that were solubilised with 2% digitonin yielded the 140 kDa Sec61 complex, the 350 kDa SEC' complex and the 380 kDa SEC complex (Supp. Fig. S5.1., D). These complexes were all observed in microsomes isolated from *sss1-6, sss1-7* and *sss1-8* (*sss1*^{H72R}) mutants (Supp. Fig. S5.2., C) further supporting the conclusion that the integrity of ER translocation complexes are not compromised in *sss1ts* mutants.

Given that activity of the Sec61 complex is essential for ER homeostasis, we tested if the unfolded protein response (UPR) was induced in *sss1*^{H72R} mutants. For this we used a LacZ reporter placed under transcriptional control of a yeast UPR enhancer (UPRE) (34). WT cells were treated with the reducing agent dithiothreitol (DTT) to gauge a typical UPR response. UPR dependent LacZ activity was significantly elevated in DTT treated cells compared to WT (Fig. 5.2., B). LacZ activity in *sss1*^{H72R} cells at 30°C and 37°C was up to 11-fold greater than that of WT. This confirms that the UPR is constitutively induced in *sss1*^{H72R} cells.

Fig. 2

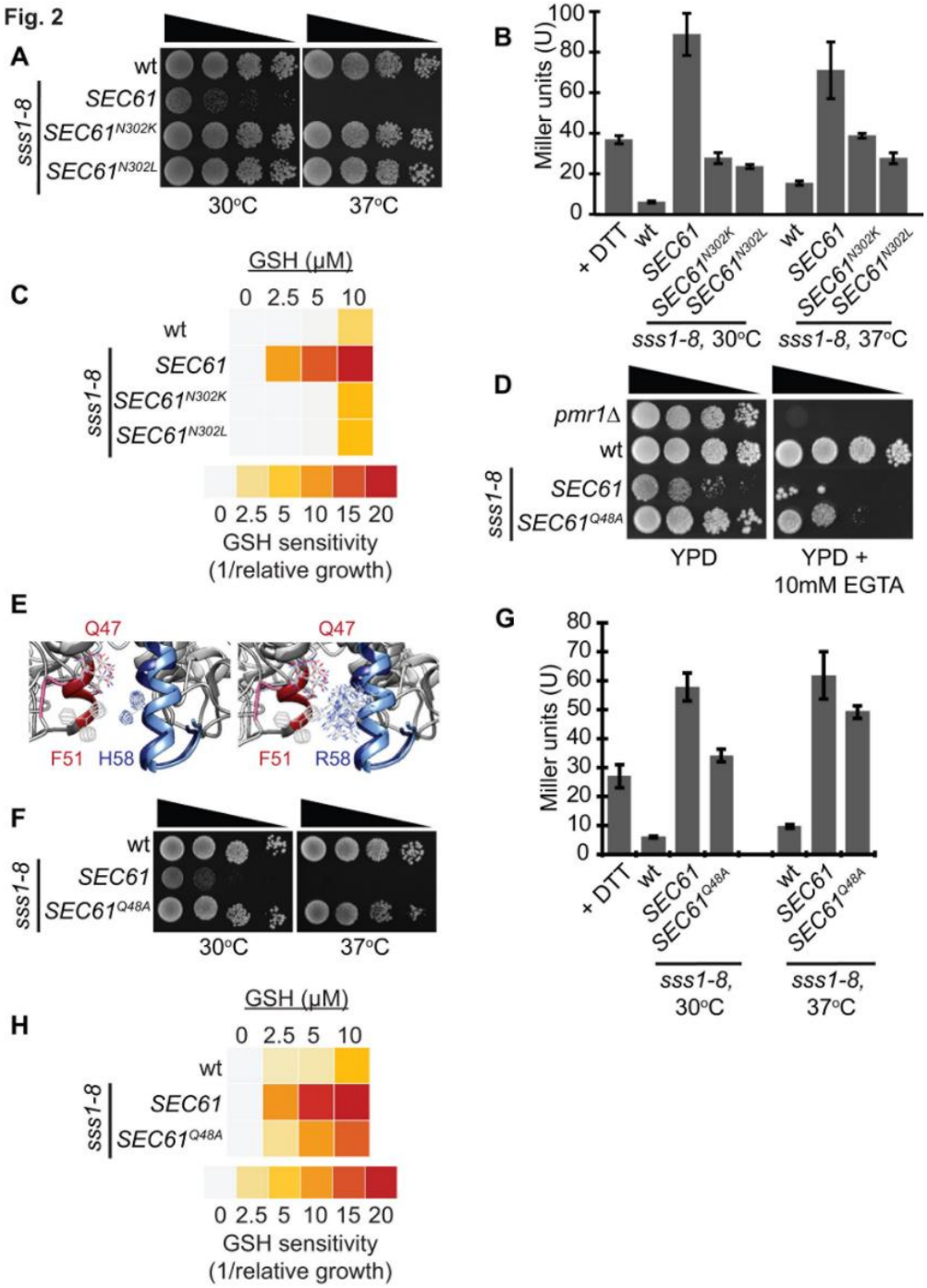
A
wt
SEC61
SEC61N302K
SEC61N302L
sss1-8
30°C
37°C
B
Miller units (U)
100
80
60
40
20
0
+ DTT
wt
SEC61
SEC61N302K
SEC61N302L
sss1-8, 30°C
sss1-8, 37°C
C
GSH (μM)
0 2.5 5 10
wt
SEC61
SEC61N302K
SEC61N302L
sss1-8
0 2.5 5 10 15 20
GSH sensitivity
(1/relative growth)
D
pmr1Δ
wt
SEC61
SEC61Q48A
sss1-8
YPD
YPD +
10mM EGTA
E
Q47
F51
H58
R58
F
wt
SEC61
SEC61Q48A
sss1-8
30°C
37°C
G
Miller units (U)
80
70
60
50
40
30
20
10
0
+ DTT
wt
SEC61
SEC61Q48A
sss1-8,
30°C
sss1-8,
37°C
H
GSH (μM)
0 2.5 5 10
wt
SEC61
SEC61Q48A
sss1-8
0 2.5 5 10 15 20
GSH sensitivity
(1/relative growth)

Fig. 5.2. The *sss1^{H72R}* mutation disrupts ER homeostasis. **(A)** Wildtype or *sss1-8* yeast transformed with either YCp *SEC61,* YCp *SEC61^{N302K}* or YCp *SEC61^{N302L}* were spotted on YPD agar in a 10-fold dilution series and incubated at 30°C or 37°C for 2 days. **(B)** Wildtype or *sss1-8* yeast transformed with either YCp SEC*61,* YCp SEC*61^{N302K}* or YCp *SEC61^{N302L}* and with pJT30 (UPRE-LacZ) were grown in –Ura selective medium and β-Galactosidase activity determined. As a positive control wildtype cells were treated with 5mM DTT for 2 hours. **(C)** Wildtype or *sss1-8* yeast transformed with either YCp *SEC61,* YCp *SEC61^{N302K}* or YCp *SEC61^{N302L}* and with YEp *HGT1* were grown in –Ura selective medium with increasing concentrations of GSH. The relative growth of each strain determined and the GSH sensitivity (1/relative growth) presented. **(D)** Wildtype or *sss1-8 (sss1^{H72R})* yeast transformed with either YCp *SEC61* or YCp *SEC61^{Q48A}* were spotted on YPD agar or YPD agar containing 10mM EGTA in a 10-fold dilution series and incubated at 30°C for 3 days. **(E)** Ribbon diagram of the open (4CG5/7.pdb) and closed (4CG5/7.pdb) Sec61 complex crystal structure (34) was composed and overlayed using Chimera software. The position of Q47 and F51 in *Sec61α* relative to H58 in *Sec61γ* are indicated. **(F)** Wildtype or *sss1-8 (sss1^{H72R})* yeast transformed with either YCp *SEC61* or YCp *SEC61^{Q48A}* were spotted on YPD agar in a 10-fold dilution series and incubated at 30°C or 37°C for 2 days. **(G)** Wildtype or *sss1-8 (sss1^{H72R})* yeast transformed with either YCp *SEC61* or YCp *SEC61^{Q48A}* and with pJT30 (UPRE-LacZ) were grown in –Ura selective medium and β-Galactosidase activity determined. **(H)** Wildtype or *sss1-8 (sss1^{H72R})* yeast transformed with either YCp *SEC61* or YCp *SEC61^{Q48A}* and with YEp *HGT1* were grown in –Ura selective medium with increasing concentrations of GSH. The relative growth of each strain determined and the GSH sensitivity (1/relative growth) presented.

The sensitivities of *sss1*^{H72R} cell growth and degree of ER stress in the absence of an obvious ER translocation defect suggested to us that the *sss1*^{H72R} mutation may compromise the permeability of the translocon. We have found in a related study (34) that the *SEC61*^{N302L} mutation, a mutation in the lumenal lateral gate described by Gilmore and co-workers which destabilises the open conformation of the translocon (29), and *SEC61*^{N302K} suppresses the growth defects of other temperature sensitive *sss1* mutants in a dominant manner. Expression of either *SEC61*^{N302L} or *SEC61*^{N302K} from a centromeric plasmid also suppressed the temperature sensitive growth of *sss1*^{H72R} cells (Fig. 5.2., A) and reduced UPR induction in this mutant (Fig 5.2., B). This suggests that translocon gating is defective in *sss1*^{H72R} mutants.

The Sec61 translocon has been shown to facilitate the diffusion of reduced glutathione (GSH) into the ER (24). WT cells that overexpress Hgt1p, the plasma membrane high-affinity GSH transporter (↑*HGT1* cells hereafter), amass high levels of GSH, when it is provided exogenously, that become cytotoxic due to a regulated response that results in hyper-oxidation of the ER lumen (24). Using this system, we show that WT ↑Hgt1p cells easily tolerate up to 10 µM GSH (Fig. 5.2., C) Moreover, *sss1*^{H72R} ↑Hgt1p growth is extremely sensitive to GSH, as growth of these cells was severely perturbed by 2.5 µM GSH and 5 µM GSH, and completely arrested by 10 µM GSH (Fig. 5.2., C). Furthermore, the GSH hypersensitive growth defect of *sss1ts* mutants is not due to differential expression of *HGT1* (Supp. Fig. S5.3., A & B). Importantly, co-expression of *SEC61*^{N302L} or *SEC61*^{N302K} also suppressed the extreme sensitivity of *sss1*^{H72R} ↑Hgt1p growth in the presence of GSH (Fig. 5.2., C).

Farnesyl pyrophosphate (FPP) synthetase (Fpp1p) activity is Mn^{2+} dependent (37-39) and Fpp1p activity is elevated when cytoplasmic Mn^{2+} levels are raised, which results in increased squalene synthesis (37). Squalene accumulation inhibits cell growth if it cannot be metabolised; such as when cells are treated with the squalene epoxidase inhibitor terbinafine (37). We used this system to determine whether *sss1*^{H72R} cells possessed increased Fpp1p activity due to defective Mn^{2+} homeostasis. *sss1*^{H72R} cell growth was extremely sensitive to terbinafine as, unlike wildtype, 1 µg/mL terbinafine completely inhibited the growth of *sss1*^{H72R} mutants at 30°C and 34°C respectively (Supp. Fig. S5.3., C). Importantly, *sss1*^{H72R} cells are not hypersensitive to

the 14α-sterol demethylase inhibitor miconazole (Supp. Fig. S5.3., D), indicating that the hypersensitivity of *sss1*^{H72R} cells to terbinafine is not due to general inhibition of the ergosterol biosynthetic pathway.

The cation content of the ER in yeast is controlled by both the Pmr1p and Spf1p/Cod1p P-type ATPases (40-42). The growth of mutants that are defective in the storage of Ca^{2+} in secretory organelles, *pmr1Δ* and *spf1Δ* specifically, is hypersensitive to the presence of the Ca^{2+} chelator EGTA in the growth medium. Given this we hypothesised that the growth of *sss1* mutants defective in translocon gating would be hypersensitive to EGTA. Wildtype cell growth is resistant to up to 20 mM EGTA. However, *sss1*^{H72R} cells showed similar hypersensitivity to EGTA as *pmr1Δ* mutants (Fig. 5.2., D). Again, the EGTA hypersensitive growth defect of *sss1ts* mutants is not due to differential expression of *PMR1* (Supp. Fig. S5.3., A & B). Importantly the deleterious effects of EGTA on *sss1*^{H72R} growth are negated by the addition of exogenous Ca^{2+} to the growth medium (Supp. Fig. S5.3., E).

Taken together we conclude that the hypersentivities of *sss1*^{ts} growth to GSH, terbinafine and EGTA are due to the increased flux of GSH, Mn^{2+} and Ca^{2+}, respectively, through the translocon in these mutants. Regarding the latter, however, we must acknowledge that we cannot rule out the possibility that the biogenesis of the Ca^{2+} pump is affected when Sss1p is mutated.

Structural Rationale for Altered Translocon Gating in Sec61γ H58R Mutant

When the structure of the translocation channel was first solved it was proposed that the most significant structural rearrangement that takes place upon opening of the translocon is the relocation of the plug domain, from within the central cavity of the closed channel, to a site adjacent to C-terminal portion of TM1 of SecY/Sec61α, the Sec61β TMD and the extreme C-terminus of SecE/Sec61γ in the open state (13). However, structural analysis of the active mammalian translocon revealed it to only undergo subtle rearrangement as it transitions from an inactive to active state (43). We note F51, located at the extreme C-terminus of Sec61α TM1, shifts and rotates towards the KLIHIPI peptide located near the extreme C-terminus of Sec61γ (43) (Fig.

5.2., E). This movement positions the sidechain of Q47 that flanks Sec61α TM1 close to that of Sec61γ H58 (43) (Fig. 5.2., E). We have modelled this structural feature in several of the most high resolution structures of the translocon, specifically 6ND1 (CryoEM structure of the Sec Complex from yeast) (44), 6R7Q (Structure of XBP1u-paused ribosome nascent chain complex with Sec61) (45), 6FTJ (Cryo-EM Structure of the Mammalian Oligosaccharyltransferase Bound to Sec61 and the Non-programmed 80S Ribosome) (46), 6Z3T (Structure of canine Sec61 inhibited by mycolactone) (47) and 6W6L (Cryo-EM structure of the human ribosome-TMCO1 translocon) (48), and have found these to be highly comparable (Supp. Fig. S5.4.). Substitution of H58 with R would position the charged moiety of these side chains closer to one another, that may result in a strengthened interaction between these two residues that could stabilise the open conformation of the translocon (Fig. 5.2., E). We reasoned that disrupting this potential interaction would phenocopy the effect of mutations in the lumenal and lateral gate that destabilise the closed conformation of the translocon. Sec61α Q47 is well conserved with the corresponding residue being Sec61p Q48 in yeast. We tested whether *SEC61*^{Q48A} could suppress the temperature sensitivity of the *sss1*^{H72R} mutant in a dominant manner. Indeed, we found the suppressive effects of *SEC61*^{Q48A} to be indistinguishable from those of the *SEC61*^{N302L} mutant (Fig. 5.2., F). Furthermore, *SEC61*^{Q48A} could dominantly suppress all phenotypes associated with altered permeability of the ER translocase (Fig. 5.2., D, G & H).

Other Sec61γ Cancer Associated Mutations Alter Translocon Gating

Mutations in *SEC61* that alter the gating dynamics of the translocon do not profoundly affect cell physiology under normal growth conditions. However, these mutations have been shown to dramatically affect the growth defects of *sss1* mutants that are defective in translocon gating; namely *sss1-6* and *sss1-7* (*sss1*$^{P74A, I75A}$ and *sss1*^{H72K} mutations respectively) (34). Specifically, mutations in the lateral gate of Sec61p that destabilise the open conformation of the translocon, *SEC61*^{N302L} (29), completely suppress the ts growth defect of both *sss1-6* and *sss1-7* mutants (34) whereas a mutation that destabilises the closed conformation of the translocon,

SEC61^{N302D} (29), further exacerbates the ts growth defect of *sss1-6* mutant, while the *sss1-7 SEC61*^{N302D} double mutant is inviable (34). Therefore, we have a novel and elegant system that allows us to screen for mutations in components of the translocon and its associated proteins that destabilise either the open or the closed conformation of the translocon. That is mutations that destabilise the closed conformation of the translocon will exacerbate *sss1-6* temperature sensitivity, while, mutations that destabilise the open conformation of the translocon will suppress *sss1-6* and *sss1-7* growth defects.

We combined each of the mutations described in Fig. 5.1., A with either *sss1*^{H72K} (*sss1-7*) or the less severe *sss1*$^{P74A,\ I75A}$ (*sss1-6*) and investigated whether they suppressed or exacerbated *sss1-6* and *sss1-7* growth defects using the plasmid shuffle strain BWY530. We were unable to counter-select for FKp53 on FOA medium in cells expressing either *sss1-6* ^{K41E} or *sss1-7* ^{K41E} (Fig. 5.3., A). The simplest explanation for this is that the incorporation of K41E into either *sss1-6* and *sss1-7* results in a completely functionless Sss1p variant. An alternative explanation is that the magnitude of the translocon gating defect when the K41E mutation is combined with either *sss1-6* and *sss1-7* is such that cells are no longer viable. To discern between these two possibilities we reasoned that co-expression of the Sec61^{N302L}p mutant, which destabilises the open conformation of the translocon, would restore viability to *sss1-6* ^{K41E} or *sss1-7* ^{K41E} if the latter scenario is correct. Indeed this was the case, as co-expression of *SEC61*^{N302L}, but not *SEC61* alone, allowed either *sss1-6* ^{K41E} or *sss1-7* ^{K41E} to sustain cell viability when expressed as the sole copy of *SSS1* (Fig. 5.3., B).

A second mutation, L70F, was also found to exacerbate the growth defects of both *sss1-6*, and *sss1-7*. The growth of *sss1-6* ^{L70F} mutants at 30°C and 32°C was barely detectable after 2 days unlike *sss1-6* (Fig. 5.3., C). Furthermore, we discovered the GSH hypersensitive cell growth of *sss1-6* ^{L70F} and *sss1-7* ^{L70F} to be exacerbated relative to *sss1-6* and *sss1-7* respectively as the former mutants were unable to grow in the presence of 2.5 µM GSH whereas growth arrest of the latter mutants is observed at 10 µM GSH (Fig. 5.3., D). However, *sss1-6* ^{L70F} mutants, but not *sss1-6*, are inviable at the semi-permissive temperature of 34°C (Fig. 5.3., C). The UPR was induced to an

Fig. 3

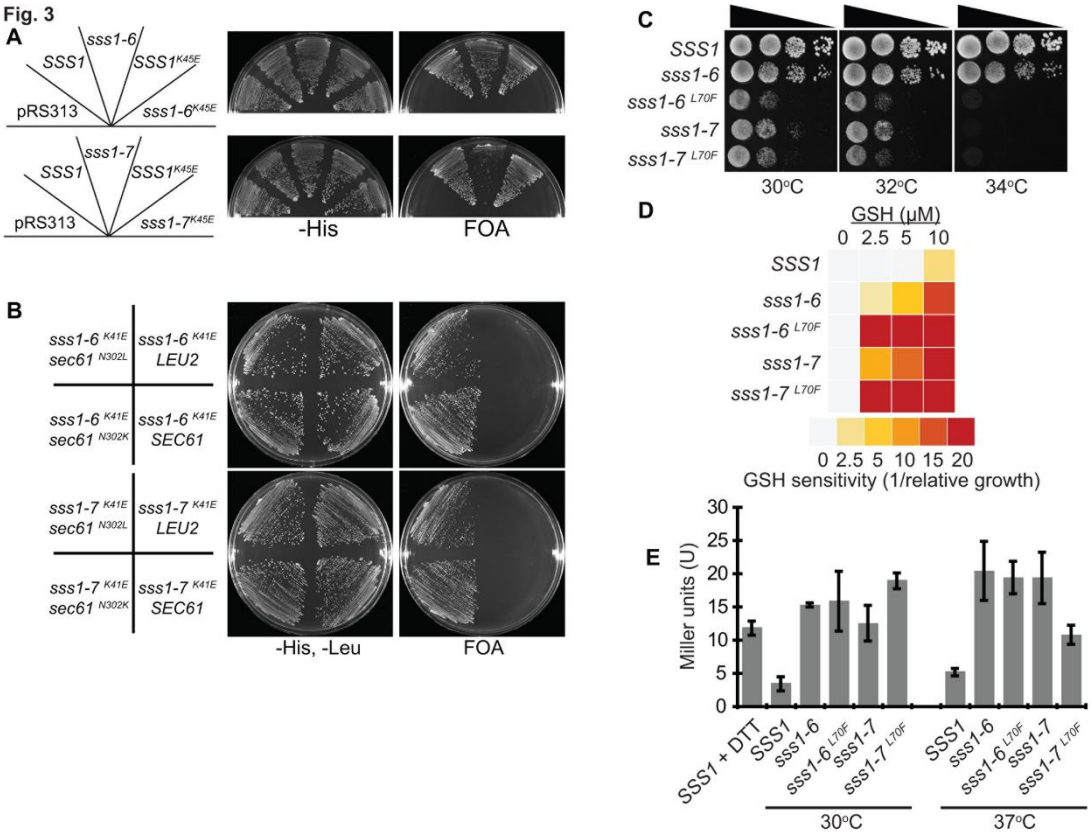
A
sss1-6
SSS1
SSS1K45E
pRS313
sss1-6K45E
sss1-7
SSS1
SSS1K45E
pRS313
sss1-7K45E
-His
FOA
B
sss1-6 K41E sec61 N302L
sss1-6 K41E LEU2
sss1-6 K41E sec61 N302K
sss1-6 K41E SEC61
sss1-7 K41E sec61 N302L
sss1-7 K41E LEU2
sss1-7 K41E sec61 N302K
sss1-7 K41E SEC61
-His, -Leu
FOA
C
SSS1
sss1-6
sss1-6 L70F
sss1-7
sss1-7 L70F
30°C
32°C
34°C
D
GSH (μM)
0 2.5 5 10
SSS1
sss1-6
sss1-6 L70F
sss1-7
sss1-7 L70F
0 2.5 5 10 15 20
GSH sensitivity (1/relative growth)
E
Miller units (U)
30
25
20
15
10
5
0
SSS1 + DTT
SSS1
sss1-6
sss1-6 L70F
sss1-7
sss1-7 L70F
SSS1
sss1-6
sss1-6 L70F
sss1-7
sss1-7 L70F
30°C
37°C

Fig. 5.3. The K27E and L56F mutations destabilise the closed conformation of the translocon. (A) BWY530 yeast transformed with either YCp *HIS3*, YCp *SSS1*, YCp *SSS1*$^{P74A, I75A}$, YCp *SSS1*$^{K41E, P74A, I75A}$, YCp *SSS1*^{H72K}, YCp *SSS1*$^{K41E, H72K}$ were streaked onto –His selective medium and medium containing FOA and incubated at 30°C for 2 days. **(B)** BWY530 yeast transformed with YCp *SSS1*$^{K41E, P74A, I75A}$ and YCp *LEU2*, YCp *SEC61*, YCp *SEC61*^{N302K} or YCp *SEC61*^{N302L} or YCp *SSS1*$^{K41E, H72KA}$ and YCp *LEU2*, YCp *SEC61*, YCp *SEC61*^{N302K} or YCp *SEC61*^{N302L} were streaked onto –His selective medium and medium containing FOA and incubated at 30°C for 2 days. **(C)** Wildtype or cells expressing either *SSS1*$^{P74A, I75A}$, *SSS1*$^{L70F, P74A, I75A}$, *SSS1*^{H72K} or *SSS1*$^{L70F, H72K}$ as the sole source of *SSS1* were spotted on YPD agar in a 10-fold dilution series and incubated at 30°C, 32°C or 34°C for 2 days. **(D)** Wildtype or cells expressing either *SSS1*$^{P74A, I75A}$, *SSS1*$^{L70F, P74A,I75A}$, *SSS1*^{H72K} or *SSS1*^{L70F,H72K} as the sole source of *SSS1* transformed with YEp *HGT1* were grown in –Ura selective medium with increasing concentrations of GSH. The relative growth of each strain determined and the GSH sensitivity (1/relative growth) presented. **(E)** Wildtype or cells expressing either *SSS1*$^{P74A, I75A}$, *SSS1*$^{L70F, P74A,I75A}$, *SSS1*^{H72K} or *SSS1*^{L70F,H72K} as the sole source of *SSS1* transformed with pJT30 (UPRE-LacZ) were grown in –Ura selective medium and β-Galactosidase activity determined. As a positive control, wildtype cells were treated with 5mM DTT for 2 hours.

equivalent extent in *sss1-6* ^{L70F} and *sss1-7* ^{L70F} relative to *sss1-6* and *sss1-7* (Fig. 5.3., E). This likely indicates that the extent with which the UPR is induced in these mutants has reached its maximum prior to the loss of cell viability.

In contrast to K41E and L70F, we find that two mutations, A53V and V78T, have suppressive effects on either both *sss1* mutants (A53V) or *sss1-7* only (V78T). *sss1-6* ^{A53V} could grow at 37°C whereas *sss1-7* ^{A53V} could grow at 34°C unlike *sss1-6* and *sss1-7* respectively (Fig. 5.4., A) and the extent with which the UPR was induced was less in both *sss1-6* ^{A53V} and *sss1-7* ^{A53V} (Fig. 5.4., B). The *sss1-7* ^{V78T} mutant could also grow at 34°C (Fig. 5.4., A) and the level to which the UPR was induced in *sss1-7* ^{V78T} was less than that observed for *sss1-7* (Fig. 5.4., B). We speculate that the P75A mutation in *sss1-6* alters the structure of the C-terminus such that the suppressive effects of the V78T mutation are negated in this mutant. The suppressive effects of both the A53V and V78T mutations also extended to overturn phenotypes associated with altered ER permeability. The A53V mutation was able to suppress the hypersensitivity of both *sss1-6* and *sss1-7* mutants to GSH (Fig. 5.4., C) and the V78T mutation did so for *sss1-7* (Fig. 5.4., C). Furthermore, A53V and V78T, have suppressive effects on either both *sss1* mutants (A53V) or *sss1-7* only (V78T) on EGTA hypersensitivity (Fig. 5.4., D) and terbinafine hypersensitivity (Supp. Fig. S5.2., B), albeit with varying strength.

Given the suppressive effects of the V78T and A53V mutations, described above, we were keen to determine whether these mutations alone were more resistant than *SSS1* to the cytotoxic effects of exogenous GSH. *SSS1*^{V78T} cells were only found to be fractionally more resistant to GSH than WT cells, however, *SSS1*^{A53V} cells were significantly more resistant to the deleterious effects of exogenous GSH (Fig. 5.4., E).

Fig. 4

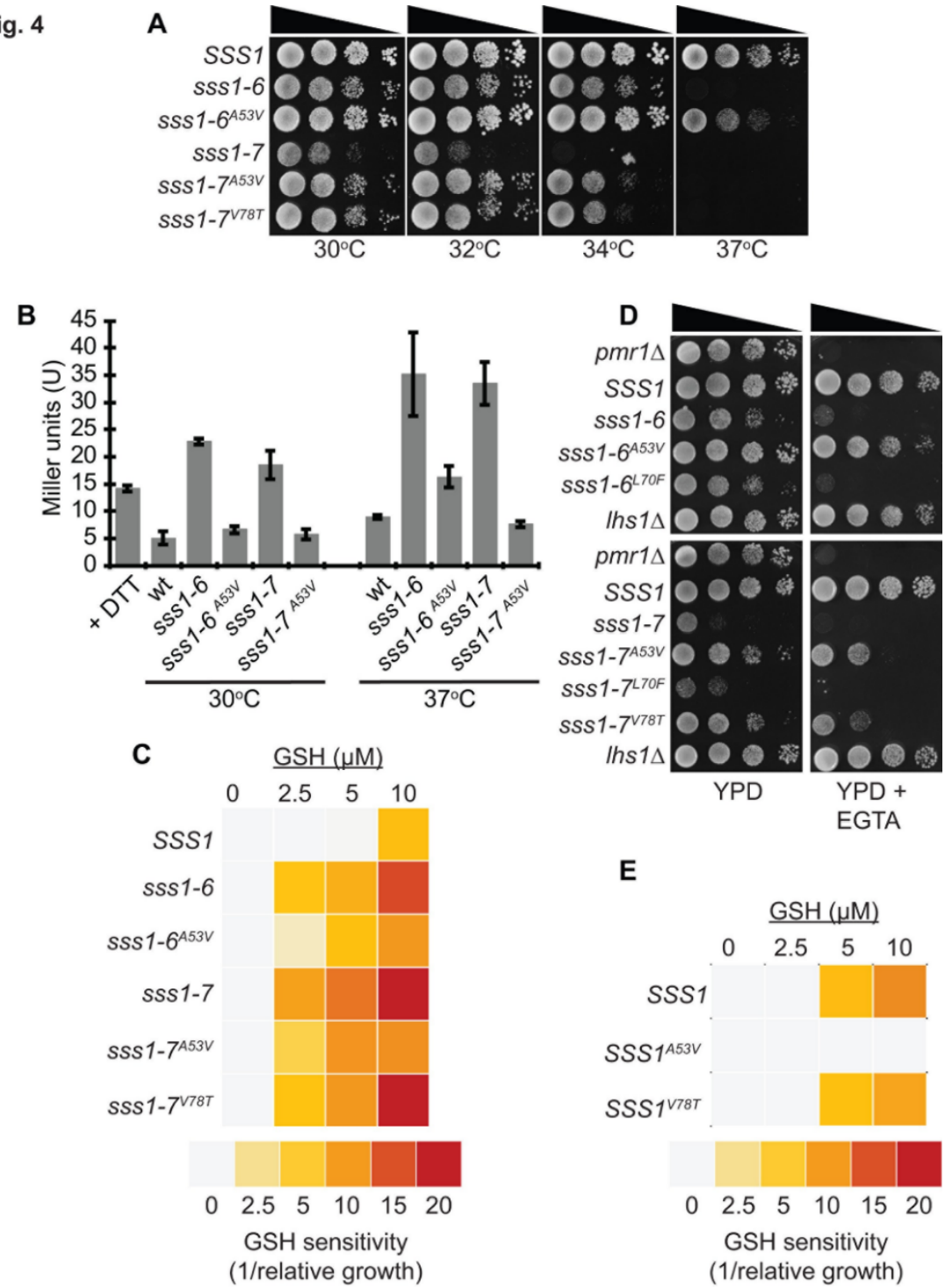
A
SSS1
sss1-6
sss1-6A53V
sss1-7
sss1-7A53V
sss1-7V78T
30°C
32°C
34°C
37°C
B
Miller units (U)
45
40
35
30
25
20
15
10
5
0
+ DTT
wt
sss1-6
sss1-6 A53V
sss1-7
sss1-7 A53V
30°C
37°C
C
GSH (μM)
0
2.5
5
10
SSS1
sss1-6
sss1-6A53V
sss1-7
sss1-7A53V
sss1-7V78T
0
2.5
5
10
15
20
GSH sensitivity
(1/relative growth)
D
pmr1Δ
SSS1
sss1-6
sss1-6A53V
sss1-6L70F
lhs1Δ
pmr1Δ
SSS1
sss1-7
sss1-7A53V
sss1-7L70F
sss1-7V78T
lhs1Δ
YPD
YPD +
EGTA
E
GSH (μM)
0
2.5
5
10
SSS1
SSS1A53V
SSS1V78T
0
2.5
5
10
15
20
GSH sensitivity
(1/relative growth)

Fig. 5.4. The A39V and I64T mutations destabilise the open conformation of the translocon. (A) Wildtype or cells expressing either *SSS1*^{P74A,I75A}, *SSS1*$^{A53V, P74A,I75A}$, *SSS1*^{H72K}, *SSS1*$^{A53V, H72K}$ or *SSS1*$^{H72K, V78T}$ as the sole source of *SSS1* were spotted on YPD agar in a 10-fold dilution series and incubated at 30°C, 32°C, 34°C or 37°C for 2 days. **(B)** Wildtype or cells expressing either *SSS1*^{P74A,I75A}, *SSS1*$^{A53V, P74A,I75A}$, *SSS1*^{H72K}, *SSS1*$^{A53V, H72K}$ or *SSS1*$^{H72K, V78T}$ as the sole source of *SSS1* transformed with pJT30 (UPRE-LacZ) were grown in –Ura selective medium and β-Galactosidase activity determined. As a positive control wildtype cells were treated with 5mM DTT for 2 hours. **(C)** Wildtype or cells expressing either *SSS1*^{P74A,I75A}, *SSS1*$^{A53V, P74A,I75A}$, *SSS1*^{H72K}, *SSS1*$^{A53V, H72K}$ or *SSS1*$^{H72K, V78T}$ as the sole source of *SSS1* transformed with YEp *HGT1* were grown in –Ura selective medium with increasing concentrations of GSH. The relative growth of each strain determined and the GSH sensitivity (1/relative growth) presented. **(D)** Wildtype or cells expressing either *SSS1*^{P74A,I75A}, *SSS1*$^{A53V, P74A,I75A}$, *SSS1*^{H72K}, *SSS1*$^{A53V, H72K}$ or *SSS1*$^{H72K, V78T}$ as the sole source of *SSS1* were spotted on YPD agar or YPD agar containing 5 mM (*sss1-7* derivatives) or 10 mM (*sss1-6* derivatives) EGTA in a 10-fold dilution series and incubated at 30°C for 3 days. **(E)** Wildtype or cells expressing either *SSS1*^{A53V} or *SSS1* ^{V78T} as the sole source of *SSS1* transformed with YEp *HGT1* were grown in –Ura selective medium with increasing concentrations of GSH. The relative growth of each strain determined and the GSH sensitivity (1/relative growth) presented.

Discussion

The Sec61 translocon facilitates the translocation of nascent proteins into the ER while maintaining the barrier between the two distinct environments of the ER lumen and cytosol. Additionally, the translocon's capability to allow the controlled flux of essential metabolites across the ER membrane is vital to maintaining these functional environments as well as coordinating cellular processes that are regulated by small molecules. The dynamic nature of the translocon is fundamental in this channel's ability to participate in these distinct functions; and while other ER channels have been described with roles in cancer and its progression (49, 50), the involvement of dysregulated translocon dynamics had yet to be reported. Herein, we have demonstrated a mechanism by which mutations in the essential translocon subunit, Sec61γ/Sss1p, influence translocon gating. Furthermore, we show that cancer associated mutations of Sec61γ/Sss1p present with an ability to influence the stability of the translocon's conformational states, stabilising either the closed or open state.

A Possible Mechanism for *sss1^{H72R}* in Disrupting Gating Dynamics

An intricate network of molecular interactions regulates the opening and closing of the translocon. N302 contributes to this network within the lateral and lumenal gate that functions in setting the hydrophobicity threshold of the translocon (29). The incorporation of a signal sequence into the channel disrupts this network under normal conditions, facilitating the transition to an open state (29). Increasing the hydrophobicity of key residues (i.e N302L) complements non-polar interactions at the lumenal and lateral gate which destabilises the open conformation (29). Seeking a mechanism by which *sss1^{H72R}* disrupts gating dynamics, we inspected the structure of the active mammalian translocon, which revealed that upon translocon opening the side chain of the Sec61α TM1 residue Q47 is juxtaposed to H58 of Sec61γ. The substitution of H58 with R positions the charged moiety of these side chains within 2.1 Å of Q47 which may facilitate the formation of a strong non-covalent interaction between these two residues. This may affect the ability of the translocon to respond

appropriately to signals for closure, therefore disrupting gating dynamics via stabilising the open state.

Disrupting Translocon Dynamics: an Outcome in Cancer Related Mutations

Data presented in the human protein atlas suggests SEC61γ to be a prognostic marker for renal and liver cancer whereby high expression is shown to be unfavourable in both cancers. In light of this we were interested to see if there existed cancer associated mutations in SEC61γ that had any effect on function. Search of the cancer genome database revealed there to be six mutations in conserved residues. Significantly, these mutations are not just natural polymorphisms as they are documented in the genome aggregation database. Rather, they represent *bona fide* mutations that have arisen in patients with cancer. Utilising our *sss1* mutants (*sss1-6* and *sss1-7*) we have developed a system for the assessment of perturbations in translocon gating dynamics. These mutants destabilise the closed conformation of the channel, therefore the introduction of a further mutation to these mutants can have one of three possible outcomes: no effect on translocon gating, suppression which indicates an ability to destabilise the open and exacerbation which is an outcome of destabilising the closed further. Initially there was no apparent phenotype observed in the cancer associated mutations of Sss1p with the exception of $sss1^{H72R}$. However, upon introduction into our system we found 4 (K41E, A53V, L70F, V78T) out of the remaining 5 also demonstrated an ability to influence translocon gating dynamics. It is important to indicate that the mutations in Sec61γ listed in the COSMIC database are alone, unlikely to be causative, driver mutations. However, these mutations legitimately alter the permeability of the ER translocase therefore we consider these mutations to be advantageous to cell fitness at a later stage of disease, such as when chemotherapy is administered or when a tumour metastasises. A subset of single nucleotide variants, proposed as passengers in cancer, has been shown to influence tumour progression (51).

Cellular compartmentalisation has served as a significant advantage for eukaryotic cells by facilitating specialisation of numerous cellular processes (52). The ER has a

distinct environment that promotes the processing and maturation of proteins (53, 54). Ca^{2+} contributes to establishing this environment and is present in abundance, particularly in mammalian cells where the ER is the major store for this ion (55) where it is utilised by molecular chaperones to facilitate protein folding (56). In addition to its role at the ER, Ca^{2+} also regulates cell signalling, metabolism, autophagy and apoptosis; i.e. pathways manipulated in cancer (57). Interestingly, the disparate effects of these cancer associated SEC61γ mutations appears to reflect the diverse way in which Ca^{2+} signalling affects cancer. The increasing energy demand of certain cancers can lead to the sustained transfer of Ca^{2+} from the ER to the mitochondria (57) which serves to fuel mitochondrial bioenergetics resulting in the production of ATP. Interestingly, in pancreatic ductal adenocarcinoma (PDAC) IP3Rs and STIM1 are reorganised to the leading edge of migrating cells (58). Inhibition of IP3Rs and SOCE repressed migration demonstrating the importance of these mechanisms in this process (58). As migration is energy demanding, the redistribution of these mechanisms likely represents the increasing demand for their role in enhancing mitochondrial bioenergetics. In the same vein, some cancers have demonstrated an ability to preferentially express certain isoforms of IP3R, i.e. upregulation of IP3R3 involved in calcium transport at MAMs (59). These findings establish a need for some cancers to hoard calcium at the ER in order to sustain energy production. The A39V and I64T mutations, identified in PDAC and endometroid carcinoma respectively, might represent a contributing factor in this process. These mutations stabilise the closed conformation of the translocon, which could serve to reduce ion leakage.

The literature reveals some lung cancer cell lines possess reduced ER Ca^{2+} levels. Down regulating the import of Ca^{2+} levels makes the ER vulnerable to calcium leak. Increased cytosolic Ca^{2+} can induce autophagic flux that acts to compensate for metabolic stress via supplying nucleotides for cellular processes such as the TCA cycle and DNA repair (60). These lung cancer cell lines show chemoresistance likely representing diminished ER to mitochondria Ca^{2+} transfer which is critical for induction of cell death (61, 62). Furthermore, cancerous cells develop an increased demand for protein and lipid biogenesis and therefore must adapt to and increasingly nutrient deprived environment. Uncontrolled ion movement from the ER can result

in cellular stress and induce the UPR (22, 63, 64). While prolonged cellular stress would typically induce apoptosis, some malignant cells can bypass apoptosis and utilise UPR to increase the protein folding capacity of the ER which can increase metastasis and chemotherapy resistance (65). Collectively these finding demonstrate that depletion of ER Ca^{2+} stores can prove beneficial to the progression of certain cancers. Sss1p cancer mutations found to destabilise the closed / stabilise the open translocon include L56F and H58R, mutations isolated from lung squamous cell carcinoma as well as K27E of endometroid carcinoma origin. We propose that mutations that impose such an effect on the translocon could perpetuate Ca^{2+} flux, contributing to cancer outcomes.

This work has served as a proof of concept for our system in determining influences on translocon gating dynamics. This system could be utilised for future studies investigating components/regions that have yet to be characterised to such a role. Here, this system has set a precedent as a useful tool in identifying potential manipulations of translocon gating dynamics which may act in benefit of carcinogenesis and tumour progression. To our knowledge this is the first study to identify mutations in the *SEC61γ* gene that affect ER permeability to be associated with pathology. Given that pathologies have been found to be associated with genes encoding for translocon components (*SEC61α1* and *SEC61β*) as well as translocon associated proteins (*SEC62* and *SEC63*) we anticipate that several channelopathies that alter the permeability of the ER membrane may be associated with mutations in Sec61γ. If so we have a novel and elegant system in place that allows screening for such mutations.

Materials And Methods

Yeast Strains

Yeast strains (Supp. Table S5.1.) were grown in YP medium (2% peptone, 1% yeast extract) in the presence of 2% glucose (YPD). Growth was predominately performed at 30°C except where defined otherwise for the purposes of TS growth analysis which involved spotting onto media at a 10-fold dilution series. Minimal medium (0.67% yeast nitrogen base; YNB) with the addition of 2% glucose and appropriate supplements (20 µg/mL) was utilised for nutrient selection. 2% (w/v) agar was additionally added for solid media. Minimal media was prepared similarly yet with the addition of 1 g/L 5-fluoroorotic acid (5-FOA) and 100 µg/mL uracil to achieve counter selection of *URA3* plasmids. 1 µg/mL terbinafine or DMSO was added to YPD agar where indicated.

Plasmid Construction – Site Directed Mutagenesis

Site directed mutagenesis was performed according to Q5 Site Directed Mutagenesis Protocol (NEB), the plasmids and oligonucleotides used are listed in Supp. Table S5.2. and Supp. Table S5.3. respectively. The plasmid pJKB2 was used as template to introduce the desired mutations into *SSS1*.

Glutathione Sensitive Growth Assay

Yeast strains containing the Yep *HGT1* were cultured at 30°C to mid-logarithmic phase. Sub-cultures at 0.01 OD_{600nm} in SC medium were produced omitting uracil and with the addition of 0-10 µM of L-reduced glutathione. Growth was followed and recorded at several key time points. Three independent biological replicates and at least two technical replicates were performed. These results were averaged with each concentration compared as a factor of the 0 µM result.

β-Galactosidase Assays

β-Galactosidase assays were performed according to Tyson and Stirling, 2000 (66). Specifically, overnight yeast cultures were diluted to 0.2 OD_{600nm} and left to recover for 4 hrs at 30°C. Following a 2 hr temperature shift cells were harvested and resuspended in 2 mL of Z buffer (60 mM Na_2HPO_4, 40 mM NaH_2PO_4, 10 mM KCl, 10 mM $MgSO_4$, 50 mM 2-mercaptoethanol, pH 7.0). Reaction mixes were made from 0.8 mL of cell suspension, 50 µL of 0.1% (w/v) SDS and 100 µL of $CHCl_3$ and placed at 30°C for 30 mins to achieve cellular permeabilisation. 160 µL of o-nitrophenylgalactopyranoside (4 mg/mL stock) was added to initiate the reaction for a 20 min duration. The addition of 400 µL of 1 M Na_2CO_3, pH 9.0 acted to halt the reaction. The OD_{420nm} was measured, and LacZ activity (U) was calculated by multiplying OD_{420nm}/OD_{600nm} by 1000. Three independent biological replicates and at least two technical replicates were performed.

Cell Lysate Preparation and Immunoblotting

Yeast cells were grown to mid-logarithmic phase where 10 OD_{600nm} of cells were isolated for generation of crude cell lysates. Pelleted cells were resuspended in sample buffer with 0.5 mm glass beads. Samples were heated for 10mins at 65°C and disrupted via FastPrep-24 (6.0m/sec for 40 sec). Samples were placed back on heat until use or stored. Samples were run via SDS page and subsequently transferred to PVDF via a semi-dry transfer apparatus. Immunoblotting Antibodies used are listed in Supp. Table S5.4.

Footnotes

Acknowledgments: We would like to thank the Curtin Medical School and CHIRI for funding.

Conflict of interest: The authors declare that they have no conflicts of interest with the contents of this article.

Author contributions: C.J.M, R.F.L.S. and B.J.S conceived, designed, and analysed the research; C.M.W., A.L.P. and L.B. performed the research. C.J.M. and R.F.L.S supervised C.M.W., A.L.P. and L.B.; C.J.M., R.F.L.S., B.L.S and C.M.W. wrote the manuscript.

References

1. Schwarz DS, Blower MD. The endoplasmic reticulum: structure, function and response to cellular signaling. Cellular and molecular life sciences : CMLS. 2016;73(1):79-94.
2. English AR, Voeltz GK. Endoplasmic reticulum structure and interconnections with other organelles. Cold Spring Harbor perspectives in biology. 2013;5(4):a013227.
3. Görlich D, Prehn S, Hartmann E, Kalies K-U, Rapoport TA. A mammalian homolog of SEC61p and SECYp is associated with ribosomes and nascent polypeptides during translocation. Cell. 1992;71(3):489-503.
4. Blobel G, Dobberstein B. Transfer of proteins across membranes. I. Presence of proteolytically processed and unprocessed nascent immunoglobulin light chains on membrane-bound ribosomes of murine myeloma. The Journal of cell biology. 1975;67(3):835-51.
5. von Heijne G, Abrahmsen L. Species-specific variation in signal peptide design. Implications for protein secretion in foreign hosts. FEBS Lett. 1989;244(2):439-46.
6. Lang S, Pfeffer S, Lee PH, Cavalie A, Helms V, Forster F, et al. An Update on Sec61 Channel Functions, Mechanisms, and Related Diseases. Frontiers in physiology. 2017;8:887.
7. Gorlich D, Rapoport TA. Protein Translocation into Proteoliposomes Reconstituted from Purified Components of the Endoplasmic-Reticulum Membrane. Cell. 1993;75(4):615-30.
8. Walter P, Ibrahimi I, Blobel G. Translocation of proteins across the endoplasmic reticulum. I. Signal recognition protein (SRP) binds to in-vitro-assembled polysomes synthesizing secretory protein. The Journal of cell biology. 1981;91(2 Pt 1):545-50.
9. Janda CY, Li J, Oubridge C, Hernandez H, Robinson CV, Nagai K. Recognition of a signal peptide by the signal recognition particle. Nature. 2010;465(7297):507-10.
10. Walter P, Blobel G. Translocation of proteins across the endoplasmic reticulum. II. Signal recognition protein (SRP) mediates the selective binding to microsomal membranes of in-vitro-assembled polysomes synthesizing secretory protein. The Journal of cell biology. 1981;91(2 Pt 1):551-6.
11. Ngosuwan J, Wang NM, Fung KL, Chirico WJ. Roles of cytosolic Hsp70 and Hsp40 molecular chaperones in post-translational translocation of presecretory proteins into the endoplasmic reticulum. The Journal of biological chemistry. 2003;278(9):7034-42.
12. Itskanov S, Park E. Structure of the posttranslational Sec protein-translocation channel complex from yeast. Science. 2019;363(6422):84-7.
13. Berg Bvd, Clemons WM, Collinson I, Modis Y, Hartmann E, Harrison SC, et al. X-ray structure of a protein-conducting channel. Nature. 2004;427(6969):36-44.
14. Mothes W, Prehn S, Rapoport TA. Systematic Probing of the Environment of a Translocating Secretory Protein during Translocation through the Er Membrane. Embo Journal. 1994;13(17):3973-82.
15. Lang S, Benedix J, Fedeles SV, Schorr S, Schirra C, Schauble N, et al. Different effects of Sec61alpha, Sec62 and Sec63 depletion on transport of polypeptides into the endoplasmic reticulum of mammalian cells. Journal of cell science. 2012;125(Pt 8):1958-69.
16. Heinrich SU, Mothes W, Brunner J, Rapoport TA. The Sec61p complex mediates the integration of a membrane protein by allowing lipid partitioning of the transmembrane domain. Cell. 2000;102(2):233-44.
17. Mandon EC, Trueman SF, Gilmore R. Translocation of proteins through the Sec61 and SecYEG channels. Current opinion in cell biology. 2009;21(4):501-7.
18. Esnault Y, Feldheim D, Blondel MO, Schekman R, Kepes F. SSS1 encodes a stabilizing component of the Sec61 subcomplex of the yeast protein translocation apparatus. The Journal of biological chemistry. 1994;269(44):27478-85.

19. Kalies KU, Rapoport TA, Hartmann E. The beta subunit of the Sec61 complex facilitates cotranslational protein transport and interacts with the signal peptidase during translocation. The Journal of cell biology. 1998;141(4):887-94.
20. Zhao X, Jantti J. Functional characterization of the trans-membrane domain interactions of the Sec61 protein translocation complex beta-subunit. BMC Cell Biol. 2009;10(1):76.
21. Laird V, High S. Discrete cross-linking products identified during membrane protein biosynthesis. The Journal of biological chemistry. 1997;272(3):1983-9.
22. Pluquet O, Pourtier A, Abbadie C. The unfolded protein response and cellular senescence. A review in the theme: cellular mechanisms of endoplasmic reticulum stress signaling in health and disease. Am J Physiol Cell Physiol. 2015;308(6):C415-25.
23. Dorner AJ, Wasley LC, Raney P, Haugejorden S, Green M, Kaufman RJ. The stress response in Chinese hamster ovary cells. Regulation of ERp72 and protein disulfide isomerase expression and secretion. The Journal of biological chemistry. 1990;265(35):22029-34.
24. Ponsero AJ, Igbaria A, Darch MA, Miled S, Outten CE, Winther JR, et al. Endoplasmic Reticulum Transport of Glutathione by Sec61 Is Regulated by Ero1 and Bip. Molecular cell. 2017;67(6):962-73 e5.
25. Giunti R, Gamberucci A, Fulceri R, Banhegyi G, Benedetti A. Both translocon and a cation channel are involved in the passive Ca2+ leak from the endoplasmic reticulum: a mechanistic study on rat liver microsomes. Arch Biochem Biophys. 2007;462(1):115-21.
26. Becker T, Bhushan S, Jarasch A, Armache JP, Funes S, Jossinet F, et al. Structure of monomeric yeast and mammalian Sec61 complexes interacting with the translating ribosome. Science. 2009;326(5958):1369-73.
27. Potter MD, Nicchitta CV. Endoplasmic reticulum-bound ribosomes reside in stable association with the translocon following termination of protein synthesis. The Journal of biological chemistry. 2002;277(26):23314-20.
28. Simon SM, Blobel G. A protein-conducting channel in the endoplasmic reticulum. Cell. 1991;65(3):371-80.
29. Trueman SF, Mandon EC, Gilmore R. A gating motif in the translocation channel sets the hydrophobicity threshold for signal sequence function. The Journal of cell biology. 2012;199(6):907-18.
30. Hamman BD, Hendershot LM, Johnson AE. BiP maintains the permeability barrier of the ER membrane by sealing the lumenal end of the translocon pore before and early in translocation. Cell. 1998;92(6):747-58.
31. Karczewski KJ, Francioli LC, Tiao G, Cummings BB, Alfoldi J, Wang Q, et al. The mutational constraint spectrum quantified from variation in 141,456 humans. Nature. 2020;581(7809):434-43.
32. McGuffin LJ, Bryson K, Jones DT. The PSIPRED protein structure prediction server. Bioinformatics. 2000;16(4):404-5.
33. Wilkinson BM, Brownsword JK, Mousley CJ, Stirling CJ. Sss1p Is Required to Complete Protein Translocon Activation. Journal of Biological Chemistry. 2010;285(42):32671-7.
34. Witham CM, Dassanayake HG, Paxman AL, Stevens KLP, Baklous L, White PF, et al. The conserved C-terminus of Sss1p is required to maintain the endoplasmic reticulum permeability barrier. The Journal of biological chemistry. 2020;295(7):2125-34.
35. Wilkinson BM, Esnault Y, Craven RA, Skiba F, Fieschi J, K'Epes F, et al. Molecular architecture of the ER translocase probed by chemical crosslinking of Sss1p to complementary fragments of Sec61p. The EMBO journal. 1997;16(15):4549-59.

36. Jermy AJ, Willer M, Davis E, Wilkinson BM, Stirling CJ. The Brl domain in Sec63p is required for assembly of functional endoplasmic reticulum translocons. The Journal of biological chemistry. 2006;281(12):7899-906.
37. Cohen Y, Megyeri M, Chen OC, Condomitti G, Riezman I, Loizides-Mangold U, et al. The yeast p5 type ATPase, spf1, regulates manganese transport into the endoplasmic reticulum. PLoS One. 2013;8(12):e85519.
38. Davis CD, Ney DM, Greger JL. Manganese, iron and lipid interactions in rats. J Nutr. 1990;120(5):507-13.
39. Hansen SL, Spears JW, Lloyd KE, Whisnant CS. Growth, reproductive performance, and manganese status of heifers fed varying concentrations of manganese. J Anim Sci. 2006;84(12):3375-80.
40. Durr G, Strayle J, Plemper R, Elbs S, Klee SK, Catty P, et al. The medial-Golgi ion pump Pmr1 supplies the yeast secretory pathway with Ca2+ and Mn2+ required for glycosylation, sorting, and endoplasmic reticulum-associated protein degradation. Molecular biology of the cell. 1998;9(5):1149-62.
41. Okorokov LA, Lehle L. Ca(2+)-ATPases of Saccharomyces cerevisiae: diversity and possible role in protein sorting. FEMS Microbiol Lett. 1998;162(1):83-91.
42. Sorin A, Rosas G, Rao R. PMR1, a Ca2+-ATPase in yeast Golgi, has properties distinct from sarco/endoplasmic reticulum and plasma membrane calcium pumps. The Journal of biological chemistry. 1997;272(15):9895-901.
43. Gogala M, Becker T, Beatrix B, Armache JP, Barrio-Garcia C, Berninghausen O, et al. Structures of the Sec61 complex engaged in nascent peptide translocation or membrane insertion. Nature. 2014;506(7486):107-10.
44. Wu X, Cabanos C, Rapoport TA. Structure of the post-translational protein translocation machinery of the ER membrane. Nature. 2019;566(7742):136-9.
45. Shanmuganathan V, Schiller N, Magoulopoulou A, Cheng J, Braunger K, Cymer F, et al. Structural and mutational analysis of the ribosome-arresting human XBP1u. eLife. 2019;8.
46. Braunger K, Pfeffer S, Shrimal S, Gilmore R, Berninghausen O, Mandon EC, et al. Structural basis for coupling protein transport and N-glycosylation at the mammalian endoplasmic reticulum. Science. 2018;360(6385):215-9.
47. Gerard SF, Hall BS, Zaki AM, Corfield KA, Mayerhofer PU, Costa C, et al. Structure of the Inhibited State of the Sec Translocon. Mol Cell. 2020;79(3):406-15 e7.
48. McGilvray PT, Anghel SA, Sundaram A, Zhong F, Trnka MJ, Fuller JR, et al. An ER translocon for multi-pass membrane protein biogenesis. eLife. 2020;9.
49. Bittremieux M, Parys JB, Pinton P, Bultynck G. ER functions of oncogenes and tumor suppressors: Modulators of intracellular Ca(2+) signaling. Biochimica et biophysica acta. 2016;1863(6 Pt B):1364-78.
50. Linxweiler M, Schick B, Zimmermann R. Let's talk about Secs: Sec61, Sec62 and Sec63 in signal transduction, oncology and personalized medicine. Signal Transduct Target Ther. 2017;2:17002.
51. Kumar S, Warrell J, Li S, McGillivray PD, Meyerson W, Salichos L, et al. Passenger Mutations in More Than 2,500 Cancer Genomes: Overall Molecular Functional Impact and Consequences. Cell. 2020;180(5):915-27.e16.
52. Gabaldón T, Pittis AA. Origin and evolution of metabolic sub-cellular compartmentalization in eukaryotes. Biochimie. 2015;119:262-8.
53. Braakman I, Hebert DN. Protein folding in the endoplasmic reticulum. Cold Spring Harb Perspect Biol. 2013;5(5):a013201-a.
54. Feige MJ, Hendershot LM. Disulfide bonds in ER protein folding and homeostasis. Current opinion in cell biology. 2011;23(2):167-75.

55. Lam AKM, Galione A. The endoplasmic reticulum and junctional membrane communication during calcium signaling. Biochimica et Biophysica Acta (BBA) - Molecular Cell Research. 2013;1833(11):2542-59.
56. Mekahli D, Bultynck G, Parys JB, De Smedt H, Missiaen L. Endoplasmic-Reticulum Calcium Depletion and Disease. 2011;3(6).
57. Ivanova H, Kerkhofs M, La Rovere RM, Bultynck G. Endoplasmic Reticulum–Mitochondrial Ca2+ Fluxes Underlying Cancer Cell Survival. 2017;7(70).
58. Okeke E, Parker T, Dingsdale H, Concannon M, Awais M, Voronina S, et al. Epithelial-mesenchymal transition, IP3 receptors and ER-PM junctions: translocation of Ca2+ signalling complexes and regulation of migration. The Biochemical journal. 2016;473(6):757-67.
59. Pierro C, Cook SJ, Foets TCF, Bootman MD, Roderick HL. Oncogenic K-Ras suppresses IP₃-dependent Ca²⁺ release through remodelling of the isoform composition of IP₃Rs and ER luminal Ca²⁺ levels in colorectal cancer cell lines. Journal of cell science. 2014;127(7):1607.
60. Kania E, Roest G, Vervliet T, Parys JB, Bultynck G. IP3 Receptor-Mediated Calcium Signaling and Its Role in Autophagy in Cancer. 2017;7(140).
61. Bergner A, Kellner J, Tufman A, Huber RM. Endoplasmic reticulum Ca2+-homeostasis is altered in Small and non-small Cell Lung Cancer cell lines. J Exp Clin Cancer Res. 2009;28(1):25-.
62. Yang H, Zhang Q, He J, Lu W. Regulation of calcium signaling in lung cancer. J Thorac Dis. 2010;2(1):52-6.
63. Lièvremont J-P, Rizzuto R, Hendershot L, Meldolesi J. BiP, a Major Chaperone Protein of the Endoplasmic Reticulum Lumen, Plays a Direct and Important Role in the Storage of the Rapidly Exchanging Pool of Ca2+. 1997;272(49):30873-9.
64. Opas M, Dziak E, Fliegel L, Michalak M. Regulation of expression and intracellular distribution of calreticulin, a major calcium binding protein of nonmuscle cells. Journal of cellular physiology. 1991;149(1):160-71.
65. Madden E, Logue SE, Healy SJ, Manie S, Samali A. The role of the unfolded protein response in cancer progression: From oncogenesis to chemoresistance. Biology of the cell. 2019;111(1):1-17.
66. Tyson JR, Stirling CJ. LHS1 and SIL1 provide a lumenal function that is essential for protein translocation into the endoplasmic reticulum. The EMBO journal. 2000;19(23):6440-52.
67. Rothblatt JA, Meyer DI. Secretion in yeast: translocation and glycosylation of prepro-alpha-factor in vitro can occur via an ATP-dependent post-translational mechanism. The EMBO journal. 1986;5(5):1031-6.
68. Wilkinson BM, Brownsword JK, Mousley CJ, Stirling CJ. Sss1p is required to complete protein translocon activation. The Journal of biological chemistry. 2010;285(42):32671-7.
69. Rentsch D, Laloi M, Rouhara I, Schmelzer E, Delrot S, Frommer WB. NTR1 encodes a high affinity oligopeptide transporter in Arabidopsis. FEBS Lett. 1995;370(3):264-8.
70. Stirling CJ, Rothblatt J, Hosobuchi M, Deshaies R, Schekman R. Protein translocation mutants defective in the insertion of integral membrane proteins into the endoplasmic reticulum. Molecular biology of the cell. 1992;3(2):129-42.
71. Young BP, Craven RA, Reid PJ, Willer M, Stirling CJ. Sec63p and Kar2p are required for the translocation of SRP-dependent precursors into the yeast endoplasmic reticulum in vivo. The EMBO journal. 2001;20(1-2):262-71.

Manuscript Supplemental Data

Invertase Secretion

Cells were grown in YPD (2% glucose) at 30°C, cultures were split, and cells incubated at 30°C or 37°C for 1h in YPD (2% glucose). Cells were then pelleted (2000g), washed twice with pre-warmed low glucose (0.1% glucose) YPD, resuspended in the low glucose YPD medium, and incubated as before for 1.5h. To halt trafficking, samples were adjusted to 10mM NaN3, and incubated on ice. The samples were washed 3X with 500 µL ice-cold 10mM NaN3 and re-suspended in 500 µL of the same. The samples were split into 10mM NaN3 buffers ± 0.2 % Triton X-100 (final) with the Triton-solubiliaed fractions also being subjected to one cycle of freeze-thaw to generate the permeabilised cell fraction. The partner non-permeabilised and permeabilised samples were used to determine extracellular and total invertase activities, respectively. The pool of secreted invertase is expressed as a fraction.

DSS Cross-linking

Yeast microsomes were prepared according to Rothblatt and Meyer, 1986 (67). Microsomes were incubated at 30°C for 30 min in the presence of either 1 mM DSS or equivalent volume of DMSO. The addition of 10 mM lysine and 10 mM Tris (final concentration) supplied excess amine groups to quench the reaction. Crosslinking was assessed through subsequent SDS PAGE, transfer and immunoblot.

Blue Native PAGE Analysis

BN-PAGE was performed according to Jermy et al., 2006 (36). Two A280nm units of microsomes were harvested by centrifugation at 10,000 × g, resuspended in 100 µL of S-buffer (20 mM Tris-HCl, pH 7.6, 250 mM NaCl, 2 mM dithiothreitol, 5 mM MgOAc, 2% digitonin, 12% glycerol, 1% (v/v) protease inhibitor mixture (Sigma)) and then incubated on

ice for 30 min. Unsolubilised material was removed by centrifugation at 10,000 × g, and then ribosomes were removed by centrifugation for 60 min at 400,000 × g. The supernatant was then diluted to 180 µL with S-buffer without NaCl and digitonin, followed by the addition of 20 µL of 10× sample buffer (5% Coomassie Brilliant Blue G250, 500 mM 6-aminocaproic acid, 100 mM Bistris-HCl, pH 7.0). 0.8 A280nm unit aliquots were loaded onto a 6–16% polyacrylamide gradient gel (buffered with 500 mM 6-aminocaproic acid, 50 mM Tris-HCl, pH 7.0). The samples were run at 200 V for 18 h with Coomassie-containing cathode buffer (50 mM Tricine, pH 7.0, 15 mM Bistris-HCl, pH 7.0, 0.02% Coomassie Brilliant Blue G250) and then for a further 3 h at 500 V in buffer lacking Coomassie (50 mM Tricine, pH 7.0, 15 mM Bistris-HCl, pH 7.0). Anode buffer (50 mM Bistris-HCl, pH 7.0) was constant throughout. The samples were then transferred to polyvinylidene difluoride membrane and analysed by Western blotting.

Reverse Transcription (RT)-PCR

Total RNA was isolated from cells using the FavorPrepTM blood cultured cell total RNA mini-Kit and 1µg was used to template reverse transcription using WarmStart® RTx Reverse Transcriptase to generate cDNA (20 µL final volume). H_2O was used in no RT controls. To analyse *HGT1*, *PMR1* or *ACT1* expression, PCR was performed using 1 µL of cDNA fraction as template and specific oligonucleotides as primers. Products were quantified with Image J software.

Supp. Table S5.1. Yeast strains used in this study.

Yeast	Genotype	Reference
BWY530	*MATα ade2- 1 ura3-1 his3-11,15 trp1-1 leu2-3,112 can1-100 sss1Δ::KanMX4* FKp53	Wilkinson et al. 2010 (68)
SSS1	*MATα ade2- 1 ura3-1 his3-11,15 trp1-1 leu2-3,112 can1-100 sss1Δ::KanMX4* pJKB2	Wilkinson et al. 2010 (68)
sss1-6	*MATα ade2- 1 ura3-1 his3-11,15 trp1-1 leu2-3,112 can1-100 sss1Δ::KanMX4* pJKB16	Witham et al., 2020 (34)
sss1-7	*MATα ade2- 1 ura3-1 his3-11,15 trp1-1 leu2-3,112 can1-100 sss1Δ::KanMX4* pCM205	Witham et al., 2020 (34)
sss1-8	*MATα ade2- 1 ura3-1 his3-11,15 trp1-1 leu2-3,112 can1-100 sss1Δ::KanMX4* pCW11	This study
sss1-KI	*MATα ade2- 1 ura3-1 his3-11,15 trp1-1 leu2-3,112 can1-100 sss1Δ::KanMX4* pCW12	This study
sss1-KE	*MATα ade2- 1 ura3-1 his3-11,15 trp1-1 leu2-3,112 can1-100 sss1Δ::KanMX4* pCW13	This study
sss1-AV	*MATα ade2- 1 ura3-1 his3-11,15 trp1-1 leu2-3,112 can1-100 sss1Δ::KanMX4* pCW14	This study
sss1-LF	*MATα ade2- 1 ura3-1 his3-11,15 trp1-1 leu2-3,112 can1-100 sss1Δ::KanMX4* pCW15	This study
sss1-VT	*MATα ade2- 1 ura3-1 his3-11,15 trp1-1 leu2-3,112 can1-100 sss1Δ::KanMX4* pCW16	This study
sss1-6 KI	*MATα ade2- 1 ura3-1 his3-11,15 trp1-1 leu2-3,112 can1-100 sss1Δ::KanMX4* pCW17	This study
sss1-6 KE	*MATα ade2- 1 ura3-1 his3-11,15 trp1-1 leu2-3,112 can1-100 sss1Δ::KanMX4* pCW18	This study
sss1-6 AV	*MATα ade2- 1 ura3-1 his3-11,15 trp1-1 leu2-3,112 can1-100 sss1Δ::KanMX4* pCW19	This study
sss1-6 LF	*MATα ade2- 1 ura3-1 his3-11,15 trp1-1 leu2-3,112 can1-100 sss1Δ::KanMX4* pCW20	This study

sss1-6 VT	*MATα ade2- 1 ura3-1 his3-11,15 trp1-1 leu2-3,112 can1-100 sss1Δ::KanMX4* pCW21	This study
sss1-7 KI	*MATα ade2- 1 ura3-1 his3-11,15 trp1-1 leu2-3,112 can1-100 sss1Δ::KanMX4* pCW22	This study
sss1-7 KE	*MATα ade2- 1 ura3-1 his3-11,15 trp1-1 leu2-3,112 can1-100 sss1Δ::KanMX4 pCW23*	This study
sss1-7 AV	*MATα ade2- 1 ura3-1 his3-11,15 trp1-1 leu2-3,112 can1-100 sss1Δ::KanMX4 pCW24*	This study
sss1-7 LF	*MATα ade2- 1 ura3-1 his3-11,15 trp1-1 leu2-3,112 can1-100 sss1Δ::KanMX4 pCW25*	This study
sss1-7 VT	*MATα ade2- 1 ura3-1 his3-11,15 trp1-1 leu2-3,112 can1-100 sss1Δ::KanMX4 pCW26*	This study
CWY46	*sss1-8* + YCp *SEC61* (pBW11)	This study
CWY47	*sss1-8* + YCp *SEC61*^{N302K} (pCW4)	This study
CWY48	*sss1-8 +* YCp *SEC61*^{N302L} (pCW7)	This study
CWY49	*sss1-8 +* YCp *SEC61*^{Q48A} (pCW27)	This study
CWY50	*sss1-6 KE* + pRS315	This study
CWY51	*sss1-6 KE* + YCp *SEC61* (pBW11)	This study
CWY52	*sss1-6 KE + YCp SEC61*^{N302L} (pCW7)	This study
CWY53	*sss1-6 KE* + YCp *SEC61*^{N302K} (pCW4)	This study
CWY54	*sss1-7 KE* + pRS315	This study
CWY55	*sss1-7 KE* + YCp *SEC61* (pBW11)	This study
CWY56	*sss1-7 KE* + YCp *SEC61*^{N302L} (pCW7)	This study
CWY57	*sss1-7 KE* + YCp *SEC61*^{N302K} (pCW4)	This study
CWY58	*SSS1*+ YCp *SEC61* (pBW11) + pJT30	Witham et al., 2020 (34)
CWY59	*sss1-6* + YCp *SEC61* (pBW11) + pJT30	Witham et al., 2020 (34)
CWY60	*sss1-7* + YCp *SEC61* (pBW11) + pJT30	Witham et al., 2020 (34)

CWY61	*sss1-6 LF* + YCp *SEC61* (pBW11) + pJT30	This study
CWY62	*sss1-7 LF* + YCp *SEC61* (pBW11) + pJT30	This study
CWY63	*sss1-6 AV* + YCp *SEC61* (pBW11) + pJT30	This study
CWY64	*sss1-7 AV* + YCp *SEC61* (pBW11) + pJT30	This study
CWY65	*sss1-7 VT* + YCp *SEC61* (pBW11) + pJT30	This study
CWY66	*sss1-8* + YCp *SEC61* (pBW11) + pJT30	This study
CWY67	*sss1-8* + YCp *SEC61*^{N302K} (pCW4) + pJT30	This study
CWY68	*sss1-8* + YCp *SEC61*^{N302L} (pCW7) + pJT30	This study
CWY69	*sss1-8* + YCp *SEC61*^{Q48A} (pCW27) + pJT30	This study
CWY70	*SSS1* + YCp *SEC61* (pBW11) + pCW10	Witham et al., 2020 (34)
CWY71	*sss1-6* + YCp *SEC61* (pBW11) + pCW10	Witham et al., 2020 (34)
CWY72	*sss1-7* + YCp *SEC61* (pBW11) + pCW10	Witham et al., 2020 (34)
CWY73	*sss1-6 LF* + YCp *SEC61* (pBW11) + pCW10	This study
CWY74	*sss1-7 LF* + YCp *SEC61* (pBW11) + pCW10	This study
CWY75	*sss1-6 AV* + YCp *SEC61* (pBW11) + pCW10	This study
CWY76	*sss1-7 AV* + YCp *SEC61* (pBW11) + pCW10	This study
CWY77	*sss1-7 VT* + YCp *SEC61* (pBW11) + pCW10	This study
CWY78	*sss1-8* + YCp *SEC61* (pBW11) + pCW10	This study
CWY79	*sss1-8* + YCp *SEC61*^{N302K} (pCW4) + pCW10	This study
CWY80	*sss1-8* + YCp *SEC61*^{N302L} (pCW7) + pCW10	This study
CWY81	*sss1-8* + YCp *SEC61*^{Q48A} (pCW27) + pCW10	This study

Supp. Table S5.2. Plasmids used in this study.

Plasmid	Description	Reference
pJT30	UPRE-LacZ reporter	Tyson and Stirling, 2000 (66)
pBW11	YCp *SEC61 LEU2*	Wilkinson et al., 1997 (35)
pDR195	YEp *URA3* containing the *PMA1* promoter and *CYC1* terminator to enable high level gene expression.	Rentsch et al. 1995 (69)
pJKB2	YCp *SSS1 HIS3*	Wilkinson et al., 2010. (68)
pJKB16	YCp *sss1*$^{P74A, I75A}$ *HIS3*	Witham et al., 2020 (34)
pCM203	YCp *SEC61 SSS1 URA3*	Witham et al., 2020 (34)
pCM205	YCp *sss1*^{H72K} *HIS3*	Witham et al., 2020 (34)
pCW4	YCp *SEC61*^{N302K} *LEU2*	Witham et al., 2020 (34)
pCW7	YCp *SEC61*^{N302L} *LEU2*	Witham et al., 2020 (34)
pCW10	YEp *HGT1 URA3*	Witham et al., 2020 (34)
pCW11	YCp *sss1*^{H72R} *HIS3*	This study
pCW12	YCp *sss1*^{K38I} *HIS3*	This study
pCW13	YCp *sss1*^{K41E} *HIS3*	This study
pCW14	YCp *sss1*^{A53V} *HIS3*	This study
pCW15	YCp *sss1*^{L70F} *HIS3*	This study
pCW16	YCp *sss1*^{V78T} *HIS3*	This study
pCW17	YCp *sss1*$^{K38I\ P74A\ I75A}$ *HIS3*	This study
pCW18	YCp *sss1*$^{K41E\ P74A\ I75A}$ *HIS3*	This study
pCW19	YCp *sss1*$^{A53V\ P74A\ I75A}$ *HIS3*	This study
pCW20	YCp *sss1*$^{L70F\ P74A\ I75A}$ *HIS3*	This study
pCW21	YCp *sss1*$^{V78T\ P74A\ I75A}$ *HIS3*	This study
pCW22	YCp *sss1*$^{K38I\ H72K}$ *HIS3*	This study
pCW23	YCp *sss1*$^{K41E\ H72K}$ *HIS3*	This study
pCW24	YCp *sss1*$^{A53V\ H72K}$ *HIS3*	This study
pCW25	YCp *sss1*$^{L70F\ H72K}$ *HIS3*	This study

pCW26	YCp *sss1*$^{V78T\ H72K}$ *HIS3*	This study
pCW27	YCp *SEC61*^{Q48A} *LEU2*	This study

Supp. Table S5.3. Oligonucleotides used in this study.

Name	Sequence
SSS1 P74A I75A_F	GATTCATATTgCAgcCAGATACGTTATTGT
SSS1 P74A I75A_R	GTATCTGgcTGcAATATGAATCAACTTGAT
SSS1 H72K_F	AAGTTGATTaAaATTCCAATCAGATACGTTATTG
SSS1 H72K_R	TGATTGGAATtTtAATCAACTTGATGGCGTAAC
SSS1 K38I_F	AATTCTTGGCCAttTGTAAGAAACCTGATT
SSS1 K38I _R	TTCTTACAaaTGGCCAAGAATTGAGTACCT
SSS1 K41E_F	CAAGTGTAAGgAACCTGATTTGAAGGAATA
SSS1 K41E_R	CAAATCAGGTTCCTTACACTTGGCCAAGAA
SSS1 A53V_F	GATTGTCAAGGtTGTTGGTATTGGTTTTAT
SSS1 A53V_R	AATACCAACAaCCTTGACAATCTTGGTGTA
SSS1 L70F_F	CATCAAGTTtATTCATATTCCAATCAGATACG
SSS1 L70F_R	GCTGCAATATGAATaAACTTGATGGCGTAACC
SSS1 H72R_F	CATCAAGTTGATTagaATTCCAATCAGATACG
SSS1 H72R_R	ATTGGAATtctAATCAACTTGATGGCGTAACC
SSS1 V78T_F	CAGATACacTATTGTTTAAAAGAGATAAAAG
SSS1 V78T_R	TCTTTTAAACAATAgtGTATCTGATTGGAAT
SSS1 L70F P74A I75A_F	CATCAAGTTtATTCATATTGCAGCCAGATACG
SSS1 L70F P74A I75A_R	ATTGGAATATGAATaAACTTGATGGCGTAACC
SSS1 L70F H72K_F	CATCAAGTTtATTaAaATTCCAATCAGATACG
SSS1 L70F H72K_R	ATTGGAATtTtAATaAACTTGATGGCGTAACC
SSS1 V78T P74A I75A_R	TCTTTTAAACAATAgtGTATCTGGCTGGAAT
*HGT1*_qpcr_F	CCCAATTGGTAGGATACTGG
*HGT1*_qpcr_R	GTAAGACCTGCAGCACCATAAC
*PMR*1_qpcr_F	GGCAACCAAGATTCTCAACC
*PMR1*_qpcr_R	GCCATAGAATTTGCGCACTC
*ACT1*_qpcr_F	GCCTTCTACGTTTCCATCCA
*ACT1*_qpcr_R	GGCCAAATCGATTCTCAAAA

Supp. Table S5.4. Antibodies used in this study.

Antibody	Dilution	Reference
Anti-Sec61p, rabbit polyclonal	1:10,000	Stirling et al., 1992 (70)
Anti-Sss1p, sheep polyclonal	1:5000	Wilkinson et al., 2010 (68)
Anti-Sec63p, sheep polyclonal	1:10,000	Young et al., 2001 (71)
Anti-DPAP B, sheep polyclonal	1:5000	Tyson and Stirling 2000 (66)
Anti-Kar2p, sheep polyclonal	1:10,000	Tyson and Stirling 2000 (66)
Anti-Prepro alpha factor	1:10,000	Young et al., 2001 (71)
HRP conjugated anti-sheep	1:20,000	N/A
HRP conjugated anti-rabbit	1:20,000	N/A

Suppl. Fig. S1

Supp. Fig. S5.1. The primary sequence of Sss1p, Sss1^{K38I}p, Sss1^{K43E}p, Sss1^{A53V}p, Sss1^{L70F}p, Sss1^{H72R}p and Sss1^{V78T}p was analysed by PSIPRED 4.0 software (32).

Suppl. Fig. S2

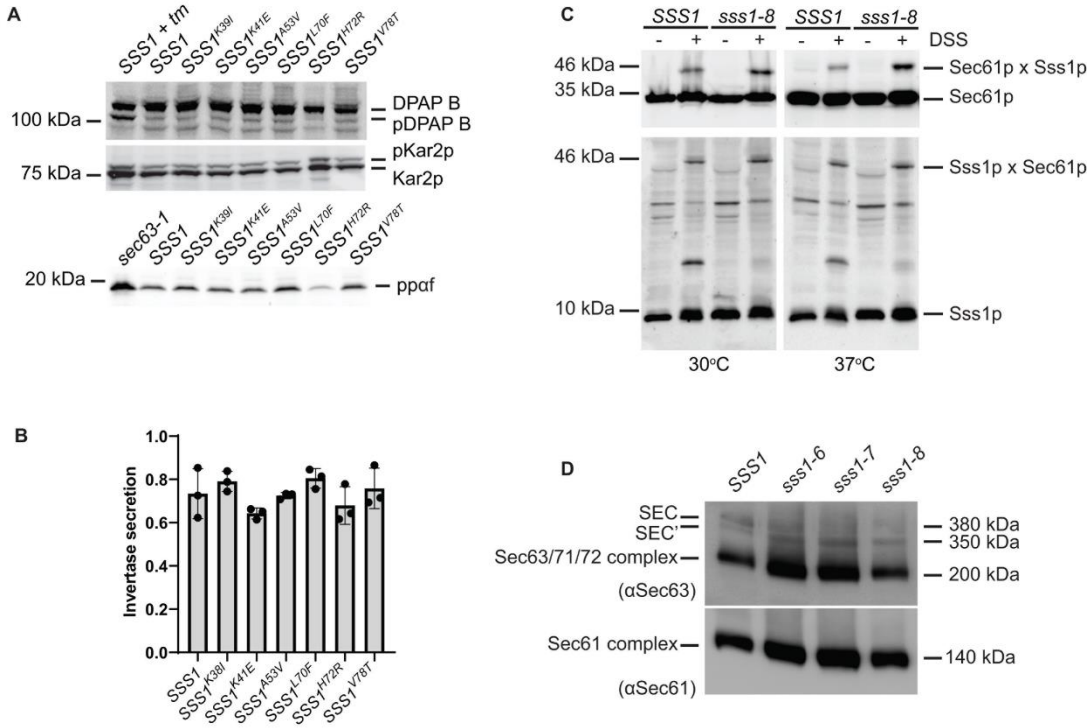

Supp. Fig. S5.2. (A) Cell extracts derived from cells expressing either *SSS1* with or without tunicamycin (tm), *SSS1*^{K39I}, *SSS1*^{K41E}, *SSS1*^{A53V}, *SSS1*^{L70F}, *SSS1*^{H72R} or *SSS1*^{V78T} were immunoblotted with anti-DPAP B, anti-Kar2p and anti-ppαf antibodies. **(B)** Invertase secretion was determined in cells expressing either *SSS1*, *SSS1*^{K39I}, *SSS1*^{K41E}, *SSS1*^{A53V}, *SSS1*^{L70F}, *SSS1*^{H72R} or *SSS1*^{V78T} **(C)** Membranes derived from wildtype or *sss1*^{H72R} yeast incubated with and without 1 mM DSS were immunoblotted with anti-Sss1p and anti-Sec61p antibodies. **(D)** Two A_{260nm} units of microsomes prepared from wild type, *sss1-6 (sss1*$^{P74A, I75A}$*), sss1-7 (sss1*^{H72K}*)* and *sss1-8 (sss1*^{H72R}*)* were resolved by 6–16% BN-PAGE and analysed by Western blotting for Sec63p (upper panel) and Sec61p (lower panel).

Suppl. Fig. S3

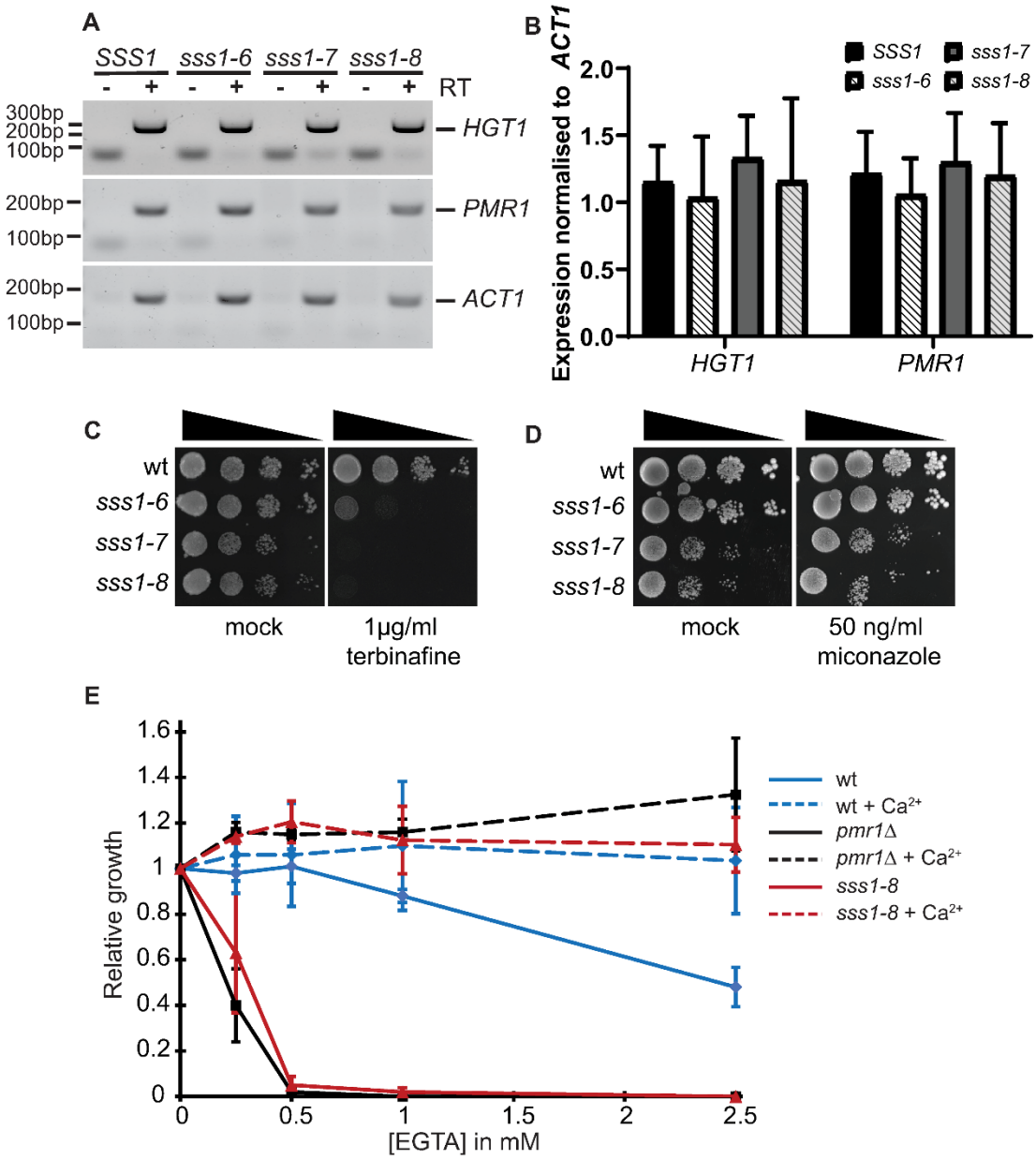
A
SSS1
sss1-6
sss1-7
sss1-8
RT
300bp
200bp
100bp
HGT1
PMR1
ACT1
B
Expression normalised to ACT1
SSS1
sss1-7
sss1-6
sss1-8
HGT1
PMR1
C
wt
sss1-6
sss1-7
sss1-8
mock
1µg/ml terbinafine
D
mock
50 ng/ml miconazole
E
Relative growth
[EGTA] in mM
wt
wt + Ca2+
pmr1Δ
pmr1Δ + Ca2+
sss1-8
sss1-8 + Ca2+

Supp. Fig. S5.3. (A) *HGT1* and *PMR1* expression was determined by RT-PCR on cDNA derived from mRNA isolated from wildtype, *sss1-6, sss1-7* and *sss1-8* yeast harbouring YEp *HGT1*. **(B)** Expression of *HGT1* and *PMR1* relative to *ACT1* in wildtype, *sss1-6, sss1-7* and *sss1-8* yeast was detetermined. The histogram shows the average of at least 6 experiments. **(C)** Wildtype, *sss1-6, sss1-7* and *sss1-8* yeast were spotted on YPD agar or YPD agar containing 1 µg/mL terbinafine in a 10-fold dilution series and incubated at 30°C for 3 days. **(D)** Wildtype, *sss1-6, sss1-7* and *sss1-8* yeast were spotted on YPD agar or YPD agar containing 50 ng/mL miconazole in a 10-fold dilution series and incubated at 30°C for 3 days. **(E)** The relative growth of wild type, *pmr1Δ* and *sss1-8* cells, grown with and without $CaCl_2$, was determined when grown with either 0, 0.25 mM, 0.5 mM, 1 mM or 2.5 mM EGTA.

Suppl. Fig. S4

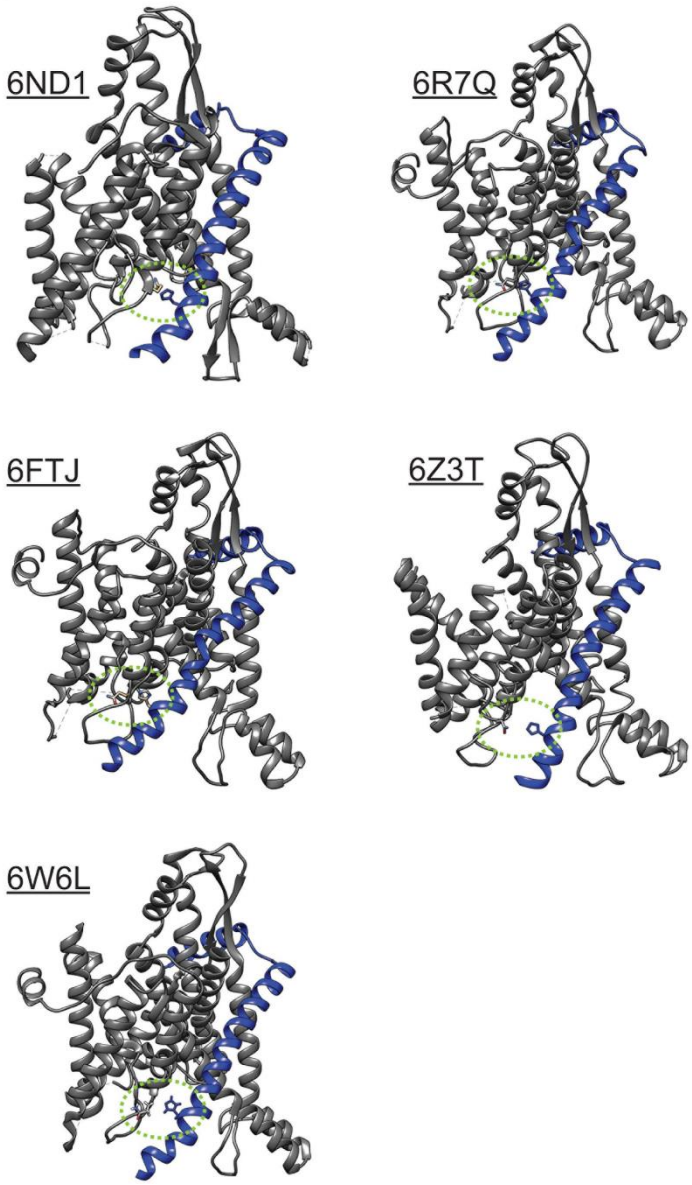

Supp. Fig. S5.4. Ribbon diagram of the Sec61 complex from five recent high resolution crystal structures; 6ND1 (44), 6R7Q (45), 6FTJ (46), 6Z3T (47) and 6W6L (48), are visualised using Chimera software. The position of Q47 in Sec61α relative to H58 in Sec61γ are indicated.

Suppl. Fig. S5

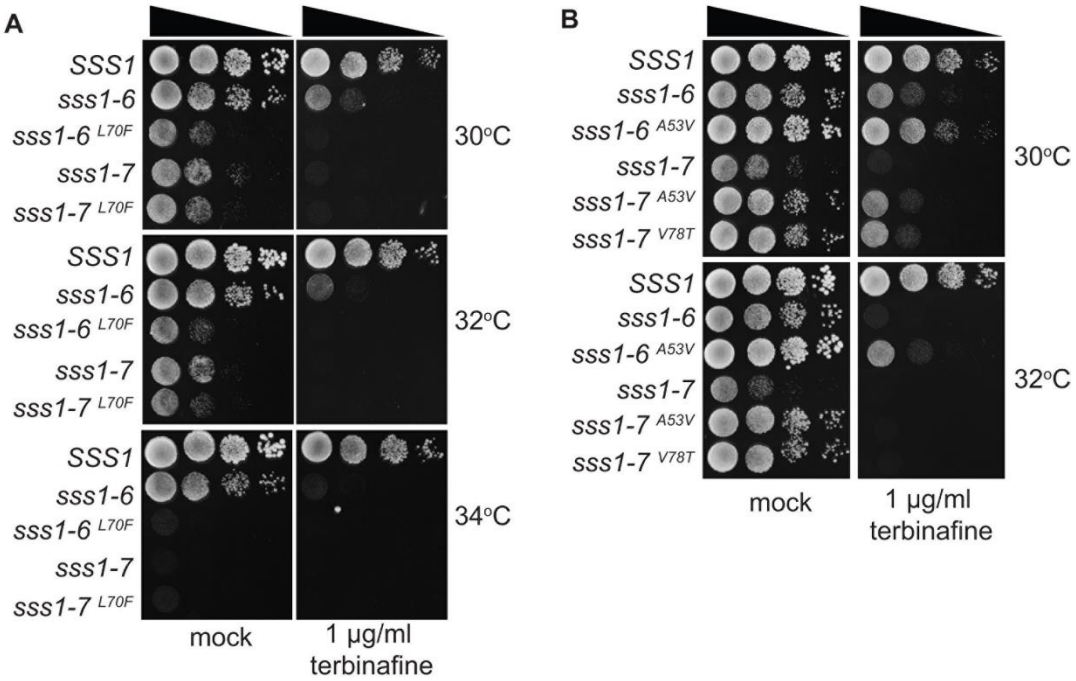

Supp. Fig. S5.5. (A) Wildtype or cells expressing either *SSS1*^{P74A,I75A}, *SSS1*$^{L70F,\ P74A,I75A}$, *SSS1*^{H72K} or *SSS1*^{L70F,H72K} as the sole source of *SSS1* were spotted on YPD agar or YPD agar containing 1 µg/mL terbinafine in a 10-fold dilution series and incubated at 30°C, 32°C or 34°C for 2 days. **(B)** Wildtype or cells expressing either *SSS1*^{P74A,I75A}, *SSS1*$^{A53V,\ P74A,I75A}$, *SSS1*^{H72K}, *SSS1*$^{A53V,\ H72K}$ or *SSS1*$^{H72K,\ V78T}$ as the sole source of *SSS1* were spotted on YPD agar or YPD agar containing 1 µg/mL terbinafine in a 10-fold dilution series and incubated at 30°C or 32°C for 2 days.

Chapter 5

Determining Protein Degradation Pathways Regulating Sss1 Abundance

Introduction

Organelles have dynamic proteomes that are in tune to the diverse needs of a cell and the conditions of their environment. Control over their individual proteomes is achieved through a coordinated balance of protein synthesis and degradation. ER associated degradation (ERAD) was previously discussed as a quality control process in the clearance of misfolded protein from the ER. The involvement of ERAD in maintaining cellular homeostasis far exceeds this purpose and lends itself to other quality control measures including maintaining stoichiometry, clearing mis-localised proteins, and quantity control of biosynthetic pathways (1, 2).

Certain motifs, often those modified post-translationally, can detail the folding state of proteins as well as their period spent within the ER lumen. This information can be used as a degradation signal to present aberrant protein for recognition via the ERAD pathways and is often referred to as the degron (3-5). The degron affords cells a level of discrimination in isolating aberrant protein from those appropriately folded or newly synthesised. Identification of the degron and subsequent degradation is facilitated through the ER resident ubiquitin ligase complexes. Mammalian systems have been demonstrated to have at least 10 such complexes whereas these processes are simplified in yeast with three prominent pathways, being HRD1, DOA10 and ASI (Fig. 6.1.) (6). These pathways work in parallel with each other to accommodate for a wide variety in substrate, with three branches of recognition granting an aspect of selectivity to each pathway. The location of the degron determines the classification of selection, which includes substrate with a degron exposed to the lumen (ERAD-L substrate), the cytosol (ERAD-C substrate) or those imbedded in the ER membrane (ERAD-M substrate) (2, 7-9). ERAD-L and

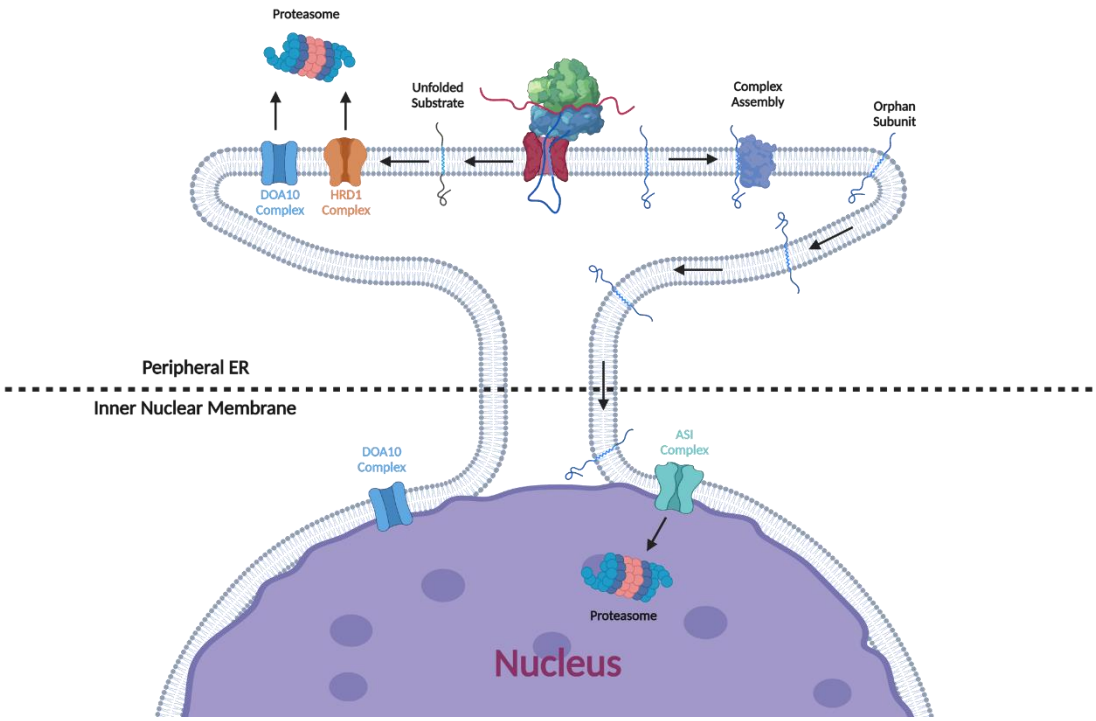

Fig. 6.1. The major ERAD pathways of yeast. Depiction of the three prominent E3 ligase complexes resident to the ER. The HRD1 complex localises to the peripheral ER processing both ERAD-L and ERAD-M substrate. The DOA10 complex can localise to both the peripheral ER and the INM and is involved recognising ERAD-C and ERAD-M substrate. The ASI complex, located solely at the INM is depicted here in its role in recognising ERAD-M substrate that, upon failing to interact with their binding partners, have now mis-localised to the INM to be degraded. Image created in BioRender.

ERAD-C substrate are exclusively processed via the HRD1 and DOA10 complexes respectively. While ERAD-M substrates make no such distinction, being suitable for processing by all three pathways.

A RING (Really interesting New Gene) finger E3 ligase constitutes the core to each ubiquitin ligase complex and operates as part of a three-step process for protein ubiquitination. First ubiquitin, a small cytosolic protein of 76 amino acids (aa) is activated by an E1 ubiquitin-activating enzyme in an ATP dependent manner (10). Second, ubiquitin then becomes fused to an E2 ubiquitin conjugating enzyme and in some cases this leads to the formation of a poly-ubiquitin chain. The ubiquitin conjugated E2 is consequently found to associate with an E3 ubiquitin-ligase. Finally, during retro-translocation of a protein substrate to the cytosol, the E3 facilitates the attachment of the ubiquitin to a lysine side chain, marking the substrate for degradation (11, 12).

The HRD1 Pathway

HRD1 represents the most extensively studied ERAD complex with well-defined modes of substrate recognition and has been further implicated in the retro-translocation of substrate, with both aspects to be explored in detail here. HRD1 complexes recognise two branches of substrate through the association of the core RING-finger Hrd1 protein with various accessory subunits. This forms two known subsidiaries. ERAD-L substrates for example, require a complex of Hrd1 with the membrane proteins Hrd3, Usa1 and Der1 in addition to the lumenal protein Yos9 (7, 13-15). Yos9 is an essential lectin involved in the recognition of misfolded glycoproteins (16, 17). However, a distinction must be made as certain glycan modifications, such as those that arise from N-linked glycosylation, aid in the folding of nascent polypeptides. As such several requirements must be met for the degradation of glycoproteins to proceed. Early glycan processing by enzymes such as glucosidases enables the recognition of substrate by lectins with protein folding activity. Yet the glycan also acts as a timer, with stubborn proteins that loiter in the ER lumen being subsequently processed via the late-stage mannosidase, Htm1 (18-

20). Yos9 binds the α1,6-linked mannose which arises from the late glycan trimming by Htm1 and is the first point of recognition. Association of Yos9 with the HRD1 complex is achieved via the lumenal domain of Hrd3. For ERAD processing of the substrate to proceed, the glycan bound to Yos9 must be within an unstructured segment that can also bind Hrd3 (2, 21). As such Hrd3 serves as the second point in substrate recognition of glycoproteins and has additionally been shown to function independently of Yos9 for the recognition of non-glycosylated ERAD-L substrates. After recognition the substrate must be retro-translocated from the ER lumen for ubiquitination at the cytosol and while the literature is still ultimately uncertain, the HRD1 complex is heavily implicated in this process. The current model suggests the involvement of Hrd1 with Der1, where together they form a channel that facilitates the movement of a substrate (5, 22, 23). Structures of Hrd1 and Der1 have revealed that their TMDs (of 6 and 8 respectively) assemble with a hydrophilic cavity with each forming as one half of a channel. Oligomerisation of the complex is facilitated through an association with Usa1 that interacts with both Hrd1 and Der1 at their cytosolic face. The hydrophilic cavities formed by Hrd1 and Der1 impact upon both the cytosolic and lumenal faces of the ER membrane respectively. In combination with molecular dynamic simulations and mutagenesis studies, these findings suggest that Hrd1 and Der1 manipulate their surrounding lipid environment, thinning the bilayer and hence reduce the energetic barrier for substrate retro-translocation. It should be mentioned that while both Hrd1 and Der1 collaborate to form a channel they do not directly interact and are separated by lipid molecules that may influence the substrate during retro-translocation (5, 6, 23).

The fully assembled HRD1 complex recruits substrate from Hrd3, which enters as a hairpin into the channel. The looped substrate is then thought to slide back and forth through the thinned bilayer until a suitable lysine residue is exposed (15, 24). Ubiquitination of the lysine by Hrd1 would prevent backflow and further engages the E2 ubiquitin conjugating enzyme, Ubc7. Ubc7 is a soluble protein that tethers to the ER via association with the membrane protein Cue1 (2, 15). Hrd1 engages with Ubc7 to facilitate the transfer of the established poly-ubiquitin chain to the substrate. The presence of a poly-ubiquitin chain permits recognition by the Cdc48

ATPase complex which serves to pull the substrate to the cytosol for subsequent degradation via the 26s proteasome (15, 25, 26).

As previously mentioned, the HRD1 complex is also involved in the degradation of ERAD-M substrate. Processing of these substrates demands an alternative Hrd1 complex in which Hrd1, Hrd3 and Usa1 remain yet Der1 is replaced for Dfm1 (27, 28). Additionally, Yos9 is absent in this complex which is indicative of the sole role this component has in the recognition of lumenal substrate. Dfm1 is related to Der1 and suggested to function in a much similar way, that is to facilitate thinning of the membrane for retro-translocation (6, 29). An ERAD-M substrate that has been of interest is that of Hmg2, homolog to the mammalian HMG-CoA reductase and rate limiting enzyme for cholesterol synthesis (30, 31). Hrd1 owes its name (**H**MG-CoA **R**eductase **D**egradation **1**) to this interaction which establishes a concept for ERAD machinery in quantity control, an aspect that will be explored again with DOA10.

The DOA10 Pathway

As the name suggests, the Doa10 (**D**egradation **O**f **A**lpha **10**) complex was first identified through its involvement in the degradation of the ERAD-C substrate and soluble transcriptional repressor, Matα2 (32). Until recently, the DOA10 complex was thought to be dedicated solely in the recognition of ERAD-C substrate. Sbh2 is a TA protein and subunit to the translocon paralog, Ssh1. Degradation of Sbh2 was found to be dependent on both their TMD and the DOA10 complex which therefore broadened the scope of DOA10 to include ERAD-M substrates (33). The core Doa10 is a 14 TMD protein with an N-terminal RING finger domain (34). A lot of how Doa10 recognises and engages substrate is still to be found, yet a conserved element at the proteins C-terminus has been implicated (35, 36). Doa10 requires the action of two E2 ubiquitin conjugating enzymes, enlisting the partnered Cue1 and Ubc7 as well as Ubc6. Differing from its action at the HRD1 complex, Ubc7 functions with Doa10 to coordinate the transfer of the first ubiquitin molecule to the substrate. This primes the substrate to now receive a pre-assembled ubiquitin chain from Ubc6 again facilitated via the E3 activity of Doa10 (6, 37). At this point

degradation proceeds as described with the HRD1 complex with the substrate recognised by the Cdc48 ATPase for removal to the cytosol for degradation. The Doa10 complex is also involved in regulating the sterol biosynthesis pathway via a negative feedback loop. Squalene monooxygenase or simply, Erg1, is one of the rate limiting enzyme that oxidises squalene to oxidosqualene as part of the mevalonate pathway (38). Erg1 is recognised for degradation by Doa10 in the presence of high levels of lanosterol, a derivative of the same pathway (39). This is critical in preventing the accumulation of toxic sterol intermediates and emphasises the role ERAD has in regulating ER homeostasis though quantity control.

The ASI Pathway

While there is a functional distinction between the inner nuclear membrane (INM) and the ER, the two domains remain contiguous with each other. This is especially relevant for the third pathway in ERAD that involves the ASI complex. The ASI complex is a trimer of two RING finger ubiquitin ligases (Asi1 and Asi3) and a recognition factor (Asi2) which engage with the E2 enzymes Ubc4 and Ubc7 (as well as Cue1 by association) (5, 40-42). Ubiquitination at ASI occurs much in the same manner as Doa10, with initial priming via Ubc7 followed by the attachment of the poly-ubiquitin chain via Ubc4. Cdc48 is again found to associate with this ERAD pathway at the end stages of degradation, with in vitro studies finding it to coordinate retro-translocation in collaboration with the ASI complex (6, 42). The ASI complex is restricted to the INM which is critical in its function in recognising mis-localised substrates. Predominantly this role falls to the removal of orphan proteins that have failed to interact with their binding partners (40, 41). The recognition of orphan proteins has been demonstrated through the removal of unassembled subunits to the oligosaccharyltransferase (OST) complex as well as Erg11, a p450 protein family member that notoriously does not assemble into stable complexes (41-44). This was found to be dependent on recognition of the protein's TMDs and hence classifies the ASI complex in the removal of ERAD-M substrate. Unassembled subunits can constitute a significant burden to cells; therefore their swift removal is pertinent to cellular homeostasis.

Experimental Design and Aims

The *sss1-6* mutant (P74A, I75A) is phenotypically similar to *sss1-7* (H72K), its growth is temperature sensitivity, the UPR is induced and unglycosylated Sil1 accumulates. However, immunoblot analysis has demonstrated Sss1-6 mutant protein to be expressed to much greater levels than WT Sss1. This has led us to hypothesise that the mutation in *sss1-6* has disrupted the degron required for efficient degradation. Our analysis has found that Sss1 is a quantity control substrate that is rapidly degraded when failing to interact with either of its major interacting partners, Sec61 and Ssh1. Furthermore, an ER resident peptidyl prolyl isomerase (PPI) appears to coordinate the ERAD of Sss1, suggesting that the stability of this subunit is regulated via the interconversion between the cis and trans isomers of the peptide bond that exists between I73 and P74. Sss1 to our knowledge is the first substrate to be implicated for recognition via multiple ERAD pathways as part of its regulated degradation.

Results

The Conserved K_{69}LIHIPI_{75} Heptapeptide Encodes the Sss1 Degron

Our characterisation of two TS mutants of the conserved translocon subunit, Sss1, revealed the TS growth defect to be the result of metabolite leak from dysregulated translocon gating. Immunoblot analysis also revealed Sss1 protein levels were elevated within the *sss1-6* strain (Fig. 3.1., D; Chapter 3). As Sss1 is known to stabilise the translocon complex, we were intrigued to determine whether the metabolite leak was the result of increased Sec61 channels formed due to increased abundance of the Sss1-6 protein. We had first endeavoured to investigate this outcome in the context of Sss1 over-expression. The WT yeast strain, BY4742 derived from *S288C*, was transformed with YCp Sss1 (pJKB2), YEp Sss1 (FKp53) an over-expression yeast episomal plasmid and the plasmid-borne copy of *sss1-6* (pJKB16). Immunoblot analysis of the BY4742 expressing pJKB16 demonstrated that the Sss1 protein was present at significantly higher levels much like that seen previously in BWY530 (*sss1Δ::KanMX4* FKp53) (Fig 3.1., D; Chapter 3), while

overexpression demonstrated only a moderate increase in Sss1 protein (Fig. 6.2., A). Collectively these findings imply a point of diversity that exists between the overexpression and *sss1-6* systems.

We attributed the difference in protein abundance observed in the immunoblot analysis to reduced turnover of Sss1-6 protein. This led us to hypothesise that the quality control for Sss1 has been perturbed within the *sss1-6* mutant. To investigate this a cycloheximide chase was performed on BWY530 cells expressing either the pJKB2, or pJKB16. Cycloheximide (chx) is a translational inhibitor, binding to the ribosomal e-site to block the translocation of tRNA during elongation (45, 46). Chx is widely used as part of chase assays designed to interrogate the degradation kinetics of the steady state population for the protein of interest. The degradation kinetics of the BWY530 strain containing either pJKB2 (BWY530 Sss1) or pJKB16 (Sss1-6) were assessed over a 90-minute time course and in agreement with previous findings (47), the half-life ($t_{½}$) of the BWY530 Sss1 was determined to be ≈ 45 min. In contrast however, Sss1-6 was found to remain stable throughout the time course (Fig. 6.3., A & B). This indicated that the regulation of Sss1 degradation had been perturbed in *sss1-6* and that perhaps we had impacted upon the signal degron of the protein.

The aa sequence of the Sss1 TMD is highly conserved and in particular at a C-terminal motif where the K_{69}LIHIPI_{75} heptapeptide is absolutely conserved. Given this conservation we hypothesised that this region may functionally encode for the degron. As part of chapter 3 we performed double-alanine scanning mutagenesis throughout this region to investigate the role of these residues in regulating Sss1. This created variants $SSS1^{I68A,\ K69A}$, $SSS1^{L70A,\ I71A}$, and $SSS1^{H72A,\ I73A}$; which together with Sss1-6 spanned the conserved motif. Sss1 is essential, as *sss1Δ* cells are not viable and as part of chapter 3 we had determined that these variants could sustain cell viability. To briefly reiterate these findings, pJKB2 along with each mutant was transformed into BWY530 and tested for the ability of these strains to grow after loss of FKp53 on 5-FOA medium. Strains harbouring pJKB2 or any of the mutants produced viable colonies, whereas strains transformed with vector alone could not. Much to the interest to the aims of this chapter, was that upon analysis of Sss1

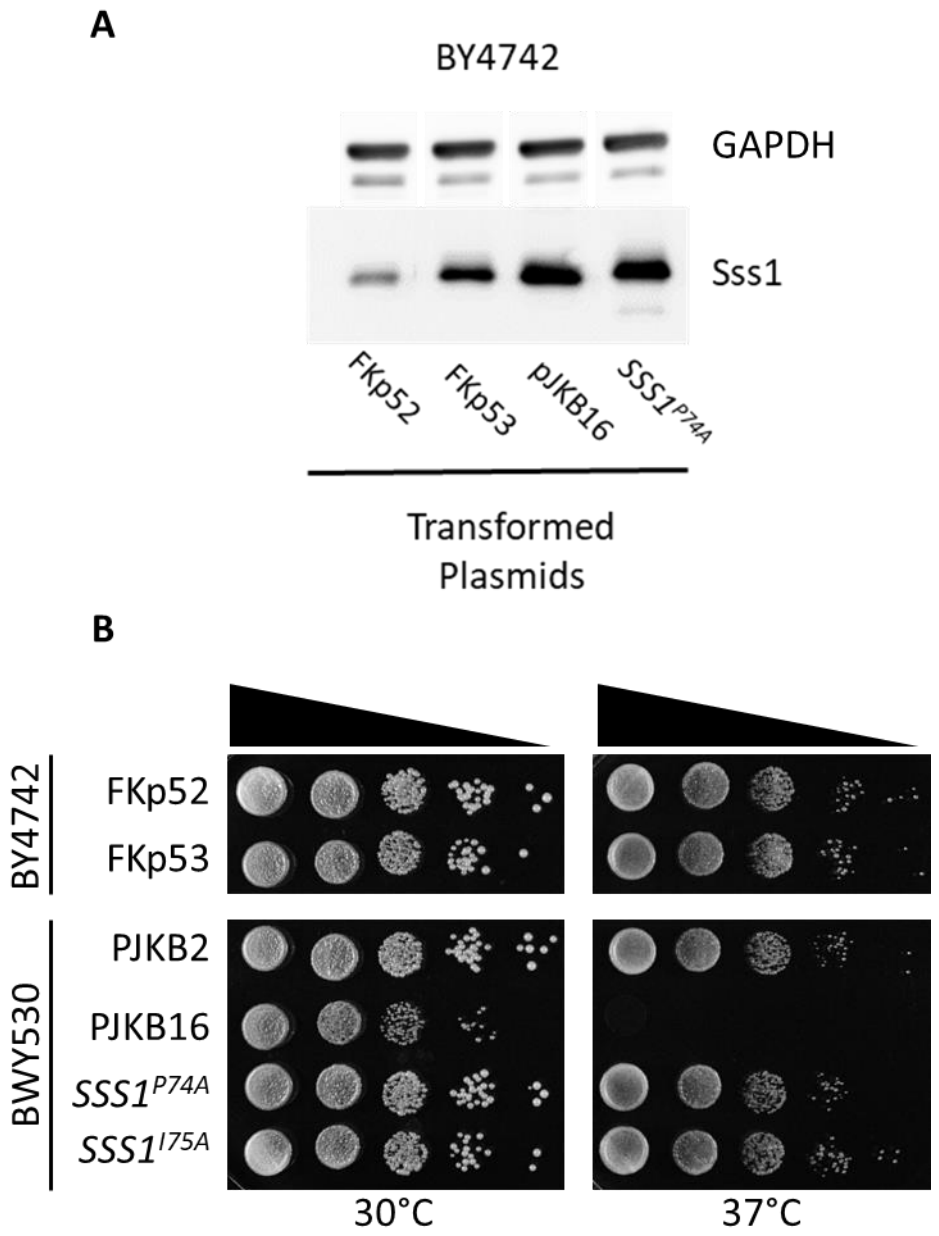

Fig. 6.2. Phenotypical characterisation of Sss1 abundance. (A) Protein lysate derived from BY4742 cells transformed with either YCp Sss1 (FKp52), YEp Sss1 (FKp53), pJKB16 (*sss1*$^{P74A, I75A}$) or *SSS1*^{P74A} were immunoblotted with anti-Sss1 or anti-GAPDH antibodies. **(B)** BY4742 cells transformed with either YCp Sss1 (FKp52) or YEp Sss1 (FKp53) as well as BWY530 cells transformed with pJKB2 (WT Sss1), pJKB16 (*sss1*$^{P74A, I75A}$), *SSS1*^{P74A} or *SSS1*^{I75A} with were spotted on YPD agar in a 10-fold dilution series and incubated at 30°C or 37°C for 3 days.

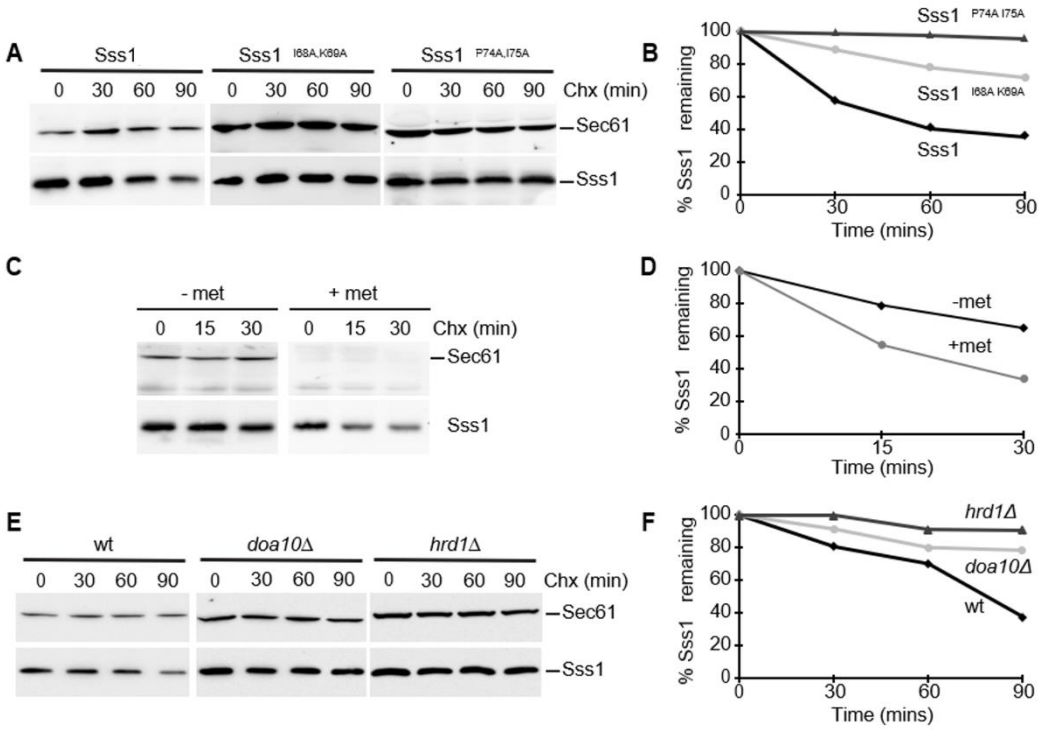

Fig. 6.3. The C-terminus of Sss1 regulates protein turnover. (A) Cells were pre-treated for 10 minutes with 0.25 mg/mL chx. Afterwards cells were removed at the indicated times and were immunoblotted with anti-Sss1 or anti-Sec61 antibodies. **(B)** Densitometric analysis of **(A)** using Image J software. **(C)** PRY14 grown in the absence or presence of methionine were pre-treated for 10 minutes with 0.25 mg/mL chx. Afterwards cells were removed at the indicated times and were immunoblotted with anti-Sss1 or anti-Sec61 antibodies. **(D)** Densitometric analysis of **(C)** using Image J software. **(E)** WT, *doa10Δ* and *hrd1Δ* cells of the *S288C* background were pre-treated for 10 minutes with 0.25 mg/mL chx. Afterwards cells were removed at the indicated times and were immunoblotted with anti-Sss1 or anti-Sec61 antibodies. **(F)** Densitometric analysis of **(E)** using Image J software.

protein within the alanine mutants, we observed a moderate increase in Sss1 protein levels of the *SSS1*$^{I68A, K69A}$ mutant, herein termed *SSS1-3* (Fig 3.1, D; Chapter 3). To determine whether this increase was conveying an enhanced protein stability as seen in Sss1-6, we performed another chx chase to include Sss1-3. Again, expression of WT Sss1 demonstrated a $t_{½} \approx 45$ min while Sss1-3 levels remained constant throughout the 90-minute chx chase, much like that observed in Sss1-6 (Fig. 6.3., A & B). Therefore, while Sss1 is usually readily turned over in cells, substitution of the residue pairs I68 & K69 and P74 & I75 with alanine is found to stabilise Sss1, indicating that these residues constitute part of the proteins degron.

P74A Individually Contributes to the Accumulation Observed in *sss1-6*

The mutant *SSS1-3* demonstrated increased protein stability likened to that of *sss1-6,* yet we found that it did not replicate the TS phenotype (data not shown) and could perhaps be indicating that these two outcomes in *sss1-6* are irrespective of each other. As such we endeavoured to find whether we could separate the two phenomena to investigate them specifically. *SSS1*^{P74A} and *SSS1*^{I75A} were each generated, and viability confirmed as previously detailed, with each mutant transformed into BWY530 demonstrating growth on 5-FOA medium. Growth analysis revealed neither mutant to possess a TS growth phenotype signifying that the double mutant is necessary for this effect (Fig. 6.2., B).

The next step was to determine whether Sss1 protein levels were higher in either mutant. Immunoblot analysis found that the *SSS1*^{P74A} mutant, but not *SSS1*^{I75A}, expressed Sss1 protein to the same extent as *sss1-6* (Fig. 6.4., A). Chx chase confirmed the stability of Sss1 protein in the *SSS1*^{P74A} mutant, with no change in protein levels over the time course (Fig. 6.4., B & C). Collectively these findings demonstrate that the P74A alone can recapitulate the increase in Sss1 protein levels, yet the two individual mutations of *sss1-6* must be combined to impart the growth defect that has been associated to dysregulated translocon gating.

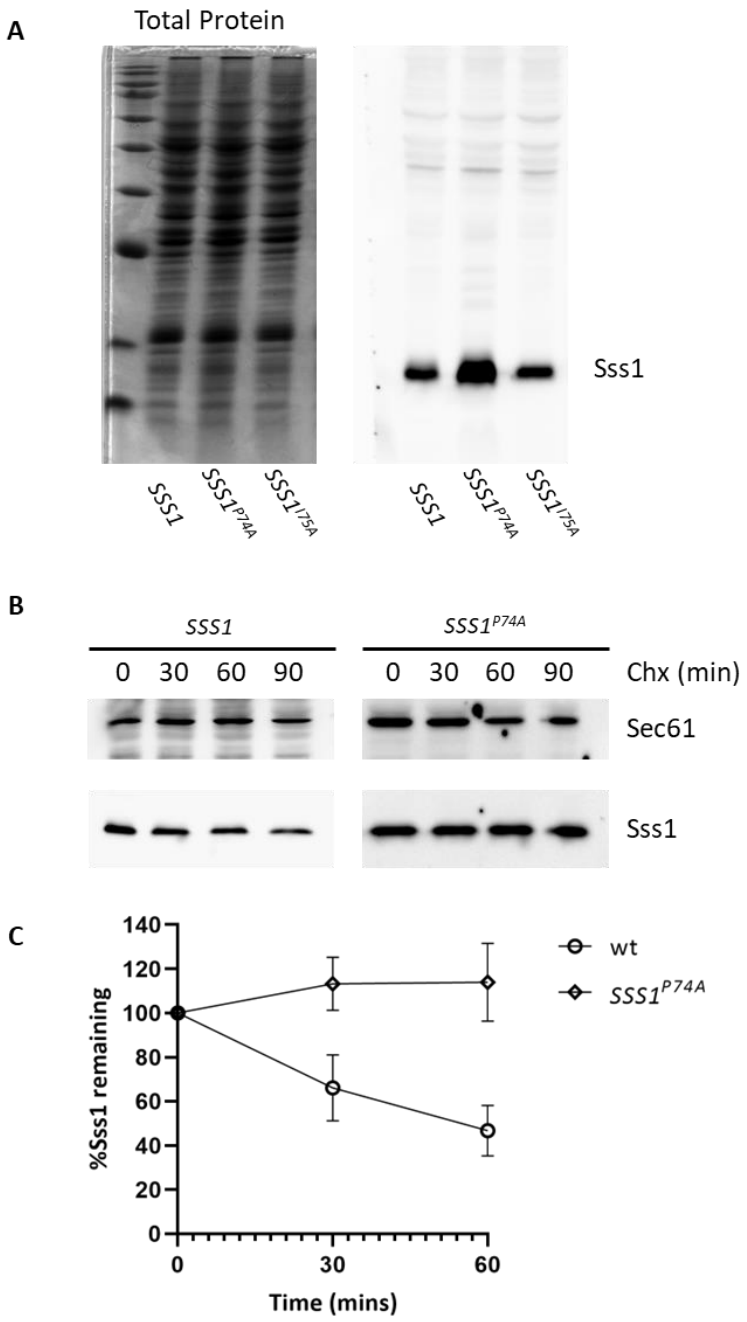

Fig. 6.4. Characterisation of the P74A mutant finds it responsible for the accumulation of Sss1 protein observed within *sss1-6*. (A) Cell extracts derived from BWY530 cells transformed with either WT Sss1 (pJKB2), *SSS1*^{P74A} or *SSS1*^{I75A} were immunoblotted with anti-Sss1 antibodies. **(B)** Cells were pre-treated for 10 minutes with 0.25 mg/mL chx. Afterwards cells were removed at the indicated times and were immunoblotted with anti-Sss1 or anti-Sec61 antibodies. **(C)** Densitometric analysis of **(B)** using Image lab software.

Sss1 is a Quantity Control Substrate Degraded by Three E3 Ligase Complexes

Sss1 is an integral membrane protein therefore it was intriguing to find it relatively labile during the chx chase experiments. As an essential component of both the Sec61 and the Ssh1 complexes, we considered the possibility that Sss1 protein levels are stabilised by its interaction with these binding partners. To determine this, we investigated Sss1 turnover in PRY14 (*ssh1Δ::kanMX4, HIS3-pMET3-SEC61*) cells grown in the presence or absence of methionine. In these cells the *SSH1* gene has been deleted (*ssh1Δ*) and *SEC61* expression is under the control of the *MET3* promoter that is transcriptionally repressed in cells grown in the presence of methionine. The Sss1 degradation profile in methionine restricted PRY14 cells resembled that observed in WT cells ($t_{½}$ ≈ 45 min). In contrast, the rate of Sss1 degradation was enhanced 3-fold upon repressed *SEC61* expression ($t_{½}$ ≈ 15 min) (Fig. 6.3., C & D). This confirmed that Sss1 is stabilised by its interactions with Sec61 and Ssh1. We therefore propose that Sss1 requires interactions with its binding partners to stabilise and avoid degradation.

Sss1 is an ER-localised TA protein and as such quality control is regulated via ERAD. *HRD1* and *DOA10* encode for the prominent major ER resident E3 ligases Hrd1 and Doa10 in yeast (14, 30, 48). As Sss1-6 protein levels accumulate due to increased stability we expected to observe a similar outcome in strains containing a knockout to the involved ERAD pathways. Initial analysis was performed in *S288C* genetic background due to availability at the time. Contrast to expectation, immunoblotting for Sss1 in BY4742, *hrd1Δ* and *doa10Δ* found no difference in protein stability between each of the strains (Fig. 6.5., B - D). To emphasise any accumulation that could be occurring from a potential lack in regulation, we opted to blot for Sss1 within the same base strains, yet were made to overexpress Sss1 via transformation with the 2-micron YEp plasmid FKp53. In this setting BY4742 had no observable differences in protein expression. However, upon over-expression of Sss1, *hrd1Δ* and to a lesser extent *doa10Δ*, did demonstrate an increase in Sss1 protein level (Fig. 6.5., B – D). We were able to further investigate the role of the HRD1 complex through the same assay with several components of the complex including Usa1, Der1, and the more universally present, Ubc7. Expression of the FKp53 plasmid in

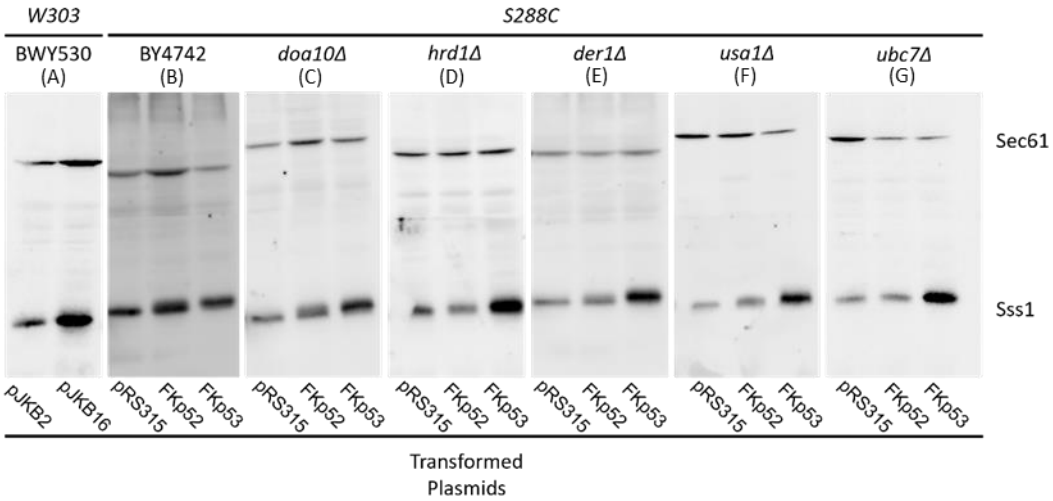

Fig. 6.5. Sss1 protein accumulates in knockouts for certain ERAD pathway components. Cell extracts derived from BWY530 cells of the *W303* background that were transformed with either YCp Sss1 (pJKB2) or pJKB16 along with WT (BY4742) *doa10Δ, hrd1Δ*, *der1Δ, usa1Δ* and *ubc7Δ* cells of the *S288C* background expressing were immunoblotted with anti-Sss1 or anti-Sec61 antibodies. The *S288C* background were all transformed with either empty vector (pRS316), YCp Sss1 (FKp52) or YEp Sss1 (FKp53).

all the tested components to the HRD1 complex demonstrated an increase in Sss1 protein that was absent in the BY4742 control (Fig. 6.5., E - G), heavily implicating Hrd1 as the major ERAD pathway involved in the degradation of Sss1.

Protein levels in the ERAD knockout strains never reached what was observed in *sss1-6*, and the need to overexpress Sss1 to observe any similarity was troubling. The *sss1-6* mutant is of the *W303* genetic background which has approximately 9700 nucleotide distinctions to *S288C* with differences across ~700 genes (49). Due to this disparity we opted to generate *W303* ERAD knockouts using the BWY530t strain (*sss1Δ::TRP1* FKp53). At this time the involvement of the ASI complex in recognising orphan subunits had come to light, and with Sss1 stability showing reliance on association to binding partners, the potential for involvement of the ASI pathway was promising. Three Knockout cassettes were generated by PCR; *hrd1Δ::KanMX6, doa10Δ::KanMX6, and asi1Δ::KanMX6*. This was approached using primers with 5' flanking regions homologous to the genes of interest and 3' regions designed to amplify the *KanMX6* gene from the pFA6a plasmid.

Successful knockouts for each ERAD pathway were generated in the BWY530t strain. Additionally, select lysine residues are known to be important during ERAD as conventional acceptors of ubiquitin. Therefore, we complemented our investigation of the ERAD pathways via generating an Sss1 mutant deficient in this process, being that of $SSS1^{K20R,\ K38R}$. $SSS1^{K20R,\ K38R}$ impacts upon ubiquitinylated lysine residues that were previously identified via a global ubiquitination proteomics screen (50). Immunoblot analysis of $SSS1^{K20R,\ K38R}$ in addition to each of the BWY530t derived ERAD knockouts revealed no substantial change in Sss1 protein levels when compared to the WT strain (data not shown). This finding was in opposition to what we had previously found in respects to the *hrd1Δ* and *doa10Δ* strains of the *S288C* background. Chx chase analysis was therefore used to determine the true extent by which any of these ERAD pathways may be influencing Sss1 protein stability. As expected, Sss1 turnover in BWY530t cells was comparable with previous findings ($t_{½}$ ≈ 45 min) (Fig. 6.6., A & B). In contrast, Sss1 levels of all E3 ligase knockouts being *hrd1Δ, doa10Δ* and *asi1Δ* appeared to demonstrate increased stability of Sss1 protein to varying extents throughout the 90-minute chase ($t_{½}$ ≈ 253 min, $t_{½}$ ≈ 204

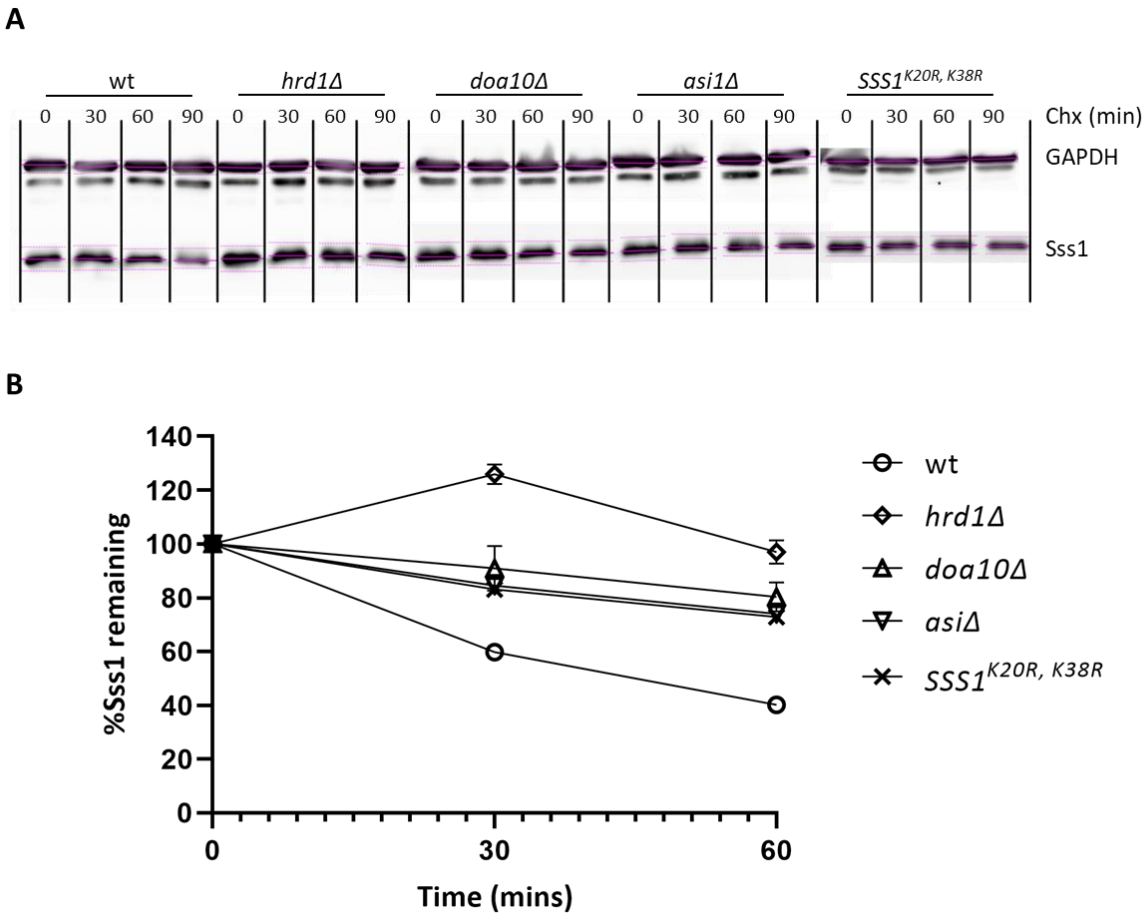

Fig. 6.6. Characterisation of Sss1 degradation pathways by chx chase of ERAD defective strains. (A) WT, *hrd1Δ, doa10Δ, asi1Δ* and *SSS1*$^{K20R, K38R}$ Cells were pre-treated for 10 minutes with 0.25 mg/mL chx. Afterwards cells were removed at the indicated times and were immunoblotted with anti-Sss1 or anti-GAPDH antibodies. **(B)** Densitometric analysis of **(A)** using Image lab software. The pink banding demonstrates the gating strategy for band identification as part of the densitometry.

min and $t_{½}$ ≈ 156 min respectively) (Fig. 6.6., A & B). *SSS1*$^{K20R, K38R}$ also demonstrated increased stability of Sss1 during the chase with a notably similar half-life to that which we had observed in the *asi1Δ* strain ($t_{½}$ ≈ 144 min) (Fig. 6.6., A & B). Taken together, these results show that Sss1 is a tightly regulated quantity control substrate that is degraded by all the major E3 ligases complexes at the ER.

PPIs Appear to Coordinate ERAD for the Essential Translocon Component Sss1

Approximately 5.2% of all peptide bonds that precede a proline are found in the cis conformation (51-53). As the proline residue was responsible for the Sss1 protein accumulation in *sss1-6*, we suspected that we had perturbed a potential cis-trans isomerisation event in the protein. Cis-trans isomerisation is a rate limiting step during protein folding that is catalysed by the PPI family of enzymes. The individual families of PPIs are highly conserved and named after the drugs they have been demonstrated to bind. Of interest to our study were the FK506-sensitive proline rotamases (FPR) and the Cyclosporin-sensitive proline rotamases (CPR) (54, 55). To assess whether PPIs were responsible in facilitating the degradation of Sss1, we treated BWY530 cells with either 50 ug/mL of FK506 or cyclosporine A (CsA). Cells treated with FK506 showed a marginal increase in protein stability ($t_{½}$ ≈ 54 min) (Fig. 6.7., A & B). Treatment with CsA on the other hand, demonstrated significant stability in Sss1 protein ($t_{½}$ ≈ 248 min) (Fig. 6.7., A & B) and hence provided more promise for the CPR family of PPIs in having a role in Sss1 degradation.

The mammalian cyclophilin, CyPB, functions within the secretory pathway and has been previously implicated in regulating ER quality control (56, 57). As there was strong evidence for the notion of CPRs in regulating quality control processes we decided to begin our investigations with the ER resident target of CsA, Cpr5. We created the knockout strain, BWY530t *cpr5Δ* (*cpr5Δ::KanMX6* + *sss1Δ::TRP1*), and put it through the same analysis previously done when probing the ERAD pathways. Immunoblotting revealed no elevation of Sss1 protein in the *cpr5Δ* strain when compared to WT BWY530. Still, the chx chase data illustrates an ability for the *cpr5Δ* strain to increase the stability of Sss1 to some extent throughout the 90-

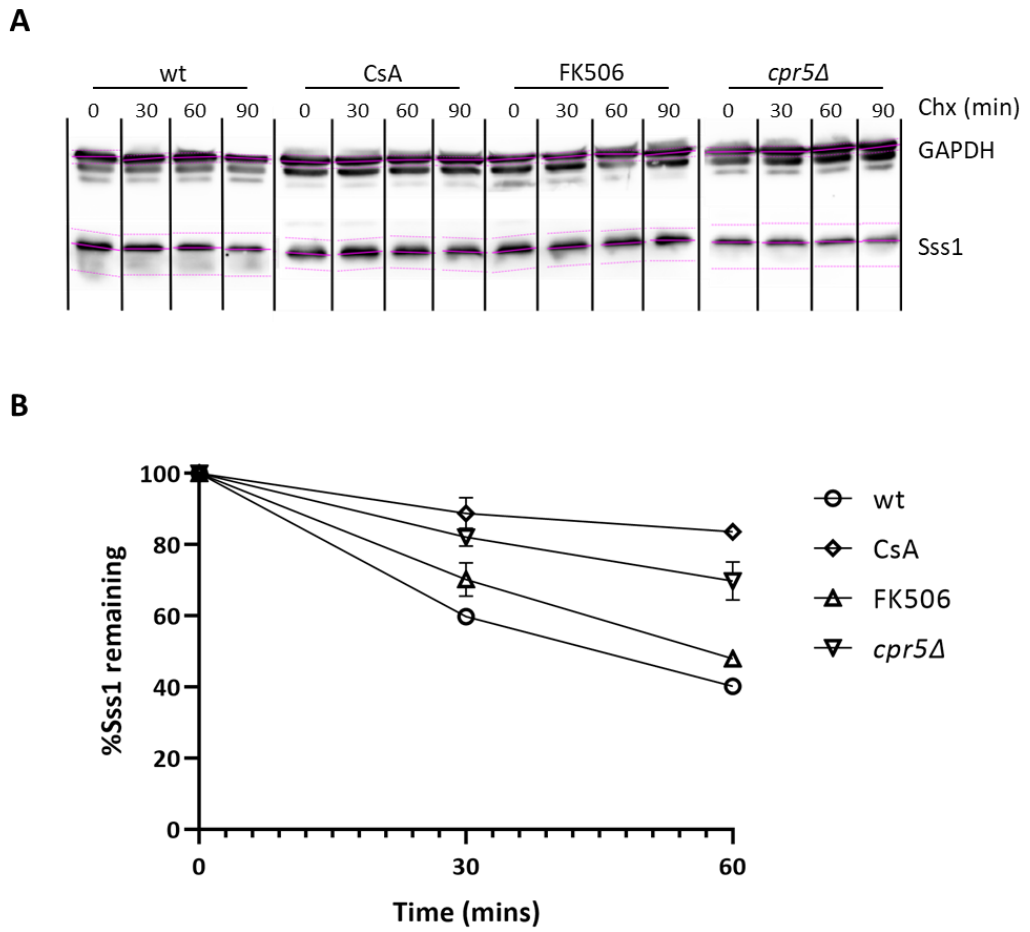

Fig. 6.7. Sss1 quality control is influenced via the action of cyclophilins. (A) WT, *cpr5Δ* and cells pre-treated with 50 ug/mL of either CsA or FK506 for 4.5 hrs were then treated for 10 minutes with 0.25 mg/mL chx. Afterwards cells were removed at the indicated times and were immunoblotted with anti-Sss1 or anti-GAPDH antibodies. **(B)** Densitometric analysis of **(A)** using Image lab software. The pink banding demonstrates the gating strategy for band identification as part of the densitometry.

mintute time course ($t_{½}$ ≈ 105 min) as opposed to the BWY530 WT cells ($t_{½}$ ≈ 43 min) (Fig. 6.7., A & B). As *cpr5Δ* does not recapitulate our findings upon treatment with CsA we suggest that it is not solely responsible in regulating Sss1 protein abundance. Our collective data is the first however to report that ER resident PPIs are involved in regulating the degradation of Sss1.

Discussion

Sss1 is an essential subunit of the Sec61 translocon with an established importance in stabilising the complex and, as we have previously discovered, regulating conformational dynamics (58, 59). The stability of protein subunits is often dictated through their association with key binding partners, with un-complexed proteins found to become rapidly degraded (33, 60). We found Sss1 to fall under such a mechanism for regulation, with the half-life of Sss1 becoming reduced significantly when neither the major pore forming subunit, Sec61 nor the paralog Ssh1 are present (Fig. 6.3., C). As to why such a level of regulation may be necessary, is that an accumulation of Sss1 may be deleterious to cellular physiology. However, we found that over-expression of Sss1 with a 2-micron yeast episomal plasmid had no observable impact on growth at normal or elevated temperatures, where the later imparts a greater demand on cells as metabolism is increased (Fig. 6.2., B). While over-expression by itself does not present with a TS phenotype this does not rule out that accumulation of Sss1 is deleterious to cell growth under exposure to certain stimuli. In-fact we found that the TS *sss1-6* mutant to accumulate Sss1 protein levels (Fig. 6.2., A). The TS growth defect of *sss1-6* was previously characterised as an outcome of dysregulated translocon gating dynamics, specifically that which facilitates an uncontrolled flux of metabolites across the translocon. A mechanism has yet to be attributed to the dysregulation observed in *sss1-6*, therefore we hypothesised that the increased accumulation of Sss1 protein contributes to the TS defect and represents a scenario where accumulation can be deleterious to cells.

We had initially thought that supply of Sss1 may be synonymous with the formation of translocon complexes, where increased channel formation exaggerates the facilitated flux of metabolites that can usually occur. The fact that overexpression of Sss1 by itself does not similarly present with a TS growth defect would suggest that this is not the case. It is worth noting however, that while the end result is the same, the accumulation observed between Sss1 overexpression and *sss1-6* does differ mechanistically. We have now characterised the accumulation in *sss1-6* to be that of increased protein stability. Following this discovery, we surmised that the ability of Sss1 to evade degradation may be necessary to achieve the observed defects to translocon dynamics. To complicate things however, both the *SSS1-3* mutant and the isolated *SSS1*^{P74A} single mutant of *sss1-6* were also found to increase the stability of Sss1 protein and yet do not replicate the TS growth defect.

If stability alone is insufficient in recapitulating the TS growth defect perhaps the very structure of the Sss1-6 protein is being perturbed. The P74 and I75 residues contribute to the extensive hydrophobicity that constitutes the TM anchor of Sss1. While we cannot completely rule out the potential for perturbations to the hydrophobicity of this region in effecting all potential Sss1 protein interactions, we do find Sss1 to assemble into the appropriate complexes for both co- and post-translational translocation as demonstrated by our collective characterisation included in chapter 3. The potential for the *sss1-6* mutation in impacting Sss1 integration within the lipid bilayer of the ER also seems unlikely as demonstrated with our previous kyte-doolittle analysis (Supp. Fig. S3.1., Chapter 3 Manuscript). We instead propose that the stability of Sss1 must be in tandem with a secondary mechanism that contributes to defects at the translocon. The synergistic effect between two such mechanisms could be foreseen as an increase in the formation of defective complexes and hence acts to exacerbate the localised issues at the translocon. Alternatively, Sss1 accumulation may in its own right impart a level of cellular stress that becomes deleterious in combination to other broad effects on cellular homeostasis. Future work is aimed to fully characterise these outcomes in the hopes of fully understanding the contributions that the Sss1 accumulation makes to the growth defect of *sss1-6*.

The chx chase analysis suggests that Sss1 protein is regulated via all major resident E3 ligases in yeast (Fig. 6.6., A & B). The HRD1 complex appears to be the predominant pathway for Sss1 degradation, with protein levels observed to have the greatest stability in the *hrd1Δ* strain. Furthermore, only in all of our BY4742 knockouts of the HRD1 complex specific components did we observe a consistent accumulation in Sss1 protein levels, offering additional plausibility to the previous statement (Fig. 6.5.). It was surprising to find that the DOA10 complex could also regulate the degradation kinetics of Sss1 and may represent a level of redundancy or cooperation that exists between the two peripherally located E3 ligases. A more expected outcome was the further involvement of the ASI complex. Located at the INM, the ASI complex is found to recognise orphan subunits that, upon failing to bind their key interacting partners, mis-localise to the INM for subsequent degradation (41-44). Through this established role we assume that the ASI complex similarly regulates Sss1 protein by clearing un-complexed subunits and therefore prevents their unwanted accumulation.

The ability of the *hrd1Δ* and *doa10Δ* strains to stabilise beyond that seen in the double lysine mutant ($SSS1^{K20R,\ K38R}$) would also suggest that these pathways work to degrade Sss1 by a manner that may potentially require ubiquitination at additional sites to those that have already been described in other studies. Other lysine residues are present within the Sss1 sequence, yet only K20 and K38 have been found to undergo ubiquitination thus far. It is also worth noting that the literature contains several instances of atypical ubiquitination of ER resident substrates. One relevant example includes the third component to the Sec61 translocon, Sbh1, which has been described to be degraded via the DOA10 complex independently from its cytosolic lysine residues (61). Furthermore, both threonine and Serine have been implicated as atypical ubiquitination sites in proteins and therefore further investigation into the ubiquitination profile of Sss1 is warranted (62, 63).

We have characterised the protein stabilisation of the *sss1-6* mutation, or more specifically, $SSS1^{P74A}$, to be the result of a disruption to the degron of Sss1. The *SSS1-3* mutant also appears to stabilise Sss1 protein levels, albeit to a lesser extent,

implicating two regions of the K_{69}LIHIPI_{75} motif in regulating the degradation of Sss1. Sss1 protein has been described here to proceed via multiple E3 ligase complexes as part of its regulated degradation. Therefore, we are left to speculate on whether the stability of the separate *SSS1-3* and *sss1-6* mutants represent two distinct sites for recognition via differing E3 ligase complexes or alternatively whether the entirety of the K_{69}LIHIPI_{75} motif is necessary for efficient association of the degron to the relevant E3 ligase complex. The P74 residue however does appear key in regulating the Sss1 degron as substitution of the proline to alanine alone is sufficient to recapitulate the observed protein accumulation.

Our analysis also suggests the involvement of cis/trans isomerisation in regulating Sss1 degradation as both treatment with the immunosuppressant, CsA and the knockout of a CsA target, the cyclophilin, Cpr5 demonstrated increased stability of Sss1 protein (Fig. 6.7., A & B). We therefore suggest that Sss1 undergoes cis/trans isomerisation at the amide bond between I73 and P74, with interconversion between the two isomers dictating protein stability. While Cpr5 demonstrates increased stability of Sss1 during the chx chase assay, we find that it does not reflect our observations in cells treated with CsA. We chose to begin our investigation into the role played by cyclophilins with Cpr5, as of all the yeast cyclophilins, it demonstrates conservation between studied yeast species (64). Furthermore, while both Cpr2 and Crp4 are also implicated to have action within the secretory pathway, Cpr5 is unique in that it presents with a HDEL targeting sequence that ensures it remains within the ER and thus specific to this domain (64, 65). Therefore, should CsA treatment be truly reflective of perturbed cis/trans isomerise activity as the causative factor in the observed stability of Sss1 protein, we would expect the comparatively limited contributions of Cpr5 to only part of a larger regulatory mechanism. Future work should hence assess the contributions of the other cyclophilins. Yeast strains containing knockouts for all the characterised cyclophilins is found to remain viable and therefore should be useful in characterising the impact that they have on Sss1 stability while additionally avoiding the potential for compensation between the individual components (66).

The effects we observe through the action of CsA may not be totally conclusive for sequestering cyclophilin activity. The drug-ligand complexes that form following treatment with an immunophilin (i.e. Cpr-CsA) have been found to interact with and inhibit additional cellular pathways. One such example is that with calcineurin where phosphatase activity is found to become diminished upon treatment with CsA and may represent an indirect mechanism for CsA to influence Sss1 (67-72). Treatment with FK506 can similarly complex with FKBPs to inhibit calcineurin, and as we saw very limited stability when cells were treated with FK506 during our chx chase analysis, it is unlikely that such mechanism is involved in this instance. However, it will still be important for future work to not only identify any and all contributing cyclophilins but perhaps also to perform mutagenesis at their active sites to fully establish their isomerise activity in regulating Sss1 stability.

The implication for PPI catalysed interconversion of cis/trans isomers in regulating protein degradation has seen some recent traction offering additional plausibility to our observations. Previous work in mammalian cells has demonstrated that CyPB, a mammalian cyclophilin resident to the secretory pathway, regulates the degradation of ERAD-L substrates (56). This work related these findings to the degradation of certain soluble proteins localised to the ER lumen. Their assessment of a membrane tethered splice variant however, was found to evade this level of regulation which would suggest that this phenomenon was exclusive to certain ER soluble proteins. Our work would disagree with this assessment, finding the degradation of the membrane bound Sss1 to be influenced by both CsA and Cpr5. It is such that we propose that this work has identified a novel class of degron, where recognition of ERAD-M substrate can be modulated by the action of PPIs.

One question that remains is how the interconversion of cis/trans isomers might dictate protein stability. One common thought in the literature is that the conversion between the two isomers may disrupt turns that are otherwise un-favourable when removing proteins from the ER membrane (56, 73, 74). Such a mechanism has been implied to be important in facilitating protein processing via the HRD1 complex, as CyPB has been found to interact with this pathway, indicating a relationship between the E3 ligase complex and CyPs (56, 75). This became of

particular interest to us as we found the ability of CsA to influence Sss1 protein stability was comparable to that of the *hrd1Δ* strain which may suggest that interconversion between the cis/trans isomers of Sss1 is important in regulating its degradation via the HRD1 complex. It is worth noting that action of PPIs in regulating the degradation of Sss1 may represent a general form of recognition by all contributing E3 ligase complexes and therefore future work aims to identify the relevant pathways with the HRD1 complex posed as a key candidate in these investigations.

Accumulation of mis-folded/localised proteins at the ER contributes a significant burden to cells and can be associated to various disease states such as tumour growth and degenerative diseases (76-78). Here, we have established the essential subunit to the translocon, Sss1, to be a highly regulated quantity control substrate regulated via a coordinated response from the collective ERAD pathways of yeast. We propose that Sss1 is predominantly degraded via the HRD1 complex in a manner that appears to require additional ubiquitination sites to the lysine residues that had been previously characterised in the literature. Furthermore, Doa10 appears to also be involved, whether as a cooperative or compensatory mechanism remains to be decided, however this outcome does highlight a potential redundancy that exists between these two E3 ligases. Sss1 that fails to interact with a key interacting partner to form a stable translocon complex will instead mis-localise to the INM where it will be targeted for degradation via the ASI complex; the action of may be dependent on the presence of the aforementioned lysine residues. Finally, the abundance of Sss1 appears to be regulated via the action of ER resident cyclophilins, with Cpr5 being the first to demonstrate any role in this process. This highly involved approach from all three analysed E3 ligases in regulating protein levels of Sss1 begins to elude a need for cells to tightly control the availability of the subunit and may be indicative of the role Sss1 accumulation can have in dyshomeostasis and disease.

References

1. Printsev I, Curiel D, Carraway KL, 3rd. Membrane Protein Quantity Control at the Endoplasmic Reticulum. The Journal of membrane biology. 2017;250(4):379-92.
2. Ruggiano A, Foresti O, Carvalho P. Quality control: ER-associated degradation: protein quality control and beyond. The Journal of cell biology. 2014;204(6):869-79.
3. Varshavsky A. Naming a targeting signal. Cell. 1991;64(1):13-5.
4. Varshavsky A. N-degron and C-degron pathways of protein degradation. 2019;116(2):358-66.
5. Christianson JC, Carvalho P. Order through destruction: how ER-associated protein degradation contributes to organelle homeostasis. The EMBO journal. 2022;41(6):e109845.
6. Krshnan L, van de Weijer ML, Carvalho P. Endoplasmic Reticulum–Associated Protein Degradation. 2022;14(12).
7. Carvalho P, Goder V, Rapoport TA. Distinct ubiquitin-ligase complexes define convergent pathways for the degradation of ER proteins. Cell. 2006;126(2):361-73.
8. Taxis C, Hitt R, Park SH, Deak PM, Kostova Z, Wolf DH. Use of modular substrates demonstrates mechanistic diversity and reveals differences in chaperone requirement of ERAD. The Journal of biological chemistry. 2003;278(38):35903-13.
9. Vashist S, Ng DT. Misfolded proteins are sorted by a sequential checkpoint mechanism of ER quality control. The Journal of cell biology. 2004;165(1):41-52.
10. Pickart CM. Mechanisms underlying ubiquitination. Annual review of biochemistry. 2001;70:503-33.
11. Koch B, Yu HG. Regulation of inner nuclear membrane associated protein degradation. Nucleus (Austin, Tex). 2019;10(1):169-80.
12. Reiss Y, Heller H, Hershko A. Binding sites of ubiquitin-protein ligase. Binding of ubiquitin-protein conjugates and of ubiquitin-carrier protein. The Journal of biological chemistry. 1989;264(18):10378-83.
13. Bays NW, Gardner RG, Seelig LP, Joazeiro CA, Hampton RY. Hrd1p/Der3p is a membrane-anchored ubiquitin ligase required for ER-associated degradation. Nat Cell Biol. 2001;3(1):24-9.
14. Bordallo J, Plemper RK, Finger A, Wolf DH. Der3p/Hrd1p is required for endoplasmic reticulum-associated degradation of misfolded lumenal and integral membrane proteins. Molecular biology of the cell. 1998;9(1):209-22.
15. Wu X, Rapoport TA. Mechanistic insights into ER-associated protein degradation. Current opinion in cell biology. 2018;53:22-8.
16. Denic V, Quan EM, Weissman JS. A luminal surveillance complex that selects misfolded glycoproteins for ER-associated degradation. Cell. 2006;126(2):349-59.
17. Gauss R, Jarosch E, Sommer T, Hirsch C. A complex of Yos9p and the HRD ligase integrates endoplasmic reticulum quality control into the degradation machinery. Nat Cell Biol. 2006;8(8):849-54.
18. Clerc S, Hirsch C, Oggier DM, Deprez P, Jakob C, Sommer T, et al. Htm1 protein generates the N-glycan signal for glycoprotein degradation in the endoplasmic reticulum. The Journal of cell biology. 2009;184(1):159-72.
19. Jakob CA, Bodmer D, Spirig U, Battig P, Marcil A, Dignard D, et al. Htm1p, a mannosidase-like protein, is involved in glycoprotein degradation in yeast. EMBO Rep. 2001;2(5):423-30.
20. Quan EM, Kamiya Y, Kamiya D, Denic V, Weibezahn J, Kato K, et al. Defining the glycan destruction signal for endoplasmic reticulum-associated degradation. Mol Cell. 2008;32(6):870-7.

21. Xie W, Kanehara K, Sayeed A, Ng DT. Intrinsic conformational determinants signal protein misfolding to the Hrd1/Htm1 endoplasmic reticulum-associated degradation system. Molecular biology of the cell. 2009;20(14):3317-29.
22. Carvalho P, Stanley AM, Rapoport TA. Retrotranslocation of a misfolded luminal ER protein by the ubiquitin-ligase Hrd1p. Cell. 2010;143(4):579-91.
23. Wu X, Siggel M, Ovchinnikov S, Mi W, Svetlov V, Nudler E, et al. Structural basis of ER-associated protein degradation mediated by the Hrd1 ubiquitin ligase complex. Science. 2020;368(6489).
24. Baldridge RD, Rapoport TA. Autoubiquitination of the Hrd1 Ligase Triggers Protein Retrotranslocation in ERAD. Cell. 2016;166(2):394-407.
25. Stein A, Ruggiano A, Carvalho P, Rapoport TA. Key steps in ERAD of luminal ER proteins reconstituted with purified components. Cell. 2014;158(6):1375-88.
26. Bodnar NO, Rapoport TA. Molecular Mechanism of Substrate Processing by the Cdc48 ATPase Complex. Cell. 2017;169(4):722-35.e9.
27. Lopata A, Kniss A, Löhr F, Rogov VV, Dötsch V. Ubiquitination in the ERAD Process. International journal of molecular sciences. 2020;21(15).
28. Neal S, Jaeger PA, Duttke SH, Benner C, C KG, Ideker T, et al. The Dfm1 Derlin Is Required for ERAD Retrotranslocation of Integral Membrane Proteins. Mol Cell. 2018;69(2):306-20.e4.
29. Nejatfard A, Wauer N, Bhaduri S, Conn A, Gourkanti S, Singh N, et al. Derlin rhomboid pseudoproteases employ substrate engagement and lipid distortion to enable the retrotranslocation of ERAD membrane substrates. Cell Reports. 2021;37(3):109840.
30. Hampton RY, Gardner RG, Rine J. Role of 26S proteasome and HRD genes in the degradation of 3-hydroxy-3-methylglutaryl-CoA reductase, an integral endoplasmic reticulum membrane protein. Molecular biology of the cell. 1996;7(12):2029-44.
31. Basson ME, Thorsness M, Rine J. Saccharomyces cerevisiae contains two functional genes encoding 3-hydroxy-3-methylglutaryl-coenzyme A reductase. Proceedings of the National Academy of Sciences of the United States of America. 1986;83(15):5563-7.
32. Swanson R, Locher M, Hochstrasser M. A conserved ubiquitin ligase of the nuclear envelope/endoplasmic reticulum that functions in both ER-associated and Matα2 repressor degradation. 2001;15(20):2660-74.
33. Habeck G, Ebner FA, Shimada-Kreft H, Kreft SG. The yeast ERAD-C ubiquitin ligase Doa10 recognizes an intramembrane degron. The Journal of cell biology. 2015;209(2):261-73.
34. Kreft SG, Wang L, Hochstrasser M. Membrane topology of the yeast endoplasmic reticulum-localized ubiquitin ligase Doa10 and comparison with its human ortholog TEB4 (MARCH-VI). The Journal of biological chemistry. 2006;281(8):4646-53.
35. Mehrtash AB, Hochstrasser M. Elements of the ERAD ubiquitin ligase Doa10 regulating sequential poly-ubiquitylation of its targets. iScience. 2022;25(11):105351.
36. Zattas D, Berk JM, Kreft SG, Hochstrasser M. A Conserved C-terminal Element in the Yeast Doa10 and Human MARCH6 Ubiquitin Ligases Required for Selective Substrate Degradation *. Journal of Biological Chemistry. 2016;291(23):12105-18.
37. Wang X, Herr RA, Rabelink M, Hoeben RC, Wiertz EJHJ, Hansen TH. Ube2j2 ubiquitinates hydroxylated amino acids on ER-associated degradation substrates. Journal of Cell Biology. 2009;187(5):655-68.
38. Jandrositz A, Turnowsky F, Högenauer G. The gene encoding squalene epoxidase from Saccharomyces cerevisiae: cloning and characterization. Gene. 1991;107(1):155-60.
39. Foresti O, Ruggiano A, Hannibal-Bach HK, Ejsing CS, Carvalho P. Sterol homeostasis requires regulated degradation of squalene monooxygenase by the ubiquitin ligase Doa10/Teb4. eLife. 2013;2:e00953.

40. Khmelinskii A, Blaszczak E, Pantazopoulou M, Fischer B, Omnus DJ, Le Dez G, et al. Protein quality control at the inner nuclear membrane. Nature. 2014;516(7531):410-3.
41. Foresti O, Rodriguez-Vaello V, Funaya C, Carvalho P. Quality control of inner nuclear membrane proteins by the Asi complex. Science. 2014;346(6210):751-5.
42. Natarajan N, Foresti O, Wendrich K, Stein A, Carvalho P. Quality Control of Protein Complex Assembly by a Transmembrane Recognition Factor. Molecular Cell. 2020;77(1):108-19.e9.
43. DeBose-Boyd RA. A Helping Hand for Cytochrome P450 Enzymes. Cell Metabolism. 2007;5(2):81-3.
44. Hughes AL, Powell DW, Bard M, Eckstein J, Barbuch R, Link AJ, et al. Dap1/PGRMC1 Binds and Regulates Cytochrome P450 Enzymes. Cell Metabolism. 2007;5(2):143-9.
45. Garreau de Loubresse N, Prokhorova I, Holtkamp W, Rodnina MV, Yusupova G, Yusupov M. Structural basis for the inhibition of the eukaryotic ribosome. Nature. 2014;513(7519):517-22.
46. Schneider-Poetsch T, Ju J, Eyler DE, Dang Y, Bhat S, Merrick WC, et al. Inhibition of eukaryotic translation elongation by cycloheximide and lactimidomycin. Nature chemical biology. 2010;6(3):209-17.
47. Christiano R, Nagaraj N, Fröhlich F, Walther TC. Global proteome turnover analyses of the Yeasts S. cerevisiae and S. pombe. Cell Rep. 2014;9(5):1959-65.
48. Swanson R, Locher M, Hochstrasser M. A conserved ubiquitin ligase of the nuclear envelope/endoplasmic reticulum that functions in both ER-associated and Matalpha2 repressor degradation. Genes Dev. 2001;15(20):2660-74.
49. Matheson K, Parsons L, Gammie A. Whole-Genome Sequence and Variant Analysis of W303, a Widely-Used Strain of Saccharomyces cerevisiae. G3 (Bethesda). 2017;7(7):2219-26.
50. Swaney DL, Beltrao P, Starita L, Guo A, Rush J, Fields S, et al. Global analysis of phosphorylation and ubiquitylation cross-talk in protein degradation. Nature methods. 2013;10(7):676-82.
51. Weiss MS, Jabs A, Hilgenfeld R. Peptide bonds revisited. Nature structural biology. 1998;5(8):676.
52. Craveur P, Joseph AP, Poulain P, de Brevern AG, Rebehmed J. Cis-trans isomerization of omega dihedrals in proteins. Amino acids. 2013;45(2):279-89.
53. Zhan YA, Ytreberg FM. The cis conformation of proline leads to weaker binding of a p53 peptide to MDM2 compared to trans. Arch Biochem Biophys. 2015;575:22-9.
54. Heitman J, Movva NR, Hiestand PC, Hall MN. FK 506-binding protein proline rotamase is a target for the immunosuppressive agent FK 506 in Saccharomyces cerevisiae. Proceedings of the National Academy of Sciences of the United States of America. 1991;88(5):1948-52.
55. Singh-Babak SD, Shekhar T, Smith AM, Giaever G, Nislow C, Cowen LE. A novel calcineurin-independent activity of cyclosporin A in Saccharomyces cerevisiae. Molecular bioSystems. 2012;8(10):2575-84.
56. Bernasconi R, Soldà T, Galli C, Pertel T, Luban J, Molinari M. Cyclosporine A-Sensitive, Cyclophilin B-Dependent Endoplasmic Reticulum-Associated Degradation. PLOS ONE. 2010;5(9):e13008.
57. Price ER, Zydowsky LD, Jin MJ, Baker CH, McKeon FD, Walsh CT. Human cyclophilin B: a second cyclophilin gene encodes a peptidyl-prolyl isomerase with a signal sequence. 1991;88(5):1903-7.
58. Falcone D, Henderson MP, Nieuwland H, Coughlan CM, Brodsky JL, Andrews DW. Stability and function of the Sec61 translocation complex depends on the Sss1p tail-anchor sequence. The Biochemical journal. 2011;436(2):291-303.

59. Gemmer M, Chaillet ML, van Loenhout J, Cuevas Arenas R, Vismpas D, Gröllers-Mulderij M, et al. Visualization of translation and protein biogenesis at the ER membrane. Nature. 2023;614(7946):160-7.
60. Finke K, Plath K, Panzner S, Prehn S, Rapoport TA, Hartmann E, et al. A second trimeric complex containing homologs of the Sec61p complex functions in protein transport across the ER membrane of S. cerevisiae. The EMBO journal. 1996;15(7):1482-94.
61. Shyu P, Jr., Ng BSH, Ho N, Chaw R, Seah YL, Marvalim C, et al. Membrane phospholipid alteration causes chronic ER stress through early degradation of homeostatic ER-resident proteins. Sci Rep. 2019;9(1):8637-.
62. McClellan AJ, Laugesen SH, Ellgaard L. Cellular functions and molecular mechanisms of non-lysine ubiquitination. Open Biol. 2019;9(9):190147-.
63. Wang X, Herr RA, Chua WJ, Lybarger L, Wiertz EJ, Hansen TH. Ubiquitination of serine, threonine, or lysine residues on the cytoplasmic tail can induce ERAD of MHC-I by viral E3 ligase mK3. The Journal of cell biology. 2007;177(4):613-24.
64. Delic M, Valli M, Graf AB, Pfeffer M, Mattanovich D, Gasser B. The secretory pathway: exploring yeast diversity. FEMS Microbiology Reviews. 2013;37(6):872-914.
65. Dolinski K, Muir S, Cardenas M, Heitman J. All cyclophilins and FK506 binding proteins are, individually and collectively, dispensable for viability in Saccharomyces cerevisiae. Proceedings of the National Academy of Sciences of the United States of America. 1997;94(24):13093-8.
66. Dolinski K, Muir S, Cardenas M, Heitman J. All cyclophilins and FK506 binding proteins are, individually and collectively, dispensable for viability in Saccharomyces cerevisiae. Proceedings of the National Academy of Sciences of the United States of America. 1997;94(24):13093-8.
67. Breuder T, Hemenway CS, Movva NR, Cardenas ME, Heitman J. Calcineurin is essential in cyclosporin A- and FK506-sensitive yeast strains. Proceedings of the National Academy of Sciences of the United States of America. 1994;91(12):5372-6.
68. Foor F, Parent SA, Morin N, Dahl AM, Ramadan N, Chrebet G, et al. Calcineurin mediates inhibition by FK506 and cyclosporin of recovery from alpha-factor arrest in yeast. Nature. 1992;360(6405):682-4.
69. Liu J, Albers MW, Wandless TJ, Luan S, Alberg DG, Belshaw PJ, et al. Inhibition of T cell signaling by immunophilin-ligand complexes correlates with loss of calcineurin phosphatase activity. Biochemistry. 1992;31(16):3896-901.
70. Liu J, Farmer JD, Jr., Lane WS, Friedman J, Weissman I, Schreiber SL. Calcineurin is a common target of cyclophilin-cyclosporin A and FKBP-FK506 complexes. Cell. 1991;66(4):807-15.
71. Walsh CT, Zydowsky LD, McKeon FD. Cyclosporin A, the cyclophilin class of peptidylprolyl isomerases, and blockade of T cell signal transduction. The Journal of biological chemistry. 1992;267(19):13115-8.
72. Wang P, Heitman J. The cyclophilins. Genome Biol. 2005;6(7):226-.
73. Bernasconi R, Molinari M. ERAD and ERAD tuning: disposal of cargo and of ERAD regulators from the mammalian ER. Current opinion in cell biology. 2011;23(2):176-83.
74. Määttänen P, Gehring K, Bergeron JJM, Thomas DY. Protein quality control in the ER: The recognition of misfolded proteins. Seminars in Cell & Developmental Biology. 2010;21(5):500-11.
75. Christianson JC, Shaler TA, Tyler RE, Kopito RR. OS-9 and GRP94 deliver mutant α1-antitrypsin to the Hrd1–SEL1L ubiquitin ligase complex for ERAD. Nature Cell Biology. 2008;10(3):272-82.
76. Qi L, Tsai B, Arvan P. New Insights into the Physiological Role of Endoplasmic Reticulum-Associated Degradation. Trends in cell biology. 2017;27(6):430-40.

77. Hetz C. The unfolded protein response: controlling cell fate decisions under ER stress and beyond. Nat Rev Mol Cell Biol. 2012;13(2):89-102.
78. Sha H, He Y, Yang L, Qi L. Stressed out about obesity: IRE1α-XBP1 in metabolic disorders. Trends in endocrinology and metabolism: TEM. 2011;22(9):374-81.

Chapter 6

Concluding Remarks

The Complexity of Regulating Translocon Dynamics

The endoplasmic reticulum is a highly efficient organelle within eukaryotic cells, capable of processing approximately one third of the cellular proteome (1). This is achieved through the establishment of a unique lumenal environment that is critical in achieving post-translational events that determine protein maturation and localisation. Certain metabolites, including calcium and glutathione, contribute to the established lumenal environment and must be kept within an optimal range to maintain ER homeostasis (2-9). The usually tight control over metabolite balance is afforded a level of flexibility, allowing the ER to react to the changing needs of the cell (10-12). This is a coordinated effort from a range of ER receptors, channels and molecular chaperones. Of specific interest to this study was the involvement of the prominent protein import channel, the Sec61 translocon. When I had first endeavoured to take on this project, the importance in maintaining the integrity of the translocon to protect the ER environment had been well established. This concept was described through the mechanisms that gated the translocon and included aspects involving both the translocon machinery itself as well as interacting partners, such as the HSP70, Kar2, and the ribosome (13-16). Association of the interacting partners with translocon machinery is part of a coordinated response that first, initiates the timely transition between the two complex states and subsequently, the stabilisation of the respective state in a manner that maintains the integrity of the ER membrane. This allows the translocon to conduct its essential function in the translocation of polypeptides while simultaneously preventing the uncontrolled flux of solutes between the unique environments of the ER lumen and cytosol.

The findings of Ponsero and colleagues would be the first to describe a third state of the translocon, that which follows the complete translocation of a nascent

polypeptide where the now idle ribosome remains bound to the translocon to sustain the open complex (2). Due to the absence of the translocating polypeptide at this stage, a facilitated diffusion of molecules was found to occur across the ER membrane, implicating the Sec61 translocon in a novel role as a leak channel. Leak channels often play a subtle role in cellular physiology, contributing to homeostasis via discreet adjustments to the metabolite balance between cellular compartments. Furthermore, the function of leak channels is essential in responding to abrupt changes to the metabolite concentrations at these compartments which usually occur via the action of active import/export channels as they respond to the needs of the cell (17-19).

As the translocon became more heavily implicated in regulating ER homeostasis as a leak channel, investigations began to characterise dysregulation of metabolites via the translocon and how this may contribute to the progression of various disease phenotypes (20-23). One aspect of this has been to characterise regulators of translocon gating dynamics with the current literature mostly describing the mechanisms of the pore forming Sec61 subunit. However, our own investigations have revealed the other essential subunit, Sss1, to be equally important in regulating these processes.

Sss1 was previously described to stabilise the translocon complex, acting to clamp the two halves of Sec61 that form the aqueous pore (24, 25). Our structural analysis of Sss1 however, found the C-terminus positioned adjacent to a critical gating motif of Sec61 and suggested to us a potential for Sss1 to influence the conformational stability of the complex. We investigated this hypothesis through the characterisation of an absolutely conserved region at the extreme C-terminus of Sss1 which we termed as the K_{69}LIHIPI_{75} motif. Two main findings came from our analysis; first, K_{69}LIHIPI_{75} constitutes an important functional region of Sss1 that can in-fact influence translocon dynamics. Second, this motif can additionally dictate protein abundance by coding the degron to Sss1. Both conclusions are novel to this study and offer greater insight into the regulatory mechanisms at the translocon which maintain ER homeostasis and respond to exogenous stimuli. Consecutively,

we expanded upon these findings to demonstrate the potential for Sss1 to influence disease progression.

Our characterisation of two temperature sensitive (TS) *sss1* mutants led to the development of a yeast-based model for determining the potential of an introduced variable in influencing translocon dynamics. The TS growth phenotype of the mutant *sss1* strains provides an observable read-out for defective gating, or more specifically that which stabilises the open translocon and hence perpetuates an uncontrolled flux across the ER membrane. The introduction of a variable, whether a protein or compound of interest, can have one of three outcomes associated with an ability to influence the TS phenotype. First, no effect upon introduction to our system indicates the variable is unlikely involved in regulating gating dynamics to any extent. Suppression of the growth defect however, indicates that the variable influences translocon dynamics through either a destabilisation of the open or stabilisation of the closed translocon states. Finally, the variable may further disrupt translocon dynamics by stabilising the open or destabilising the closed translocon and hence observed to exacerbate the TS growth defect of the mutant yeast strains. It is worth noting that the TS *sss1* mutants are considered as "unhealthy" strains with a poor base fitness profile and as such, the effects of exacerbation may be indirect to the gating of the translocon. As such any findings from the growth evaluation within our model should likely be followed up with further analysis to more accurately depict the effects on translocon dynamics. Fortunately, we have included such analysis in the development of our system through several "gating assays". These involved assessing cell survival to extreme perturbations to the availability of certain metabolites such as GSH, Ca^{2+} and Mn^{2+}. Complementing our yeast system with the described gating assays provided us with knowledge to the exact direction in which translocon dynamics are being influenced, an essential distinction to make when assessing these outcomes in disease.

Outcomes for Analysing Disease

The translocon is critical in regulating cellular physiology through the prominent role as the entry-point into the secretory pathway. This is highlighted in the fact that disrupted translocation can contribute to many diseases associated with irregular metabolism and folding kinetics (26). Furthermore, the translocation machinery may also be manipulated to the advantage of certain diseases. Fast-growing cancers for example, rely on efficient translocation to maintain viability, while viruses have been found to employ the host machinery for synthesis of viral proteins and host related entry receptors (26-33). While the contribution that the translocation process has in these disease outcomes cannot be understated, we found ourselves following a different avenue. The observations we made from the investigation of our *sss1* mutants lead us to fully consider the contributions the translocon makes to cellular homeostasis through the facilitated flux of molecules. The potential for dysregulated translocon dynamics to have outcomes in metabolic disease has been previously discussed in this document. To briefly revise the topic, the introduction of a Sec61 mutant (Y344H) into a mice model resulted in the inability of Kar2 to bind the lumenal face of the translocon (34). This facilitated the uncontrolled flux of Ca^{2+} and ultimately leads to the development of ER stress induced apoptosis, with the mice presenting with phenotypes often associated with type 2 diabetes (T2D). While this work contributed to initial insights linking translocon gating to disease outcomes, this exact pathway has yet to be implicated as part of human pathologies. In what has been found to be a more relevant pathway to disease, is the involvement of the free fatty acid (FFA), palmitate (22). A major risk factor for T2D is a high-fat, high-sucrose-diet which can lead to increased palmitate in the blood and subsequently lipotoxicity (22, 35). This has been linked to the induction of ER stress through the depletion of ER Ca^{2+} stores via the Sec61 translocon (22, 36, 37). Pancreatic B cells respond poorly to these conditions, as signalling pathways begin to promote apoptosis which consequently can lead to the development of T2D phenotypes, as seen with the Y344H mutant. The translocon represents a key driver in this scenario, contributing to the defects in Ca^{2+} signalling that in this case promotes sustained ER stress. This presents a generalised pathway

to dyshomeostasis that we thought may be common to a variety of broader disease outcomes.

Cancer cells are notorious in their ability to leverage survival pathways to their advantage with processes involving Ca^{2+} often highlighted as significant routes for exploration (38, 39). In our assessment of six cancer associated mutations of the Sss1 subunit we found these mutations could facilitate either an uncontrolled flux of metabolites via the translocon or opposingly reduce the flux of metabolites. With this in mind, we hypothesised that mutations that arise in malignancies can dynamically manipulate the translocon, likely in the later stages of progression, to meet the needs of the diseased cell. Manipulation of Ca^{2+} at the ER within cancerous cells is not a wholly novel topic, with one such example involving the IP3R active Ca^{2+} transporters in mammalian cells. These receptors can be reorganised in certain tumours to exacerbate the efflux of Ca^{2+} at the ER face that contacts the mitochondria, fuelling ATP production (40, 41). This level of regulation is likely critical in energy demanding processes such as propagating migration of certain tumours. Prevention of Ca^{2+} flux on the other hand, can be found to aid in survival of certain cancer cells, as a sustained increase in Ca^{2+} at the mitochondria can lead to the induction of apoptosis (41-45). Furthermore, inducing apoptosis is often leveraged in a clinical setting through the mode of action of certain chemotherapeutic drugs such as Cisplatin (46). The reliance of Ca^{2+} homeostasis in regulating apoptosis presents the prevention of Ca^{2+} flux from the ER as an aspect that may also confer chemotherapeutic resistance.

Of the two TS *sss1* mutants that we assessed, the *sss1-6* mutant was unique in that while it had similarly demonstrated dysregulation through the uncontrolled flux of metabolites, it also presented with an increase accumulation in Sss1 protein. We found this to be noteworthy as the mammalian *SEC61γ* is found to be overexpressed in various cancers including head and neck squamous cell carcinoma (HNSCC), Hepatocellular carcinoma (HCC), breast cancer, gastric cancer, glioblastoma and lung adenocarcinoma (LUAD) (47-53). *SEC61γ* expression appears to be important in these cancers for cell migration and invasion and is also negatively correlated to immune cell infiltration (47-53). Knockdown of *SEC61γ* is

found to ablate these negative outcomes and impairs tumour cell survival (47, 48, 52, 53). The exact mechanisms by which *SEC61γ* overexpression contributes to cancer progression is still being elucidated yet an increased propensity for Sec61γ to bind other regulatory factors is found to be relevant as demonstrated in A549 cells where an interaction between Sec61γ and the ER membrane-bound transcription factor, CREB3 is thought to influence migration, invasiveness, and cell survival (52). We contribute the increase of Sss1 protein observed in *sss1-6* to be that of increased stability through a disruption of the proteins degron rather than an increase in *SSS1* expression. Nevertheless, the end result remains the same where we believe that the increase in Sss1 within *sss1-6* contributes to the dysregulated homeostasis that we have observed. Through our characterisation of *sss1-6* we have also found that the subunit is subject to a highly involved form of quality control that likely highlights the need for cells to regulate the availability of Sss1. Future work aims to understand the contribution that the accumulation of Sss1 protein has in the phenotypical growth defect of *sss1-6* with the hope of revealing mechanisms by which Sss1 expression contributes to the afore mentioned cancers.

It is unlikely that the Sss1 cancer associated mutations we assessed result in the development of the initial tumour and instead we suspect that they function as passenger mutations. By manipulating translocon dynamics, cancer associated mutations may discreetly modulate metabolic signalling to sustain cellular fitness throughout aspects such as metastasises and chemotherapeutic resistance. The ability of single nucleotide variants to influence tumour progression as passengers has been previously demonstrated, emphasising the need to assess an individual's variability at a single nucleotide level (54). Here in lies the advantage of our yeast system in the context of disease. By introducing an associated mutation, we can determine both the ability and manner in which these mutations may influence translocon dynamics.

How Can Yeast Help You

Translational research has since its conception provided an avenue for discovery science to contribute to human health and is often viewed with a bench to bedside attitude. The contribution of such research has been that of a “one size fits all” approach, as observations in a laboratory setting are generalised to the subset population. This approach can lead to the disregard of an individual’s unique factors such as environmental conditions, cultural background and, variation in both symptoms and genomics. On that last example specifically, while we as humans share ~99.1% identity in genetics, the diversity of the remaining ~0.9% leads to the greatest variability between individuals (55-57). The significance of such variation comes down to not only an individual’s propensity to develop certain diseases but also their response to treatment options (58-61). It is as such that recent times have initiated a paradigm shift to the perception of healthcare, with observations made on an individual basis in a clinical setting being taken back into the laboratory for analysis. The results from such a workflow can be used by clinicians to tailor treatment options to the patients’ individual needs in what is being termed as “personalised medicine”. Growth in this domain of healthcare relies on basic research to not only establish a foundation, through the characterisation of the conventional physiological processes, but also to drive improvements in the speed and accuracy of the laboratory techniques. A notable example is the vast improvements to genomic sequencing. These techniques allow us to generate large scale genomic databases that contribute a vast array of clinically relevant data for comparative analysis in a manner synonymous with quality, consistency, and cost effectiveness. We made use of such a database in the development of this project, sourcing relevant mutations to assess the applications of our system in health-based outcomes. This ultimately led us to infer that mutants of Sss1 that arise in cancer contribute to the progression of the disease.

Personalised medicine is not without constraint, often requiring the discovery of a mechanism related to the individual’s disease progression. This is not only important for the identification of disease-causing mutations, but also in establishing an effective treatment plan where optimal drug choices and patient

response can be comparatively assessed. To illustrate the importance of establishing such a physiological mechanism; Ca^{2+} contributes to signal transduction pathways that regulate both cell survival and death responses (17, 62). These two contrasting processes are maintained at a balance in healthy individuals, with defects in the distribution of Ca^{2+} able to tip the scale to favour of one response and leads to the progression of various diseases (38, 39, 62, 63). The opposing spectrums at which specific defects may operate towards disease progression emphasises the importance in ensuring necessary distinctions are made when considering a treatment plan.

There is an increasing need to discover new compounds and pathways for targeted inhibition, particularly on the forefront of rising cases of antibiotic and chemotherapeutic resistance. In the context of metabolite flux at the translocon, novel small molecule inhibitors are beginning to reveal potential avenues for disease intervention (64-66). High throughput screening assays are critical in the discovery of novel therapeutic agents, yet the properties of Sec61 are notoriously problematic for finding small molecule inhibitors, as the complex lacks any sort of self-enzymatic activity, is limited in accessibility to compounds in live cells and difficult to reconstitute functionally as part of in-vitro assays (26). It may be of interest as part of future studies to see how our model system can respond to certain translocon inhibitors with the hope that future aspects may aid in aspects of drug discovery. We can infer some initial success in this avenue, for as part of our analysis we have demonstrated the ability of our system to respond to several inhibitors, that of the antifungal terbinafine and the immunosuppressant, peptidyl-prolyl isomerase (PPI) inhibitor, FK506. Both of which impose an increased sensitivity in our stabilised open translocon mutants. Furthermore, we found another PPI inhibitor, Cyclosporine A (CsA), to regulate the quality control of Sss1. This outcome may be implicated, through the observations made with the TS *sss1-6*, to influence translocon dynamics and hence we also suggest that cyclophilins present as a novel mechanism that could be used to target the translocon.

In summary, our investigation into the absolutely conserved K_{74}LIHIPI$_{75}$ motif has revealed a novel function for the translocon subunit, Sss1, in regulating gating

dynamics of the Sec61 translocon. This finding was predominantly achieved through the characterisation of two TS mutants of this region, where the observed growth defect was related to perturbed translocon dynamics. This was crucial in our design of a yeast model that can be utilised to find novel regulators of translocon dynamics, assess the impact of translocon dynamics in disease and may have future applications as part of drug discovery. In addition to these outcomes, we found the K_{74}LIHIPI_{75} motif to code the degron for Sss1 and revealed a level of complexity to regulation of Sss1 degradation that appears to involve ER localised PPIs. These collective findings contribute to our greater understanding of the fundamental processes that regulate ER homeostasis, with implications for the dysregulation of these pathways in the development of disease.

References

1. Lang S, Zimmermann R. Mechanisms of ER Protein Import. International journal of molecular sciences. 2022;23(10).
2. Ponsero AJ, Igbaria A, Darch MA, Miled S, Outten CE, Winther JR, et al. Endoplasmic Reticulum Transport of Glutathione by Sec61 Is Regulated by Ero1 and Bip. Molecular cell. 2017;67(6):962-73.e5.
3. Huang EP. Metal ions and synaptic transmission: think zinc. Proceedings of the National Academy of Sciences of the United States of America. 1997;94(25):13386-7.
4. Hershfinkel M, Moran A, Grossman N, Sekler I. A zinc-sensing receptor triggers the release of intracellular Ca2+ and regulates ion transport. Proceedings of the National Academy of Sciences of the United States of America. 2001;98(20):11749-54.
5. Bennett BD, Kimball EH, Gao M, Osterhout R, Van Dien SJ, Rabinowitz JD. Absolute metabolite concentrations and implied enzyme active site occupancy in Escherichia coli. Nature chemical biology. 2009;5(8):593-9.
6. Park JO, Rubin SA, Xu YF, Amador-Noguez D, Fan J, Shlomi T, et al. Metabolite concentrations, fluxes and free energies imply efficient enzyme usage. Nature chemical biology. 2016;12(7):482-9.
7. Henry CS, Broadbelt LJ, Hatzimanikatis V. Thermodynamics-based metabolic flux analysis. Biophysical journal. 2007;92(5):1792-805.
8. Deponte M. Glutathione catalysis and the reaction mechanisms of glutathione-dependent enzymes. Biochimica et Biophysica Acta (BBA) - General Subjects. 2013;1830(5):3217-66.
9. Cuozzo JW, Kaiser CA. Competition between glutathione and protein thiols for disulphide-bond formation. Nature Cell Biology. 1999;1(3):130-5.
10. Kitano H. Towards a theory of biological robustness. 2007;3(1):137.
11. Hackett SR, Zanotelli VRT, Xu W, Goya J, Park JO, Perlman DH, et al. Systems-level analysis of mechanisms regulating yeast metabolic flux. 2016;354(6311):aaf2786.
12. Küken A, Eloundou-Mbebi JMO, Basler G, Nikoloski Z. Cellular determinants of metabolite concentration ranges. PLoS computational biology. 2019;15(1):e1006687.
13. Alder NN, Shen Y, Brodsky JL, Hendershot LM, Johnson AE. The molecular mechanisms underlying BiP-mediated gating of the Sec61 translocon of the endoplasmic reticulum. The Journal of cell biology. 2005;168(3):389-99.
14. Crowley KS, Liao S, Worrell VE, Reinhart GD, Johnson AE. Secretory proteins move through the endoplasmic reticulum membrane via an aqueous, gated pore. Cell. 1994;78(3):461-71.
15. Crowley KS, Reinhart GD, Johnson AE. The signal sequence moves through a ribosomal tunnel into a noncytoplasmic aqueous environment at the ER membrane early in translocation. Cell. 1993;73(6):1101-15.
16. Hamman BD, Hendershot LM, Johnson AE. BiP Maintains the Permeability Barrier of the ER Membrane by Sealing the Lumenal End of the Translocon Pore before and Early in Translocation. Cell. 1998;92(6):747-58.
17. Clapham DE. Calcium Signaling. Cell. 2007;131(6):1047-58.
18. Lemos FO, Bultynck G, Parys JB. A comprehensive overview of the complex world of the endo- and sarcoplasmic reticulum Ca2+-leak channels. Biochimica et Biophysica Acta (BBA) - Molecular Cell Research. 2021;1868(7):119020.
19. Enyedi P, Czirják G. Molecular Background of Leak K+ Currents: Two-Pore Domain Potassium Channels. 2010;90(2):559-605.
20. Lang S, Pfeffer S, Lee P-H, Cavalié A, Helms V, Förster F, et al. An Update on Sec61 Channel Functions, Mechanisms, and Related Diseases. 2017;8.

21. Linxweiler M, Schick B, Zimmermann R. Let's talk about Secs: Sec61, Sec62 and Sec63 in signal transduction, oncology and personalized medicine. Signal Transduction and Targeted Therapy. 2017;2(1):17002.
22. Parys JB, Van Coppenolle F. Sec61 complex/translocon: The role of an atypical ER Ca(2+)-leak channel in health and disease. Front Physiol. 2022;13:991149-.
23. Sicking M, Lang S, Bochen F, Roos A, Drenth JPH, Zakaria M, et al. Complexity and Specificity of Sec61-Channelopathies: Human Diseases Affecting Gating of the Sec61 Complex. Cells. 2021;10(5):1036.
24. Van den Berg B, Clemons WM, Jr., Collinson I, Modis Y, Hartmann E, Harrison SC, et al. X-ray structure of a protein-conducting channel. Nature. 2004;427(6969):36-44.
25. Wilkinson BM, Brownsword JK, Mousley CJ, Stirling CJ. Sss1p is required to complete protein translocon activation. The Journal of biological chemistry. 2010;285(42):32671-7.
26. Pauwels E, Schülein R, Vermeire K. Inhibitors of the Sec61 Complex and Novel High Throughput Screening Strategies to Target the Protein Translocation Pathway. International journal of molecular sciences. 2021;22(21):12007.
27. Gillece P, Pilon M, Römisch K. The protein translocation channel mediates glycopeptide export across the endoplasmic reticulum membrane. Proceedings of the National Academy of Sciences of the United States of America. 2000;97(9):4609-14.
28. Greiner M, Kreutzer B, Jung V, Grobholz R, Hasenfus A, Stöhr RF, et al. Silencing of the SEC62 gene inhibits migratory and invasive potential of various tumor cells. International journal of cancer. 2011;128(10):2284-95.
29. Heaton NS, Moshkina N, Fenouil R, Gardner TJ, Aguirre S, Shah PS, et al. Targeting Viral Proteostasis Limits Influenza Virus, HIV, and Dengue Virus Infection. Immunity. 2016;44(1):46-58.
30. Jung V, Kindich R, Kamradt J, Jung M, Müller M, Schulz WA, et al. Genomic and expression analysis of the 3q25-q26 amplification unit reveals TLOC1/SEC62 as a probable target gene in prostate cancer. Molecular cancer research : MCR. 2006;4(3):169-76.
31. Linxweiler M, Linxweiler J, Barth M, Benedix J, Jung V, Kim YJ, et al. Sec62 bridges the gap from 3q amplification to molecular cell biology in non-small cell lung cancer. The American journal of pathology. 2012;180(2):473-83.
32. Lu Z, Zhou L, Killela P, Rasheed AB, Di C, Poe WE, et al. Glioblastoma proto-oncogene SEC61gamma is required for tumor cell survival and response to endoplasmic reticulum stress. Cancer research. 2009;69(23):9105-11.
33. Ravindran MS, Bagchi P, Cunningham CN, Tsai B. Opportunistic intruders: how viruses orchestrate ER functions to infect cells. Nature reviews Microbiology. 2016;14(7):407-20.
34. Lloyd DJ, Wheeler MC, Gekakis N. A point mutation in Sec61alpha1 leads to diabetes and hepatosteatosis in mice. Diabetes. 2010;59(2):460-70.
35. Bensellam M, Laybutt DR, Jonas JC. The molecular mechanisms of pancreatic β-cell glucotoxicity: recent findings and future research directions. Molecular and cellular endocrinology. 2012;364(1-2):1-27.
36. Cassel R, Ducreux S, Alam MR, Dingreville F, Berlé C, Burda-Jacob K, et al. Protection of Human Pancreatic Islets from Lipotoxicity by Modulation of the Translocon. PLoS One. 2016;11(2):e0148686.
37. Cnop M, Abdulkarim B, Bottu G, Cunha DA, Igoillo-Esteve M, Masini M, et al. RNA sequencing identifies dysregulation of the human pancreatic islet transcriptome by the saturated fatty acid palmitate. Diabetes. 2014;63(6):1978-93.
38. Prevarskaya N, Ouadid-Ahidouch H, Skryma R, Shuba Y. Remodelling of Ca2+ transport in cancer: how it contributes to cancer hallmarks? Philosophical transactions of the Royal Society of London Series B, Biological sciences. 2014;369(1638):20130097.

39. Roderick HL, Cook SJ. Ca2+ signalling checkpoints in cancer: remodelling Ca2+ for cancer cell proliferation and survival. Nature reviews Cancer. 2008;8(5):361-75.
40. Okeke E, Parker T, Dingsdale H, Concannon M, Awais M, Voronina S, et al. Epithelial-mesenchymal transition, IP3 receptors and ER-PM junctions: translocation of Ca2+ signalling complexes and regulation of migration. The Biochemical journal. 2016;473(6):757-67.
41. Ivanova H, Kerkhofs M, La Rovere RM, Bultynck G. Endoplasmic Reticulum–Mitochondrial Ca2+ Fluxes Underlying Cancer Cell Survival. 2017;7(70).
42. Madden E, Logue SE, Healy SJ, Manie S, Samali A. The role of the unfolded protein response in cancer progression: From oncogenesis to chemoresistance. Biology of the cell. 2019;111(1):1-17.
43. Lièvremont J-P, Rizzuto R, Hendershot L, Meldolesi J. BiP, a Major Chaperone Protein of the Endoplasmic Reticulum Lumen, Plays a Direct and Important Role in the Storage of the Rapidly Exchanging Pool of Ca2+. 1997;272(49):30873-9.
44. Opas M, Dziak E, Fliegel L, Michalak M. Regulation of expression and intracellular distribution of calreticulin, a major calcium binding protein of nonmuscle cells. Journal of cellular physiology. 1991;149(1):160-71.
45. Pluquet O, Pourtier A, Abbadie C. The unfolded protein response and cellular senescence. A review in the theme: cellular mechanisms of endoplasmic reticulum stress signaling in health and disease. Am J Physiol Cell Physiol. 2015;308(6):C415-25.
46. Mandic A, Hansson J, Linder S, Shoshan MC. Cisplatin induces endoplasmic reticulum stress and nucleus-independent apoptotic signaling. The Journal of biological chemistry. 2003;278(11):9100-6.
47. Gao H, Niu W, He Z, Gao C, Peng C, Niu J. SEC61G plays an oncogenic role in hepatocellular carcinoma cells. Cell cycle (Georgetown, Tex). 2020;19(23):3348-61.
48. Jin L, Chen D, Hirachan S, Bhandari A, Huang Q. SEC61G regulates breast cancer cell proliferation and metastasis by affecting the Epithelial-Mesenchymal Transition. J Cancer. 2022;13(3):831-46.
49. Liu B, Liu J, Liao Y, Jin C, Zhang Z, Zhao J, et al. Identification of SEC61G as a Novel Prognostic Marker for Predicting Survival and Response to Therapies in Patients with Glioblastoma. Medical science monitor : international medical journal of experimental and clinical research. 2019;25:3624-35.
50. Lu T, Chen Y, Gong X, Guo Q, Lin C, Luo Q, et al. SEC61G overexpression and DNA amplification correlates with prognosis and immune cell infiltration in head and neck squamous cell carcinoma. Cancer Med. 2021;10(21):7847-62.
51. Tsukamoto Y, Uchida T, Karnan S, Noguchi T, Nguyen LT, Tanigawa M, et al. Genome-wide analysis of DNA copy number alterations and gene expression in gastric cancer. The Journal of pathology. 2008;216(4):471-82.
52. Zhang Q, Guo Z. SEC61G participates in endoplasmic reticulum stress by interacting with CREB3 to promote the malignant progression of lung adenocarcinoma. Oncol Lett. 2022;24(1):233.
53. Zheng Q, Wang Z, Zhang M, Yu Y, Chen R, Lu T, et al. Prognostic value of SEC61G in lung adenocarcinoma: a comprehensive study based on bioinformatics and in vitro validation. BMC Cancer. 2021;21(1):1216.
54. Kumar S, Warrell J, Li S, McGillivray PD, Meyerson W, Salichos L, et al. Passenger Mutations in More Than 2,500 Cancer Genomes: Overall Molecular Functional Impact and Consequences. Cell. 2020;180(5):915-27.e16.
55. Finishing the euchromatic sequence of the human genome. Nature. 2004;431(7011):931-45.
56. Ahmed Z, Zeeshan S, Mendhe D, Dong X. Human gene and disease associations for clinical-genomics and precision medicine research. Clin Transl Med. 2020;10(1):297-318.

57. Venter JC, Adams MD, Myers EW, Li PW, Mural RJ, Sutton GG, et al. The sequence of the human genome. Science. 2001;291(5507):1304-51.
58. Jackson FL. Human genetic variation and health: new assessment approaches based on ethnogenetic layering. British Medical Bulletin. 2004;69(1):215-35.
59. Lu YF, Goldstein DB, Angrist M, Cavalleri G. Personalized medicine and human genetic diversity. Cold Spring Harbor perspectives in medicine. 2014;4(9):a008581.
60. Schärfe CPI, Tremmel R, Schwab M, Kohlbacher O, Marks DS. Genetic variation in human drug-related genes. Genome Medicine. 2017;9(1):117.
61. Torkamani A, Pham P, Libiger O, Bansal V, Zhang G, Scott-Van Zeeland AA, et al. Clinical implications of human population differences in genome-wide rates of functional genotypes. Frontiers in genetics. 2012;3:211.
62. Bagur R, Hajnóczky G. Intracellular Ca(2+) Sensing: Its Role in Calcium Homeostasis and Signaling. Mol Cell. 2017;66(6):780-8.
63. Berridge MJ, Bootman MD, Roderick HL. Calcium signalling: dynamics, homeostasis and remodelling. Nature Reviews Molecular Cell Biology. 2003;4(7):517-29.
64. Domenger A, Choisy C, Baron L, Mayau V, Perthame E, Deriano L, et al. The Sec61 translocon is a therapeutic vulnerability in multiple myeloma. 2022;14(3):e14740.
65. Itskanov S, Wang L, Junne T, Sherriff R, Xiao L, Blanchard N, et al. A common mechanism of Sec61 translocon inhibition by small molecules. 2022:2022.08.11.503542.
66. Pauwels E, Schülein R, Vermeire K. Inhibitors of the Sec61 Complex and Novel High Throughput Screening Strategies to Target the Protein Translocation Pathway. International journal of molecular sciences. 2021;22(21).